FLUID BED THERMAL RECOVERY OF SYNTHETIC CRUDE FROM BITUMINOUS SANDS OF UTAH

by

Valadi N. Venkatesan

Sunnyside
Tar Sand Triangle

A dissertation submitted to the faculty of The
University of Utah in partial fulfillment of the requirements
for the degree of

Doctor of Philosophy

in

Fuels Engineering

Department of Mining and Fuels Engineering

The University of Utah

March 1980

ABSTRACT

The bituminous sand deposits of Utah are estimated to contain 25 - 29 billion barrels of oil in place and are the largest petroleum resource of this type in the United States. There are six major deposits of commercial importance, some of them potentially amenable to surface mining techniques. In this investigation an experimental program was conducted to determine the feasibility of an aboveground fluidized bed thermal process for the recovery of a synthetic crude from the minable bituminous sand deposits of Utah.

A continuous bench-scale, fluidized bed reactor, designed for a maximum throughput capacity of 2.25 kilograms of feed sand per hour, was developed for this investigation. Bituminous sands of distinctly different origin were processed, that is, (i) the Sunnyside bituminous sand, a deposit of fresh water origin having a bitumen content of 8.5 percent by weight, and (ii) the Tarsand Triangle sand, a deposit of marine origin having a bitumen content of 4.5 percent by weight. The effects of the following variables on the synthetic liquid yield and on the liquid quality were studied:

Reactor Temperature: 698 - 898 K
Solids Retention Time: 20.4 - 31.4 minutes
Particle Size of Feed Sand: 162 - 507.5 microns

The maximum liquid yield for the Sunnyside sand, 70 weight percent of the bitumen fed, was obtained at 773 K and a solids retention time of 20.4 minutes for a feed sand particle size of 358.5 microns. The remaining 30 weight percent of the bitumen was converted to coke and light hydrocarbon gases. Increasing the solids retention time lowered the liquid yield and shifted the temperature for maximum liquid yield to a lower value. The physical properties and chemical nature of the synthetic liquid obtained were correlated with the reactor temperature. The synthetic liquid obtained was paraffinic and contained a low percentage of heteroatoms. A mechanism for the thermal cracking of the bitumen has been developed to explain the results obtained.

Extrapolation of the data to a solids retention time of 16 minutes predicts a yield of 80 weight percent synthetic liquid, 8 weight percent light hydrocarbon gases (C_1 - C_4), and 12 weight percent coke.

The thermal processing of Tarsand Triangle sand was studied as a function reactor temperature in the range 723 - 898 K. It was found that the liquid yield was lower than that obtained with the Sunnyside feed. The maximum liquid yield of 51 weight percent based on bitumen fed was obtained at 798 K and a retention time of 27.2 minutes. Despite the differences in the origin of the feed sand and the operating temperature range, the yield of coke (19 - 22 wt %) was comparable to Sunnyside coke yields. The liquid product was more aromatic than the Sunnyside liquid product.

TABLE OF CONTENTS

Page

ABSTRACT iv

LIST OF FIGURES. x

LIST OF TABLES xiv

ACKNOWLEDGEMENTS xvi

CHAPTER

I. INTRODUCTION. 1

1.1 Reserves and Utilization of Coal and Oil Shale . . . 2
1.2 Bituminous Sand Definition 4
1.3 World and U.S. Reserves of Bituminous Sands. 5
1.4 Origin and Geology 7
1.5 Properties of Bituminous Sands 14
1.6 Nature of Bitumen in Bituminous Sands. 22

II. RECOVERY OF BITUMEN OR PRODUCTION OF SYNTHETIC CRUDES FROM BITUMINOUS SANDS. 30

2.1 Interest in Commercial Development of Bituminous Sands 31
2.2 Factors Influencing the Choice of Recovery Methods 32
2.3 *In-situ* Recovery Schemes 35
    2.3.1 Emulsion Steam Drive Process. 38
    2.3.2 Partial Oxidation Recovery Processes. 41
    2.3.3 Combination of Combustion and Water Flooding Processes. 46
2.4 Surface-Mined Aboveground Recovery Methods 47
    2.4.1 Solvent Extraction Processes. 50
    2.4.2 Cold Water-Solvent Extraction Processes . . . 51
    2.4.3 Hot Water-Solvent Extraction Processes. . . . 52
2.5 High Temperature Aboveground Recovery Processes. 63

CHAPTER Page

2.5.1 Fundamentals of High Temperature Thermal Processing 63
2.5.2 Fluidized Bed Coking Processes 65
2.5.3 Nonfluidized Direct Coking Processes. 73
2.6 Process Selection 80
2.7 Research Objectives 88

III. EXPERIMENTAL WORK. 89

3.1 Fluid Bed Reactor Assembly. 92
3.2 Introduction and Withdrawal of Solids 109
3.3 Oil Product Recovery System 118
3.4 Bituminous Sand Feed Preparation. 127
3.5 Calibrational Procedures. 131
3.5.1 Calibration of Screw Feeder. 131
3.5.2 Calibration of Rotameter 132
3.5.3 Calibration of Differential Pressure Controller 140
3.6 Operational Procedures. 143
3.7 Product Analysis. 146
3.7.1 Gas Analysis 146
3.7.2 Coke Analysis. 147
3.7.3 Synthetic Liquid Product Analysis. 147
3.8 Material Balance. 147

IV. RESULTS AND DISCUSSION 151

4.1 Effect of Operating Variables on Yield and Product Distribution. 151
4.1.1 Effect of Temperature on Product Yield and Distribution 152
4.1.2 Effect of Solids Retention Time on Yield and Product Distribution 163
4.1.3 Effect of Feed Sand Particle Size and Particle Size Distribution on Yield and Product Distribution 181
4.1.4 Effect of Feed Bituminous Sand Source and its Bitumen Content on Product Yield and Distribution 187
4.2 Characterization Studies on Extracted Bitumen and Synthetic Liquid. 198
4.2.1 Properties of the Extracted Bitumens 200
4.2.2 Effect of Temperature on Synthetic Liquid Product Quality 208
4.2.3 Potential Reaction Pathways for Bitumen Cracking 246
4.2.4 Effect of Solids Retention Time on Synthetic Liquid Product Quality 248

CHAPTER Page

V. CONCLUSIONS AND RECOMMENDATIONS. 254

5.1 Conclusions 254
5.2 Recommendations 256

APPENDIX A. THERMOGRAVIMETRIC ANALYSIS OF THE BITUMINOUS SANDS OF UTAH. 259

APPENDIX B. DESIGN OF THE FLUIDIZED BED REACTOR. 276

B.1 Rheological Properties of the Bituminous Sands. 276
B.2 Behavior of Bituminous Sand Under Fluidizing Conditions 277
B.3 Heat Demand for the Pyro-Distillation of the Bituminous Sand. 278
B.4 Fluidized Bed Reactor Design. 278

APPENDIX C. FLUIDIZED STUDIES AT HIGH TEMPERATURES 281

C.1 The Fluidized State 281
C.2 Estimation of Minimum Fluidization Velocity . . 285
C.3 Fluidization Studies on Coked Sand. 287

APPENDIX D. HYDROCARBON MIST REMOVAL 298

APPENDIX E. MATERIAL BALANCE CALCULATIONS. 304

REFERENCES. 307

VITA. 319

Copyright © Valadi N. Venkatesan 1980
All Rights Reserved

THE UNIVERSITY OF UTAH GRADUATE SCHOOL

SUPERVISORY COMMITTEE APPROVAL

of a dissertation submitted by

Valadi N. Venkatesan

I have read this dissertation and have found it to be of satisfactory quality for a doctoral degree.

September 28, 1979 Alex G. Oblad
Date

Alex G. Oblad
Chairman, Supervisory Committee

I have read this dissertation and have found it to be of satisfactory quality for a doctoral degree.

September 28, 1979 Francis V Hanson
Date

Francis V. Hanson
~~Member, Supervisory Committee~~
Cochairman , Supervisory Committee

I have read this dissertation and have found it to be of satisfactory quality for a doctoral degree.

September 28, 1979 David M Bodily
Date

David M. Bodily
Member, Supervisory Committee

I have read this dissertation and have found it to be of satisfactory quality for a doctoral degree.

September 28, 1979 Wendell H Wiser
Date

Wendell H. Wiser
Member, Supervisory Committee

I have read this dissertation and have found it to be of satisfactory quality for a doctoral degree.

September 28, 1979
Date

Jan D. Miller
Member, Supervisory Committee

I have read this dissertation and have found it to be of satisfactory quality for a doctoral degree.

September 28, 1979 Norman W. Ryan
Date

Norman W. Ryan
Member, Supervisory Committee

THE UNIVERSITY OF UTAH GRADUATE SCHOOL

FINAL READING APPROVAL

To the Graduate Council of The University of Utah:

I have read the dissertation of Valadi N. Venkatesan in its final form and have found that (1) its format, citations, and bibliographic style are consistent and acceptable; (2) its illustrative materials including figures, tables, and charts are in place; and (3) the final manuscript is satisfactory to the Supervisory Committee and is ready for submission to the Graduate School.

October 5, 1979
Date

Francis V. Hanson
Francis V. Hanson
Member, Supervisory Committee

Approved for the Major Department

David M. Bodily
David M. Bodily
Chairman, Dean

Approved for the Graduate Council

James L. Clayton
Dean of The Graduate School

05

Dedicated to

My Beloved Father

LIST OF FIGURES

Figure Page

1.1 Location of Major Bituminous Sand Deposits in Utah. 9

1.2 Physical Arrangement of Utah and Canadian Bituminous Sands. 16

1.3 Effect of Temperature on the Viscosity of Bitumens. 25

2.1 Types of Fire Flooding Schemes. 43

2.2 Temperature Dependence of Water and Bitumen Densities . . . 53

2.3 Flow Diagram of Syncrude Canada Process 56

2.4 Flow Diagram of the Laboratory Fluidized Bed Thermal Recovery Unit 66

2.5 Flow Diagram of the Fluidized Bed Pilot-Plant Operation for Canadian Bituminous Sands 69

2.6 Flow Diagram of Lurgi Rührgas Direct Coking Process 75

2.7 Flow Diagram of Berg's Rotary Kiln Direct Coking Process. 78

2.8 Material Balance Comparison of Direct Coking and Hot Water Extraction/Primary Fluid Coking Upgrading 82

2.9 Energy Comparison of Direct Coking and Hot Water Extraction/Primary Fluid Coker Upgrading. 85

3.1 Flow Diagram of Fluidized Bed Thermal Recovery Unit 90

3.2 Physical Arrangement of Fluid Bed Reactor Assembly. 93

3.3 Detailed Diagram of the Fluidizing Gas Pre-heater 95

3.4 Schematic of the Reactor Unit 99

3.5 Detail of the Gas Distributor 102

3.6 Schematic of the Expansion Chamber. 105

Figure Page

3.7 Differential Pressure Controller - Piping Diagram. 110

3.8 Schematic of the Screw Feeder. 113

3.9 Schematic of the Feed Sand Hopper. 116

3.10 Solids Control Valve 119

3.11 Sand Fines Cyclone Separator Configuration 122

3.12 Stainless Steel Filter Configuration 125

3.13 Configuration of the Cyclone Separator for Mist Removal. . 128

3.14 Feed Rate Characteristic Curves for Sunnyside Bituminous Sand. 133

3.15 Feed Rate Characteristic Curves for Tarsand Triangle Bituminous Sand 135

3.16 Characteristic Flow Curve for Fluidizing Gas (Nitrogen) 138

3.17 Differential Pressure Unit Calibration Arrangement 141

3.18 Typical C_1 to C_6 Hydrocarbon Gas Chromatogram. 148

4.1 Effect of Reactor Temperature on Yield and Product Distribution (Sunnyside Feed). 154

4.2 Effect of Reactor Temperature on Gas Make and Product Distribution (Sunnyside Feed). 159

4.3 Effect of Retention Time of Solids, θ_{avg}, on Product Yield and Distribution (Sunnyside Feed). 166

4.4 Effect of Retention Time of Solids, θ_{avg}, on Product Yield and Distribution (Sunnyside Feed). 169

4.5 Effect of Retention Time of Solids, θ_{avg}, on Product Yield and Distribution (Sunnyside Feed). 172

4.6 Solids Slugging. 175

4.7 Effect of Retention Time of Solids on the Optimum Temperature for Maximum Yield of Synthetic Crude (Sunnyside Feed) 179

Figure Page

4.8 Particle Size Distribution of Coked Sand (Sunnyside Feed) 185

4.9 Effect of Reactor Temperature on Product Yield and Distribution (Tarsand Triangle Feed) 190

4.10 Effect of Reactor Temperature on Gas Make and Product Distribution (Tarsand Triangle Feed) 192

4.11 Effect of Feed Sand Source and Bitumen Content on the Optimum Temperature for Maximum Yield of Synthetic Crude 196

4.12 Distillation Curves for Extracted Bitumens 206

4.13 Effect of Coking Reactor Temperature on the API Gravity of Synthetic Liquid. 211

4.14 Effect of Coking Reactor Temperature on the Conradson Carbon Residue of the Synthetic Liquid 214

4.15 Effect of Coking Reactor Temperature on the Viscosity of Synthetic Liquid. 217

4.16 Effect of Coking Reactor Temperature on the Distillation Curve (Sunnyside Feed). 221

4.17 Effect of Coking Reactor Temperature on the Distillation Curves. 224

4.18 Proton Magnetic Resonance Spectra of Extracted Bitumen and Synthetic Liquid (Sunnyside Feed). 230

4.19 Effect of Coking Reactor Temperature on the Chemical Nature of Synthetic Liquid (Sunnyside Feed). 242

4.20 Effect of Solids Retention Time on the Viscosity of Synthetic Liquid. 252

A-1 Isothermal Thermal Analysis (TGA) Curves (Asphalt Ridge Bituminous Sand). 262

A-2 Isothermal Thermal Analysis (TGA) Curves (Sunnyside Bituminous Sand). 264

A-3 Temperature Programmed Thermal Analysis (TGA) Curve (Tarsand Triangle Bituminous Sand) 267

A-4 Temperature Programmed Thermal Analysis (TGA) Curve (Tarsand Triangle Bituminous Sand) 269

Figure Page

A-5 Temperature Programmed Thermal Analysis (TGA) Curve (Tarsand Triangle Coked Sand) 272

A-6 Temperature Programmed Thermal Analysis (TGA) Curve (Tarsand Triangle Coked Sand) 274

C-1 Ideal Pressure Drop-Gas Velocity Diagram. 283

C-2 Bed Pressure Drop Versus Gas Velocity Coked Sand (Tarsand Triangle Deposit). 290

C-3 Bed Pressure Drop Versus Gas Velocity Coked Sand (Tarsand Triangle Deposit). 292

C-4 Effect of Reactor Temperature on Minimum Fluidization Velocity Coked Sand (Tarsand Triangle Deposit) 295

LIST OF TABLES

Table Page

1.1 Estimates of World and U.S. Fossil Fuel Resources 3

1.2 Major Bituminous Sand Deposits of the World 6

1.3 Major United States Bituminous Sand Deposits. 8

1.4 Extent of Major Utah Tar Sand Deposits. 11

1.5 Bulk Properties of Utah and Canadian Bituminous Sand Deposits 21

2.1 Existing and Proposed Commercial Bituminous Sand Projects in Canada. 33

2.2 Bitumen and/or Synthetic Liquid Recovery Schemes. 36

2.3 Syncrude Canada, Ltd. Project Details 58

3.1 Differential Pressure Controller Specifications. 108

4.1 Effect of Reactor Temperature on Product Yield and Distribution (Sunnyside Feed) 153

4.2 Typical Composition of the Gaseous Product (Sunnyside Feed). 162

4.3 Effect of Retention Time of Solids on Product Yield and Distribution (Sunnyside Feed) 165

4.4 Effect of Retention Time of Solids on Product Yield and Distribution (Sunnyside Feed) 168

4.5 Effect of Retention Time of Solids on Product Yield and Distribution (Sunnyside Feed) 171

4.6 Effect of Feed Sand Particle Size and Particle Size Distribution on Product Yield and Distribution (Sunnyside Feed). 183

Table Page

4.7 Effect of Reactor Temperature on Product Yield and Distribution (Tarsand Triangle Feed) 189

4.8 Comparison of Product Yield and Distribution with Feed Sand Source and its Bitumen Content. 195

4.9 Properties of Extracted Bitumens 201

4.10 Effect of Reactor Temperature on Synthetic Liquid Product Quality (Sunnyside Feed) 209

4.11 Effect of Reactor Temperature on Synthetic Liquid Product Quality (Tarsand Triangle Feed). 210

4.12 Effect of Reactor Temperature on the Distillation Fractions for Synthetic Liquid (Sunnyside Feed). 220

4.13 Effect of Reactor Temperature on the Distillation Fractions for Synthetic Liquid (Tarsand Triangle Feed) . . 223

4.14 Effect of Reactor Temperature on the Percentage Distribution of Carbon Type in the Bitumen and in the Synthetic Liquid (Sunnyside Feed) 233

4.15 Chemical Structure of Bitumen and Synthetic Liquid (Sunnyside Feed) 238

4.16 Effect of Retention Time of Solids on Synthetic Liquid Product Quality (Sunnyside Feed) 249

4.17 Properties of Synthetic Liquid at Optimum Reactor Temperatures (Sunnyside Feed). 250

C-1 Bed Pressure Drop Versus Gas Velocity at Different Reactor Temperatures 289

C-2 Comparison of Experimental and Theoretical Values of Minimum Fluidization Velocity. 294

D-1 Comparison of the Performance of Various Liquid Recovery Systems 302

ACKNOWLEDGEMENTS

I am greatly indebted to Professor Alex G. Oblad for the help, guidance and encouragement which he generously gave, especially during the difficult moments of this research project. I consider myself fortunate to have had the opportunity of working with him and this experience will be long remembered.

I am thankful to Professor Francis V. Hanson who readily agreed to be the cochairman of my supervisory committee. I am extremely grateful for his invaluable guidance, encouragement and friendship during this investigation and in the preparation of this manuscript.

Special thanks are extended to the members of my supervisory committee, Professors Wendell H. Wiser, Norman W. Ryan, David M. Bodily and Jan D. Miller.

The author wishes to acknowledge the assistance of Mr. Jeff Utley during the experimental phase of this project in particular for the characterization of the synthetic liquid product. Gratitude is also expressed to the faculty and staff and to my colleagues of the Department of Fuels Engineering for these memorable years of graduate school. My sincere thanks go to Mr. Keith McCleery (Central Machine Shop) and Mr. D. Steinmann (Mechanical Machine Shop) for their help in the fabrication of the experimental apparatus. The financial support of the United States Department of Energy (Grant EF 77-S-04-3953), the National Science Foundation (Grant AER 74-21867) and the Mobil Foundation are gratefully acknowledged.

Finally, my sincere thanks to my mother, brothers and sisters for their love, encouragement and understanding during my long absence from my homeland. To my mother, I owe a debt of gratitude for recognizing the need for a rigorous educational background and for providing me with the opportunity to obtain one. In particular, I thank her for sharing my failures and successes during these years of my life.

CHAPTER 1

INTRODUCTION

The depletion of petroleum and natural gas reserves in the United States concomitant with an increasing demand for energy has created a supply-demand imbalance(1). The growth in energy demand has been met by increased petroleum and natural gas imports and according to the Exxon Corporation petroleum imports will increase from 40 to 50% by 1990(2). Although there are different opinions regarding the rate of growth for energy demand, it is accepted that the requirements at the end of this century will be enormous by present standards. In addition, the energy demand growth rate of the rest of the world will increase faster than the United States', resulting in an even greater demand for petroleum and natural gas products. A long range solution to the energy imbalance could be achieved by the development of technology dedicated to the production of synthetic crudes from alternate fossil fuels like coal, oil shale and bituminous sand. These alternate fossil energy resources are available in sufficient quantities to alleviate and perhaps eliminate the dependence of the United States on imported petroleum crude provided that a firm committment is made in developing these resources soon.

1.1 Reserves and Utilization of Coal and Oil Shale

The proven reserves of coal and oil shale in the United States exceed our proven reserves of petroleum crude. The estimated fossil energy reserves for the world and the United States are presented in Table 1.1(1,3). Although there is an abundant supply of coal the use of coal, at present, is limited by its lack of versatility and the high sulfur content of many of the more readily mineable eastern coals.

Despite the high yield of synthetic crude per ton of coal (3 to 3.5 barrels), the coal liquefaction process requires large amounts of hydrogen due to the low hydrogen to carbon atomic ratio of coal (the atomic hydrogen to carbon ratio in coal is in the range of 0.7 - 0.9 compared to a value of 1.6 for bituminous sand). There are no commercial operations for the production of coal derived synthetic crudes, however, several coal liquefaction processes are at various stages of development. Some of the processes, such as the solvent refined coal (SRC II) process, the char oil energy development (COED) process, H-Coal (Hydrocarbon Research) process and the Exxon donor solvent (EDS) process, are at the demonstration plant level. Howard and Hottel(4) have discussed the difficulties associated with coal liquefaction processes such as heat transfer in liquids containing suspended solids, catalyst activity and regeneration, solids separation, etc.

The recovery of synthetic crude from shale kerogen can be accomplished either by _in-situ_ techniques or by the above ground

Table 1.1

Estimates of World and U.S. Fossil Fuel Resources[a]

	United States		World	
	Proved and Currently Recoverable	Estimated Remaining Recoverable	Proved and Currently Recoverable	Estimated Remaining Recoverable
Dry Natural Gas				
Trillion Cubic Feet	209.0	760-1170	2118-2450	9090-9490
Quintillion (10^{18}) BTU	0.21	0.78-1.19	2.18-2.52	9.36---9.78
Natural Gas Liquids				
Billion Bbl	6.0	21---33	55---65	241--251
Quintillion BTU	0.02	0.09-0.13	0.23-0.27	0.99---1.03
Crude Oil				
Billion Bbl	29.5	144--371	538--606	1500-1840
Quintillion BTU	0.17	0.84-2.15	3.12-3.52	8.7---10.67
Coal				
Billion Short Tons	214.0	1036-1788	662	5367-6119
Quintillion BTU	4.72	20.71-35.75	13.67	107.34-122.3
Shale Oil				
Billion Bbl	74.0	1026 (4000)[a]	190	1865 (19000)[b]
Quintillion BTU	0.43	5.95	1.10	10.82

Notes: [a] Adapted from references 1, 3 and 5.

[b] The values in the parenthesis were estimated by Duncan and Swanson whose results are summarized by Hendrickson(5).

retorting of mined shale. Hendrickson(5) has reviewed the various in-situ and above ground retorting processes for the recovery of a synthetic crude from shale. The above ground recovery techniques, such as the Tosco-II and the Paraho retorting processes, give high yields of synthetic liquid (92 - 95 Vol. % Fisher Assay of shale feed), but require the disposal of large amounts of spent shale. The in-situ methods, such as the Occidental process, recover less synthetic liquid than the surface retorting methods and much research (on site) must be carried on to determine pressure and flow rate requirements for the injected retorting fluids, fracturing of the shale zones, and control of the combustion zone.

In light of the above problems associated with the development of coal and oil shale, commercialization of synthetic crudes from these two fossil fuels may be delayed until 1985 - 1990. On the contrary, commercial operations for the recovery of synthetic crudes from bituminous sands have been carried out in Canada since 1967. Even though the 25 - 30 billion barrels of oil in place in the U.S. bituminous sand reserves is small compared to the vast reserves of coal and oil shale, exploitation of this resource can be achieved with a shorter lead time. In the remainder of this chapter, the world reserves of bituminous sands and their characteristics are discussed.

1.2 Bituminous Sand Definition

There are several different names for describing the oil saturated sand deposits, but the most commonly used term in the literature is 'tar sand'. 'Tar sand' refers to a mixture of sand and a dense, viscous petroleum-like material(6). However, tars and pitches are the products obtained from the destructive distillation of organic matter. As used, 'tar sand' refers to consolidated or unconsolidated rocks with interstices containing a highly viscous hydrocarbon material not recoverable in its natural state through a well bore or by primarily petroleum production methods. Other names used to describe this material are oil sands, bituminous sands, bituminous sandstone or oil-impregnated rock and rock asphalt. The black or heavy oil deposits are different from bituminous sand deposits due to the difference in viscosity and can be recovered by primary petroleum methods, but not at economic rates. Because the term 'bituminous sand' adequately describes the material as a mixture of sand and bitumen and is technically correct, it is used herein.

1.3 World and U.S. Reserves of Bituminous Sands

Bituminous sand deposits are found throughout the world, often in the same geographical area as conventional petroleum. There are sixteen major bituminous sand deposits containing a total of 2,100 billion barrels of oil in place(7). McRae and Dudas(8) have reported the geographical distribution of this resource (Table 1.2). Three deposits, the Orinoco tar belt of Eastern Venezuela(9), the Alberta deposit of Western Canada(10,11), and the bituminous sand deposits of Columbia(8) are individually comparable in size to the proven reserves of petroleum of the entire Middle East. A figure of three trillion barrels of oil in place has even been proposed as a possible upper limit for the reserves of the Venezuelan tar belt(12). A number of

Table 1.2

Major Bituminous Sand Deposits of the World

	Proved and Currently Recoverable[a] (billion barrels)	Estimated Total Recoverable[b] (billion barrels)
North America		
Canada	300	900 - 1200
Trinidand and Tobago	-	60 - 70
United States	-	27 - 30
South America		
Colombia	-	1139 - 1140
Venezuela	60 - 70	200 - 1050
Africa		
Malagasy Republic	-	1.7 - 1.75
Europe		
Albania	-	0.3
Rumania	-	0.03
Asia		
USSR	-	150

Note: [a] Estimated from information in the literature.
[b] Adapted from references 5, 7 and 8.

excellent reviews discussing the geology and the reserves of the major bituminous sand deposits are reported in the literature(13,14).

The bituminous sand reserves of the United States are estimated at 25 - 30 billion barrels of bitumen-in-place and are located in 22 states(15). Only six states contain deposits which could be recovered commercially (Table 1.3) and more than 90% of the estimated reserves of oil in place in the bituminous sand deposits are located in the state of Utah. Some of the national deposits are shallow(16) and provide easy access for 'mining' oil. Based on the information available in the literature(17-19), there are 97 deposits in Utah which are estimated to contain 25 - 29 billion barrels of bitumen-in-place. The locations of major Utah deposits are shown in Figure 1.1, while the average bitumen content and the estimated amount of bitumen in place in each of the major deposits are presented in Table 1.4. The extent of Utah deposits seems small compared to the vast bituminous sand reserves of Alberta, Canada. Nevertheless, the bitumen in place in Utah deposits is equivalent to three times the recent oil discoveries (10.1 billion barrels) in Prudhoe Bay, Alaska(20). A number of reviews have been reported dealing with the exploitation of Utah bituminous sand resources(21,22).

1.4 Origin and Geology

The origin of the bituminous sands has long been a subject of speculation among geologists. There are two theories regarding the origin of the bitumen. One suggested that the bitumen in the sand is locally generated and has not been subjected to great overburden pressures(5). Under these conditions, the hydrocarbon material would not

Table 1.3

Major United States Bituminous Sand Deposits[a]

Location	Estimated Resource (millions of barrels)
Alabama	1,180
California	270 - 323
Kentucky	149
New Mexico	57
Texas	154
Utah	25,000 - 29,500

Note: [a] Adapted from references 7, 8, 14, 17 and 19.

Figure 1.1

Location of Major Bituminous
Sand Deposits in Utah

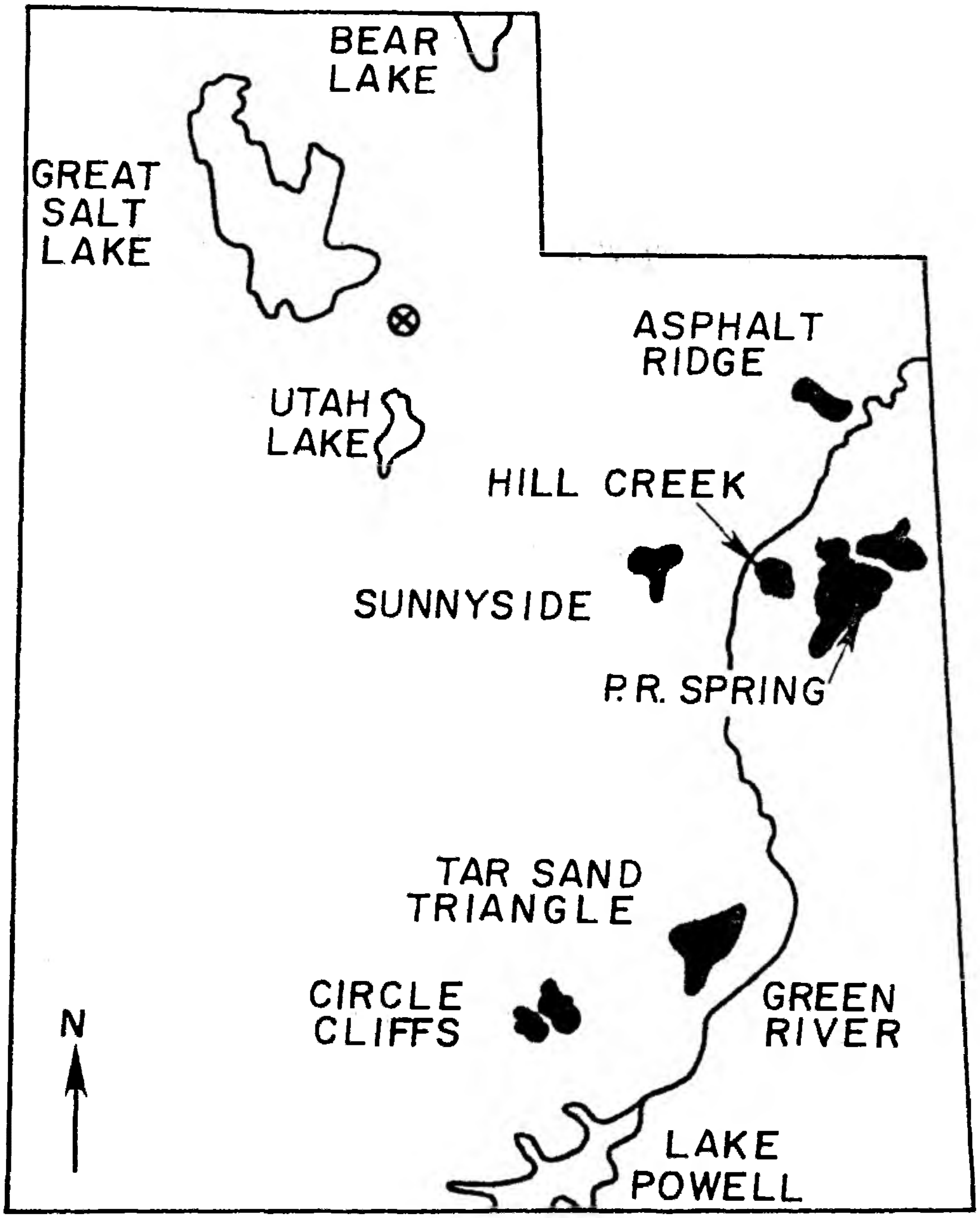
BEAR LAKE
GREAT SALT LAKE
UTAH LAKE
ASPHALT RIDGE
HILL CREEK
SUNNYSIDE
P.R. SPRING
TAR SAND TRIANGLE
CIRCLE CLIFFS
GREEN RIVER
LAKE POWELL
N

Table 1.4

Extent of Major Utah Tar Sand Deposits [17-19]

Deposit	In-Place Bitumen (billion barrels)	Average Bitumen Content (Wt. %)
Tar Sand Triangle	12.5-16.0	5
PR Spring	4.0-4.5	8
Sunnyside	3.5-4.0	9
Hill Creek	1.2	6
Circle Cliff	1.3	5
Asphalt Ridge	1.15	8
Whiterocks	0.06-0.125	6-8

have been subjected to thermal cracking resulting in a geologically young, viscous substance. The second theory suggested that the original petroleum crude is assumed to have migrated into the sand deposits, which may initially have been filled with water. Later, when the overburden pressures were relieved, the light ends evaporated leaving a highly viscous residue(5). Recently, a geochemical theory based on biodegradation by bacterial action has also been proposed(23).

Considerable information regarding the geology and the origin of the bitumen of the Alberta bituminous sands has been published(10,24,25). A large portion of the bituminous sand deposits in the Athabasca deposits, are contained within the lower Cretaceous Mannville group, which has been subdivided into McMurray, Clear Water and Grand Rapid formations. The Peace River deposits occur in sands equivalent to the McMurray formation. An estimated 625 billion barrels of bitumen-in-place in the Athabasca bituminous sand deposits are contained in the McMurray formation. The distribution of bitumen is controlled by the presence of clean, porous and permeable sandstones and the distribution of the sands is controlled by the depositional history of the basin. The migration theory and the local formation theory have both been put forward to explain the origin of the Athabasca bitumen, however, the exact origin is still debated. The geochemical theory(23) appears to successfully explain the origin of the highly viscous bitumens in the Athabasca deposits(10), however, this issue is unresolved.

Much of the work on the origin of bitumen of the Orinoco tar belt of Venezuela indicates some similarities with the bituminous sands of Alberta. The bitumen is hosted in the Cretaceous and Tertiary sands(26) and the density of the bitumen varies between 8 to 18 °API. Gutierrez, et. al.(27) have indicated that a major portion of the bitumen in the Orinoco tar belt is found in the Tertiary formation with appreciable quantities occuring in the Paleozoic formation. The bitumen in the tar belt is not isolated but grades into prolific producing oil fields of the north, suggesting the origin of the bitumen may be related to the migration of the petroleum crude into the sand deposits. Bacterial degradation of normal crude oil has also been proposed to explain the origin of the bitumen or extra heavy oil in the Orinoco tar belt(28).

Most of the studies regarding the origin and the geology of the United States' bituminous sand deposits have been concentrated on the Utah resources. Detailed information regarding the geology of the major Utah deposits has been reported by Ritzma(29,30), Campbell(19,31) and Covington(18). In most of the deposits of the northern region such as Asphalt Ridge, P. R. Spring and Sunnyside, the bitumen occurs in sandstone rocks and is generally related to the Tertiary sediments of the basin, primarily the Green River formation of Eocene age; while in the deposits of the southern region, in particular Tarsand Triangle, the bitumen occurs in Permian White Rim sandstone. The bitumen in the deposits of the southern region are assumed to have migrated from source beds. Moreover, some of the Utah deposits exhibit multiple zones of bitumen saturation. Information on the reservoir characteristics for Asphalt Ridge(32,33), P. R. Spring(34-36), Sunnyside(37), Circle Cliff(38) and Tarsand

Triangle(39) have been reported and have been summarized by Campbell(31). The deposits in the southern region of Utah (Tarsand Triangle, Circle Cliff) appear to be similar in origin (marine origin) to the bituminous sand deposits of Canada; while the origin of the bitumen in the northern deposits (Asphalt Ridge, P. R. Spring, Hill Creak, Sunnyside) is of fresh or brackish water origin(29) and appears to be unique.

Recently, studies on the geology and bitumen characteristics for the Alabama deposits(40) and the New Mexico bituminous sandstone deposits(41) have been reported. The bitumen occuring in the Santa Rosa sandstone deposit of New Mexico is generally related to the Permian and Triassic sediments of the basin. The properties of the bitumen are similar to the bitumen from the Tarsand Triangle deposit, having a high percentage of sulfur (3 - 4 wt %) and a low nitrogen content (less than 1 wt %). The reservoir characteristics include an average porosity of 10 - 13% and an air permeability in the range of 100 - 200 millidarcies.

1.5 Properties of Bituminous Sands

An understanding of the physical and chemical properties of the bituminous sands is essential to the development of a synthetic crude recovery technique. Since the technology for the recovery of the bitumen and/or a synthetic crude from the Canadian bituminous sands has been developed to the commercial stage, it is appropriate to compare the properties of Utah sands to the properties of Canadian sands. This will permit us to evaluate the possiblity of applying the Canadian technology for recovering the bitumen to the Utah bituminous sands.

There are significant differences in the physical and chemical natures of the Canadian and Utah bituminous sands. The Utah deposits contain an average of 0.5% by weight connate water compared to an average of 4.5% by weight connate water for the Canadian deposits. Typical physical arrangements of the Canadian and Utah bituminous sands are presented in Figure 1.2. A film of water separates the bitumen and the sand granule in the Canadian bituminous sands and it is believed the film of water facilitates the separation of the bitumen from the sand in the hot water extraction process; while direct contact of the bitumen with sand granules prevails with the Utah sands. The bitumen is also found in the void spaces and in some instances, a small volume of gas may also be present. Scanning electron micrographs of Canadian bituminous sands(42) and Utah bituminous sands(43) support this view regarding the physical arrangement of bituminous sands of Canada and Utah.

The physical properties of the bituminous sands, such as the extent and nature of mineral matter, the bulk properties, the amount of sand fines and the bitumen content, may significantly influence the selection of a recovery method and the ease of processing the bituminous sands. Bituminous sands are classified as lean, medium and rich depending upon their bitumen content. Lean grade bituminous sand contains less than 4% by weight bitumen, medium grade bituminous sand has a bitumen content of 4 to 10% by weight, while the rich grades have more than 10% by weight bitumen(44). More than 65% of the

Figure 1.2

Physical Arrangement of Utah and
Canadian Bituminous Sands

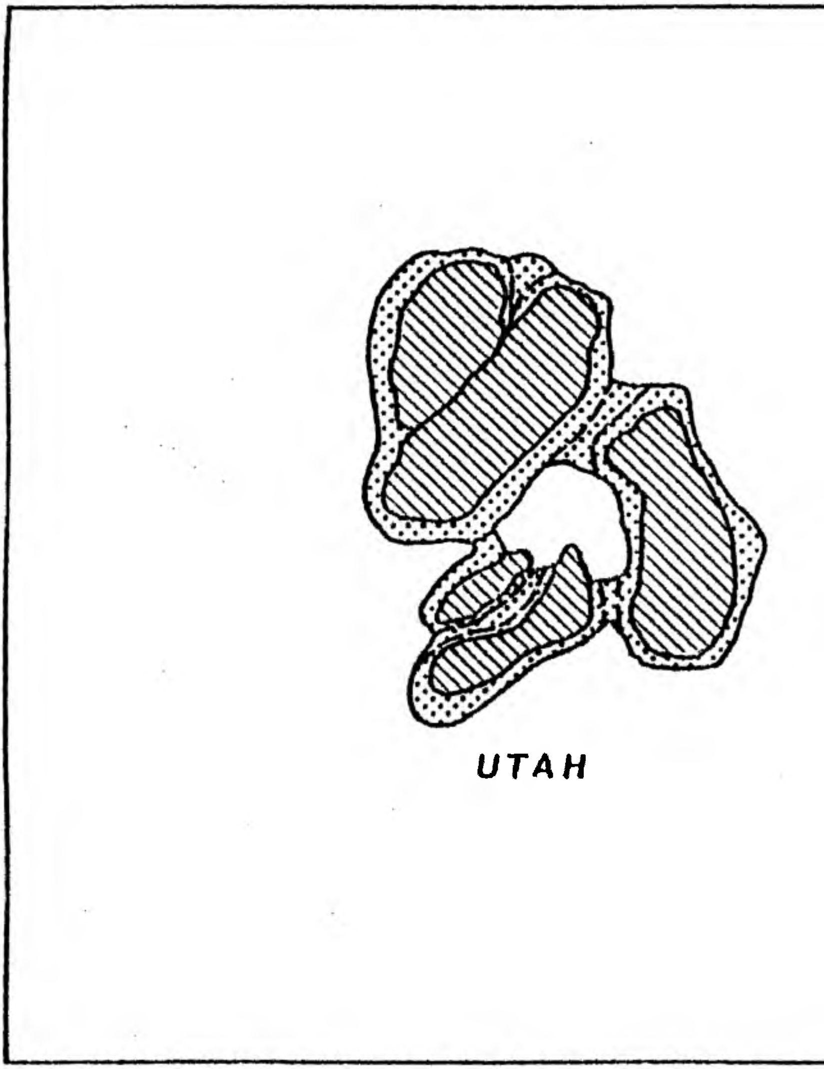
UTAH

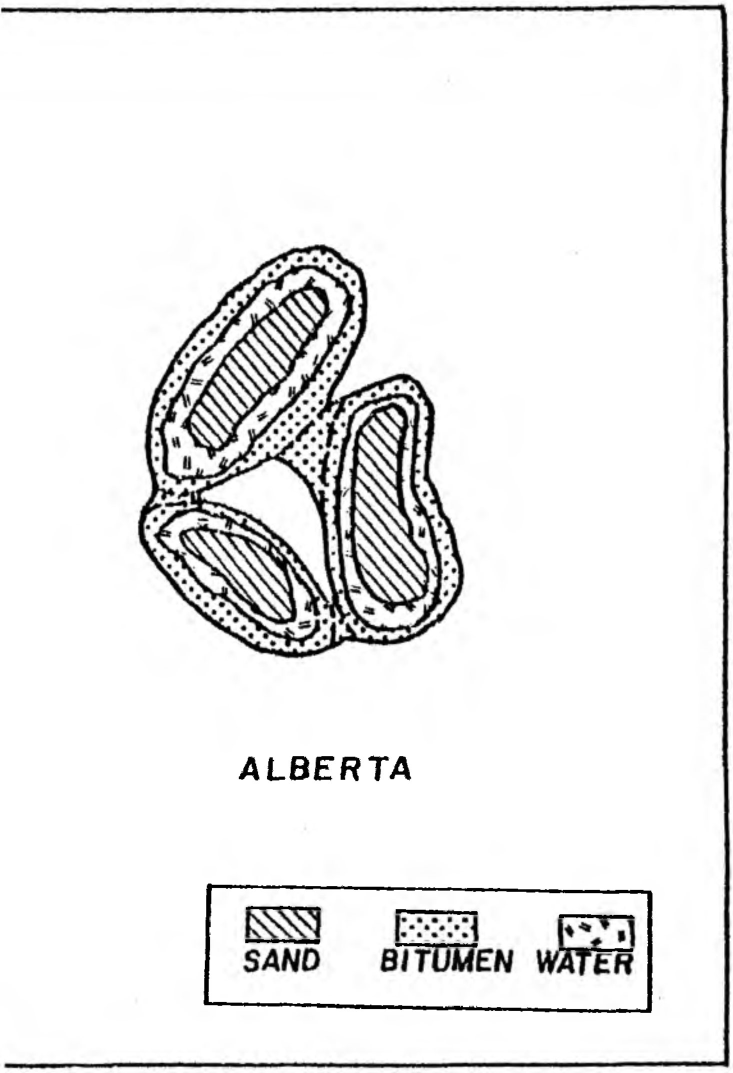
ALBERTA
SAND
BITUMEN
WATER

Canadian bituminous sand reserves are rich grade(45), while most of the Utah bituminous sand reserves belong to the medium grade class.

The bitumen concentration has a profound influence on the appearance and the nature of bituminous sands. In rich grade samples, the individual sand particle is coated with a continuous film of bitumen and it appears that the sand grains are suspended in the bitumen matrix forming an unconsolidated sample. In low and medium grade samples, the sand granules are coated with a non-continuous film of bitumen. This allows the sand granules to fuse to each other during the rock-forming process resulting in the consolidated nature of the bituminous sand. Because of its rich grade, most of the Canadian deposits appear black in color and are unconsolidated. The bitumen surrounding the water-wet sand appears to be a continuous film. In fact, when a sample of Canadian bituminous sand is compressed, a small portion of the oil is released from the sample. Except for the Asphalt Ridge sample, most of the Utah bituminous sand samples appear light to dark brown in color and are largely consolidated sandstone deposits. The bitumen content of the Utah reserves varies from deposit to deposit and significant variations have been observed within a given deposit(46). Some of the high bitumen content Asphalt Ridge samples (bitumen content greater than 10% by weight) are unconsolidated and these samples are similar to the Canadian sands in their physical properties. In the high bitumen content Asphalt Ridge deposit, the bitumen surrounding the sand grains is continuous; while in the medium and low grade deposits such as Sunnyside, P. R. Spring and Tarsand Triangle deposits, the bitumen film surrounding the sand grains appears to be discontinuous(47). One of the most significant differences between Utah and Canadian bituminous sand deposits is the consolidated nature of Utah deposits and this may dictate the processing approaches for the bituminous sand reserves of Utah that are different from the technology used for the Athabasca deposits in Canada.

Due to the consolidated nature, most of the Utah bituminous sand deposits are amenable to conventional size reduction methods. Crushed and size classified bituminous sand samples of Tarsand Triangle exhibit free-flowing properties. With increasing bitumen content of the sample, for example the Sunnyside sand, the size reduction becomes more difficult. In addition, the free-flowing or rheological properties of the sand decreases with increasing bitumen content of the sand. Other factors which influence the rheological behavior of the crushed and size classified bituminous sand samples include temperature and time duration while handling.

The size distribution of the sand in the bituminous sands is an important consideration in the surface recovery methods. A high percentage of fines in the bituminous sand feed would result in an increased amount of sand fines in the bitumen froth during hot water extraction processes, while a high percentage of fines in the feed would require better sand fines collecting equipment in the thermal recovery methods. Carrigy(44) classified the Canadian bituminous sands into three self-defined categories based on the size distribution of the sand and found that the amount of sand fines (less than Tyler 325 mesh) was inversely correlated with the bitumen content of the Athabasca deposit of the McMurray formation. Sepulveda(47) reported the size distribution of bituminous sands from four major deposits of Utah and his results indicate the absence of any relationship between the fines content and the bitumen saturation of the deposit. The amount of sand fines in the Utah deposits is generally small compared to the Canadian bituminous sands(48).

Information on the composition of the mineral matter for the various bituminous sand samples is not available. However, Shea and Higgins(49) have qualitatively reported the composition of mineral matter found in Asphalt Ridge and Sunnyside bituminous sands. The mineral matter in Asphalt Ridge bituminous sand is mainly clear quartz and dark-gray quartzite; while the mineral matter in Sunnyside bituminous sand consists of quartz with small amounts of muscovite and chalcedony. Also, Shea and Higgins(49) noted the absence of ferromagnesian minerals in Sunnyside bituminous sands. The bituminous sands of Utah contained no clay and silt, but the presence of clay and silt has been reported in Canadian sands(45). The composition of the mineral matter in Canadian sands indicates about 99% of the bituminous sand mineral matter consists of quartz grains and clay minerals. The remaining 1% contains over twenty-five ferromagnesian minerals. The presence of clay and silt in the Canadian bituminous sands requires large settling ponds in the hot water extraction process because in water, clays tend to form stable emulsions(45,50).

The bulk properties of Utah bituminous sands vary significantly from the Canadian bituminous sands. The estimated bulk properties of Utah bituminous sands(17-19,31-36,51) and Canadian bituminous sands(44,45) are presented in Table 1.5. It is evident that most of

Table 1.5

Bulk Properties of Utah and Canadian Bituminous Sand Deposits[a]

Deposit	Sample[b] Type	Porosity (% volume)	Air Permeability (millidarcies)	Bitumen Saturation (% P.V.)	Water Saturation (% P.V.)	Bulk Density (g/cc)
Asphalt Ridge	C	19 - 31	5 - 745	51 - 71	2.7	1.9 - 2.03
Asphalt Ridge (N.W.)	C	23	603	45	20	NA
P. R. Spring	C	7 - 37	0 - 6954	1.0 - 91.0	3.0	NA
Sunnyside	C	21 - 30	154 - 729	45	NA	NA
Tarsand Triangle	C	20 - 35	2 - 3200	21 - 71	NA	NA
	S	20	207	6.0	NA	NA
Athabasca (Canada)		65	0 - 215	34 - 98	1 - 39	1.9

Notes: [a] References 17-19, 31-36, 44, 45, 51.

[b] C refers to core sample and S refers to surface sample.

NA - not available.

the Utah deposits have low porosity but higher air permeability compared to the Canadian sand. The higher air permeability would permit the establishment of a better communication path between injection and production wells and should enhance the bitumen recovery by in-situ processes.

The behavior of lumps of consolidated bituminous sand samples of Utah upon heating is different from the bituminous sands of Canada. Lumps of Canadian bituminous sands became free flowing sand after being debituminized, when heated in a muffle furnace at 773 K. Similar observations were made by Oblad(52). On the other hand, the lumps of Sunnyside and Tarsand Triangle bituminous sand samples, ranging in size from 1.5 to 4.0 cm, would not disintegrate after being debituminized when subjected to heat in the muffle furnace at 773 K. This indicates that the sand grains in the Utah deposits are fused together and possess higher mechanical strength compared to the Canadian bituminous sands. The stability of Utah samples should be given serious consideration in processing lumps of bituminous sands in an above ground thermal recovery porcess using a fluidized bed technique, where higher flow rates of fluidizing gas would be required with large diameter particles.

1.6 Nature of Bitumen in Bituminous Sands

The bitumen in the bitumen-sand mixture is highly viscous in its natural state. The interfacial bond between the sand and the bitumen is related to the physical and chemical properties of the raw bitumen. Considerable differences and similarities exist in the properties of the bitumens from different deposits. In all studies, the bitumen samples were obtained by solvent extraction of the particular bituminous sand under study. Various solvents such as benzene or toluene, aqueous solvents(50) and chlorinated solvents(53) have been used for the extraction of the bitumen.

The density of the extracted Canadian bitumen was 6 - 10 °API at 290 K indicating that the bitumen is heavier than water and normal crude oils. Camp(45) reported that the density of the Canadian bitumen exhibited an inverse relationship with increasing temperature in the temperature range 290 - 420 K. The density of the Canadian bitumen was dependent upon the source of the deposit and the location of the sample within the deposit. Similar conclusions can be drawn from the work of Wood and Ritzma(46) who reported the bitumen densities of various Utah deposits. The densities of Venezuelan bitumen fall in the same range as for the Canadian bitumen.

Although the densities of bitumens from Canada, Utah and Venezuela are similar, marked differences exist in the viscosities of these bitumens. Moreover, the high viscosities are responsible for the difficulties encountered in recovering the bitumen by conventional primary petroleum recovery methods. Bowman(50) and Camp(45) have summarized the work of several investigators on the viscosity of Canadian bitumen. The viscosities of various Canadian bitumen samples increased with increasing specific gravities of the bitumen(44). However, no correlation exists between viscosities and specific gravities for the Utah bitumen samples. The studies of Misra and Miller(54), Sepulveda(47) and Bunger, et. al.(55) indicated that the viscosities of the bitumens from the northern bituminous sand deposits (Asphalt Ridge, P. R. Spring, Sunnyside deposits) were higher then the viscosity of the bitumen from the southern deposit (Tarsand Triangle). Rojas, et. al.(56) have reported the viscosities of the bitumen of the Orinoco tar belt. The viscosities of the bitumens from different locations varied between 11,000 - 234,000 centipoises at 300 K but showed a decreasing trend with increasing temperature. A substantial reduction in the viscosities of the bitumens was observed when normal crude oils from the region were used as a diluent. The viscosities of bitumens from the northern deposits of Utah were one to two orders of magnitude higher than Canadian and Venezuelan bitumens indicating no relationship exists between the viscosity and the grade of the bituminous sands (Figure 1.3). While the viscosity studies on the Canadian and Utah bitumens predict the Newtonian behavior, the bitumen from eastern Venezuela exhibited a non-Newtonian Bingham Plastic type, behavior. The high viscosities of the Utah bitumens were related to their molecular weight(55). Generally, the molecular weights of the Utah bitumens were much higher than the Canadian bitumen. The molecular weight of Utah bitumens was in the range of 660 - 900, while the molecular weight of Canadian bitumens was between 540 - 600(45,50,54,55). Information on the molecular weight of Venezuelan bitumen was not available in the literature and could not be compared with Utah and Canadian bitumens.

The distillation characteristics and the elemental analysis of the bitumen from different bituminous sand deposits have been investigated. Excellent reviews on the studies conducted on Canadian bitumens have been reported by Camp(45) and Bowman(50). Wood and

Figure 1.3

Effect of Temperature on the Viscosity
of Bitumens

Source: References 45, 47, 54, and 56.

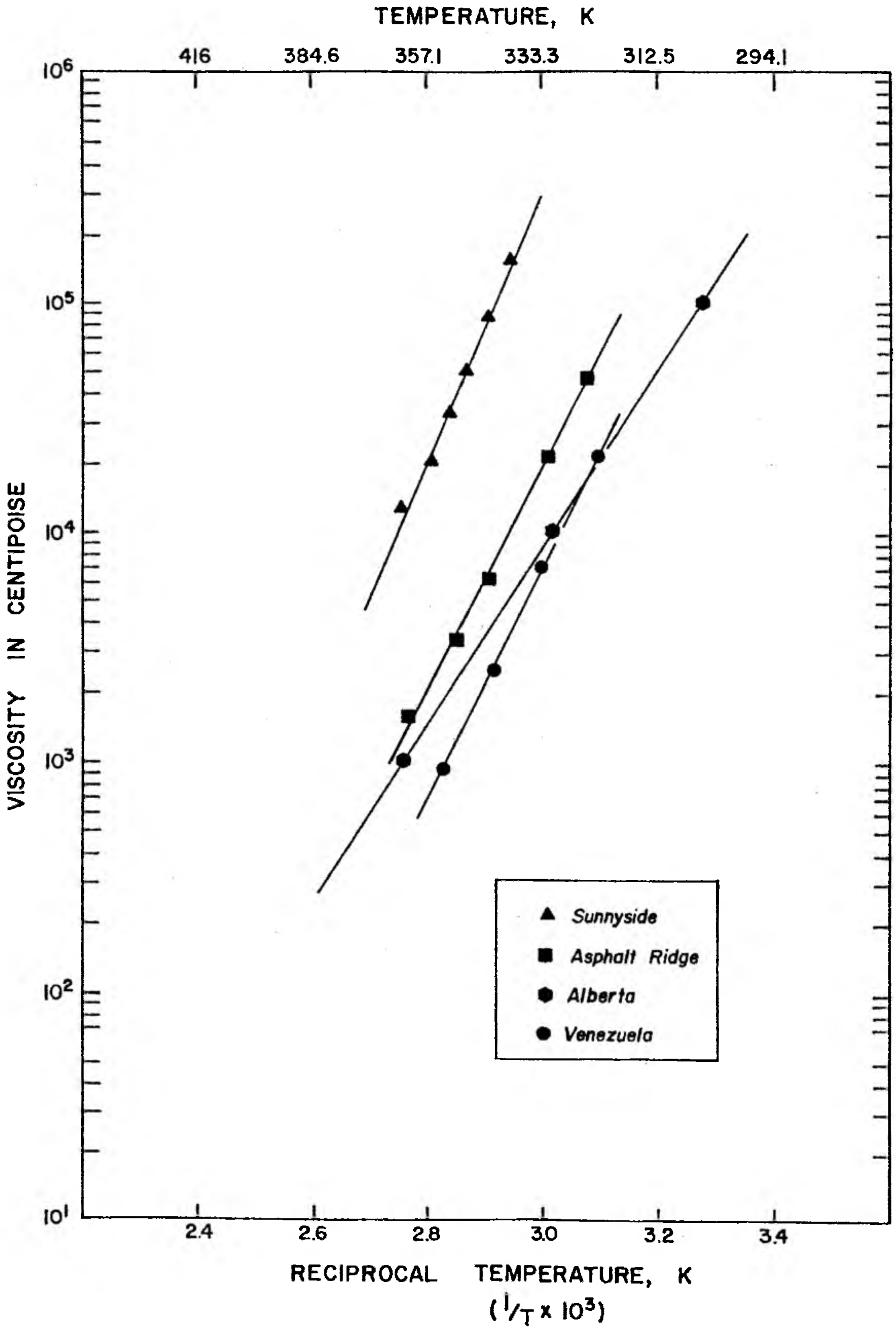
TEMPERATURE, K
416
384.6
357.1
333.3
312.5
294.1
10^6
10^5
10^4
10^3
10^2
10^1
VISCOSITY IN CENTIPOISE
2.4
2.6
2.8
3.0
3.2
3.4
RECIPROCAL TEMPERATURE, K
($^1/_T$ x 10^3)
▲ Sunnyside
■ Asphalt Ridge
⬢ Alberta
● Venezuela

Ritzma(46) and Wenger, et. al.(57) have reported the elemental composition and ASTM distillation data on the Utah bitumens, while Bunger, et. al.(55) have compared the boiling point distributions of various Utah bitumens with the Athabasca bitumen using the simulated distillation procedure(58). The simulated distillation curves of Utah bitumens indicate that only between 30 - 45 weight percent of the bitumen is distillable to an end point of 811 K, while the distillation data for the Canadian bitumen indicate that 50 weight percent of the bitumen is distillable to an end point of 811 K(55). The higher distillate yields obtained in the ASTM distillation data(46) compared to the yields from the simulated distillation data might be attributed to the thermal cracking taking place during the distillation. The elemental compositions of Utah bitumens indicate that the bitumens of the northern or Uinta Basin have a higher hydrogen content compared to bitumens from Tarsand Triangle and Athabasca deposits. Bunger(59) classifies the Utah and Canadian bitumens into two groups based on the geochemical origin of the bitumen: group I consisting of all northern deposits of Utah, that is, Asphalt Ridge, P. R. Spring, and Sunnyside deposits; group II consisting of Tarsand Triangle (Utah) and Athabasca (Canada) deposits. The bitumens of group I were of fresh or brackish water origin, while the group II bitumens were of marine origin. The following conclusions can be drawn from these studies: (i) the lower distillate yields of Utah bitumens compared to the distillate yield of Athabasca bitumen were related to the high viscosities and higher molecular weight of Utah bitumens, and (ii) significant differences in the hetero-atom contents were observed between the bitumens of the

Uinta Basin, Utah and bitumens of southern Utah, Canada and Venezuela. The Uinta Basin bitumens have low sulfur concentrations (less than 1% by weight), while the bitumens of Tarsand Triangle, Athabasca and Venezuela contain 3 - 5% by weight sulfur. The high sulfur content of these bitumens was related to the marine origin(7). Also, the high sulfur bitumens have been observed to contain higher metal impurities. The high sulfur content and high metal impurities in the bitumen would require preliminary processing steps to lower the metal impurities and sulfur content before conventional refining methods could be employed for upgrading the bitumen to produce the synthetic crude.

The chemical composition of the bitumen has been studied to explain the interfacial bonding extant between the bitumen and the sand. The chemical composition of the bitumen will also dictate the compatability of the bitumen and the synthetic crude derived from the bitumen with conventional petroleum crude. Knowledge of the composition of the bitumen could be used to elucidate the reaction pathways of different primary upgrading processes for bitumen(60). A brief summary of the available literature is presented here.

The chemical composition of the bitumen has been studied by subdividing the bitumen by solvent separation followed by detailed analysis of the fractions. A historical summary of the earlier investigations on the chemical composition of Canadian bitumen has been published by Bowman(50). In most of the studies with Canadian bitumen, the bitumen was separated into oils, resins and asphaltenes(61-64). The results indicate the following average composition of the bitumen: oils 61%, resins 22%, and asphaltenes 17%.

Minor variations in the amount of the fractions have been observed depending upon the solvents used in the separation. Ruberto, _et. al._(65) have reported a comparative study of the chemical composition of Canadian bitumen with synthetic liquids derived from coal and oil shale. Their study indicates that in samples of the same boiling range but from a different fossil fuel source, the amount of asphaltenes and resins were higher for coal and shale liquids, while the bitumen contained a relatively higher percentage of saturates. Bunger, _et_. _al_.(55) have reported the composition of Utah and Athabasca bitumens based on functional groups. The bitumens from Asphalt Ridge, P. R. Spring, Tarsand Triangle and Athabasca were separated into five major fractions, that is, acids, bases, neutral nitrogen bases, saturated hydrocarbons and aromatic hydrocarbons, according to USBM-API 60 scheme(66). The principal functional groups of each fraction were identified. The analyses indicate the percentage of non-hydrocarbons (acids + bases + neutral nitrogen bases) based on 100% bitumen is higher for high sulfur bitumens (Tarsand Triangle, Athabasca) than for the low sulfur bitumens of the Uinta Basin, Utah (P. R. Spring, Asphalt Ridge). The total hydrocarbon content in all the samples was in the range of 50 - 60% of the bitumen. However, the aromatic hydrocarbon content in high sulfur bitumens was higher than the aromatic hydrocarbon content in low sulfur bitumens. In addition, the saturated hydrocarbon content (26 - 28 weight percent) is comparable to the aromatic hydrocarbon content (25 - 27 weight percent) in the Uinta Basin bitumens.

CHAPTER 2

RECOVERY OF BITUMEN OR PRODUCTION OF SYNTHETIC CRUDES FROM BITUMINOUS SANDS

This chapter discusses the development of the extraction or separation technology required for the production of bitumen or a synthetic liquid from bituminous sands. Prior to reviewing the various extraction methods, it was deemed appropriate to present a brief discussion regarding the interest in the commercial development of bituminous sand deposits and the factors controlling the choice of recovery methods. The price of synthetic liquid produced from bituminous sands by any of the recovery schemes should be comparable with the price of petroleum crude in order to provide an economic incentive in developing these alternate fossil fuels. Also, the capital investment requirements for any new recovery scheme should be compared to the capital investment for the existing operations such as Great Canadian Oil Sands Ltd. (GCOS) process and/or Syncrude Canada Ltd., process for capital investment.

The emphasis in reviewing the literature was placed on the above ground thermal recovery schemes in keeping with the major objective of this research study.

2.1 Interest in Commercial Development of Bituminous Sands

The prime commercial use for extracted bitumen or for the high grade bituminous sands prior to 1967 was as road paving material. The production of bituminous sands derived synthetic liquids commenced in 1967 when the GCOS project was brought on stream. The passage of Canadian bituminous sand development programs from the laboratory to the commercial plant has been extensively reported in the literature. Unfortunately, only a limited number of programs has been initiated in the United States aimed at the production and utilization of synthetic liquids derived from bituminous sands. However, the rapid escalation of petroleum crude prices since the 1973 oil embargo by the Organization of Petroleum Exporting Countries (OPEC) has focused considerable attention on bituminous sands as an alternative energy resource.

Commercial processing of bituminous sands is being carried on only in Canada among the non-communist countries having bituminous sand deposits. The GCOS Ltd. operation processes 120,000 tons of bituminous sand per day to produce 58,000 barrels per day of synthetic crude(67,68). The processing scheme is based on the extraction of the bitumen by the hot-water process followed by delayed coking of the bitumen to obtain the synthetic crude. The second commercial scheme based on hot-water extraction technology is operated by Syncrude Canada Ltd. and has a rated capacity of 129,000 barrels per day(69). The plant started in 1978 has been operating at 50% capacity due to technical problems in one of the two parallel processing trains. The selling price of the synthetic crude per barrel produced at the site is $17 - $18 (1979 Canadian dollars), which is comparable with the current crude oil price. McMillan(70) discussed the capital requirements and the capacities for the current and planned bituminous sand projects. A summary of McMillan's analysis is presented in Table 2.1.

Surface mined recovery processes like Syncrude are economical for bituminous sand deposits with an overburden to payzone ratio of 1.0 to 1.5. On the other hand, in-situ recovery processes appear to be attractive for deeper bituminous sand deposits, for which mining methods become uneconomical due to the large amount of overburden to be removed. The factors influencing the choice between the above ground and in-situ recovery methods are discussed in section 2.2.

2.2 Factors Influencing the Choice of Recovery Methods

A feasible synthetic crude recovery process applicable to bituminous sands must be able to separate the bitumen or bitumen derived synthetic crude from the sand matrix. The choice of a suitable recovery technique will depend upon the following:

(i) the extent of the bituminous sand deposit
(ii) the thicknesses of the overburden and the bituminous sand zones
(iii) the bitumen content of the sand
(iv) the ratio of overburden to bituminous sand zones, and
(v) the nature of mineral matter associated with the sand.

In addition to these deposit-specific factors, geographical location

Table 2.1

Existing and Proposed Commercial Bituminous Sand Projects in Canada[a]

Company	Project Size Syncrude (BPCD)	Method of Processing	Capital Cost per Barrel of Daily Capacity (Current U.S. dollars)	Start-up Date
Great Canadian Oil Sands Ltd.	58,000	Mining	4,400	1967
Syncrude Canada, Ltd.	129,000	Mining	19,400	1978
Imperial Oil Co.	145,000	In-situ	32,900	1985
Alsands Mining Project	140,000	Mining	35,000	1987
Shell Canada	100,000	Mining	-	1982

Note: [a] Adapted from McMillan(70).

and climatic conditions will influence the selection of the recovery scheme. Among the above, the critical factors are the overburden to bituminous sand zones ratio, the size of the deposit, and the bitumen content of the sand. Camp(45) discussed in detail the effect of these factors for the Canadian bituminous sand deposits. According to him, the overburden thickness of Athabasca deposits vary from 0 - 600 meters (0 - 2000 feet) and the average thickness of the bituminous sand pay zone is 45 meters. The economic ratio of the overburden to bituminous sand zone thicknesses for surface mined recovery method is about 1.0 to 1.5, which indicates that 15% of the total Canadian reserves is amenable for current mining methods. The remaining 85% has to be recovered by in-situ methods. The weight percent of bitumen in the sand is also important from the view point of selecting the method of recovery. The quantity of bituminous sand to be mined per barrel of synthetic crude increases with decreasing bitumen content. For example, Syncrude does not process bituminous sands below six weight percent bitumen content in the hot-water extraction process.

The overburden thicknesses of northern deposits of Utah vary from 0 - 150 meters, while the overburden thickness of the Tarsand Triangle deposit varies from 0 - 500 meters(31). Moreover, most of the Utah deposits exhibit multiple bituminous sand pay zones. There is no information in the literature regarding the economic ratio of the overburden to bituminous sand zone ratio for surface mined recovery methods for the Utah deposits. Furthermore, the percentage of the total bituminous sand reserves of Utah amenable for current mining methods has not been determined. However, Glassett and Glassett(71) have classified the major deposits of Utah according to their suitability for mining methods. According to Glassett and Glassett(71), the Sunnyside and Tarsand Triangle deposits are most favorable for surface mined recovery processes.

The extraction of the bitumen or production of synthetic crude from bituminous sands can be carried either by in-situ recovery schemes or by surface mined above ground separation schemes. Each category can be subdivided according to thermal energy requirements of the recovery scheme. The potential in-situ and above ground separation schemes are presented in Table 2.2.

2.3 In-situ Recovery Schemes

In spite of the lower percent recovery of bitumen compared to the above ground recovery schemes, the ability of in-situ recovery schemes for recovering the bitumen from the unminable bituminous sand deposits make them attractive. The viscous nature of the bitumen makes it immobile and non-recoverable by conventional techniques. The lack of reservoir energy does not permit the application of conventional primary recovery methods that are used in the recovery of petroleum crude. In the primary recovery of crude from petroleum reservoirs, the reservoir energy diminishes with production over a period of time, thus an outside or external stimulant is required to compensate for the loss of natural energy. In secondary and tertiary recovery schemes for crude petroleum, the external stimulant is usually usually steam/water or compressed high pressure gases. The low temperature in-situ schemes applied to the recovery of bitumen from the bituminous sand deposit are either direct or modified versions of

Table 2.2

Bitumen and/or Synthetic Liquid Recovery Schemes

- In-situ Recovery Methods
  - A: Low Temperature Operations
    1. Emulsion-Steam Drive Process
  - B: High Temperature Operations
    1. Partial Oxidation Processes
    2. Combination of Combustion and Water Flooding Processes
- Surface-Mined Above Ground Recovery Methods
  - A: Low Temperature Operations
    1. Solvent Extraction Processes
    2. Cold Water-Solvent Extraction Processes
    3. Hot Water-Solvent Extraction Processes
  - B: High Temperature Operations
    1. Fluidized Coking Processes
    2. Non-Fluidized Direct Coking Processes

the secondary and tertiary recovery schemes applied to crude petroleum.

The lack of natural mobility of the bitumen in bituminous sand deposits is due to the low API gravities and the high viscosities of the bitumen. The other characteristic features of bituminous sand reservoirs such as their inhomogeneity, variations in porosity, low to moderate permeability within the reservoir also make the recovery of bitumen difficult. The main objective of the in-situ recovery methods is to improve the mobility of the bitumen or heavy oils by decreasing the viscosity. The viscosities of bitumen and heavy oils can be reduced by the use of chemical solvents or the injection of high pressure gases, both of which are expensive. Instead, water/ steam injection and partial oxidation techniques are more economical and have been successfully applied to the recovery of the bitumen or production of synthetic crude.

The in-situ recovery schemes will have to meet the following requirements:

1. establishment of a communication path between the production and injection wells through the bituminous sand deposit,
2. necessary pressure gradients between the wells for introducing the external stimulant through the injection well to increase the mobility of the bitumen and for withdrawing products from the production well,
3. reservoirs will have to be mapped for bitumen saturation, depth, continuity, permeability, porosity variations, areal extent of the deposit to facilitate proper design and operation of an in-situ recovery scheme.

In addition to these requirements, devices to determine the pressure and the flow rate requirements for the injected retorting fluids and the temperature of the combustion zone are necessary to monitor the progress of the recovery process employed.

Apart from its ability to recover the bitumen from deeper bituminous sand deposits, in-situ recovery methods have other distinct advantages which have been outlined by Decora and Schrider(72), that is, (i) little or no mining is required thus eliminating hauling, crushing and above ground processing; (ii) land requirements and land disruptions are minimized; (iii) fewer people are required to operate an in-situ operation; (iv) waste disposal is greatly reduced; and (v) health and safety hazards are lessened.

Further descriptions of each in-situ scheme are presented below.

2.3.1 Emulsion-Steam Drive Process

The emulsion steam drive recovery of bitumen is similar to secondary recovery of petroleum crude using water. The basic concept of an emulsion steam drive process is the formation of a bitumen-in-water emulsion (20 - 30% bitumen) by steam injection. The viscosity of this emulsion is almost equal to that of water rendering the bitumen recoverable through a well bore. The injection of steam increases the reservoir temperature with a concommitent decrease in the viscosity of the bitumen or heavy oil thus facilitating the formation of an emulsion. The bitumen recovered is generally in the range of 25 - 30% of the total resource in place. The steam generation is commonly carried out on the surface and is pumped through the injection wells into the bituminous sand reservoir. Recently, Bader, et.

al.(73) have reported methods of generating steam deep in the reservoir face and the results obtained in the pilot-plant studied indicate the process may have future applications.

Many of the surface generated steam drive processes are being used in the recovery of bitumen or heavy oil of Venezuela, Canada, and the United States. All of the different processes are at the demonstration plant stage, however, each has promising commercial potential. Because a number of articles have been published on the steam drive recovery of bitumen from Canadian deposits(45,74-77), and extra-heavy oil deposits of Orinoco tar belt, Venezuela(77), however, it is not possible to review all of them in this report. A number of reviews(78,79) dealing with the status of various in-situ processes for the recovery of bitumen from bituminous sands of Alberta have been published. A number of papers on steam drive in-situ schemes were presented at the First International Conference on the future of Heavy Crude and Tarsands (1979) held in Edmonton, Alberta, Canada. Among the various pilot-plant in-situ processes, two were chosen as representative of the different approaches because both of them were on the threshold of being commercialized.

The in-situ oil extraction from Cold Lake deposits, Canada, by steam injection, developed by Imperial Oil Ltd.(80), uses high temperature steam at 593 K and 14 MPa pressure. The Cold Lake bitumen has an API gravity ranging from 9 - 11 and is lighter than the Athabasca bitumen. A five-spot pattern with the production wells on the corners of the square and the injection well at the center of the square was employed. Steam was injected for four to six weeks (huff), later the bitumen was pumped from the wells for as long as six months (puff) and, therefore, this process is often referred to as the "huff and puff" process. Imperial Oil plans to recover 1.5 billion barrels of the seven billion barrels of bitumen in place. This process has been licensed for commercial production in 1985 with a capacity of 145,000 barrels per day.

The second process, operated by Shell Canada Ltd., is being used for the extraction of Athabasca bitumen in the McMurray formation(79). The process uses a combination of caustic solution and steam drive approach. The caustic solution used appears to displace the bitumen and the injected steam decreases the viscosity enabling the bitumen to be pumped out from the ground. The field experiments were conducted using a five-spot pattern of wells (four injection wells at the four corners of a square with a producing well located at the center) and the communication between the production and injection wells was established through a horizontal fracture in the reservoir. In the pilot-plant operations, according to Shell Canada Ltd., the steam consumption was 0.685 tons per barrel of bitumen recovered. Based on the results obtained in the pilot-plant operations, Shell hopes to recover 50 - 70% of the oil-in-place in its commercial operation.

The application of the steam injection technique to Utah deposits has had limited success due to the high viscosity of the bitumen. Thurber and Welbourn(81) have reported the pilot-plant in-situ recovery of bitumen from the Sunnyside deposit. This process, operated by Shell Oil Co., and operated intermittently, used 70 - 80% quality steam at pressures in the range of 2050 - 4033 kPa. The pilot-plant was abandoned because of low production rate of crude due to high viscosity of the bitumen and the thief characteristics of the natural reservoir fracture system.

The economic viability of the in-situ recovery of bitumen using steam injection depends upon a number of factors, in particular the steam requirement per barrel of oil recovered. Theoretically about 0.5 tons of steam is required per barrel of oil recovered assuming 100% efficiency(79). However, in practice, the steam requirements increase due to the loss of thermal energy; the inefficient communication between injection and producing wells; the slumping of the sand structure during the recovery operation leading to obstruction of the communication between the injection and the producing wells; and the cooling of the hot unemulsified bitumen before it arrives at the production well could disrupt the communication between the wells(82). The use of chemical additives with steam injection has been studied to evaluate the performance of chemical additives in lowering the interfacial tension between bitumen and sand, thereby increasing the oil recovery. Shell Canada Ltd. uses sodium hydroxide as chemical additive with steam injection and the pilot-plant results have indicated 50 - 70% of the bitumen-in-place can be recovered compared to 25 - 30% recovery in the direct steam flooding process. The use of chemical additives also helps in preventing the disruption of the communication between injection and producing wells(83).

2.3.2 Partial Oxidation Recovery Processes

The partial oxidation recovery processes are often referred as fire-flooding thermal methods. These high temperature *in-situ* recovery processes consume a portion of the in-place bitumen to supply the thermal energy needed to reduce the viscosity of the bitumen. The bitumen is consumed in the combustion zone fed by injected air. Moreover, mild thermal cracking of the bitumen occurs yielding a less viscous synthetic liquid. Two types of partial oxidation or partial combustion in-situ processes have been proposed: (i) forward combustion, and (ii) reverse combustion (Figure 2.1). The difference between these two operations is that in forward combustion the flame front and the released hydrocarbon vapor move in the same direction, but in reverse combustion the movement of flame front opposes the flow of the hydrocarbon vapor. The fuel source in the forward combustion scheme is a coke-like residue which was deposited on the sand when the bitumen was thermally decomposed to produce the synthetic crude. The bitumen itself serves as the fuel source in the reverse combustion scheme. In reverse combustion the hydrocarbon vapors pass through the heated portion of the reservoir to the production well minimizing plugging of the pores. In forward combustion, the hydrocarbon vapors move through the unheated portion of the reservoir to the production well. The passage of the vapor through the colder region of the reservoir can cause condensation of the vapor which, in turn, can lead to plugging of the communication path between the combustion/production zone and the production well bore. Consequently, the majority of the fire-flooding processes use reverse combustion.

Limited information has been published on the recovery of the bitumen or synthetic crude using fire-flooding techniques due to the proprietary nature of the processes, however, numerous articles

Figure 2.1

Types of Fire Flooding Schemes

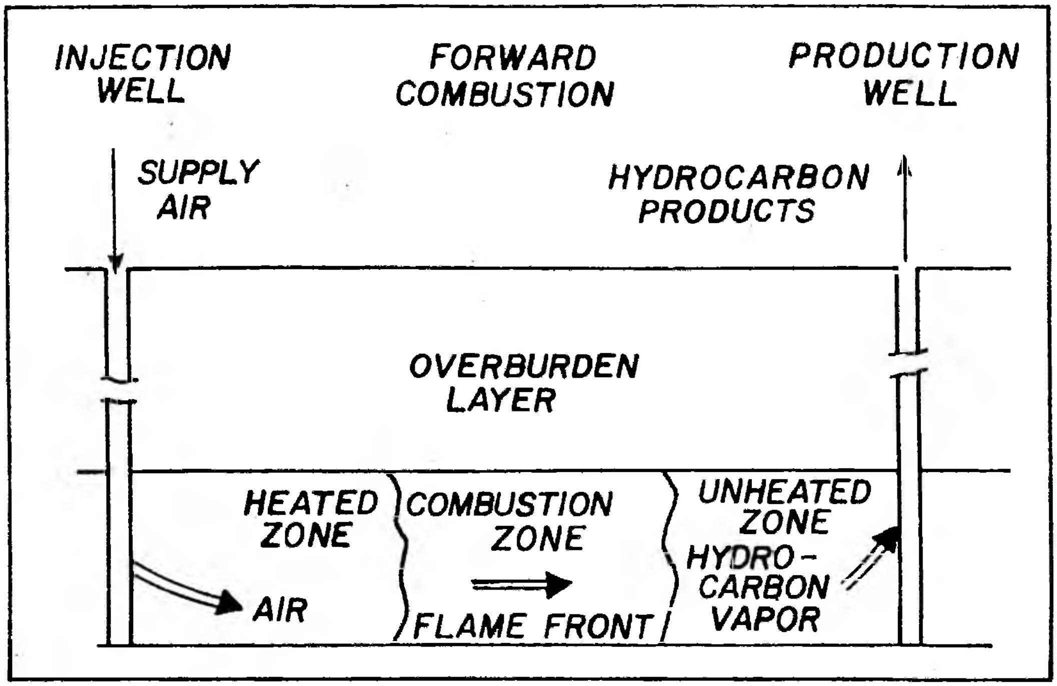
INJECTION WELL
FORWARD COMBUSTION
PRODUCTION WELL
SUPPLY AIR
HYDROCARBON PRODUCTS
OVERBURDEN LAYER
HEATED ZONE
COMBUSTION ZONE
UNHEATED ZONE
HYDRO-CARBON VAPOR
AIR
FLAME FRONT

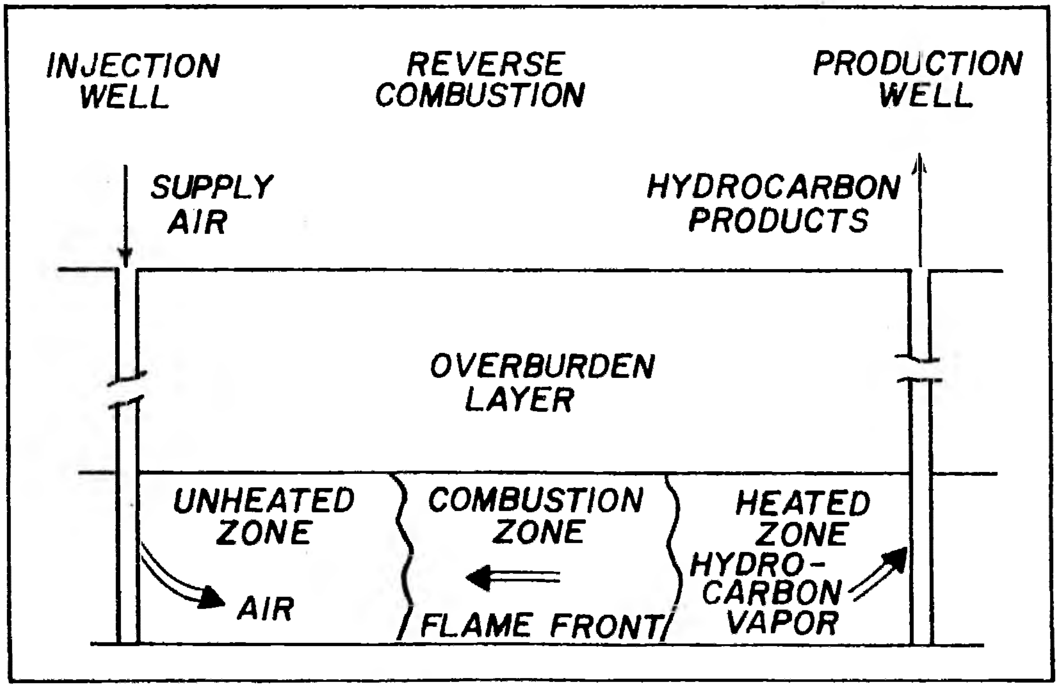
INJECTION WELL
REVERSE COMBUSTION
PRODUCTION WELL
SUPPLY AIR
HYDROCARBON PRODUCTS
OVERBURDEN LAYER
UNHEATED ZONE
COMBUSTION ZONE
HEATED ZONE
HYDRO-CARBON VAPOR
AIR
FLAME FRONT

reporting the results of the laboratory studies supporting these field experiments have been published. Perry, et. al.(84) have discussed briefly the differences in the operating variables affecting the performance of both forward and reverse combustion schemes. The laboratory studies include both theoretical(85-87) and experimental analyses(88,89) of a range of process variables. The conclusions as summarized by Reed and Reed(90) were as follows: (i) the average peak temperature can be adequately represented as a function of air flux alone and increasing the air flux increases the peak temperature; (ii) the heat loss decreases the rate of advance of the combustion zone; (iii) the oil recovery for reverse combustion type varied with air flux, with a maximum oil recovery of nearly 50% for an air flux in the range of 35 - 40 scf/hr-ft^2; (iv) when the air flux was below the optimum value, the oil was left in the reservoir along with the coke. The oil can be recovered by forward combustion following the reverse combustion, but still the total recovery remained constant.

Among the pilot-plant operations being conducted at present, information is available on the field experiments conducted by the Laramie Energy and Technology Center (LETC), Wyoming, on the Asphalt Ridge deposits of Utah. Two field experiments were conducted using reverse combustion. In the first test, the fire channeled through the deposit and did not heat the deposit effectively(91). Johnson, et. al.(92) have reported the results of the second experiment, in which the reverse combustion was followed by forward combustion. The recovery of oil was only 25% at an air injection pressure of 2580 kPag.

Further field tests are planned and in the next test the recovery of bitumen using steam injection will be attempted(93).

2.3.3 Combination of Combustion and Water Flooding Processes

In the combined fire and water flooding processes, the temperature of the deposit is increased by fire-flooding using the forward combustion technique, after which water is injected along with air. The amount of water injected with air is controlled to lower the peak temperature of the combustion zone and coke-like material is left behind as the combustion front moves towards the production well. The injected water accelerates the rate of advance of the combustion front and the steam generated moves ahead to spread the heat uniformly and helps in driving the synthetic crude to the production well. In addition, the amount of bitumen consumed as fuel is reduced and the percentage of oil-in-place recovered is higher than when no water is injected.

The combination of forward combustion and water flooding process (COFCAW), developed by Amoco Canada Ltd., is the only pilot-plant process being carried out on the Athabasca deposits. The project, still continuing, consists of a five-spot pattern of wells with four wells drilled at the corners of a square and the injection well drilled at the center(94). Combustion is initiated at the center well as air is injected at pressures high enough to fracture the bituminous sand zone. After fracturing has been achieved and the temperature of the deposit has reached a peak value of about 620 K, the pressure is decreased and the water is injected together with air. The water lowers the combustion temperature and the steam thus generated moves ahead of the combustion front and spreads the heat to the formation on a broader front. The steam improves the effectiveness of extraction and a recovery of 50 - 55% of the oil-in-place is feasible with an in-situ combustion process with steam injection, while only 7 - 8% of the bitumen is consumed for energy requirements.

2.4 Surface-Mined Aboveground Recovery Methods

The surface-mined above ground recovery of bitumen methods are complex processing schemes which include a sequence of individual but fully integrated processes. The factors involved in the selection of surface-mined above ground recovery methods were discussed in Section 2.2. Though the hot-water extraction technique has been proven commercially viable for the extraction of bitumen from Athabasca bituminous sands, its earlier success, perhaps, is specific to the deposits because of the physical arrangement of the bituminous sand (Chapter 1). The need for a process to be competitive with the hot-water extraction method has resulted in numerous laboratory and pilot-plant studies using different extraction techniques. These studies are classified into two main groups, namely low temperature operations and high temperature operations, and are further sub-classified as shown in Table 2.2. Prior to discussing the various recovery methods, it is important to address briefly the problems that might be encountered in other phases of the integrated process such as mining of the bituminous sand and the disposal of spent sand either coked or burned clean.

All the surface-mined above ground recovery processes will have a number of common factors in the over-all operation, although the method of bituminous sand extraction might be different from process to process. These principal common factors have been outlined by McConville(78) as follows:

1. clearing and drainage of the mine area,
2. removal of the overburden and the inter-ore waste,
3. mining of the sands,
4. transportation of the sands to the process site,
5. construction of the tailings impoundment dikes,
6. reconstruction of the surface,
7. extraction of the bitumen from the sand,
8. separation of clay from the bitumen,
9. disposal of sand tailings,
10. reclamation of process water,
11. upgrading of the bitumen to produce a synthetic crude,
12. provisions for utilities-electric power and steam generation, water and fuel supply (if required)
13. provision for waste disposal and pollution control,
14. disposition of products - synthetic crude and other products (sulfur, excess coke).

The compilation of these factors is specific to the GCOS operation and to the Athabasca bituminous sand deposits. Some of the factors mentioned above may or may not be important for the Utah deposits, however, additional factors specific to Utah deposits may have to be considered.

The mining and conveying of the bituminous sand has been one of the critical operations at the GCOS and Syncrude plants. Due to large quantities of material handled, a number of mining problems are being confronted in both these plants. The high grade and the unconsolidated nature of the bituminous sand of the Athabasca deposit and the extreme variations in climatic conditions have led to problems such as the rapid and extreme wear of mining equipment, in particular, the bucketwheel excavators, the bituminous sand sticking to both mining and conveying equipment, and the dissolution of rubber in the conveyor belts by the bitumen during conveying. A chemical coating (proprietary information) is used to minimize the dissolution of rubber in the conveyor belts by the bitumen.

With Utah bituminous sand deposits located in rough, mountainous terrain, a combination of different mining methods, such as mountain-top removal, open-pit mining, and contour mining may be required for mining Utah bituminous sands(71). The mountain-top removal mining method appears to be more attractive for bituminous sand pay zones where the ratio of bituminous sand and overburden zones is less than 1.5. Open-pit mining may be used for bituminous sand zones located near the top of a canyon. Due to the consolidated nature of Utah deposits, drilling and blasting of both overburden and bituminous sand zones may be required in assisting the surface mining of Utah bituminous sands. Additionally, all consolidated bituminous sandstones except Asphalt Ridge would require size reduction before being processed.

The reclamation of the mined land is an important consideration common to the development of all fossil fuels. For example, one of the reasons impeding the development of oil shale and strip mining of coal in the western United States is the land reclamation. The development of industrial processes for the recovery of bitumen from bituminous sands depends upon the way the spent sand is disposed.

As indicated in Table 2.2, the recovery of bitumen or production of synthetic crude from the bituminous sand can be conducted at low temperature or at high temperatures. The product obtained in the high temperature processing is a liquid and will be referred to in this report as synthetic crude.

2.4.1 Solvent Extraction Processes

Perhaps the easiest method of recovering the bitumen at low temperature is by chemical solvent extraction. Generally, ideal separation between the bitumen and sand takes place and for this reason it is widely used for preparing samples in the laboratory for examining the nature of the bitumen.

A number of small scale field operations based on the solvent extraction technique have been undertaken for extracting Asphalt Ridge bituminous sands and have been summarized by Glassett and Glassett(71). Among the recent studies on solvent extraction of the Athabasca bituminous sand, the investigation by Exxon Engineering appears to hold the most promise. The dissolution behavior of Athabasca bituminous sand in low molecular weight paraffinic solvents at ambient temperature was investigated by Funk(95) in a laboratory scale to obtain the effective diffusional coefficients between the solvent and deasphaltened oil. The asphaltene fraction of the bitumen precipitated as small aggregates during the extraction and the particle size of these aggregates decreased with increasing molecular weight of the solvent. The amount of the asphaltene aggregates entrained at various liquid velocities was determined when the bituminous sand was extracted with a solvent in a fluidized bed type contactor. Based on the particle size distribution of the sand and the asphaltene aggregates, it appears that for a paraffinic solvent there is a range of liquid flow rates (0.5 - 1.0 cm/sec) which gives carry over of asphaltenes from a fluidized bed type contactor but does not entrain the sand.

Chemical solvent extraction methods, although simple, have several inherent disadvantages. A portion of the low molecular weight solvent, which is more expensive than the bitumen product, is lost when the spend sand is discarded after each extraction cycle. The size of the extraction and recovery vessels is large because of the large volumes of solvent needed per barrel of bitumen extracted, thus requiring high capital investments for process equipment. The operating cost will also be high due to the large volumes of solvent, thus making the over-all economics of solvent recovery processes unattractive.

2.4.2 Cold Water-Solvent Extraction Processes

The cold water-solvent extraction processes reported in the literature have been mostly applied to Athabasca bituminous sands. The objective behind the cold water extraction technique is to minimize the thermal energy requirements during the extraction step. Clark$^{(96)}$ has reported the extraction of Athabasca bituminous sand using tap water unassisted by solvent. The bitumen, separated from the sand, formed lumps and settled to the bottom of the extractor along with the spent sand. The bitumen lumps were found to contain sand particles enmeshed in it, thus resulting in the low recovery of the bitumen. Several investigators have conducted solvent aided cold water extraction and have reported better recovery of the bitumen. These investigations have been summarized by Perrini(97). Djingheuzian(98) has successfully operated a pilot-plant for extracting Athabasca bituminous sands using the solvent assisted cold water extraction method. Because of the use of solvent, the drawbacks of these processes are similar to solvent extraction methods.

2.4.3 Hot Water-Solvent Extraction Processes

The initial hot water scheme as applied to the extraction of bitumen from Canadian bituminous sands was developed by Clark(96) and was later modified by others(99,100). The hot water technique involves the conditioning of the bituminous sand with water in the presence of an alkaline wetting agent. The operating temperature is in the range of 355 - 372 K at near atmospheric pressures. At this temperature, the density of the bitumen is less than that of the water (Figure 2.2). Thus, the bitumen can be recovered in a flotation cell. The mechanism of bitumen displacement from the sand partilces during the hot water extraction is not yet well understood. A number of investigators(50,101,102) have attempted to explain the bitumen displacement based on the thermodynamic equilibrium of surface energies between the different phases in the sand-bitumen-water system. Accordingly, the total free energy of the system should decrease during bitumen displacement from the sand particle. However, this thermodynamic approach

Figure 2.2

Temperature Dependence of Water
and Bitumen Densities*

Athabasca Bituminous Sand

---

*Source: Camp(45)

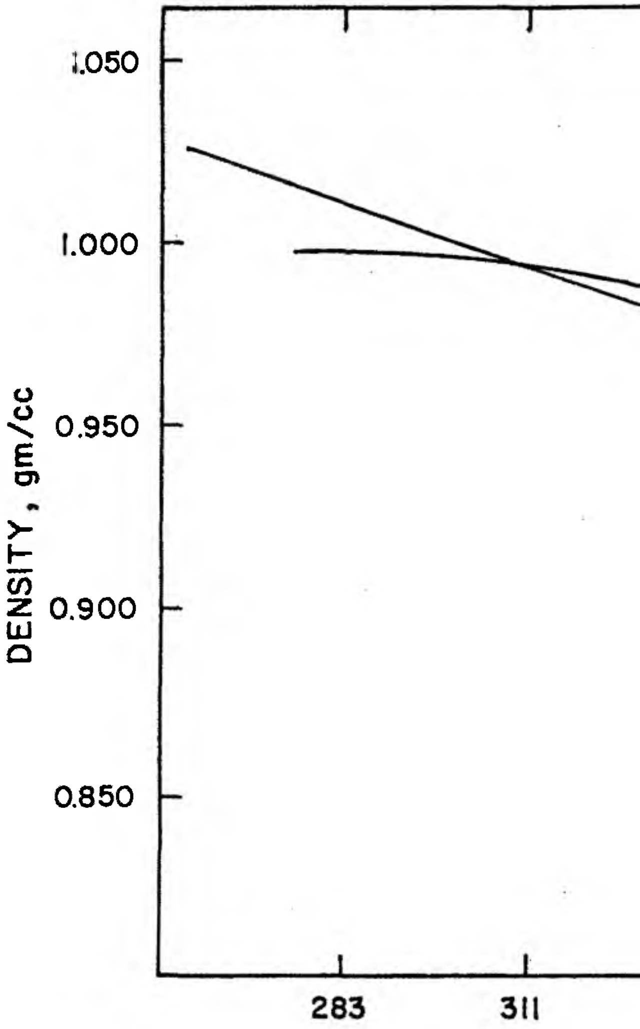
DENSITY, gm/cc
1.050
1.000
0.950
0.900
0.850
283
311

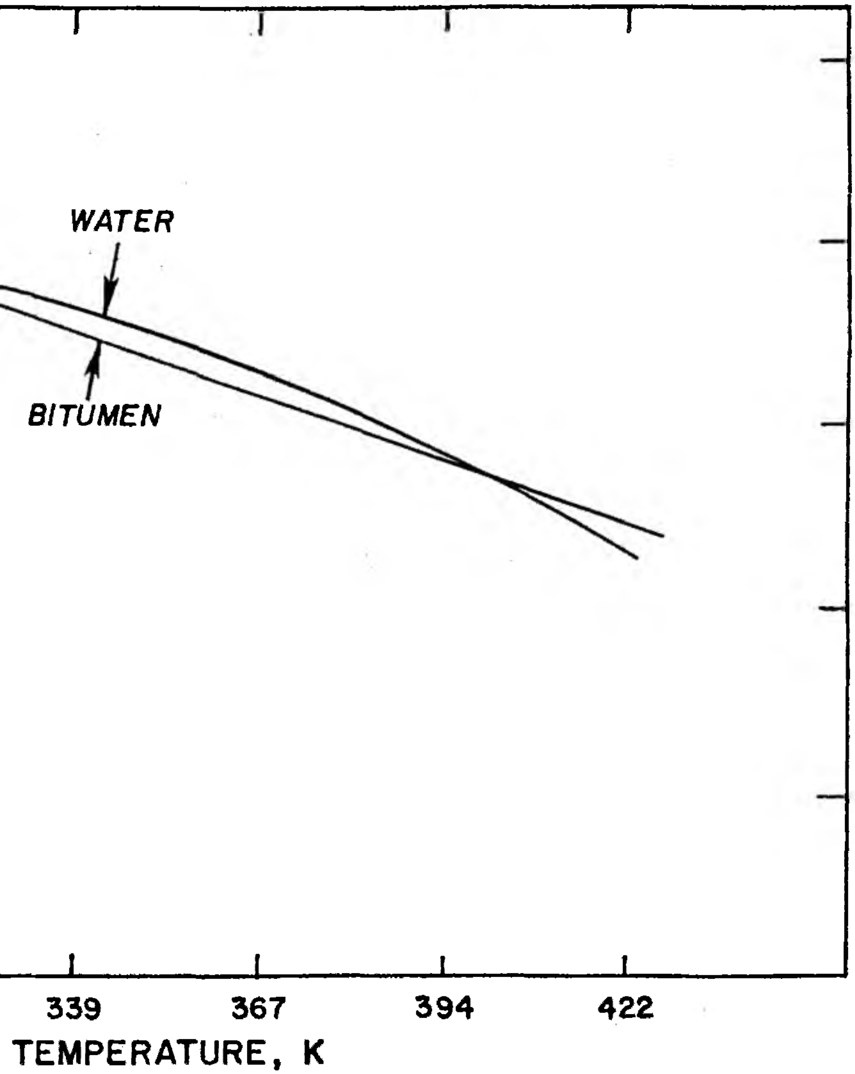
WATER
BITUMEN
339
367
394
422
TEMPERATURE, K

describes only the final equilibrium conditions and fails to account for possible physical and electrostatic barriers which might be operative during the bitumen displacement. Nutting(103,104) has attempted to explain the displacement of bitumen based on chemical reaction theory. According to him, a strong attachment exists between the siloxyl radicals formed on the hydrated silica surface and the basic constituents of the bitumen. During the conditioning of the bituminous sand with the alkaline wetting agent, the strong hydroxyl radicals tend to displace the weak basic radicals of the bitumen enabling the displacement of the bitumen from the sand particles. This chemical reaction theory appears to be more realistic in explaining the bitumen displacement. In 1967, GCOS Ltd. utilized a modified hot water extraction method in their commercial plant producing 58,000 barrels per day of synthetic crude from Athabasca bituminous sands(100). In 1978, a second commercial plant based on hot water separation technology was brought on stream by Syncrude Canada Ltd.. The rated capacity of this plant was 129,000 barrels per day of synthetic crude. In the GCOS and Syncrude plants both primary and final extraction operations for recovering bitumen are exactly the same. The GCOS Ltd. plant, the first in pioneering commercial operation, offers on a royalty basis the technical know-how of all stages of the extraction operation. Syncrude Canada Ltd. adapted the GCOS extraction technology but used the fluid coking method for upgrading the bitumen for the production of synthetic crude. Because the GCOS and Syncrude extraction processes are similar, the Syncrude operation is described here. The process flow diagram and the

Figure 2.3

Flow Diagram of Syncrude Canada Process*

A. Rotating Drum

B. Primary Separation Tank

C. Secondary Separation Tank

D. Dilution Tank

E. Centrifuges

F. Flash Drum

G. Fluid Cokers

H. Fractionator

I. Naphtha Hydrotreater

J. Gas Oil Hydrotreater

---

*Source: Syncrude(105)

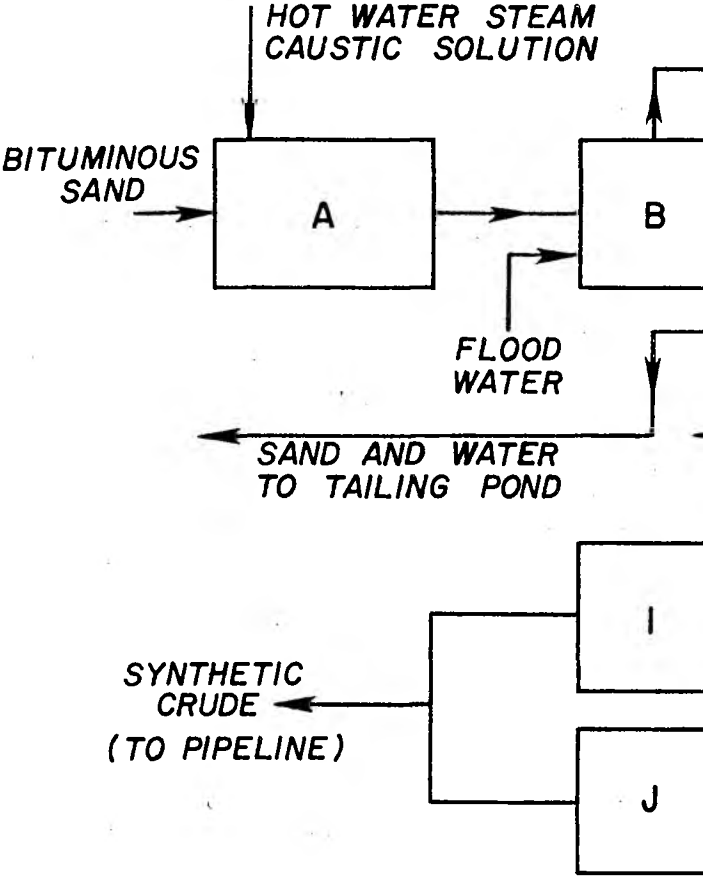
HOT WATER STEAM
CAUSTIC SOLUTION
BITUMINOUS SAND
A
B
FLOOD WATER
SAND AND WATER TO TAILING POND
I
J
SYNTHETIC CRUDE
(TO PIPELINE)

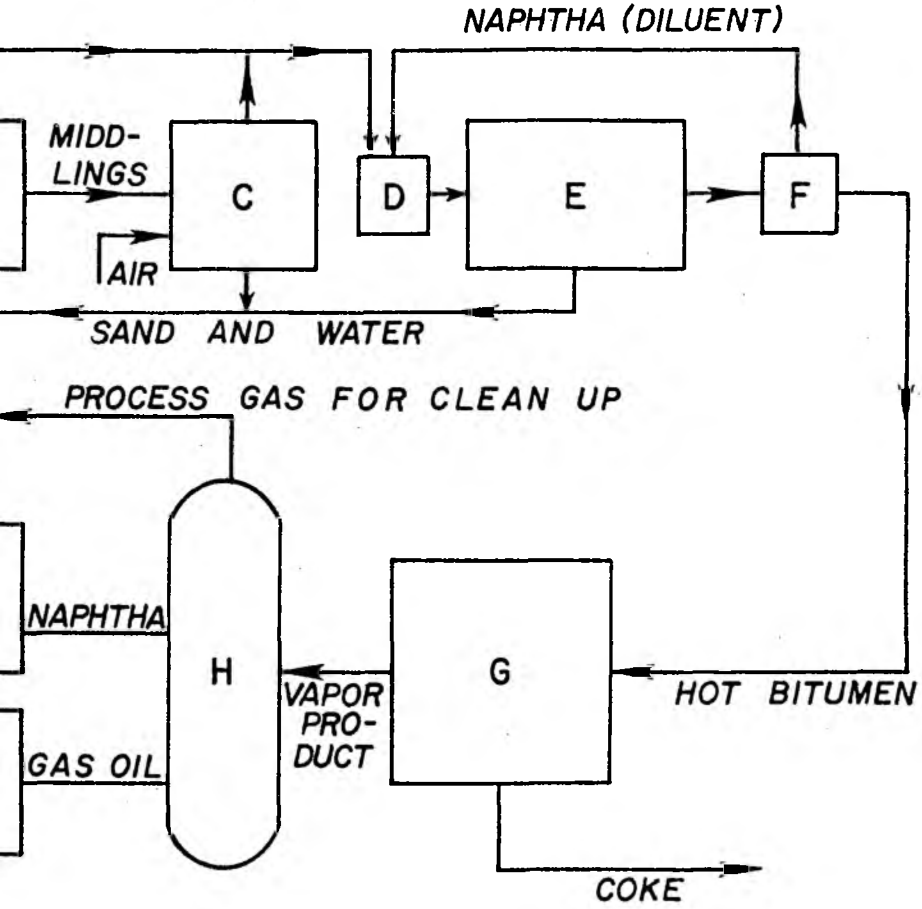
NAPHTHA (DILUENT)
MIDD-
LINGS
C
D
E
F
AIR
SAND AND WATER
PROCESS GAS FOR CLEAN UP
NAPHTHA
H
VAPOR
PRO-
DUCT
G
HOT BITUMEN
GAS OIL
COKE

Table 2.3

Syncrude Canada, Ltd. Project Details*

Daily production of synthetic crude oil (initial)		109,000 bbl
Daily production of synthetic crude oil (1982)		129,000 bbl
Total Investment	$2.1 billion	
Mining Operation		
Mine Dimensions	4.2 km long 7.5 km wide 60 m deep	
Extraction Plant		
Amount of bitumionous sand processed		11,800 tons/hr
Amount of bituminous froth produced		2,050 tons/hr
Synthetic Crude Properties		
Gravity, ^{o}API	33.0	
Sulfur, wt %	0.27	
Nitrogen, wt %	0.07	
Liquid Analysis, vol %		
C_5 - 380^{o}F	25.5	
380 - 650^{o}F	29.5	
650 - 975^{o}F	25.0	
Extraction Unit Material Balance	Input	Output
	1 m^3 of bituminous sand	1.2 m^3 of sand; 1 barrel of bitumen
Upgrading Unit Material Balance	Input	Output
	1 barrel of bitumen	0.85 barrels of synthetic crude; 15 m^3 of gas

---

*Source: Syncrude(105)

operational details for the Syncrude plant are presented in Figure 2.3 and Table 2.3.

The Syncrude process(105) consists of two parallel process trains and the hot water extraction unit is similar to the GCOS operation, however, the capacity is much greater, that is, 11,800 tons per hour ($t.h^{-1}$) of bituminous sands. The bituminous sand is conditioned by the hot water-caustic solution (pH is maintained between 8.0 - 8.5) in a rotating drum into which steam is introduced below the slurry surface by means of a sparger. This causes the sand particles to disintegrate, liberating the bitumen from the sand and the associated clay particles. The slurry is screened to remove the stones and clay agglomerates and is fed to the primary separation cell where it is mixed with additional water. The sand particles settle to the bottom of the cell as tailings and the bitumen floats to the top where it is removed by rakes to a peripheral launder. From the launder the bitumen is pumped to the final extraction plant, while the sand tailings and the water are sent to a tailings pond where the suspended solids settle and clarified water is obtained. A middling stream containing clay, silty particles, water and minute droplets of bitumen is drawn from the center of the primary cell delivered to the secondary separation cell. Air is introduced into the secondary cell to enhance the bitumen recovery from the middlings fraction. The bitumen froth from both the primary and the secondary separation cells is diluted with naphtha and centrifuged to remove the final traces of water and the remaining solids. The naphtha is then separated out by distillation, leaving very thick, black, tar-like bitumen. The bitumen has an API gravity of 8 -

10 and contains 5% sulfur plus trace amounts of metal contaminants such as nickel (75 - 100 ppm) and vanadium (150 - 250 ppm).

The bitumen is upgraded by a fluid coking process where it is thermally cracked to lighter hydrocarbons and coke. The hydrocarbon vapor from the fluid coker is fractionated into a light process gas, naphtha, and heavy gas oil. The naphtha and gas oil fractions are individually hydrotreated to remove the remaining sulfur and trace metals. The hydrotreated products are blended to obtain a synthetic crude of 33 API gravity and pipelined to the refinery.

There are at least two major areas of the hot water extraction in which further research needs to be conducted. The hot water extraction technology as applied to Canadian bituminous sands requires large settling ponds to clarify the reject water of sand, fine clay, and other mineral matter. The disposal of tailings sludge poses an environmental problem due to an increase in the volume of the sludge (Table 2.3)(106). Moreover, the spent sand is usually returned to the mined-out area. The increase in the volume or 'bulking' of the spent sand would require larger space than that occupied by bituminous sand itself. Research efforts should be concentrated in reducing the volume increase of the spent sand. Secondly, due to the clarification process the thermal energy loss in the reject water from the primary processing step is high(107). Research studies should be carried in reducing the energy input during extraction in order that less energy will be lost in the reject water. Alternately, research should be conducted in ways and means of recovering the energy from the reject water before it is sent to the tailings ponds. Recently, a novel laboratory hot water extraction method using electrical energy for heating the water has been reported(108). The method claims a reduction in the over-all thermal energy input requirements thereby decreasing the heat loss.

Research activities on the recovery of bitumen or a synthetic crude from Utah's bituminous sands have been limited to laboratory studies. The first systematic investigation using hot water extraction was reported by Shea and Higgins(49). In this laboratory process, developed by the Bureau of Mines, the bituminous sand was digested in a cylindrical pulper with an aqueous sodium silicate solution and a light oil diluent at 365 K. The bitumen was separated as a froth in a series of flotation cells. Bituminous sand samples from the Asphalt Ridge and Sunnyside deposits were used in this investigation. The reported bitumen contents for the Asphalt Ridge and Sunnyside samples were 12 weight percent and nine weight percent, respectively. The percentage recovery based on the bitumen fed was 96% with the composition of the bitumen froth being 54% bitumen, 38% sand, and 8% water. Although the bitumen recovery for the Sunnyside samples was nearly comparable to the Asphalt Ridge sample, the bitumen froth contained a higher percentage of water and sand. The reported density of the Asphalt Ridge bitumen was 8.6 °API, while the density of the Sunnyside bitumen was 7.6 °API. The light oil diluent requirements per ton of bituminous sand was 8 - 10 gallons with 0.1 - 0.3 gallons of diluent lost in the tailings stream. On the contrary, a modified, solvent unassisted, hot water extraction method has been developed at the University of Utah(43). In this modified hot water extraction method, the bituminous sand was digested with an aqueous alkaline solution under high shear conditions to liberate the bitumen from the sand. With the bitumen in direct contact with the sand particles in the Utah deposits, the high shear applied during the digestion step helped in breaking this bitumen-sand interface enabling the release of the bitumen from the sand(109). Sepulveda(47) successfully applied this modified extraction technique for recovering the bitumen from Utah's bituminous sands, in particular Asphalt Ridge bituminous sand. The quality of bitumen separation was reported in terms of a coefficient of separation ranging from zero (no separation) to one (ideal separation). The process variables, temperature, caustic concentration, and percent solids in the digester were optimized. At the optimum digester conditions (70 - 80% solids, 0.58M caustic solution, 368 K), the coefficient of separation and the percent recovery of bitumen were 0.9 - 0.95 and 93 - 96, respectively.

Misra and Miller(54) have applied the modified hot water extraction method described by Sepulveda and Miller(109) to a representative sample from the Sunnyside deposit (bitumen content 9 - 10 weight percent). In this study, sodium carbonate was used as the alkaline wetting agent in the digestion step and the results indicated a low coefficient of separation (0.5 - 0.55). The addition of diluents, such as toluene and No. 1 fuel oil, during the digestion stage improved the coefficient of separation from 0.55 to 0.69, however, this was still below the coefficient of separation achieved for the Asphalt Ridge sample. The authors feel that the separation can be improved by adding hydrophobic solid additives as an external agent.

2.5 High Temperature Aboveground Recovery Processes

Surface-mined above ground recovery processes operating at high temperature offer an alternative to the hot water extraction techniques for the recovery of a bitumen derived synthetic crude from the bituminous sand. No previous investigations have been reported on the above ground high temperature processing of Utah's bituminous sands, however, a considerable volume of material has been published on the above ground thermal processing of the Canadian bituminous sands. Noyes Data Corporation has published a detailed summary of all patented thermal processing schemes(97).

2.5.1 Fundamentals of High Temperature Thermal Processing

In high temperature thermal processing, the feed sand is heated to temperatures in the range of 673 - 873 K in the absence of air or oxygen. This process is often described by various names such as direct coking, retorting, destructive distillation, etc.. These names are often used interchangeably in the description of a process. Essentially at these high temperatures the high molecular weight hydrocarbon species in the bitumen undergo distillation and cracking simultaneously (often called as pyro-distillation) to produce species of low molecular weight. Concomitant with the release of the synthetic crude and light gases, a portion of the bitumen undergoes polymerization, condensation reactions to form coke-like material on the sand particles. The process is endothermic and the over-all reaction can be represented as

$$\text{Bitumen} + \text{Heat} \rightarrow \text{Synthetic Crude} + \text{Gas} + \text{Coke} \qquad (2.1)$$

The heat required for the above reaction can be obtained from the combustion of the carbonaceous material on the sand, according to the reaction

$$\text{Coke (Carbon, Hydrogen)} + \text{Air (Oxygen)} \rightarrow CO_2 + H_2O + \text{Heat} \qquad (2.2)$$

The over-all process can be made energy self-sufficient by proper selection of operating conditions and by developing a suitable method of transfering the energy produced by the combustion reaction (2.2) to the pyro-distillation reaction (2.1). The objective of this investigation was to study the process variables (described later) that influence the products obtainable in reaction (2.1).

Several processes with differing reactor configurations have been studied to carry out the combined pyro-distillation - combustion processes. The various processes can be classified, according to the procedure of Moore, et. al.(110), into two general groups, that is, direct heated and indirect heated processes. In the direct heated process, the coking reactor is generally located above the combustor and the heat generated in the combustor according to reaction (2.2) is generally transported to the coking reactor by the hot flue gases. In the indirect heated process, the pyro-distillation reaction and the combustion reaction are carried out in two separate reactor vessels and the heat generated in the combustion reaction (2.2) is transported to the pyro-distillation reaction (2.1) by the hot spent sand. The thermal processes are classified as follows(110):

(i) direct heated, fluidized processes
(ii) direct heated, non-fluidized processes
(iii) indirect heated, fluidized processes
(iv) indirect heated, non-fluidized processes

These four classifications are based upon the choice of the reactor vessel (fluidized or non-fluidized) in which reaction (2.1) is carried out and the method by which the heat is supplied to the pyrodistillation reaction (2.1) (direct heated or indirect heated). In addition, it is possible that the combustion reaction (2.2) can be carried out in a fluidized bed process or in a non-fluidized process. Processes in which the combustion of coke was not carried out and the heat required for reaction (2.1) supplied by electrical energy are termed indirect heated processes.

2.5.2 Fluidized Bed

Coking Processes

Fluidized bed coking has been successfully applied to the production of synthetic crude from bituminous sands. The earliest reported work is that of Gishler(111), who studied the direct distillation of Canadian bituminous sands in a small laboratory unit (Figure 2.4). Nitrogen was used as the fluidizing gas and the reactor unit was electrically heated. The main objective of this investigation was to obtain the necessary engineering data to permit scale-up for a large scale operation. The data indicated the existence of an optimum temperature range at which the liquid yields were maximized. The liquid obtained was less viscous than the extracted

Figure 2.4

Flow Diagram of the Laboratory Fluidized Bed Thermal Recovery Unit*

A. Preheater
B. Reactor
C. Cyclone Separator
D. Oil Trap
E. Electrostatic Precipitator
F. Charcoal Adsorber
G. Steam Preheater
H. Water Still
I. Condenser
J. Gil Receivers

---

*Source: Gishler(111)

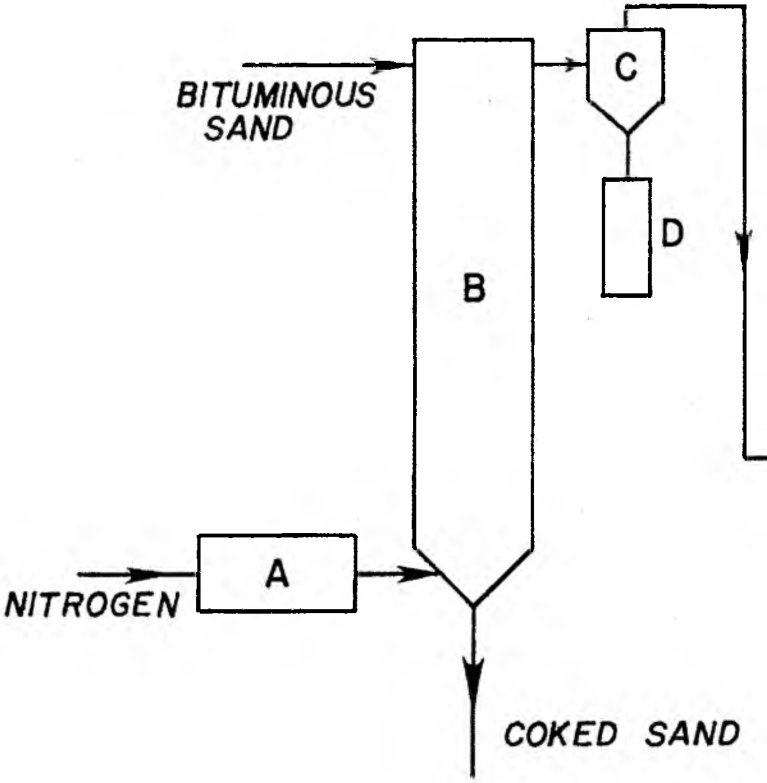
BITUMINOUS SAND
C
D
B
NITROGEN
A
COKED SAND

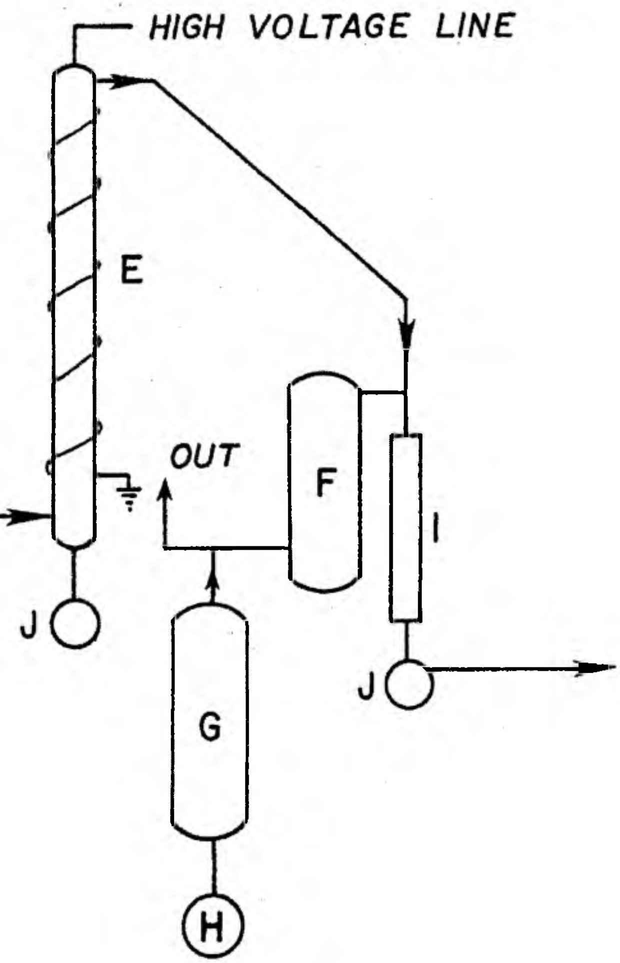
HIGH VOLTAGE LINE
E
OUT
F
I
J
J
G
H

bitumen and had an API gravity in the range of 13 - 15 and a sulfur content of 3 - 4 %, while the API gravity and the sulfur content of the extracted bitumen were 7.5 and 5%, respectively. Experimental runs were also conducted using steam as the fluidizing gas. The presence of water vapor resulted in a significant increase in the yield of light hydrocarbon gases above the coking reactor temperature of 773 K. The high yields of light gases were due to steam cracking of the bitumen and were similar to the steam cracking of petroleum crude for the production of light olefins(112,113). Peterson and Gishler(114-116) developed a large scale, fluidized bed pilot-plant based on the data obtained in the preliminary studies by Gishler(111). A flow diagram of this indirectly heated fluidized process is presented in Figure 2.5. The coking vessel was a 15 cm pipe, 1.8 meters in height; while the combustor was a 22.5 cm diameter pipe, 1.8 meters in height. The bituminous sand was added continuously to the coking reactor which was maintained at a predetermined temperature above 755 K. The vapor product was carried by the fluidizing gas into the collection system. The residual coked sand was withdrawn continuously from the coking reactor and transported into the combustor by a preheated air stream where the coke was burned off at 922 K. A part of this hot, spent sand was recycled (the recycle ratio of hot spent sand to fresh sand was four) to the coking reactor to supply the heat required for the pyro-distillation of the bitumen from the fresh bituminous sand. The remaining spent sand was discarded. Bituminous sand samples from the Bitumont and Abasand deposits were used in the pilot-plant investigation. The experiments generally lasted 6 - 10 hours at feed rates of 35 - 65 $kg.h^{-1}$. Synthetic liquid yields were dependent

Figure 2.5

Flow Diagram of the Fluidized Bed Pilot-Plant Operation for Canadian Bituminous Sands*

A. Coker
B. Combustor
C. Product Receiver

---

[*] Source: Peterson and Gishler(114-116)

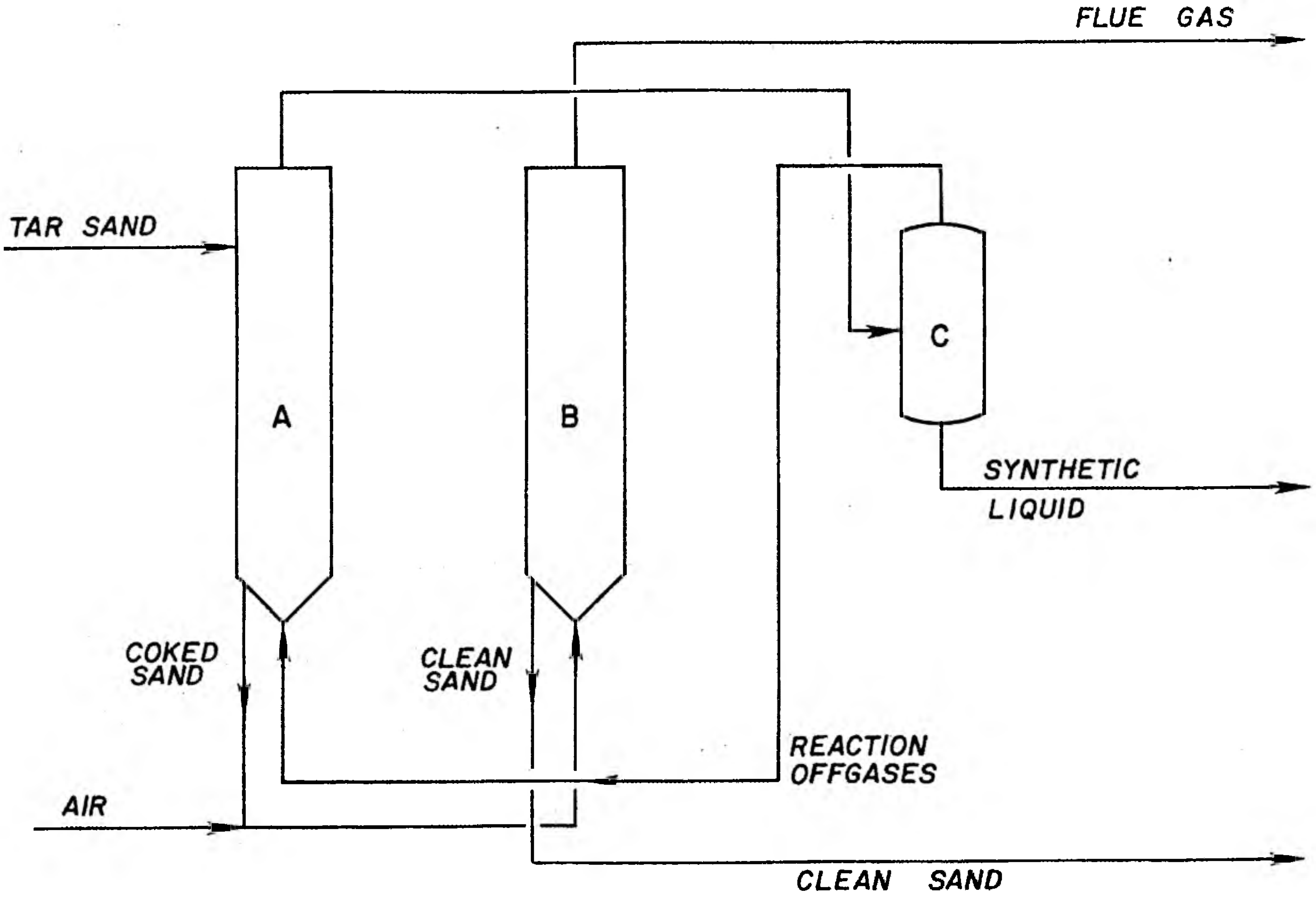
FLUE GAS
TAR SAND
A
B
C
SYNTHETIC LIQUID
COKED SAND
CLEAN SAND
REACTION OFFGASES
AIR
CLEAN SAND

dependent upon the coking reactor temperature and the temperature for the maximum liquid yield was in the range of 773 - 798 K. Moreover, synthetic liquid yields of 84 - 86% by volume were obtained for both feed sand sources and the liquid gravities were 16 °API. In spite of these high yields, the process did not gain further attention because of the heat losses associated with the discarded sand and the requirements of high recycle ratio of hot, spent sand to supply the energy required for the liberation of the bitumen leading to erosion of the processing vessels by the circulating sand(107).

A direct heated process using a fluidized bed coking reactor-moving bed combustor developed at the University of Calgary was used to study the recovery of a synthetic liquid from the Canadian bituminous sands(110). The fluidized bed coking reactor was located directly above the moving bed combustor. The feed sand was fed to the coking reactor through a disengaging section. After the release of the vapor, the hot coked sand passed into the combustor as a moving bed of solids. Air was injected at the bottom of the combustor and the combustion products which flow upward act as the fluidizing gas for the coking section. The heat required for the liberation of the bitumen was transported by combustion gases and was supplemented by electrical heating. The process has been successfully operated on a small scale, however, large scale operation has not yet been attempted. One of the major drawbacks of this process is the possibility of bitumen combustion in the coking reactor. The fluidizing gas entering the coking reactor may contain oxygen depending upon the quantity of air used in the combustor. If oxygen is present, the bitumen in the coking reactor could undergo combustion. This would result in the decrease of liquid yield due to (i) the loss of bitumen from combustion, and (ii) the increase in the coking reactor temperature due to bitumen combustion would result in the additional cracking of the bitumen, thereby increasing the production of light gases.

The recovery of synthetic liquid from the bituminous sand deposit of Kirmak in the Soviet Union by a fluidized bed coking technique has also been reported(117,118). The bituminous sand was crushed to less than one centimeter diameter and was fed to the fluidized bed coking reactor held at a temperature which ranged from 733 - 753 K(117). The product vapor was carried by the fluidizing gas to the liquid recovery collection system. The coked sand was transported to an air fluidized combustor held at 813 - 833 K where the coke was burnt. A portion of the hot, spent sand was returned to the fluidized coking reactor. The feed sand charged to the coking reactor contained 3.5 percent moisture and 7 percent bitumen. The process yielded two percent by weight light gases, 50 - 55% by weight synthetic liquid based on the bitumen fed and the balance was converted to coke.

In a similar study(118) on a Kirmak bituminous sand having a bitumen content of 7.0 - 7.5 weight percent and an initial moisture content of six percent, the moisture content was reduced to 3.5 percent by treatment with flue gases from the combustor in a counter-current contactor. During the drying step a liquid hydrocarbon product was collected and amounted to 10% of the bitumen fed. The dried bituminous sand having a bitumen content of six percent was fed to the fluidized bed coking reactor. The coking reactor was operated in the temperature range of 738 - 773 K and at a solids retention time of 8 to 15 minutes. The liquid yield appeared to be insensitive to the sand retention time in this investigation. The recovery of liquid from this stage was 53% giving an over-all yield of 63%.

A novel process for simultaneous volatilization and catalytic cracking of the bituminous sand was described by Haensel(119). In this process, bituminous sand - cracking catalyst mixture was added to the fluidized coking reactor. The coked sand and coked catalyst were recycled from the regenerator. The heat carrier to the coking reactor was individual streams of catalyst and spent sand. The catalyst and sand particles were kept separate from each other forming two layers using the density difference and the proper gas flow rates. Common cracking catalysts such as silica-alumina, silica-magnesia, silica-zirconia or a natural catalyst such as Superfiltrol were used. No yield data were reported. The maintenance of catalytic activity and loss of catalyst along with sand fines could be important in the economic evaluation of the process.

2.5.3 Nonfluidized Direct Coking Processes

Among the non-fluidized direct coking processes, the Lurgi-Ruhrgas process appears to have considerable potential for commercialization. Recently, the Alberta Oil Sands Technology and Research Authority (AOSTRA) has commissioned a study to conduct a preliminary evaluation of the comparative economics of the Lurgi-Ruhrgas direct, dry distillation process and the most advanced hot water process for extraction and primary conversion of bitumen from the Athabasca bituminous sands.

Rammler(120,121) has described the application of this process to coal, oil shale, and bituminous sands for the production of synthetic liquids. The pilot-plant operation was tested with a feed bituminous sand from the Edna deposit in California. A flow diagram of the process is shown in Figure 2.6.

In this process, the feed sand (bitumen content 9 - 10 percent by weight) and the heat carrier (hot spent sand) were continuously supplied to a mechanical mixer where a major portion of the cracking of the bitumen took place. The product vapors were withdrawn at the end of the mixer. The newly formed coked sand and the heat carrier were discharged into a surge hopper. This flowed from the hopper to the lower portion of a lift pipe. The coke on the sand was burned in air in the lift pipe and the solids were raised pneumatically by the combustion products to a collecting bin. After separating the flue gases, the hot sand was recycled to the mechanical mixer with fresh feed sand. The surplus spent sand was continuously removed from the surge hopper.

The report contained little quantitative data, however, the yield of synthetic liquid was more than 90% by weight at a coking temperature of 773 K. The synthetic crude yield was influenced by the operating capacity of the pilot-plant. The synthetic crude yield increased from 75 weight percent to 90 weight percent corresponding to the feed rate (related to the operating capacity) increase from 0.36 $t.h^{-1}$ to 0.49 $t.h^{-1}$.

The "Direco" Process, developed by Syncrude Canada Ltd., was similar to the Lurgi Ruhrgas process in concept, but was a bench scale unit used to study the direct coking of Canadian bituminous sands(122). The

Figure 2.6

Flow Diagram of Lurgi-Rührgas Direct Coking Process*

A.	Mechanical Mixer	E.	Cyclone Separator
B.	Surge Hopper	F.	Product Receiver
C.	Lift Pipe	G.	Waste Heat Boiler
D.	Collecting Bin		

---

*Source: Rammler(121)

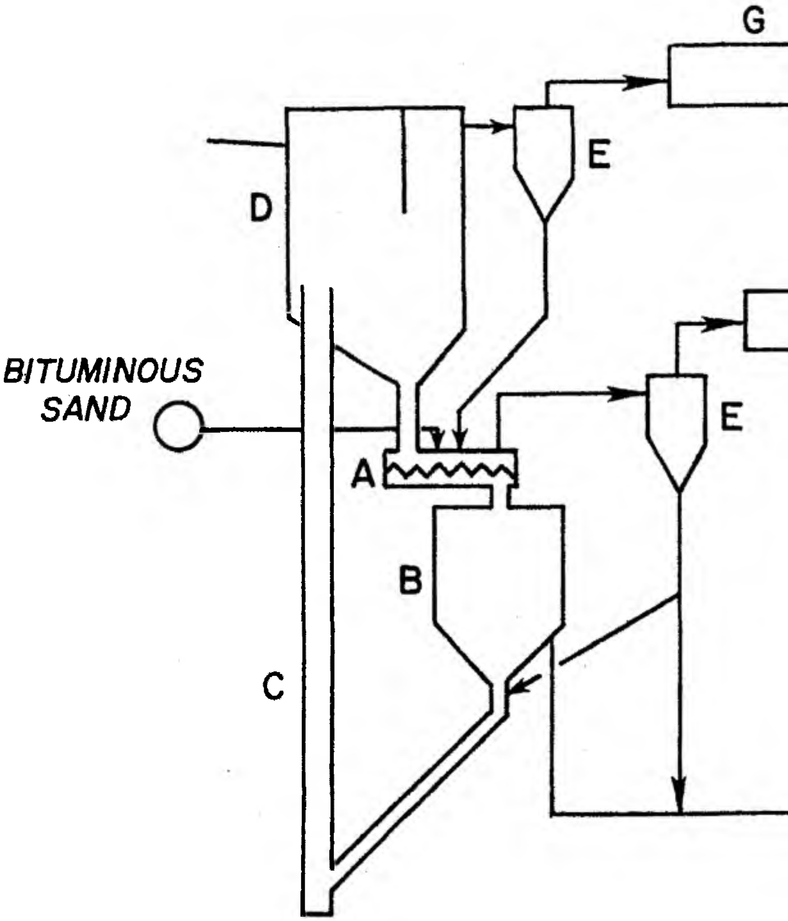
G
E
D
BITUMINOUS SAND
E
A
B
C

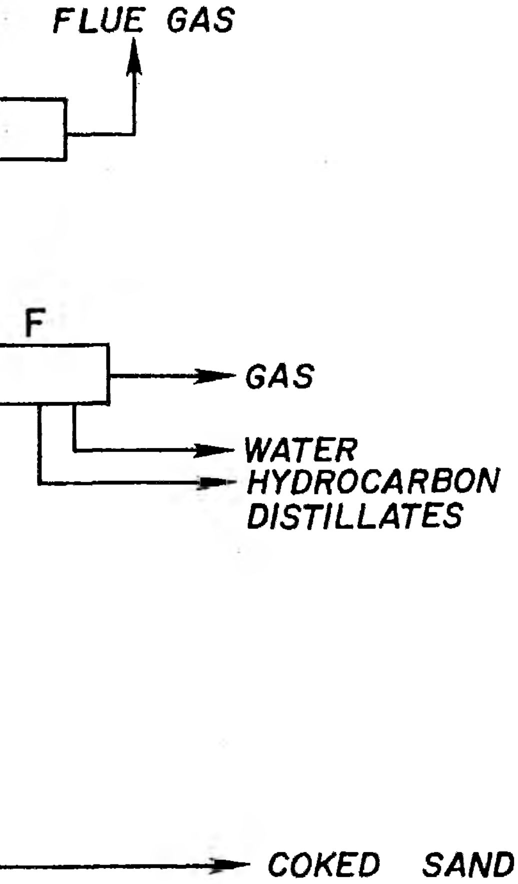
FLUE GAS
F
GAS
WATER
HYDROCARBON DISTILLATES
COKED SAND

bituminous sand was supplied to an electrically heated screw conveyor where the pyro-distillation of the bitumen took place. The data reported were corrected to a 797 K end point using the weight percent of Conradson carbon of the resid portion of the synthetic liquid. The operating temperature and the vapor residence time inside the reactor had significant effect on the yield pattern of the products. The yields of coke, light gases, and naphtha based on the bitumen fed increased at the expense of heavy and light gas oil fractions with increasing reactor temperature. The yield of light gases increased from 2 percent at 748 K to about 18 percent at 848 K, the yield of naphtha increased from 3 to 8 percent, while the total gas oil (light gas oil plus heavy gas oil) yield decreased from 82 - 84 percent to 58 - 60 percent between the above temperatures. The bitumen converted to coke increased with increasing reactor temperature up to 793 K. Above 793 K the coke yield attained a stationary value of 20 percent by weight. The light gases, naphtha, coke yields increased at the expense of heavy gas oil as the hydrocarbon vapor residence time in the coking zone increased. In addition, the density and weight percent sulfur of the light gas oil and heavy gas oil fractions increased, while the density and weight percent sulfur of the naphtha fraction decreased with increasing reactor temperature.

In a non-fluidized bed process described by Berg(123), the coking of the bituminous sand was carried out in a kiln as shown in Figure 2.7. The fresh bituminous sand and the hot, spent sand were mixed and fed to the kiln. The product vapors from the kiln were withdrawn from the disengager using the light hydrocarbon gas, which was recycled.

Figure 2.7

Flow Diagram of Berg's Rotary Kiln
Direct Coking Process*

A. Rotary Kiln
B. Surge Hopper
C. Combustor
D. Lift Pipes
E. Distillation Column

---

*Source: Berg(123)

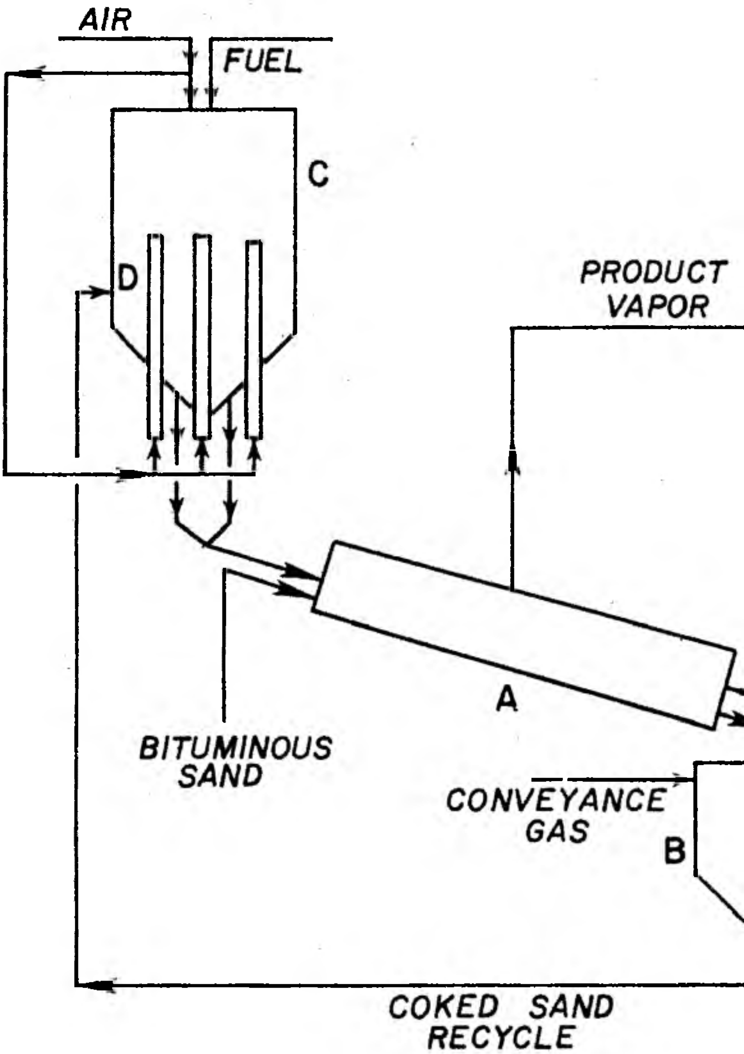
AIR
FUEL
C
D
PRODUCT
VAPOR
A
BITUMINOUS
SAND
CONVEYANCE
GAS
B
COKED SAND
RECYCLE

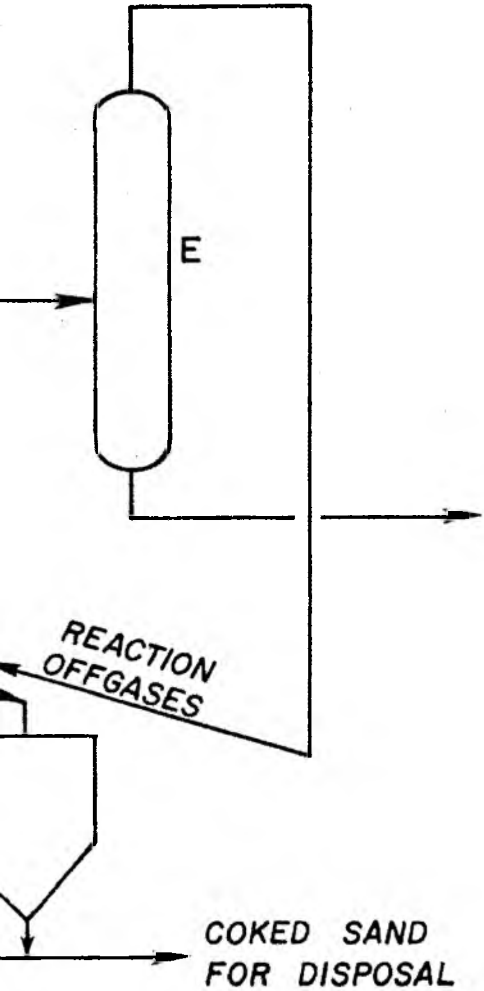
E
REACTION OFFGASES
COKED SAND FOR DISPOSAL

The coked sand from the kiln was discharged into a surge hopper. The coked sand was transported to the combustor by a conveyance gas which was admitted to the surge hopper. The hot coked sand passed downward as a moving bed of solids inside the combustor. Air, required for combustion, was admitted at the bottom of the combustor. The mixing of solids in the combustor was achieved by internal circulation of solids via lift pipes. The combustion of coke in the combustor produced 65% of the heat required for the pyro-distillation of the bituminous sand. The remaining 35 percent was supplied by the fuel gas. For a feed sand containing 12 percent bitumen, the yields of synthetic liquid and coke were 73 percent and 18 percent, respectively.

Stinmatz(124) described a process in which the fresh bituminous sand was mixed with extracted bitumen obtained by a hot water extraction method. This feed preparation technique could be attractive for processing low grade bituminous sand (bitumen content less than four percent by weight) because the energy requirements for the pyro-distillation of the bituminous sand increases as the bitumen content of the sand decreases(116), however, this uniform feed mixture would eliminate the variations in the bitumen content thereby improving the thermal efficiency of the high temperature thermal process.

2.6 Process Selection

The selection of an appropriate processing scheme for the recovery of the bitumen or for the production of a synthetic crude from the bituminous sands of Utah will be dependent upon the following factors: (1) the selected process or a combination of processes should produce higher yields at minimum cost, (2) the process must have minimum technological risk, and (3) the data for commercial operation should be obtainable at a reasonable cost and time.

The hot water extraction process and the fluidized bed thermal recovery process are prime choices for the processing of minable bituminous sands of Utah. However, a direct comparison cannot be made on the individual processes alone because of the differences in the nature of products produced and the thermal energy requirements. The hot water process produces a tar-like material, while the high temperature fluidized bed thermal process produces a less viscous, higher gravity (API^o) synthetic crude. Generally, the bitumen from the hot water extraction process is upgraded by a standard thermal coking process to produce a synthetic crude(5). Accordingly, the coking process must be considered as an integral part of the over-all scheme for the production of synthetic crude from bituminous sands by hot water extraction. Thus, the heat and mass balances for the hot water extraction-coking scheme can now be directly compared with the high temperature fluidized bed thermal recovery process.

The yields of synthetic crude obtained with the Canadian bituminous sands from the two processing schemes are compared in Figure 2.8. The data are based on the assumption of 100% bitumen in the feed. The percent yield of liquid obtainable from the high temperature direct coking process is in the range of 82 - 86, while the yield of liquid from the hot water extraction-coking process is in the range of 65 - 68 percent. However, in the high temperature fluidized bed processing scheme, the thermal energy demand caused by the inorganic portion of the bituminous sand is large and a significant amount of thermal

Figure 2.8

Material Balance Comparison of Direct Coking
and Hot Water Extraction/Primary
Fluid Coking Upgrading

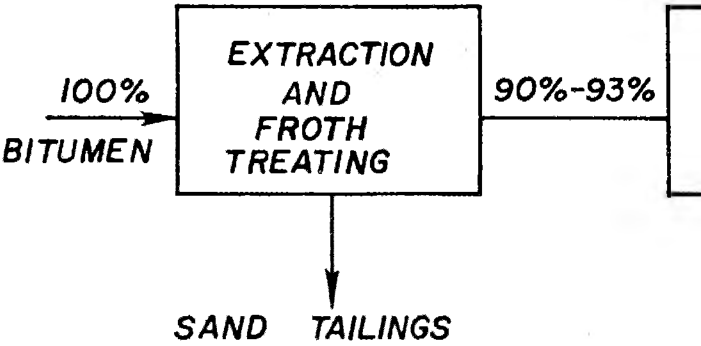
100%
BITUMEN
EXTRACTION AND FROTH TREATING
90%-93%
SAND TAILINGS

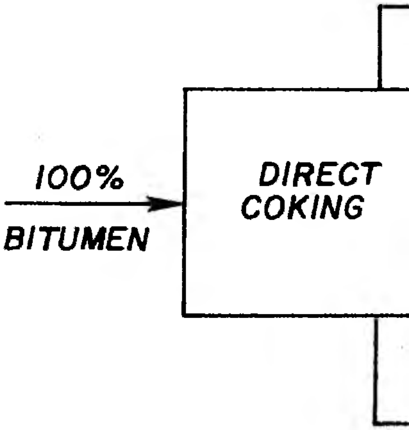
100%
BITUMEN
DIRECT COKING

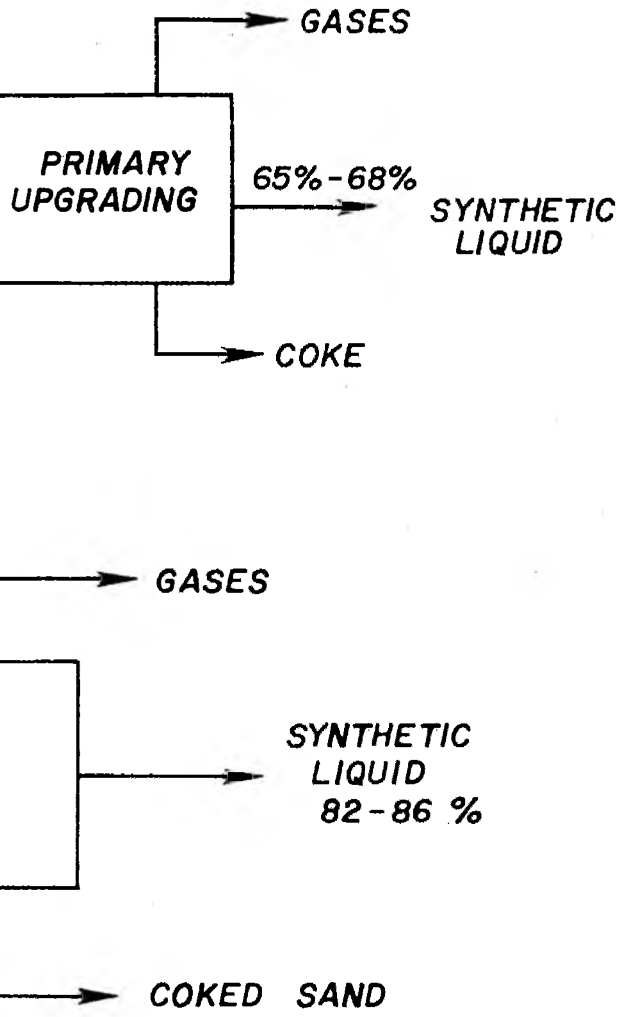
GASES
PRIMARY UPGRADING
65%-68%
SYNTHETIC LIQUID
COKE
GASES
SYNTHETIC LIQUID 82-86 %
COKED SAND

energy is lost in the hot, spent sand. Furthermore, the physical arrangement of the Canadian bituminous sand (a film of water separating the bitumen and the sand) and the simplicity of the hot water extraction method led to the selection of the hot water extraction-coking scheme in the commercial process of Athabasca bituminous sand deposits. However, Flynn, et. al. (107) have compared the net thermal energy efficiencies of the thermal recovery process and the hot water extraction-coking scheme (Figure 2.9) and have concluded that they are nearly the same. However, they point out that the thermal efficiency of the high temperature process can be markedly high if sensible heat from the hot, spent sand is recovered and reused. In such a case the thermal efficiency of the high temperature scheme is about 82 percent whereas the most efficient hot water process is only 70 percent.

Additional advantages of the fluidized bed thermal coking method as a choice for recovering the bitumen derived synthetic liquid are listed here:

(i) The water availability for the development of the bituminous sand resource is a serious problem in an arid state like Utah. Process water requirements are reduced in thermal schemes relative to hot water recovery schemes.

(ii) A dry sand is produced, thus eliminating the huge tailing ponds. Moreover, there is no increase in the volume of the dry sand relative to the bituminous sand which would allow dumping the sand into the mined-out area.

(iii) Bituminous sands with low bitumen content can be processed in the high temperature thermal recovery process whereas the hot water

Figure 2.9

Energy Comparison of Direct Coking and
Hot Water Extraction/Primary
Fluid Coker Upgrading*

---

*Source: Flynn, *et*. *al*.(107)

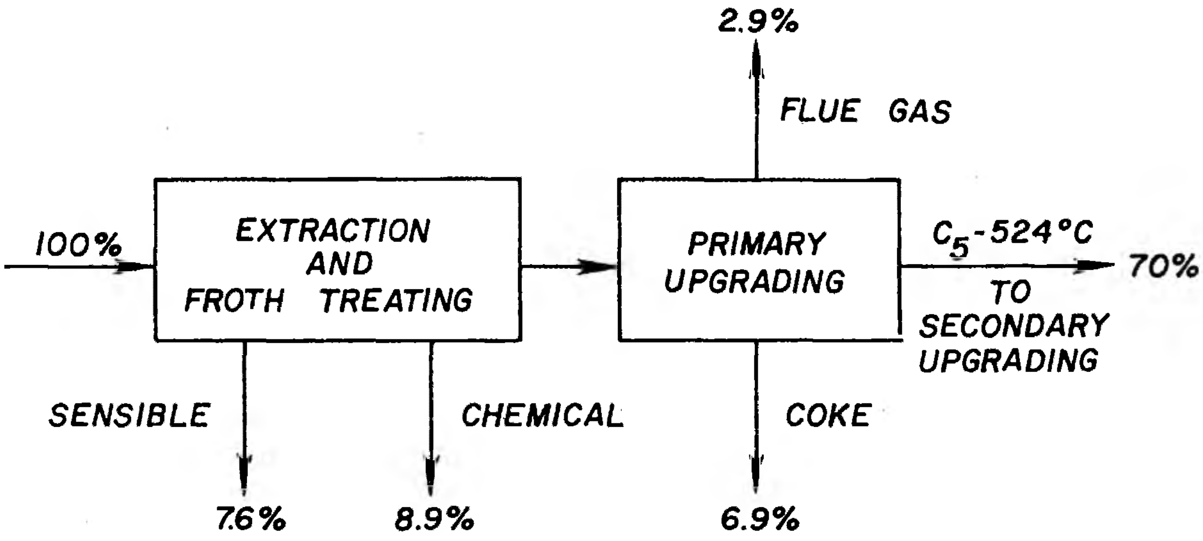
100%
EXTRACTION AND FROTH TREATING
SENSIBLE
7.6%
CHEMICAL
8.9%
PRIMARY UPGRADING
2.9%
FLUE GAS
COKE
6.9%
C_5-524°C
70%
TO SECONDARY UPGRADING

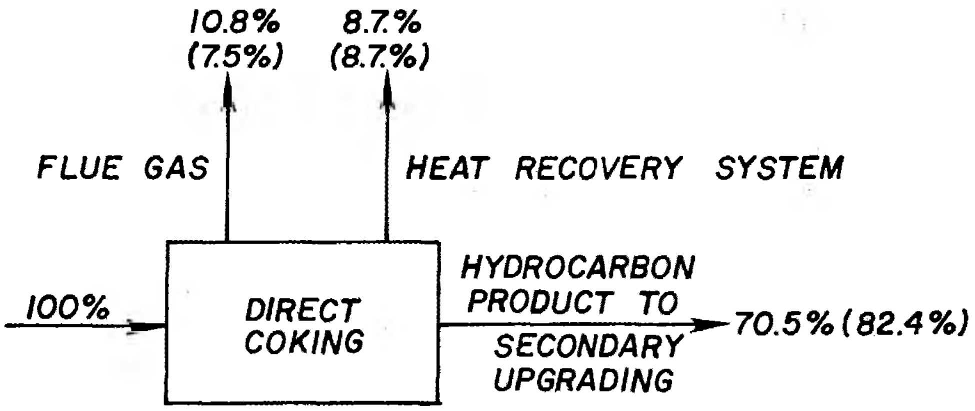
10.8%
(7.5%)
8.7%
(8.7%)
FLUE GAS
HEAT RECOVERY SYSTEM
100%
DIRECT COKING
HYDROCARBON PRODUCT TO SECONDARY UPGRADING
70.5% (82.4%)

extraction method resulted in a low coefficient of separation for lower bitumen content Utah deposits such as Tarsand Triangle(47).

(iv) Among the various thermal schemes, the fluidized bed thermal recovery process is attractive because fluidized beds are highly efficient in maintaining uniform temperature and have higher heat transfer rates.

(v) The synthetic liquid product is less viscous and can be transported by pipeline without further upgrading. The bitumen obtained in hot water must be upgraded by coking processes.

(vi) When substantial amounts of sand fines present in the feed material, the separation of bitumen becomes difficult in the hot water method. The high percentage of fines in the Sunnyside bituminous sand feed resulted in a high percentage of middlings stream, thus lowering the coefficient of separation from 0.9 to 0.55(54). On the other hand, fines do not pose any serious problem and can be collected effectively in the thermal process by available fines collection technology.

(vii) The application of the fluidization technology developed by the petroleum industry for the fluid catalytic cracking process would reduce the technological risk involved in commercializing the recovery of synthetic crude from bituminous sands of Utah using a fluidized bed thermal recovery process.

In spite of these advantages, fluidized beds do pose a few problems such as:

(i) Erosion of process vessels due to sand abrasion.

(ii) The combustion of coke on the sand may produce air pollutants. The high nitrogen content in the bitumen of Utah deposits may cause the formation of NO_x compounds in the combustion process, however, a recent study on the catalytic cracking of shale-oil with a high percentage of nitrogen has claimed the elimination of NO_x problem in the regenerator flue gases by controlled combustion of coke on the catalyst(125).

The advantages of fluidized bed and the quality of the liquid obtainable appear to outweigh the minor objectionable features of the fluidized bed, thermal processing of bituminous sands of Utah.

2.7 Research Objectives

This investigation was undertaken with the following objectives:

(1). to determine the feasibility of the fluidized bed thermal recovery technique for the production of a synthetic crude from the bituminous sands of Utah;

(2). to design, fabricate, and operate a bench scale unit for processing bituminous sands of Utah;

(3) to study the effect of the following variables on the production of synthetic crude, coke formation and bed operation:

i. source of feed and feed particle size
ii. bitumen content of feed
iii. fluidization bed temperature
iv. retention time of solids
v. method of introduction of bituminous sand;

(4) to analyze and characterize the synthetic crude obtained in the process.

CHAPTER 3

EXPERIMENTAL WORK

This investigation was concerned with the development of a fluidized bed reactor in which a synthetic crude oil could be thermally liberated from bituminous sands. The advantages of the fluid bed thermal recovery scheme were discussed in Chapter 2.

The design of a bench-scale fluid bed reactor is dependent upon a knowledge of the "ease of liberation" of the bitumen from the bituminous sand with time at elevated temperatures (between 673-900 K). Thermogravimetric studies were conducted at isothermal conditions to determine the relationship between the cumulative weight loss, temperature, and time for the various bituminous sand deposits of Utah (Appendix A). The minimum solids holding time necessary to liberate the synthetic crude was calculated from the thermogravimetric analysis (TGA). A bench-scale fluidized bed reactor was designed to process a maximum of 2.25 kg h^{-1} of bituminous sand based on the TGA data. The details of the fluid bed reactor design are reported in Appendix B.

A schematic of the fluid bed thermal recovery unit is presented in Figure 3.1. The unit will be described in detail under three distinct headings:

1. Fluid Bed Reactor Assembly

Figure 3.1

Flow Diagram of Fluidized Bed Thermal Recovery Unit

A.	Nitrogen Supply
B_1,B_2.	Rotameters
C.	Pre-heater
D.	Reactor
E.	Expansion Chamber
F.	Screw Conveyor
G.	D.C. Motor
H.	Feed Sand Hopper
I.	Speed Controller
K_1,K_2.	Cyclone Separators
L_1,L_2.	Sand Fines Receiver
M.	Filter
N.	Water Cooled Condenser
O_1,O_2.	Oil Receivers
S.	Orifice Meter
T.	Solids Receiver
U.	Cyclone Separator
W.	Fiber Mist Eliminators
X.	Glass Bottle
Y.	Differential Pressure Recorder Controller
Z.	Differential Pressure Cell

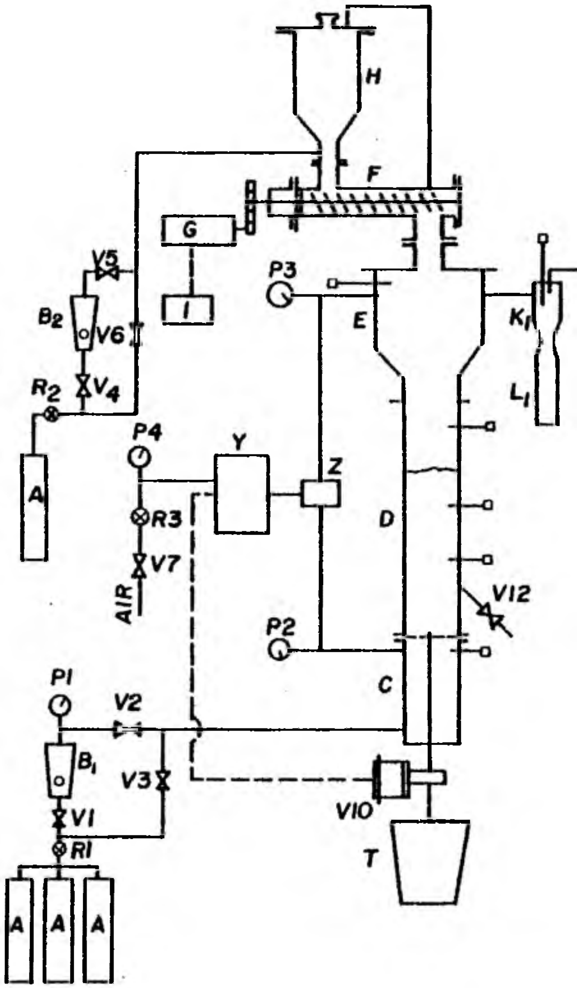
H
F
G
I
V5
B_2
V6
V_4
R_2
A
P3
E
K_1
L_1
P4
Y
Z
D
R3
V7
AIR
V12
P2
C
P1
V2
B_1
V3
V1
R1
A
A
A
V10
T

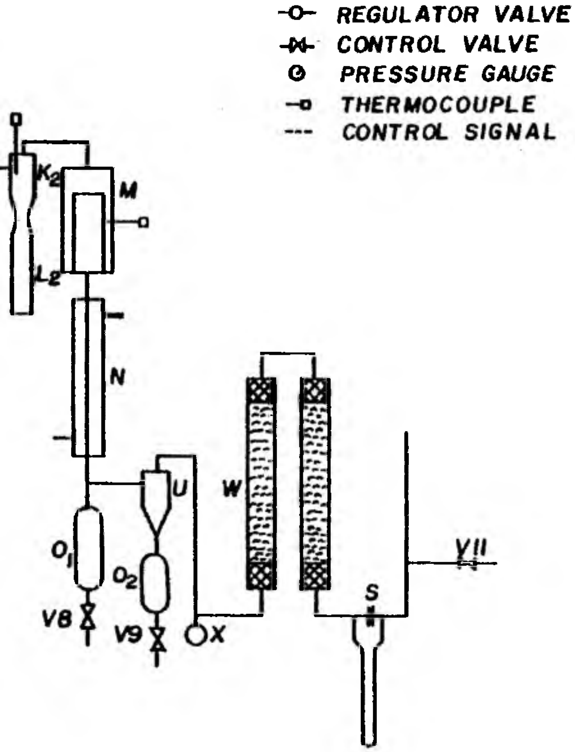

-o- REGULATOR VALVE
-⋈- CONTROL VALVE
⊙ PRESSURE GAUGE
-▫ THERMOCOUPLE
--- CONTROL SIGNAL
K2
L2
M
N
U
O1
O2
V8
V9
X
W
S
VII

2. Solids Introduction and Withdrawal Systems
3. Synthetic Crude Product Recovery System

The control and instrumentation systems associated with each of the sections will also be described.

The fluidizing gas (nitrogen), metered through a rotameter, entered the bottom of the reactor assembly where it was preheated to the coking reactor temperature (Figure 3.1). Bituminous sand was added to the reactor under free-fall conditions by a screw conveyor. The oil vapor, along with the fluidizing gas leaving the reactor, entered the product recovery system. The two cyclones and the filter, which were maintained at high temperature, removed the sand fines elutriated from the reactor. The gas-vapor stream was cooled in a water condenser, where the oil was partially condensed and collected. The mist resulting from the cooling of the oil vapor was removed by a series of fiber mist eliminators. The gas leaving the mist eliminators was sampled, metered, and vented.

3.1 Fluid Bed Reactor Assembly

The physical arrangement of the fluid bed reactor assembly is shown in Figure 3.2. It consisted of a preheater, reactor, and an expansion or disengaging chamber.

The purpose of the preheater was to provide the sensible heat to the fluidizing gas and to prevent any sensible heat addition to the gas in the reactor when bituminous sand was added to the reactor bed.

The preheater (Figure 3.3) was fabricated from a 3.13 cm nominal diameter 316 stainless steel schedule 10 pipe (3.6 cm inside diameter and 4.15 cm outside diameter) and was 25 cm in length. A standard

Figure 3.2

Physical Arrangement of Fluid Bed Reactor Assembly

A. Pre-heater
B. Main Reactor
C. Expansion Chamber
D. Connecting Section
E. Solids Standpipe
F. Gas Distributor
G. Standard 150 lb Flange

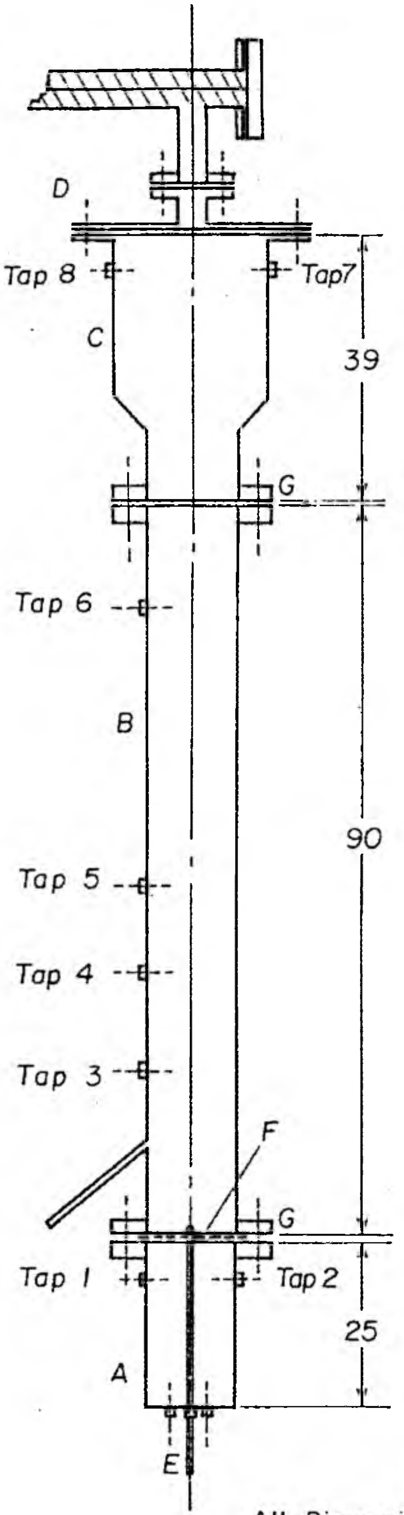
D
Tap 8
Tap7
C
39
G
Tap 6
B
90
Tap 5
Tap 4
Tap 3
F
G
Tap 1
Tap 2
25
A
E

All Dimensions In Cms.

Figure 3.3

Detailed Diagram of the Fluidizing Gas Pre-heater

A. Pre-heater Body
B. Standard 150 lb Stainless Steel Flange
C. Temperature Tap (Tap 2)
D. Pressure Tap (Tap 1)
E_1 and E_2. Fluidizing Gas Ports
F. Solids Standpipe Port

SECTIONAL FRONT VIEW

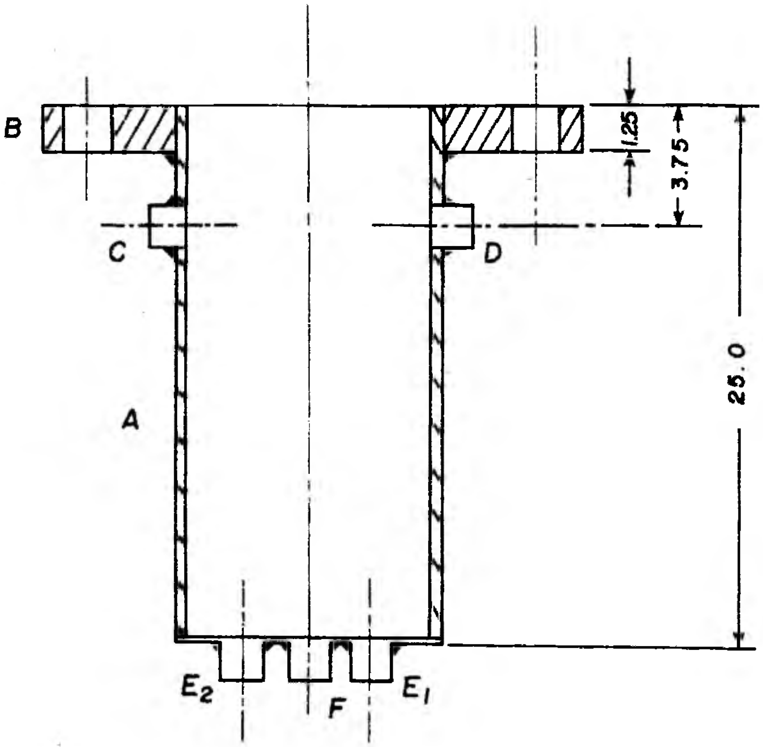
B
1.25
3.75
C
D
A
25.0
E$_2$
F
E$_1$

TOP VIEW

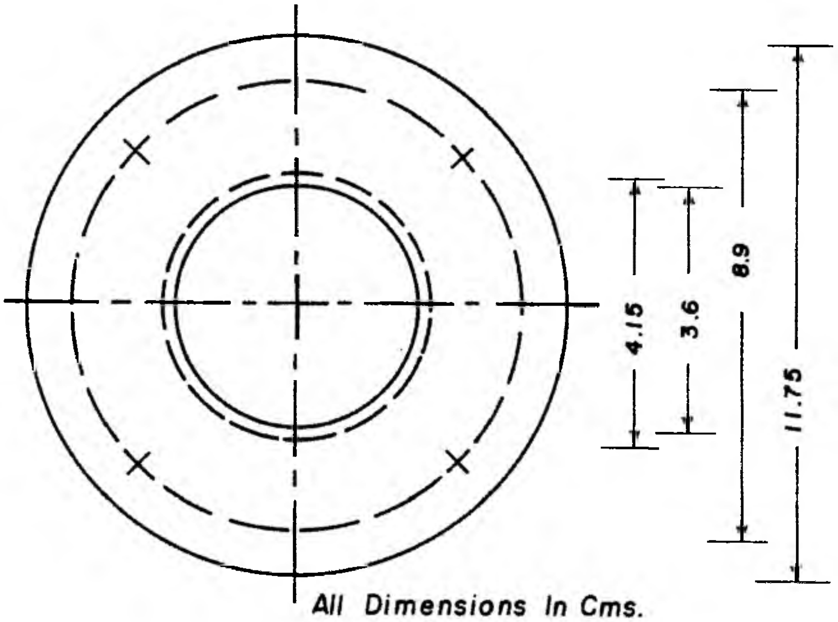
4.15
3.6
8.9
11.75

All Dimensions In Cms.

150 lb flange (304 stainless steel) for the above pipe size was welded to one end of the pipe. The other end was closed with provisions for introducing the fluidization gas and for withdrawing solids (coked sand) through a stand pipe. The preheater flange was bolted to the bottom flange of the main reactor. The inlet pressure and the temperature of the fluidization gas entering the reactor were measured at taps 1 and 2, respectively. These taps were located opposite each other and were 2.5 cm below the preheater flange. The preheater was packed with inert ceramic pellets. The purpose of the packing was to provide a calming section in which a uniform gas flow could be established and to provide improved heat transfer to the gas.

The preheater was heated by means of a tubular furnace rated for 1030 watts at 115 volts. The temperature of the fluidizing gas leaving the preheater was measured by a Type-K (Chromel-Alumel) thermocouple (supplied by Industrial Instrument Division, Illinois), which was introduced through Tap 2. All thermocouples used in this experimental set-up were 0.31 cm in diameter and 22.5 cm in length.

The recording control thermocouple and the heating element were connected to a Love Model 49 Proportioning Controller (manufactured by Love Controls Corporation, Illinois).

The preheater and the furnace were insulated outside by two layers of 2.5 cm thick Cerafelt insulation cloth (supplied by Bullough Asbestos Co., Utah) to minimize heat loss to the surroundings. The pressure tap (Tap 1) was connected to a 0-35 kPa (1 kPa = 0.15 psi) pressure gauge (manufactured by Marshalltown Manufacturing, Inc., Iowa), and to the high pressure side of a differential pressure controller (described later).

The construction details of the fluid bed reactor are presented in Figure 3.4. The reactor was constructed from a 3.13 cm nominal diameter 304 stainless steel schedule 10 pipe with standard 150 lb flanges welded at each end to give a total length of 90 cm between the flange faces. Four taps were provided along the length of the reactor and are marked as 3, 4, 5, and 6 in Figure 3.4. The distance of each tap from the bottom of the reactor is also given in Figure 3.4. Tap 3 was used to monitor the bed height during the experiment using a manometer. The procedure for bed height measurement is described in Appendix C. Taps 4, 5, and 6 were used to measure the temperature.

A nichrome wire (20 B & S gauge) of 12 ohms total resistance was would around the reactor on 2.3 cm centers as a heating element to provide uniform heating along the length of the reactor. The reactor wall and the heating element were separated by a silica cloth, which prevented electrical conductance between the nichrome wire and the metal wall of the reactor. The heating element was rated for 1200 watts at 120 volts. The temperature of the bed of solids was measured by the thermocouples (Type-K) introduced through Taps 4 and 5. The thermocouple at Tap 4 was also connected to a Barber-Coleman Model 472 P temperature controller (manufactured by Industrial Instruments Division, Illinois) for temperature control of the bed of solids in the reactor. The vapor phase temperature within the reactor was monitored by the thermocouple inserted through Tap 6. The

Figure 3.4

Schematic of the Reactor Unit

A.	Reactor Body
B.	Coked Sand Sampling Port
C.	Standard 150 lb Flange
Tap 3.	Manometer Connection Port
Taps 4, 5 and 6.	Thermocouple Ports

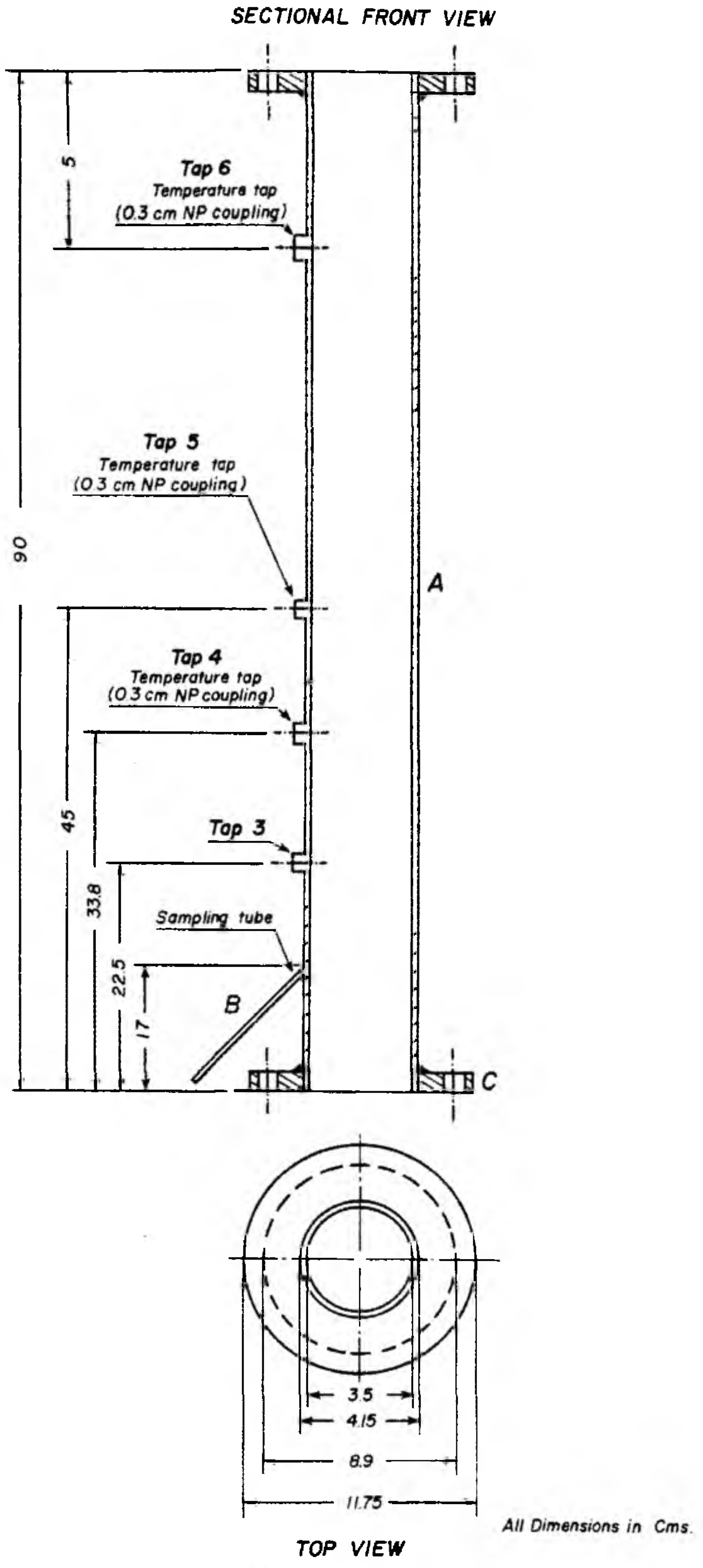
SECTIONAL FRONT VIEW
5
Tap 6
Temperature tap
(0.3 cm NP coupling)
Tap 5
Temperature tap
(0.3 cm NP coupling)
90
A
Tap 4
Temperature tap
(0.3 cm NP coupling)
45
Tap 3
33.8
Sampling tube
22.5
17
B
C
3.5
4.15
8.9
11.75
TOP VIEW

All Dimensions in Cms.

temperature indicated by the thermocouple at Tap 5 was generally within 5 K of the control temperature indicated by the thermocouple at Tap 4. The thermocouples of Taps 5 and 6 were connected to a Wheelco temperature indicator (manufactured by Wheelco Instruments Co., Illinois) through a Barber-Coleman Model 801 A-6 thermocouple selector switch (manufactured by Industrial Instruments Division, Illinois). An 0.625 cm O.D. (304 stainless steel schedule 10) tubing of 15.2 cm in length was braced to the reactor at 17 cm from the bottom flange of the reactor. The other end of this tubing was connected to an 0.625 cm stainless steel ball valve. This tubing served as a sampling tube for periodically withdrawing coked sand samples from the reactor during the experimental run. The reactor was insulated on the outside by two layers of high temperature Cerafelt insulation cloth of 2.5 cm thickness.

The gas distributor was located between the lower flange of the reactor and upper flange of the preheater as shown in Figure 3.2. The distributor screen was cut from a Tyler 325 mesh stainless steel screen cloth and was held in place between two stainless steel rings which were welded together.

The details of the gas distributor are shown in Figure 3.5. The gas distributor also served to support the bed of solids, when the bed was not fluidized. At the center, the gas distributor had a 1 cm orifice through which the sand standpipe passed. Standard 150 lb Flexitallic metal gaskets (supplied by Elastomer Products, Utah) were placed above and below the gas distributor to form a gas seal.

Figure 3.5

Detail of the Gas Distributor

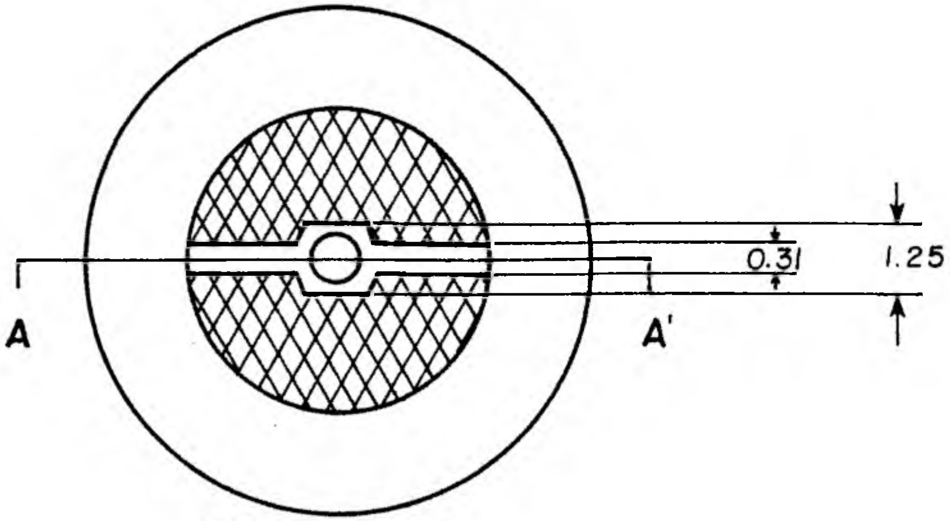

TOP VIEW

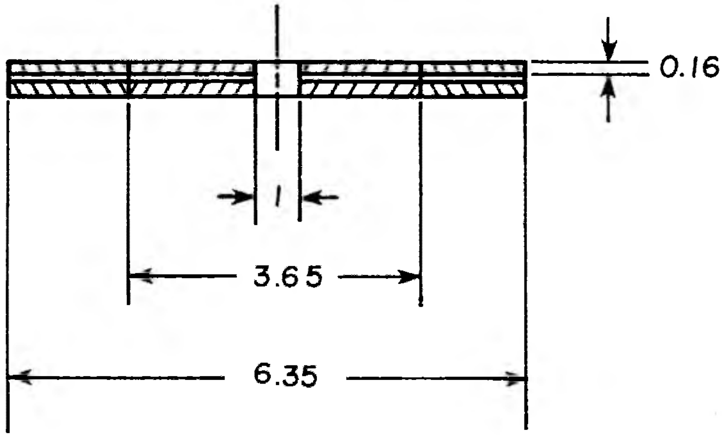
0.16
1
3.65
6.35

SECTIONAL FRONT VIEW ON AA'

▩ SCREEN CLOTH (SS 304)

▨ SS 304

▧ SS 304

All Dimensions In Cms.

The details of the expansion chamber, which was located above the reactor, are presented in Figure 3.6. The purpose of the expansion chamber was to decrease the velocity of the gas leaving the reactor facilitating the separation of the solids and gas, decreasing the entrainment of solids from the reactor. Furthermore, the chamber facilitated the easy addition of fresh bituminous sand to the reactor.

The expansion chamber was fabricated from a 7.5 cm nominal diameter 304 stainless steel schedule 10 pipe 22.5 cm in length and a 3.13 cm nominal diameter 304 stainless steel schedule 10 pipe 8.75 cm in length. The two pipes were connected to each other by a conical section as shown in Figure 3.6. A standard 150 lb flange was welded to the 3.13 cm nominal diameter pipe (lower end of the expansion chamber). A flange, made from an 0.625 cm thick 304 stainless steel plate, was welded to the 7.5 cm nominal diameter pipe (upper end of the expansion chamber). Two taps (Taps 7 and 8) were located 3.8 cm from the upper end of the expansion chamber. A pipe nipple 0.63 cm in diameter and 7.5 cm in length was connected to Tap 7. The other end of the nipple was connected to an 0.63 cm pipe tee. A Type-K thermocouple was introduced through one port of the tee, while the other port was used as a pressure tap. The pressure tap was connected to a Marshalltown pressure gauge (0-35 kPa range) for pressure measurement and to the differential pressure controller (described below). The gas stream containing the oil vapor exited from the chamber through Tap 8.

The heating element for the expansion chamber was a nichrome wire of 17 ohms total resistance. The wire was wound around the

Figure 3.6

Schematic of the Expansion Chamber

A. Expansion Chamber Body

Tap 7. Pressure and Temperature Measuring Port

Tap 8. Vapor-Gas Mixture Exit Port

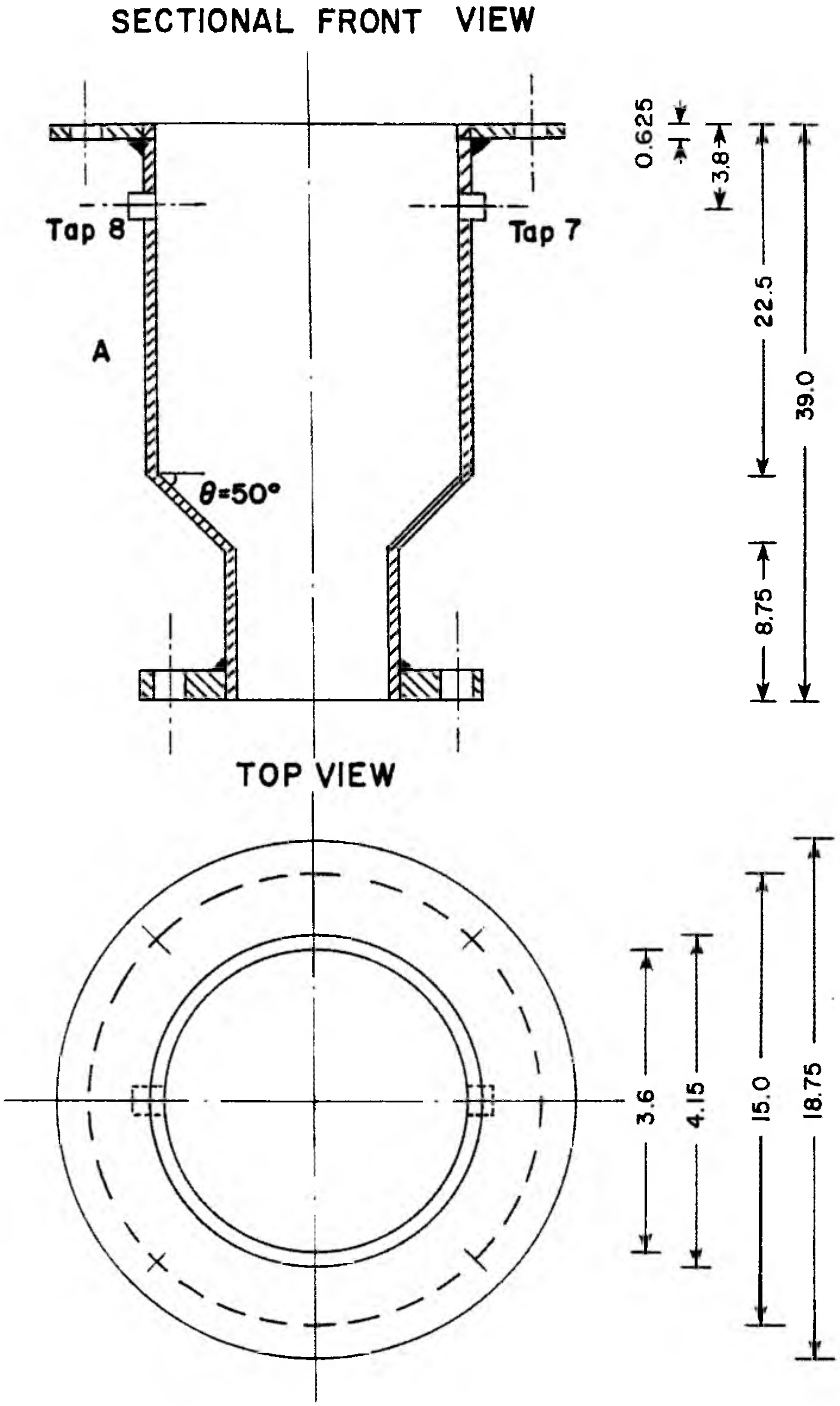
SECTIONAL FRONT VIEW
Tap 8
Tap 7
A
θ=50°
0.625
3.8
22.5
39.0
8.75
TOP VIEW
3.6
4.15
15.0
18.75

ALL DIMENSIONS IN Cms.

expansion chamber on 1.5 cm centers and was separated from the walls of the expansion chamber by a silica cloth. The expansion chamber heating element was rated for 1000 watts at 120 volts. The Type-K thermocouple (Tap 7) was connected to a Barber-Coleman Model 272 P temperature recorder-controller (Industrial Instruments Division, Illinois) for temperature measurement and control. Two layers of high temperature Cerafelt insulation cloth 2.5 cm thick were wrapped around the expansion chamber to minimize heat losses. The lower flange of the expansion chamber was bolted directly onto the top flange of the reactor. Two standard 150 lb Flexitallic metal gaskets were used to provide a gas seal between the expansion chamber and the reactor.

Since the system was operated as a continuous process, in which the bituminous sand was continuously added to the expansion chamber and coked sand was continuously withdrawn from the bottom of the reactor, the solids bed weight was maintained constant to prevent accumulation of solids within the bed. This was achieved by the differential pressure controller in combination with a pneumatically operated solids discharge valve (described in detail in section 3.2).

The specifications for the ITT Barton Model 338 pressure recording pneumatic controller (manufactured by Barton Instruments, California) are presented in Table 3.1.

The primary function of the recorder-controller was to maintain the bed of solids in the reactor at a fixed level ('set point'). The 'set point' in this system was the differential pressure (ΔP) corresponding to a fixed bed weight of solids.

Table 3.1

Differential Pressure Controller Specifications

Actuator:	Model 199 Differential Pressure Unit
Instrument Air:	20.7 - 103.5 kPa
Output Air:	20.7 - 103.5 kPa
Temperature Limits:	222 K to 367 K (Ambient)
Differential Pressure (DP) Range:	0 - 125 cm water column
Accuracy of DP Recording:	± 1/2% full scale differential pressure
Safe Working Pressure:	6890 kPa
Bellows Material of Construction:	316 stainless steel
Operating Fluid of the Bellows:	Mineral oil, Grade 1005

The system was maintained at the 'set point' by measuring the actual differential pressure across the bed of solids and comparing it with the 'Set point'. The controller actuated the solids discharge valve to close or open position, depending upon the deviation between the actual differential pressure and the 'set point'.

The reactor pressure taps (Tap 1 and Tap 7) were connected to the Differential Pressure unit (DPU) of the recorder-controller as shown in Figure 3.7. The regulating valves, as shown in Figure 3.7, were used to damp the pressure impulse from the reactor. The calibration procedure of the differential pressure recording controller is described in section 3.5.

3.2 Introduction and Withdrawal of Solids

An integral part of the thermal recovery scheme was the method of introducing the bituminous sand to the fluidized bed of solids and the withdrawal of the coked sand from the bed. The selection of a solids feeding device was dependent upon a thorough understanding of the rheological characteristics of the material which was fed. The critical parameters which must be considered in the selection of a solids feeding device have been reviewed(126,127).

Screw feeders were versatile enough to handle a range of material from powders to lumps, relatively inexpensive, and easily sealed to prevent the emission of dust or vapor. Since the crushed and sized bituminous sands of Tarsand Triangle and Sunnyside deposits exhibited acceptable rheological behavior, they were fed at a uniform rate using

Figure 3.7

Differential Pressure Controller - Piping Diagram

REACTOR ASSEMBLY

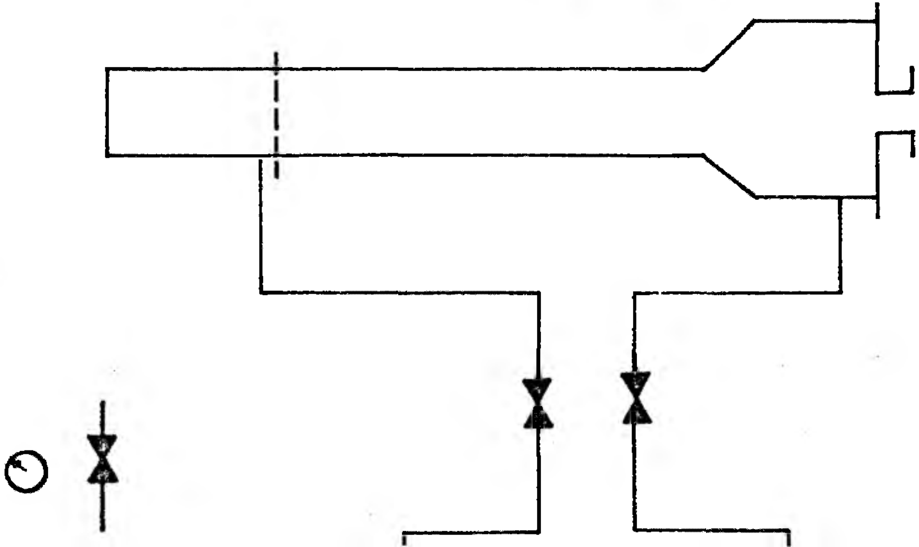

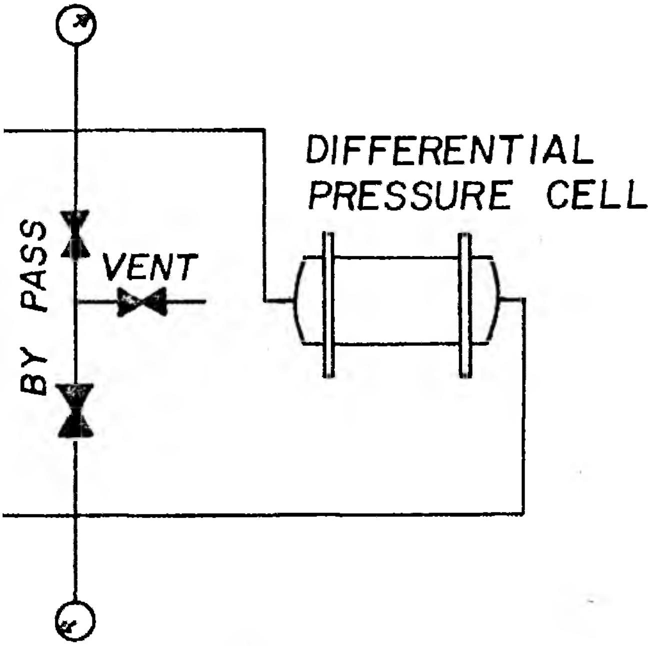
DIFFERENTIAL PRESSURE CELL
VENT
BY PASS

REGULATING VALVE

PRESSURE GAUGE

a screw feeder. Although there were several design variations that promoted uniform solids withdrawal from the hopper, a standard, full pitch screw configuration was found to be satisfactory.

The design features of the screw feeder used in this study are shown in Figure 3.8. The screw was made from 304 stainless steel and had the following dimensions: diameter 4.38 cm, and length 25.4 cm, with a pitch of 3.13 cm. The screw flight thickness was 0.16 cm and the screw shaft diameter was 1.27 cm. The screw was housed in a tube (5.08 cm O.D. and 4.7 cm I.D.) and the clearance between the screw flight and the housing tube was 0.16 cm. The end of the screw shaft was housed in the brass bushing, located at the center of the flange (1.88 cm thick 304 stainless steel disc). The other end of the shaft was connected to the motor drive assembly.

The inlet tube of the screw feeder was a 2.5 cm I.D. (304 stainless steel schedule 10) tube and was 7.3 cm in length. One end of this tube was welded to the screw housing and the other end to a 10.8 cm diameter flange. The outlet tube was a 3.13 nominal diameter pipe (304 stainless steel schedule 10) and was 12.7 cm in length. One end of this pipe was welded to the screw housing. A standard 150 lb flange was welded to the other end of the tube. A tap was provided in the screw housing for admitting nitrogen as a purge gas. The nitrogen purge prevented the oil vapor-fluidizing gas mixture leaving the reactor from entering the screw feeder and condensing on the bituminous sand feed. In the absence of the purge gas, the vapor condensed on the walls of the feeder outlet tube which caused the bituminous sand feed to stick to the walls and let to the eventual plugging of the

Figure 3.8

Schematic of the Screw Feeder

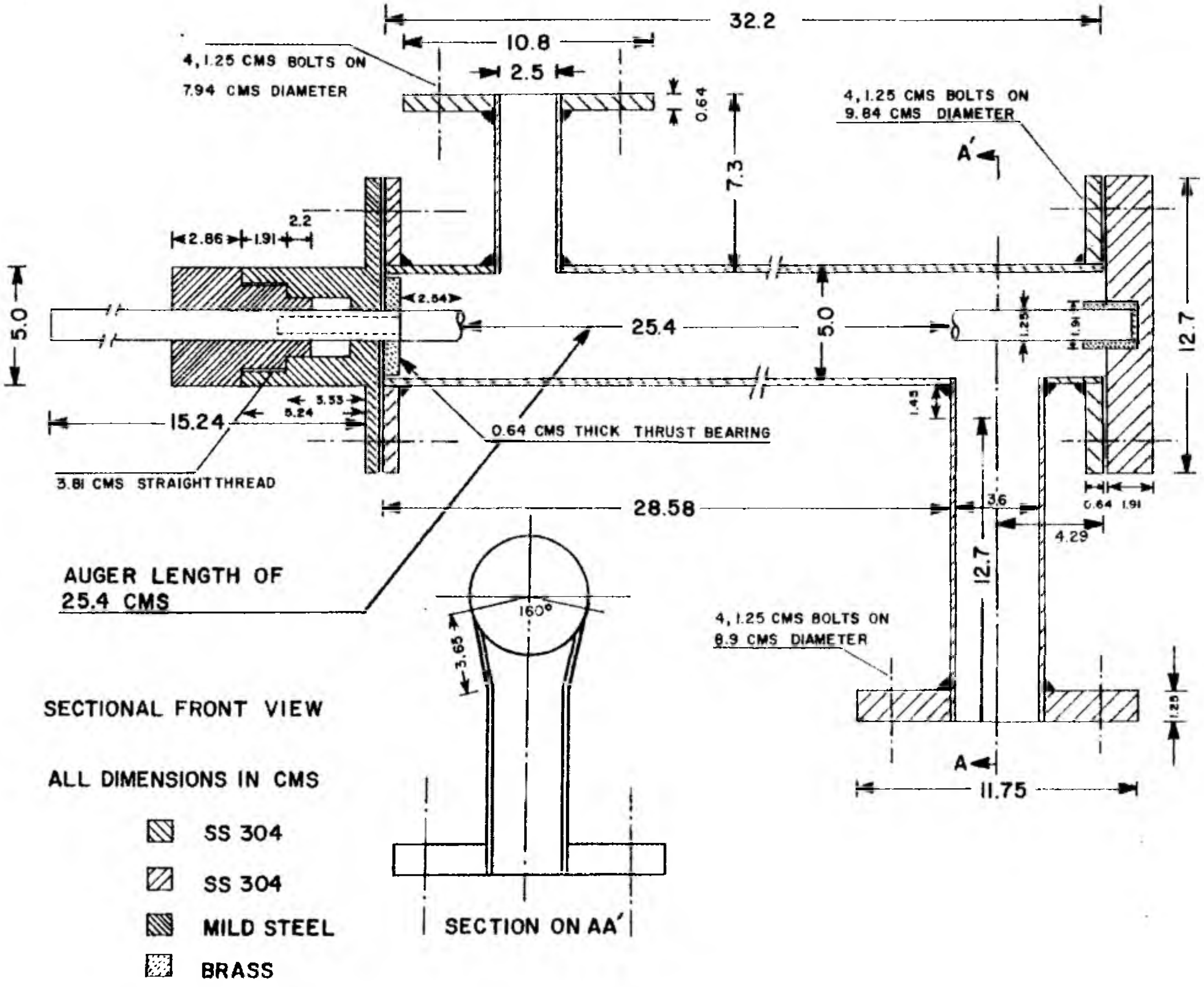

32.2
10.8
2.5
4, 1.25 CMS BOLTS ON
7.94 CMS DIAMETER
0.64
7.3
4, 1.25 CMS BOLTS ON
9.84 CMS DIAMETER
A'
2.2
2.86
1.91
2.54
5.0
25.4
5.0
1.25
1.91
12.7
3.53
5.24
15.24
1.45
0.64 CMS THICK THRUST BEARING
3.81 CMS STRAIGHTTHREAD
28.58
.36
0.64
1.91
4.29
12.7
AUGER LENGTH OF
25.4 CMS
160°
3.65
4, 1.25 CMS BOLTS ON
8.9 CMS DIAMETER
1.25
A
11.75
SECTION ON AA'
▧ SS 304
▨ SS 304
▩ MILD STEEL
▒ BRASS

SECTIONAL FRONT VIEW

ALL DIMENSIONS IN CMS

outlet. The nitrogen purge also prevented bridging of bituminous sand feed at higher feed rates.

The outlet flange of the screw feeder was bolted directly onto the top flange of the connecting section. Thus, the axes of the feeder outlet and the reactor were co-linear enabling the feed sand to fall through the expansion chamber into the fluid bed under free-fall conditions. The bituminous sand became softened as the temperature of the feed sand was raised during the free-fall. Upon release of the oil at higher reactor temperatures, the sand became free flowing and did not adhere to the reactor wall. The outlet of the feeder was thermally isolated from the connecting section by a series of asbestos and standard Flexitallic gaskets. Also, the outlet of the feeder was cooled periodically by spraying water onto the wet cloth wrapped around the outlet pipe. This prevented agglomeration of the bituminous sand during feeding.

A variable speed 1/2 h.p. D.C. Motor, with a Speed-A-Matic VP-150 controller (manufactured by U.S. Electric Motors, Connecticut), and a speed reduction gear assembly was used to drive the screw.

A schematic of the feed hopper is presented in Figure 3.9. It was made from an 0.31 cm thick mild steel plate. The plate was rolled to form the cylindrical section of 27.5 cm diameter and 25.4 cm in length and welded. The cylindrical section of the hopper and one end of the outlet tube (2.54 cm O.D. and 2.54 cm in length) were connected by a conical section as shown in Figure 3.9. A flange of 10.8 cm outside diameter and 1.25 cm thick was welded to the other end of the outlet tube. The hopper was bolted to the inlet of the screw feeder.

Figure 3.9

Schematic of the Feed Sand Hopper

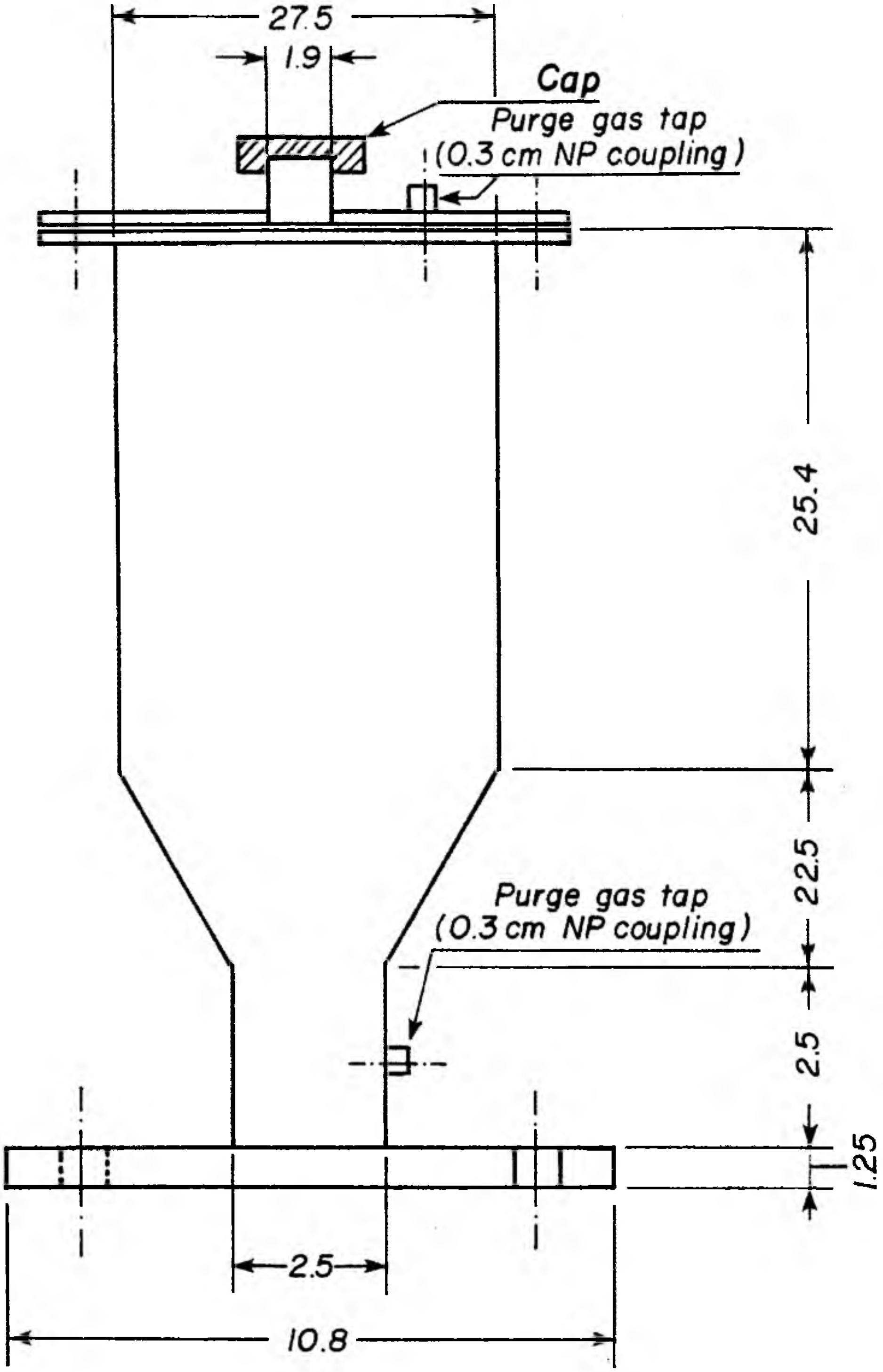
27.5
1.9
Cap
Purge gas tap
(0.3 cm NP coupling)
25.4
22.5
Purge gas tap
(0.3 cm NP coupling)
2.5
1.25
2.5
10.8

All Dimensions in Cms.

The coked sand must be removed continuously to maintain a constant weight of solids in the bed in a continuous steady state process. This was achieved by a sand withdrawal standpipe combined with a solids control valve, which was operated pneumatically.

A detailed diagram of the solids control valve is presented in Figure 3.10. The solids control valve was made of a brass body with an inlet port and an outlet port. A cylindrical opening of 1.25 cm in diameter was machined such that a 1.25 cm diameter cylindrical rod slid as a piston. The inlet and the outlet were also connected through a 0.93 cm valve opening. The piston had a travel length of 0.93 cm. The valve was packed with Sepco 910 high temperature packing and was operated by a pneumatic Honeywell actuator. The valve opening could be varied between 0 to 100% (100% full open, 0% fully closed), depending upon the air pressure applied to the actuator by the differential pressure controller.

The inlet port of the solids control valve was connected to the sand standpipe, which extended above the gas distributor screen (about 0.5 cm) (Figure 3.2). The outlet port was connected to a coked sand receiver.

3.3 Oil Product Recovery System

The oil vapor leaving the fluid bed reactor formed an aerosol which was observed at the condenser outlet. The recovery of oil from an aerosol or mist can be achieved by various techniques. The efficiency of a variety of aerosol or mist eliminating devices was investigated and the performance and limitations of each are discussed in Appendix D.

Figure 3.10

Solids Control Valve

A. Brass Body

B. Valve Piston

C. Adjustable Lock Nut

D. Sepco High Temperature Packing

E. Inlet and Outlet Ports

SECTIONAL

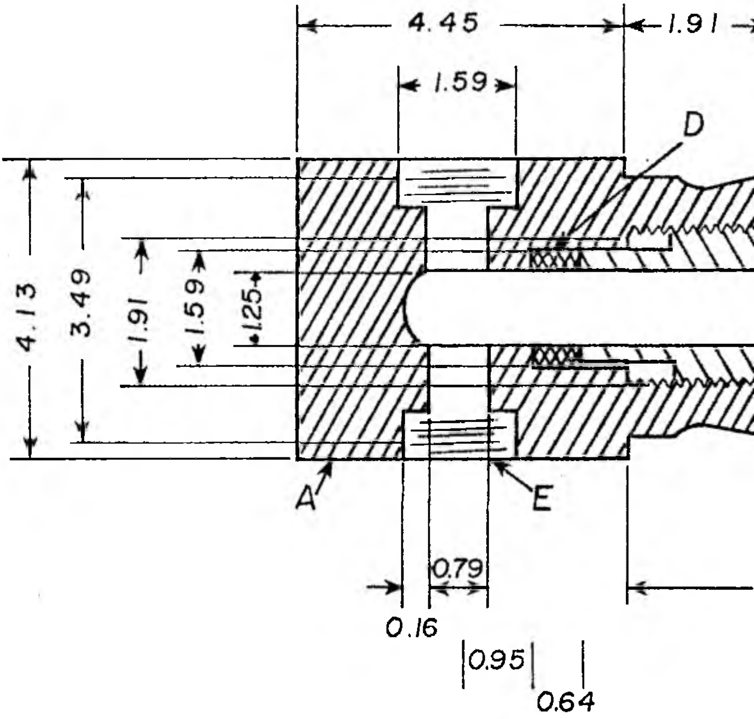
4.45
1.91
1.59
D
4.13
3.49
1.91
1.59
1.25
A
E
0.79
0.16
0.95
0.64

FRONT VIEW

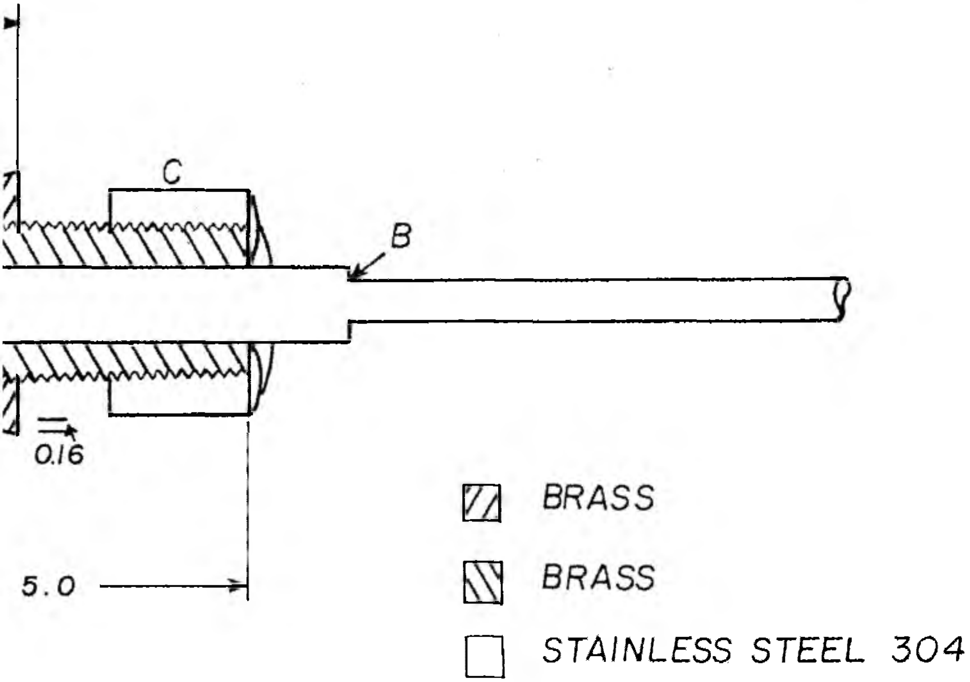
C
B
0.16
5.0
▨ BRASS
▧ BRASS
☐ STAINLESS STEEL 304

All Dimensions In Cms.

The oil product recovery system used in this study consisted of a series of cyclones and a filter, which were operated at high temperature (673 K), for recovering sand fines. The fines, which were elutriated from the bed, were carried along with the oil vapor-fluidizing gas mixture. The oil vapor-gas mixture was cooled in a water cooled condenser after the fines had been removed. The presence of an aerosol or an oil mist was observed at the condenser outlet. A cyclone separator removed a fraction of the oil from the oil mist. The gas and the remaining oil mist were passed through an air cooled condenser tube before entering a series of fiber mist eliminators where the oil was quantitatively removed. The oil collected on the fibers was washed with solvent and the solvent was recovered and reused.

The two cyclones used for sandfines removal were identical and were designed according to the procedure given in the Chemical Engineering Handbook(127). The first cyclone, used for fines removal, was connected to the gas outlet part of the expansion chamber (Tap 8) by a 0.93 cm diameter and 7.5 cm in length flexible Cajon tubing. This was to allow for the thermal expansion of the fluid bed reactor assembly, when it was heated from the ambient temperature to the operating temperature. The configuration of the cyclone separator is presented in Figure 3.11. The combined efficiency of the two cyclones was greater than 95%. The cyclones were heated by means of Briskeat flexible heating tapes (manufactured by Briscoe Manufacturing Co., Nevada) rated at 384 watts at 115 volts. The Cajon flexible tubing was heat traced with a Briskeat heating tape rated at 192 watts at 115 volts. The temperature of the gas stream leaving each cyclone

Figure 3.11

Sand Fines Cyclone Separator Configuration

A. Inlet Port

B. Cyclone Body

C. Gas Outlet

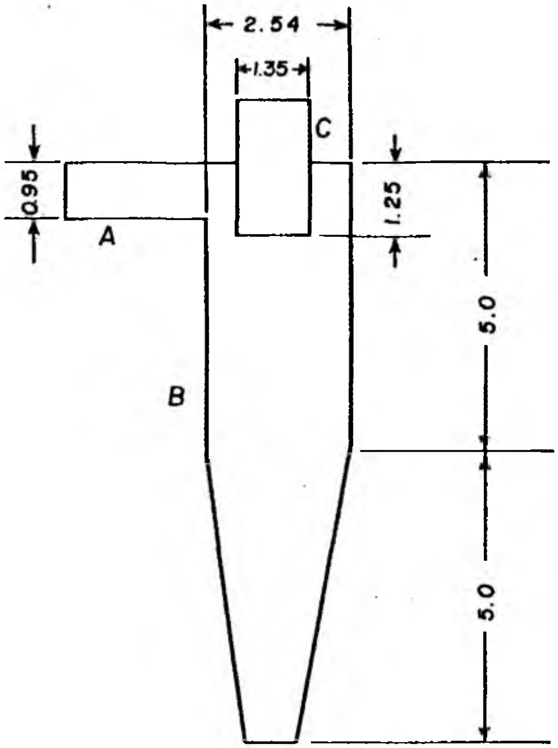
2.54
1.35
C
0.95
A
1.25
5.0
B
5.0

FRONT VIEW

All Dimensions In Cms.

outlet was measured by a Type-K thermocouple. The thermocouples were connected to a Wheelco temperature indicator through a multi-point switch. The temperature of each cyclone was controlled by a pre-calibrated Variac, to which the heating tapes were connected. The cyclones and the connecting sections were insulated with Cerafelt insulation cloth.

The filter, which removed the remaining sand fines, was connected to the outlet of the second cyclone. The filter element was a MCS 1001 PE sintered stainless steel cartridge (supplied by Pall Trinity Micro Corporation, New York). The schematic diagram of the filter is presented in Figure 3.12. The filter element housing was a 12.5 cm O.D. 304 stainless steel schedule 40 pipe and was 37.5 cm long. One end of the pipe was closed, with a 1.25 cm NPT coupling welded into the center of the plate as inlet port. The filter cartridge was attached to a 2.5 cm thick stainless steel disc, which could be screwed on to the other end of the housing as shown in Figure 3.12. A Type-K thermocouple was introduced through a coupling to measure the gas temperature. The filter heating element was a nichrome wire wound on 2 cm centers of 14 ohms total resistance and was rated at 900 watts at 120 volts. The heating element was wrapped with a Cerafelt insulation cloth. The operating temperature of both the cyclones and filter was about 693 ± 5 K.

The carrier gas and the oil vapor leaving the filter were cooled in a double pipe single pass condenser. The inner tube of the condenser was an 0.93 cm O.D. (304 stainless steel schedule 10) tube through which the carrier gas-oil vapor stream flowed, while the

Figure 3.12

Stainless Steel Filter Configuration

A. Filter Cartridge
B. Housing
C. Gas Outlet
D. Gas Inlet
E. Thermocouple Port
F. Threaded Disc

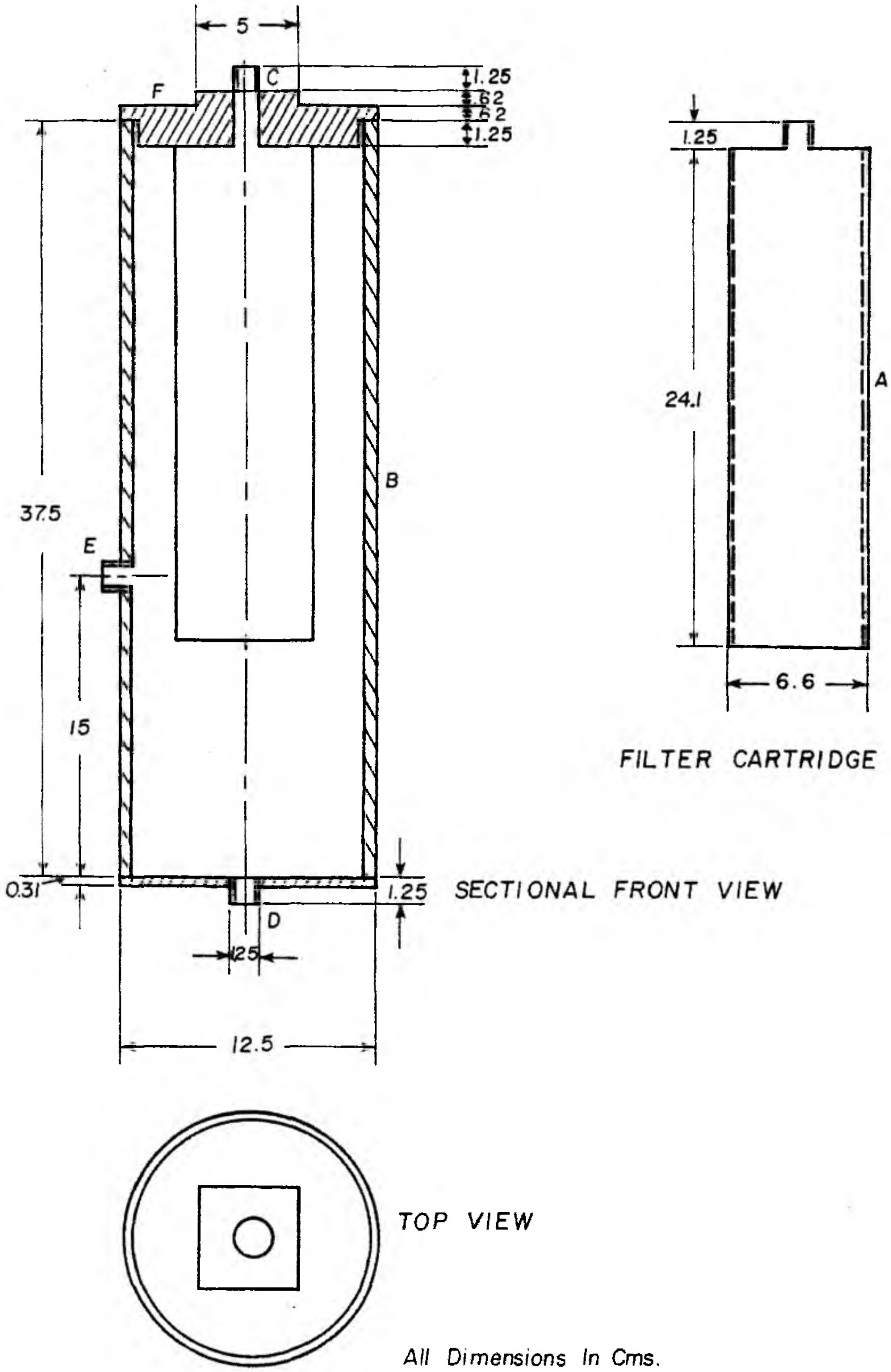
5
C
F
1.25
.62
.62
1.25
37.5
E
B
15
0.31
1.25
D
125
12.5
SECTIONAL FRONT VIEW
1.25
24.1
A
6.6
FILTER CARTRIDGE
TOP VIEW

All Dimensions In Cms.

outlet tube was a 5 cm pipe through which cold water was circulated. The condenser was 90 cm long.

A fraction of the oil which condensed on the walls of the inner tube was collected in a receiver. The remaining condensable vapor observed as oil mist was then passed through a cyclone separator, similar in design to the Figure 3.11, where a portion of the mist was condensed and collected. The cyclone dimensions are given on Figure 3.13.

The remaining mist leaving the cyclone separator was further cooled in an air cooled condensor (0.93 cm O.D. copper tube, 90 cm in length) before entering the fiber mist eliminators operated in series. The fiber mist eliminators were 3.8 cm O.D. (3.0 cm I.D.) pyrex glass columns 75 cm in length and were packed with cellulose fibers. The ends of the glass column were packed tightly with a wire mesh pad (7.5 cm in length) to prevent the entrainment of cellulose fibers. The combined efficiency of the fiber mist eliminators was greater than 92%. The exit gas leaving the second fiber mist eliminator was clean and contained only the light hydrocarbon gases. The oil collected on the cellulose fibers was extracted from the fibers at the end of each run with a solvent (benzene) and the solvent was recovered later (details in section 3.6). The gases leaving the mist eliminators were metered, sampled, and vented to the stack.

3.4 Bituminous Sand Feed Preparation

The bituminous sands used in this study were from the Tarsand Triangle and Sunnyside bituminous sand deposits. The Tarsand Triangle sample was an outcrop sample from NE¼, NE¼ Section 31,

Figure 3.13

Configuration of the Cyclone Separator
for Mist Removal

A. Inlet Port
B. Cyclone Body
C. Gas Outlet

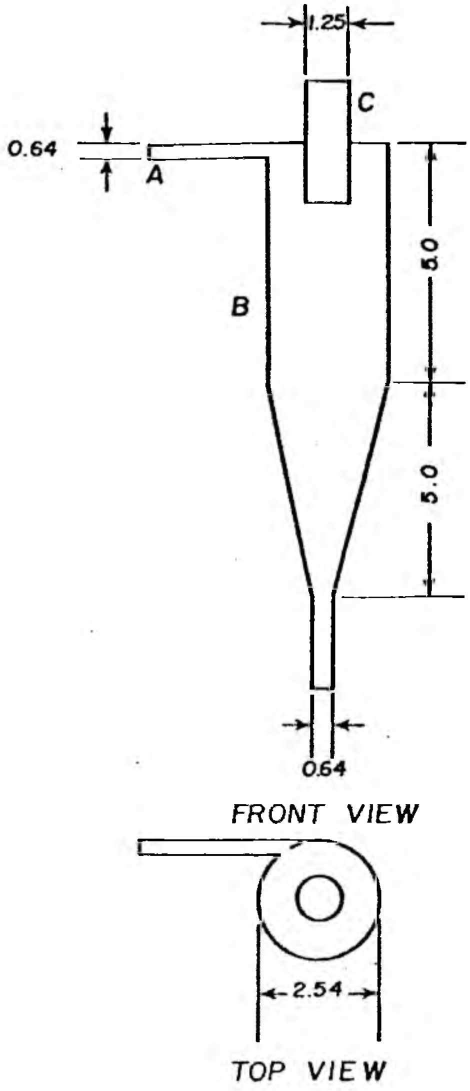
1.25
C
0.64
A
B
5.0
5.0
0.64
FRONT VIEW
2.54
TOP VIEW

All Dimensions In Cms.

T 31 S, R 16 E (near Garfield County, Utah), while the Sunnyside sample was obtained from an old asphalt quarry located northeast of Dragerton, Utah.

Both the Tarsand Triangle and Sunnyside sands are consolidated, oil-impregnated sandstone rocks. The size of the rocks was 20 - 30 cm when received. The rocks were broken into smaller size (8 - 15 cm) using a hammer and the smaller chunks were crushed in a jaw crusher. The product from the jaw crusher was screened into various size fractions using a set of Tyler mesh screens (the screen numbers were 28, 35, 48, 65, 100 and pan).

The oversize fraction (retained on Tyler 28 mesh screen) was ground in a roll crusher. When the Sunnyside sand was ground in the roll crusher, each batch was soaked in liquid nitrogen before grinding. This prevented the agglomeration of the particles during the grinding operation. The product obtained from the roller crusher was also sized. The liquid nitrogen soaking procedure was also used when the Sunnyside sand was screened. The remaining oversize fraction was ground in a pulverizer and size classified.

Each size fraction was thoroughly mixed to make the sample homogeneous. The samples were stored in five gallon buckets, which were closed with tightly sealed lids to prevent oxidation during storage.

The bitumen 'saturation' or 'content' on the sand was determined in a modified soxhlet extraction unit. About 100 - 125 g of the particular bituminous sand was loaded into the extraction thimble. The loaded thimble was placed in the extraction column. Benzene was used as the extracting solvent and the solvent reservoir was kept stirred using a magnetic stirrer. The stirring of the solvent reservoir kept the temperature constant. After several hours of extraction, the extract was replaced with a fresh batch of solvent in the reservoir. When the color of the overflow liquid from the column was clear, the extraction was stopped. The debituminized sand was dried in an oven at 383 K for two hours to remove the solvent. After cooling, the weight of the extracted sand was determined. The drying was continued until a constant weight was obtained.

The extract was filtered several times using Whatmann No. 42 filter paper to remove any sand fines that might have been entrained by the solvent during the extraction. The solvent (benzene) was stripped from the bitumen-solvent mixture using a Büchi rotoevaporator Model RE (manufactured by Brinkmann Instruments, Inc., New York) under a vacuum of 47.1 kPa and a temperature of 353 K. After a major portion of the solvent was stripped from the bitumen-solvent mixture, the pressure was reduced to 0.63 kPa at T = 353 K. This condition was maintained until no more solvent was vaporized, condensed, and collected. The weight percent bitumen content in the sand was determined from the weight of the bitumen. This value was compared with the value obtained from extracted sand. The two values were found to agree reasonably well and the average value was reported.

The bitumen contents for the Tarsand Triangle and Sunnyside bituminous sand were 4.5 wt % and 8.5 wt %, respectively.

3.5 Calibrational Procedures

3.5.1 Calibration of Screw Feeder

The bituminous sand feed rate influences the average holding time of solids in the reactor, for a given bed height of solids. The sand feed rate can be varied by changing the speed at which the screw turns. The calibration of the screw feeder was done as described below. During the calibration of the screw, the feeder and the drive assembly were arranged such that the sand coming from the outlet tube could be collected in a beaker.

The speed of the D.C. motor that drove the screw could be varied by the 10-turn speed control knob located on the Speed-A-Matic VP-150 solid state controller. The dial on the speed control knob was set at 10. With the motor running and using a tachometer, its speed was adjusted to the rated speed of 1750 rpm according to the instruction manual.

Five to six kilograms of sand were loaded into the hopper. The dial on the speed control knob was set at a particular value and the flow rate of solids from the feeder outlet was established. The hourly flow rate of solids was obtained by collecting the sand for 10 minutes and weighing it. This procedure was repeated at least three times to obtain the average flow rate for that setting of the speed control knob. Likewise, the average flow rates for the other dial settings were determined. The results of the sand feed rate calibration for different particle sizes are presented in Figures 3.14 and 3.15.

3.5.2 Calibration of Rotameter

The precise measurement of fluidization gas flow rates is important in this study for the following reasons:

(i) At high temperatures, the velocity of the gas flowing through the reactor can be far greater than required for

Figure 3.14

Feed Rate Characteristic Curves for
Sunnyside Bituminous Sand

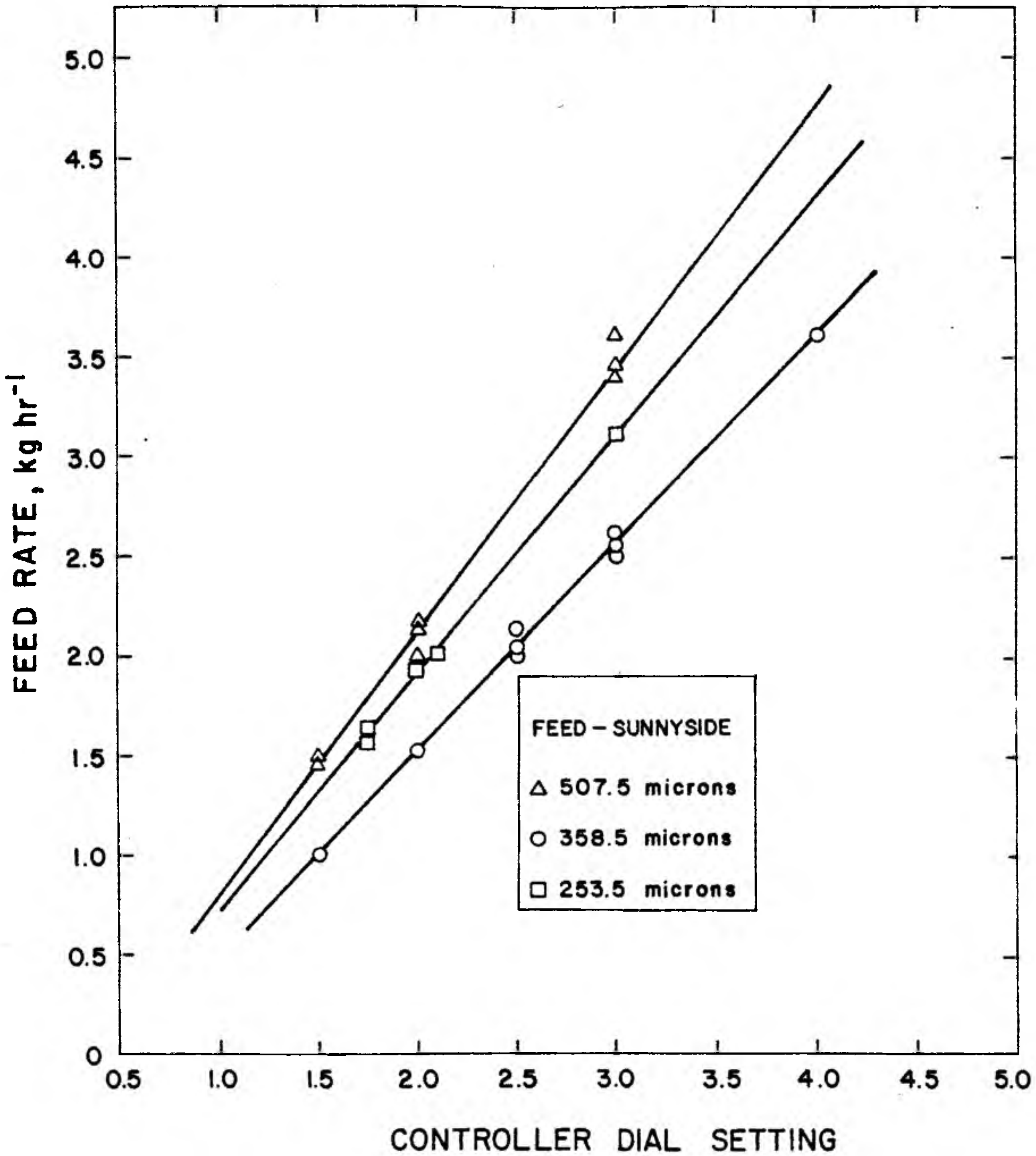
FEED RATE, kg hr⁻¹
0
0.5
1.0
1.5
2.0
2.5
3.0
3.5
4.0
4.5
5.0
0.5
1.0
1.5
2.0
2.5
3.0
3.5
4.0
4.5
5.0
CONTROLLER DIAL SETTING
FEED – SUNNYSIDE
△ 507.5 microns
○ 358.5 microns
□ 253.5 microns

Figure 3.15

Feed Rate Characteristic Curves for
Tarsand Triangle Bituminous Sand

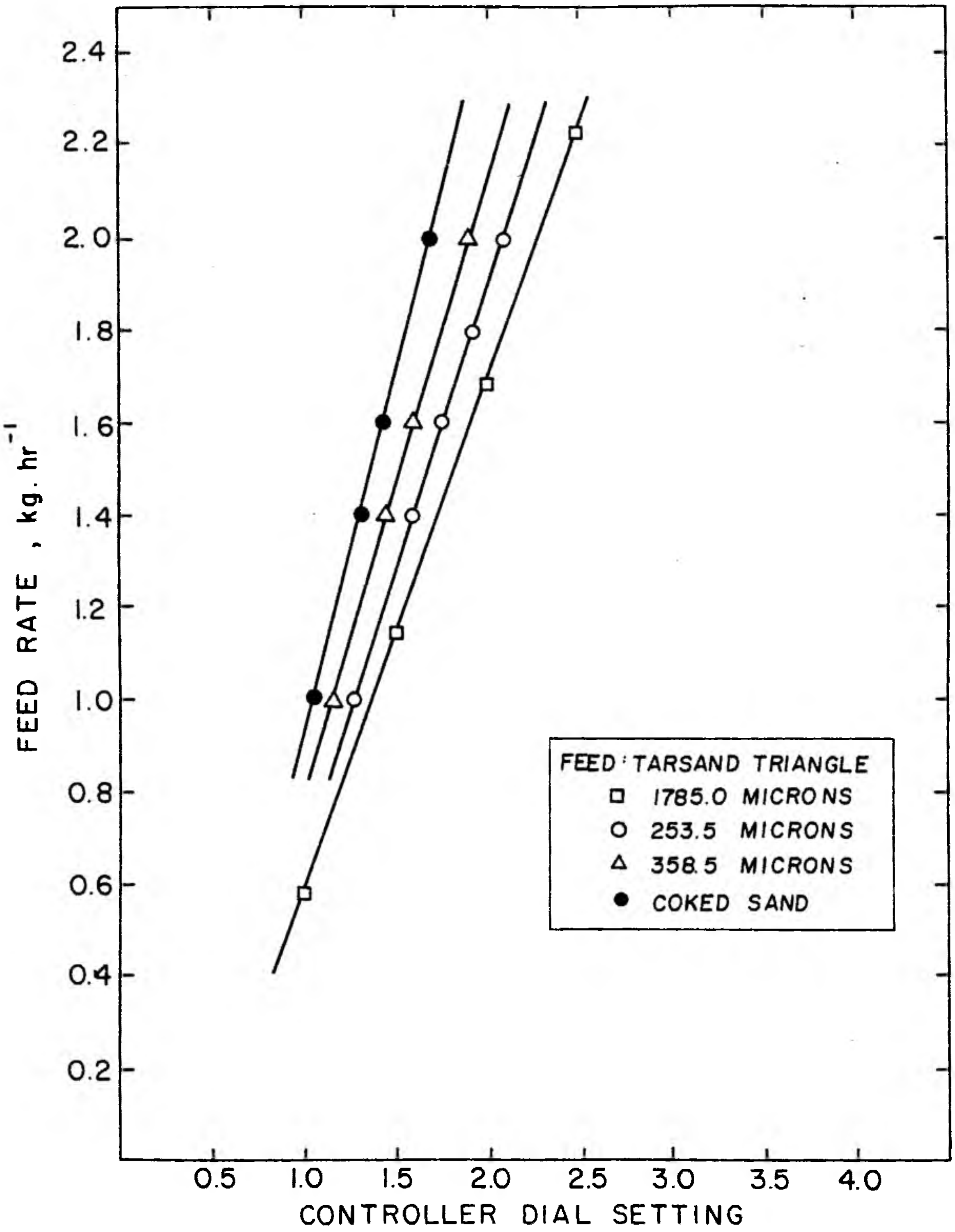
FEED RATE , kg. hr^{-1}
2.4
2.2
2.0
1.8
1.6
1.4
1.2
1.0
0.8
0.6
0.4
0.2
0.5
1.0
1.5
2.0
2.5
3.0
3.5
4.0
CONTROLLER DIAL SETTING
FEED: TARSAND TRIANGLE
□ 1785.0 MICRONS
○ 253.5 MICRONS
△ 358.5 MICRONS
● COKED SAND

for minimum fluidization. This could result in severe "slugging" of the bed (Appendix C). "Slugging" of the bed can be minimized by operating at velocities slightly higher than the maximum fluidization velocity.

(ii) Because the fluidizing gas (nitrogen) does not participate in the cracking reactions of the bitumen, it is used as the internal standard to calculate the product gas make.

A rotameter (manufactured by Fischer and Porter Co., Pennsylvania) was installed as shown in Figure 3.1. The rotameter float was a constant density glass ball (density 2.28 g/cc). A wet test meter (manufactured by Precision Scientific, Illinois) was used to measure the volumetric flow rate of the gas. The manometer fluid of the wet test meter was a liquid with a specific gravity of 2.92. Since the gas was compressible, the pressure gauge (P1) was installed in the downstream side and ahead of the control valve (V2) for correcting the indicated flow for pressure. The nitrogen flow was established with the inlet valve (V1) and control valve (V2) closed and the by-pass valve (V3) fully open. The outlet pressure of the two-stage regulator was adjusted to 240 kPa. The valve (V1) was opened slowly to equalize the pressure, then it was opened all the way. The valve (V2) was opened slowly and the float was brought to the desired scale reading. The cumulative volume of gas flow during a fixed time interval of 10 minutes was calculated from the wet test meter and the volumetric flow rate at standard conditions was computed for that scale reading. The calibration curve for fluidization gas (nitrogen) is presented in Figure 3.16.

Figure 3.16

Characteristic Flow Curve for
Fluidizing Gas (Nitrogen)

Tube: Fisher Porter - $\frac{1}{4}$ - 16 - G - 5

Float - Constant Density Glass Ball

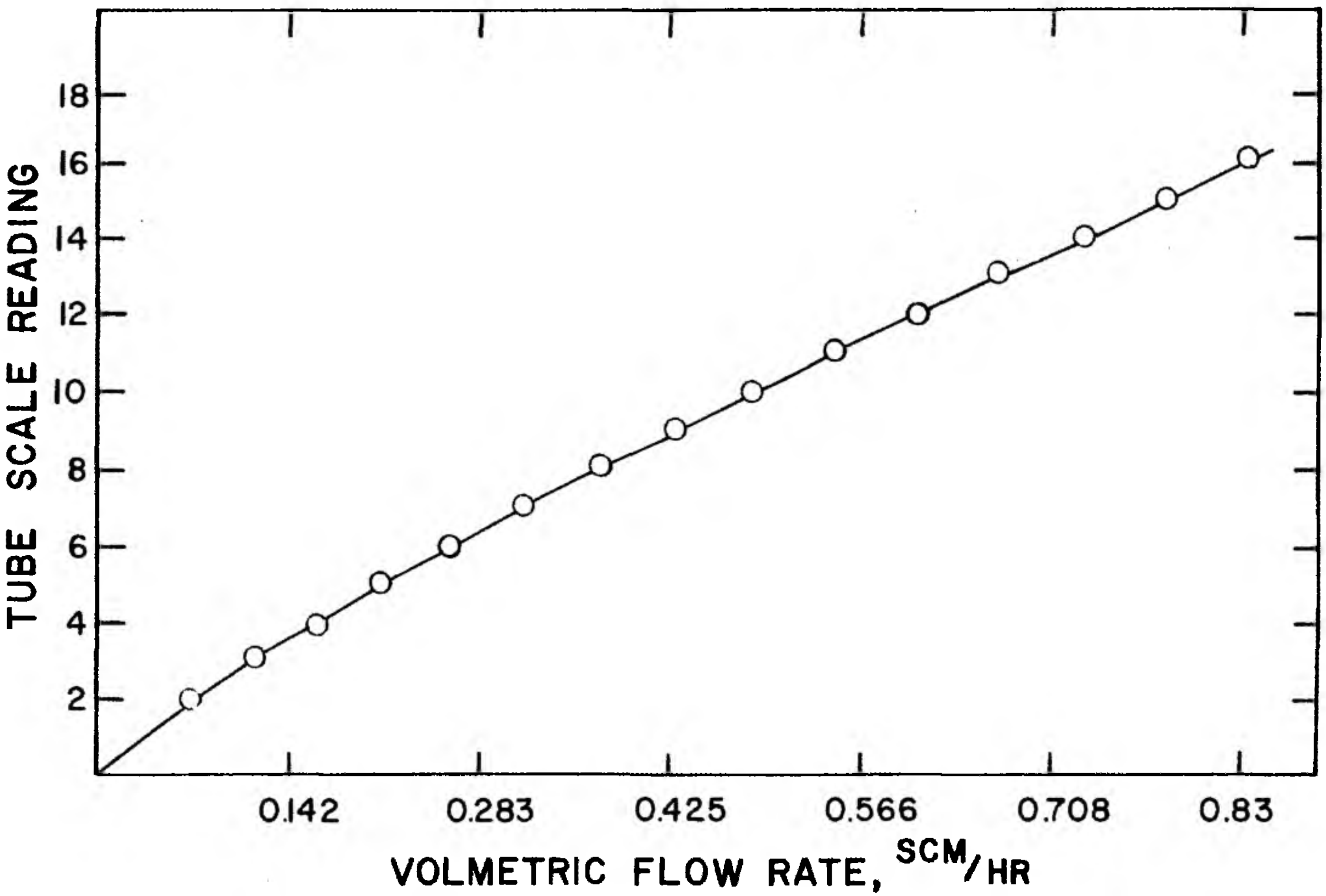
TUBE SCALE READING
2
4
6
8
10
12
14
16
18
0.142
0.283
0.425
0.566
0.708
0.83
VOLMETRIC FLOW RATE, SCM/HR

3.5.3 Calibration of the Differential Pressure Controller

The weight of solids in the bed has a direct influence on the retention time of the solids. At the onset of fluidization, the pressure drop across the bed (ΔP_{eq}) is directly related to the weight of solids (W) in the bed as given by

$$\Delta P_{eq} = \frac{W}{A_c}$$

where A_c is the cross-sectional area for flow.

The differential pressure unit (DPU), which was used to measure ΔP, was recalibrated using coked sand. The range of the DPU was 0 - 125 cm water column (W.C.) and the circular chart of the recorder had 0 - 100 divisions. A U-tube manometer of one meter in length was connected across the DPU as shown in Figure 3.17. With no gas flowing through the reactor, the position of the indicator pointer was made to coincide with the zero on the circular chart using the "zero adjusting" screw, if necessary. The pressure drop across the gas distributor was then measured in the desired temperature range (673 - 873 K) for different gas flow rates. This pressure drop was found to be small. With the screw feeder removed from the connecting section, the reactor was loaded with a known weight of coked sand. Before the coked sand was loaded, the gas flow was stopped. The calibration of the DPU was first done at room remperature. The pressure drop across the bed was measured and checked with the position of the indicator pointer on the recorder scale. The gas flow was increased slowly until the bed reached the fluidized state. The pressure drop measured in centimeters of water by the manometer was compared with the differential pressure

Figure 3.17

Differential Pressure Unit Calibration Arrangement

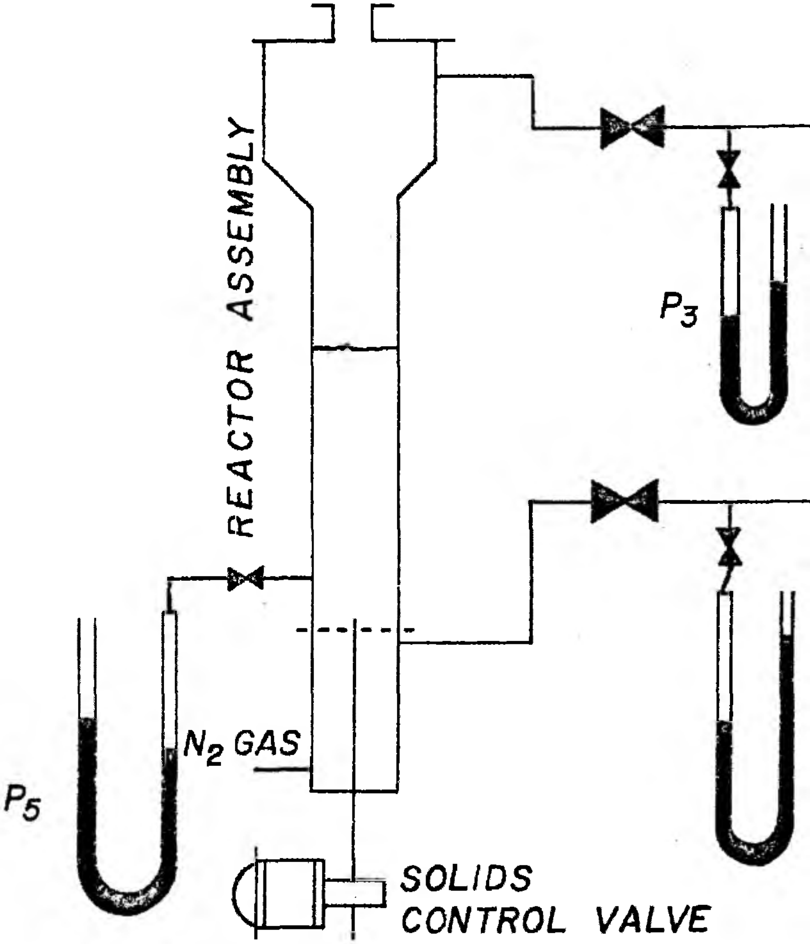
REACTOR ASSEMBLY
P3
P5
N2 GAS
SOLIDS CONTROL VALVE

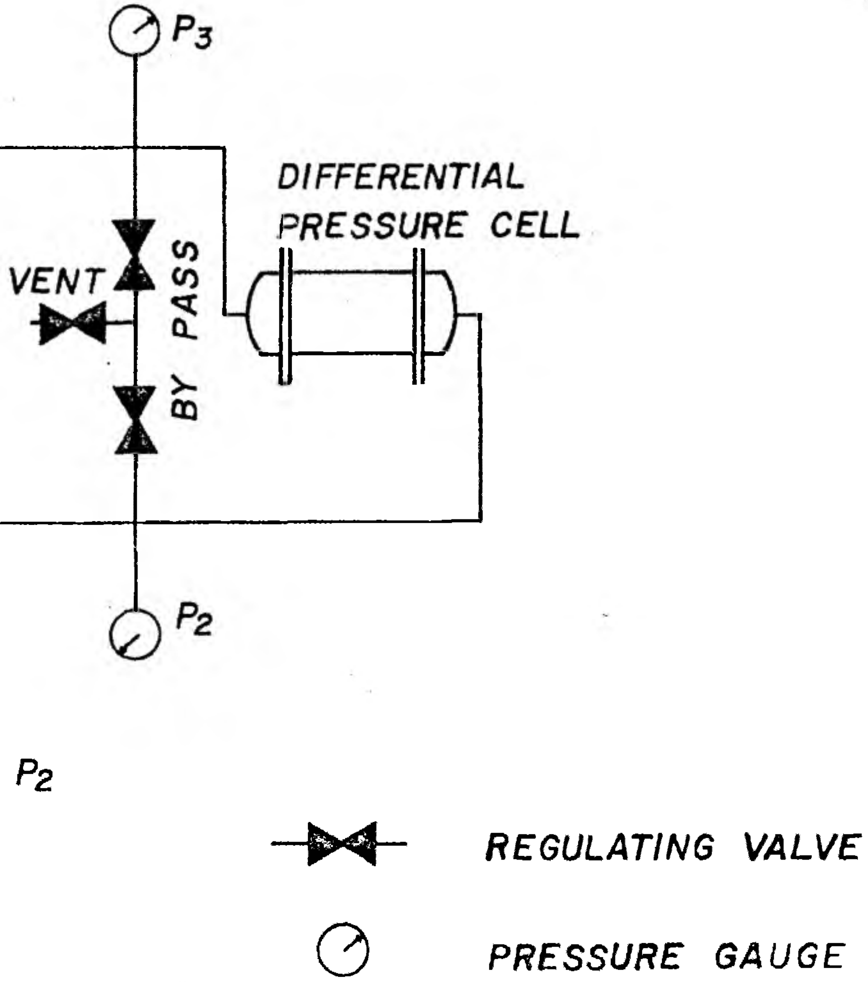
P3
DIFFERENTIAL
PRESSURE CELL
VENT
BY PASS
P2
P2
REGULATING VALVE
PRESSURE GAUGE

value indicated by the DPU and the agreement was found to be satisfactory. Each division of the circular chart was found to represent a pressure drop of 1.25 cm W.C.. The procedure was repeated in its entirety at a higher temperature (723 K). The calibration results agreed satisfactorily for these two temperatures.

3.6 Operational Procedures

In the description of the operating procedures, the identifying numbers and letters refer to Figure 3.1.

1. Before starting the experiment, approximately 6-8 kg of coked sand from the previous runs was screened through Tyler 28 mesh to eliminate aggregates of sand.

2. A known quantity of the desired bituminous sand was weighed and the lumps were removed. When the feed sand source was Sunnyside, the bituminous sand was mixed with the coked sand in a weight ratio of 1:1. This improved the flow characteristics and facilitated feeding the sand to the reactor.

3. The electrical connections to all heaters were checked and the 'set points' on the temperature controllers were adjusted to the desired operating temperatures.

4. The cooling water flow to the condenser (N) and the exhaust fan of the vent system were started.

5. The main valve (V7) of the air line connected to the differential pressure recorder-controller supply was opened. The instrument air pressure to the recorder-controller was adjusted to a gauge pressure of 68.9 kPa using the regulator valve (R3).

6. The outlet pressure of the two-stage regulator, connected to the nitrogen gas manifold, was adjusted to 240 kPa with the by-pass valve (V3) open.

7. The control valve (V2) was opened after opening the inlet valve (V1) fully. The by-pass valve (V3) was closed and the fluidizing gas flow rate was adjusted to the desired value [rotameter (B_1)] using control valve (V2).

8. The empty bed pressure drop was noted along with the readings on the pressure gauges P2 and P3.

9. The coked sand was charged to the hopper (H) and the D.C. motor drive (G) was engaged with the screw feeder (F).

10. The purge gas flow rate was adjusted to the desired value [rotameter (B_2)] using the valve (V5).

11. The coked sand feed rate was adjusted to the desired value using the speed control knob on the VP-150 controller (I).

12. With the control mode on "auto" position, the set point of the differential pressure controller (Y) was increased in steps of 10 divisions of the circular recorder chart until the final pressure drop of 6.46 kPa, corresponding to the bed weight of 0.68 kg, is reached. This incremental increase in the pressure drop facilitated smooth operation of the solids control valve (V10).

13. The heaters of the pre-heater (C), the reactor (D), the expansion chamber (E), the cyclones (K1 and K2) and the filter (M), were energized after the desired bed height and bed pressure drop was reached.

14. The temperatures indicated by each thermocouple was monitored and recorded periodically.

15. When the temperatures of the individual sections reached their set values, the pressure indicated by P2 and P3 were noted.

16. The feed sand was added to the hopper with a small amount of coked sand still remaining in the hopper (H). The desired feed rate was set prior to adding the bituminous sand.

17. The differential pressure controller was set on "auto" control mode after the addition of the bituminous sand to the hopper.

18. When the oil mist was observed at the inlet of the fiber mist eliminator (W), a stop-clock was started. This starting time was refered to as "zero" time.

19. Gas samples were taken at 15 - 20 minute intervals starting from the time "zero".

20. Coked sand samples were also taken periodically through the solid sampling valve (V11), the first sample being taken 30 minutes after the mist was first observed in the product recovery train. Care was exercised to minimize the oxidation of coked sand while sampling.

21. When all the bituminous sand was fed (indicated by the decrease in the oil mist output), the heaters were shut-off.

22. The purge gas was shut-off, the fluidizing gas flow was kept to a minimum. This prevented the oxidation of the syncrude oil.

23. After 24 hours, the coked sand in the reactor was emptied and its weight was determined. The weight was compared to the weight corresponding to the pressure drop across the bed as measured during the experiment.

24. The weight of syncrude oil in the condenser receiver (O_1) and the cyclone receiver (O_2) was determined.

25. The absorbed oil from the fiber mist eliminators was recovered by washing with benzene.

26. The benzene was stripped in a Büchi roto-evaporator under an absolute pressure of 47 kPa and a temperature of 353 K. The final pressure of stripping was 4.7 kPa.

27. The gas and coke samples were analyzed as described in section 3.7.

28. The cyclone fines collected in receivers (L1 and L2) were weighed. The cyclones and the filter were cleaned.

29. The hopper and the screw feeder were dismantled and the reactor was inspected for plugging.

30. The inspected reactor was cleaned by backflushing with compressed air.

31. A small amount of sand containing condensed oil adhered to the screw feeder outlet tube. This material was removed and the amount of oil condensed on the sand was determined.

The above operational steps were found to be successful and were adhered to during each experiment.

3.7 Product Analysis

3.7.1 Gas Analysis

The gases were analyzed using a (3.18 mm O.D. x 6.1 meter long) chromosorb 102 column in a 5830A Hewlett Packard Gas Chromatograph with a microprocesser and with a combination of dual flame ionization detector (FID) and dual thermal conductivity detector (TCD). A typical gas chromatogram is presented in Figure 3.19. Hydrogen was determined using a molecular sieve column (3.18 mm O.D. x 2.44 meters long) with 8% hydrogen in helium as carrier gas.

3.7.2 Coke Analysis

The determination of coke on the sand could not be carried out at higher temperatures (say 1023 K) due to the decomposition of the inorganics in the sand matrix. Therefore, the coke on the sand was determined by burning a weighed sample of coked sand in a muffle furnace at 773 K for 16-18 hours. The percentage of coke was determined from the weight loss. For Sunnyside bituminous sand feed, the percentage of coke on the coked sand used to mix with the bituminous sand feed was also determined. The difference in the percentage of coke on the sand before and after the run was the actual coke on the sand made during the run.

3.7.3 Synthetic Liquid Product Analysis

The analysis and characterization of the synthetic liquid is reported in detail in Chapter IV.

3.8 Material Balance

The material balance of each run exceeded 90 wt % of the bitumen fed to the reactor. The data was normalized by adding the remaining wt % to the liquid yield. This was done to correct for (i) the liquid lost with benzene during the stripping of benzene-synthetic crude mixture, and (ii) the oil condensing on the screw feeder outlet, which

Figure 3.18

Typical C_1 to C_6 Hydrocarbon Gas Chromatogram

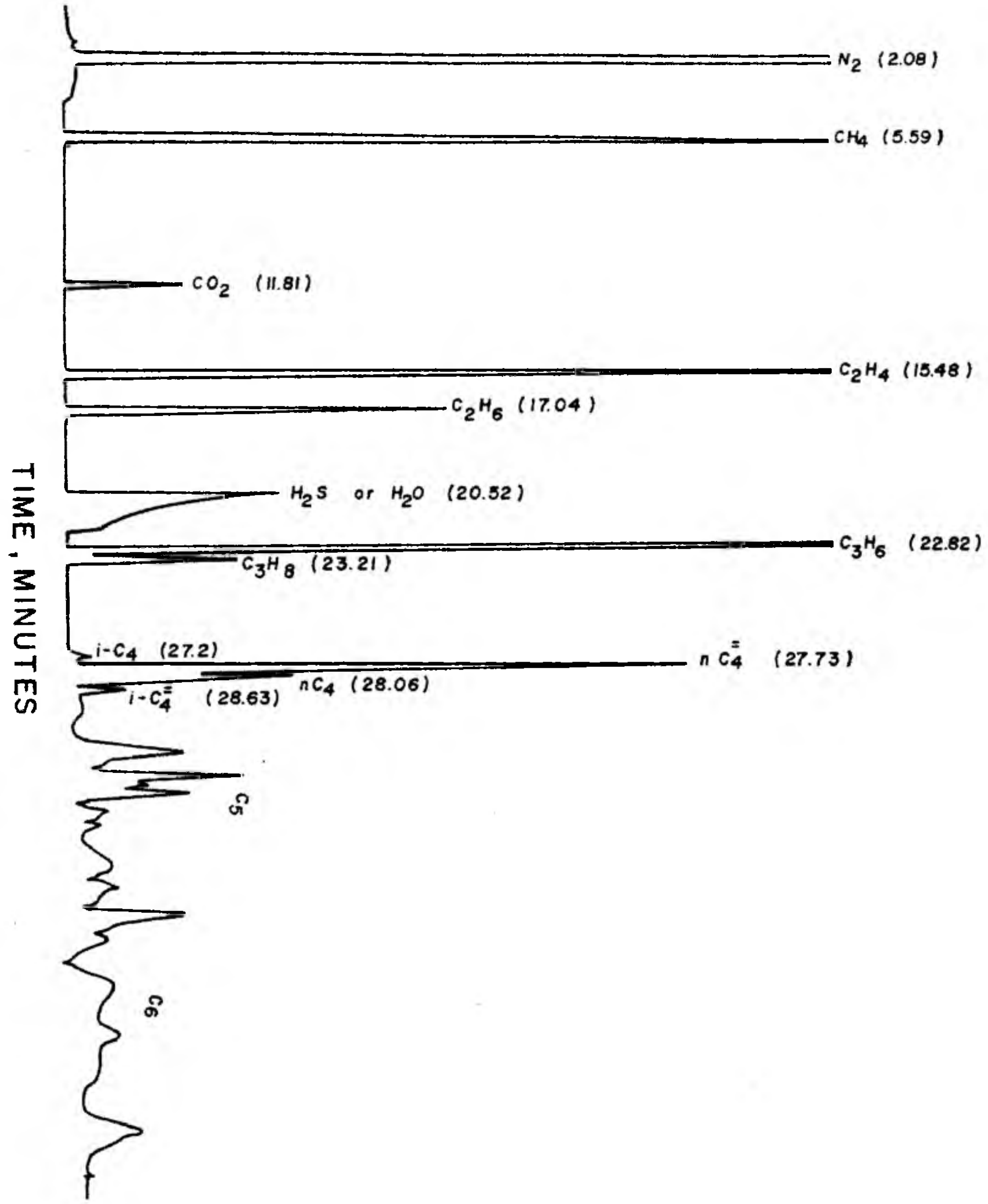
N_2 (2.08)
CH_4 (5.59)
CO_2 (11.81)
C_2H_4 (15.48)
C_2H_6 (17.04)
H_2S or H_2O (20.52)
C_3H_6 (22.82)
C_3H_8 (23.21)
i-C_4 (27.2)
n $C_4^=$ (27.73)
nC_4 (28.06)
i-$C_4^=$ (28.63)
C_5
C_6
TIME, MINUTES

cannot be recovered. The material balance calculations for a typical experiment are presented in Appendix E.

CHAPTER 4

RESULTS AND DISCUSSION

The primary operating variables investigated in the study of the thermal recovery of a synthetic crude from the bituminous sand deposits of Utah were the reactor temperature, the average retention time of the bituminous sand in the fluidized bed, and the particle size of the feed sand. The effects of the feed sand source and the bitumen content were studied using the bituminous sand of the Sunnyside and Tarsand Triangle deposits. The Sunnyside deposit is of fresh water origin and contains an average of 8 - 9 weight percent bitumen content and 0.5 - 0.8 weight percent sulfur, whereas the Tarsand Triangle deposit is of marine origin and contains an average of 4 -5 weight percent bitumen and 3.5 - 4.5 weight percent sulfur.

4.1 Effects of Operating Variables on Yield and Product Distribution

All yields are reported as weight percent based on the bitumen fed. In this investigation the C_5 plus liquid was termed as synthetic crude, while the liquid product obtained was referred to as synthetic liquid.

4.1.1 Effect of Temperature on Product Yield and Distribution

The effect of the fluid-bed reactor temperature on the yield pattern is presented in Table 4.1 and Figure 4.1. These data were obtained with a sample of the bituminous sand from the Sunnyside deposit which had an average bitumen content of 8.5 weight percent. The sand particle size (d_p) was 358.5 microns and the average retention time of solids (θ_{avg}) was 27.2 mins in all these experimental runs. The weight percent yield of synthetic crude varied from 51% at 698 K to 45% at 798 K, with a maximum yield of 61.2 weight percent at 723 K. Gishler(111) observed a similar trend for the influence of reactor temperature on the synthetic crude yield with the Canadian bituminous sands (bitumen content 16 weight percent). In the Canadian studies, Gishler allowed the bed depth to increase before withdrawing the coked sand from the reactor. In the present study, the coked sand was continuously withdrawn from the fluid bed reactor and the bed depth was kept constant by means of a differential pressure controller and a pneumatically operated solids flow valve. Thus, the influence of the bed depth on the yield of synthetic crude with reactor temperature was minimized. The coked sand withdrawn from the reactor was dry and unwetted by the synthetic liquid product produced. Filby, _et_. _al_.(122) have reported trace amounts of their synthetic liquid product was carried out of the reactor with the coked sand.

The synthetic liquid product was analyzed in terms of three fractions according to boiling range: a gasoline fraction (C_5^+ -

Table 4.1

Effect of Reactor Temperature on Product Yield and Distribution

Sunnyside Feed

Experiment Number	56	52	54	53	55
Reactor Temperature, K	698	723	748	773	798
Retention Time of Solids, min.	27.2	27.2	27.2	27.2	27.2
Feed Sand Particle Size, μ	358.5	358.5	358.5	358.5	358.5
Fluidizing Gas Flow Rate, SCM·h^{-1}	0.142	0.142	0.142	0.142	0.142
Gas Make, LPH at STP	7.3	7.3	10.6	14.5	16.0
Synthetic Liquid Yield, gm h^{-1}	19.8	23.9	18.4	22.2	22.9
Mass Balance (weight percent)					
CO_2	1.2	1.3	1.8	1.5	2.7
C_1 - C_3	12.5	10.8	18.1	21.0	22.9
C_4	4.1	4.0	5.9	6.5	6.7
C_5^+ liquid (synthetic crude)	51.0	61.2	55.1	47.5	45.0
Coke	31.2 (15.8)[a]	22.6	19.2	23.5	22.8

[a] Weight percent of soft coke determined by solvent extraction.

Figure 4.1

Effect of Reactor Temperature on Yield and Product Distribution

Sunnyside Feed

Retention Time of Solids, θ_{avg} = 27.2 mins.

Feed Sand Particle Size, d_p = 358.5 microns

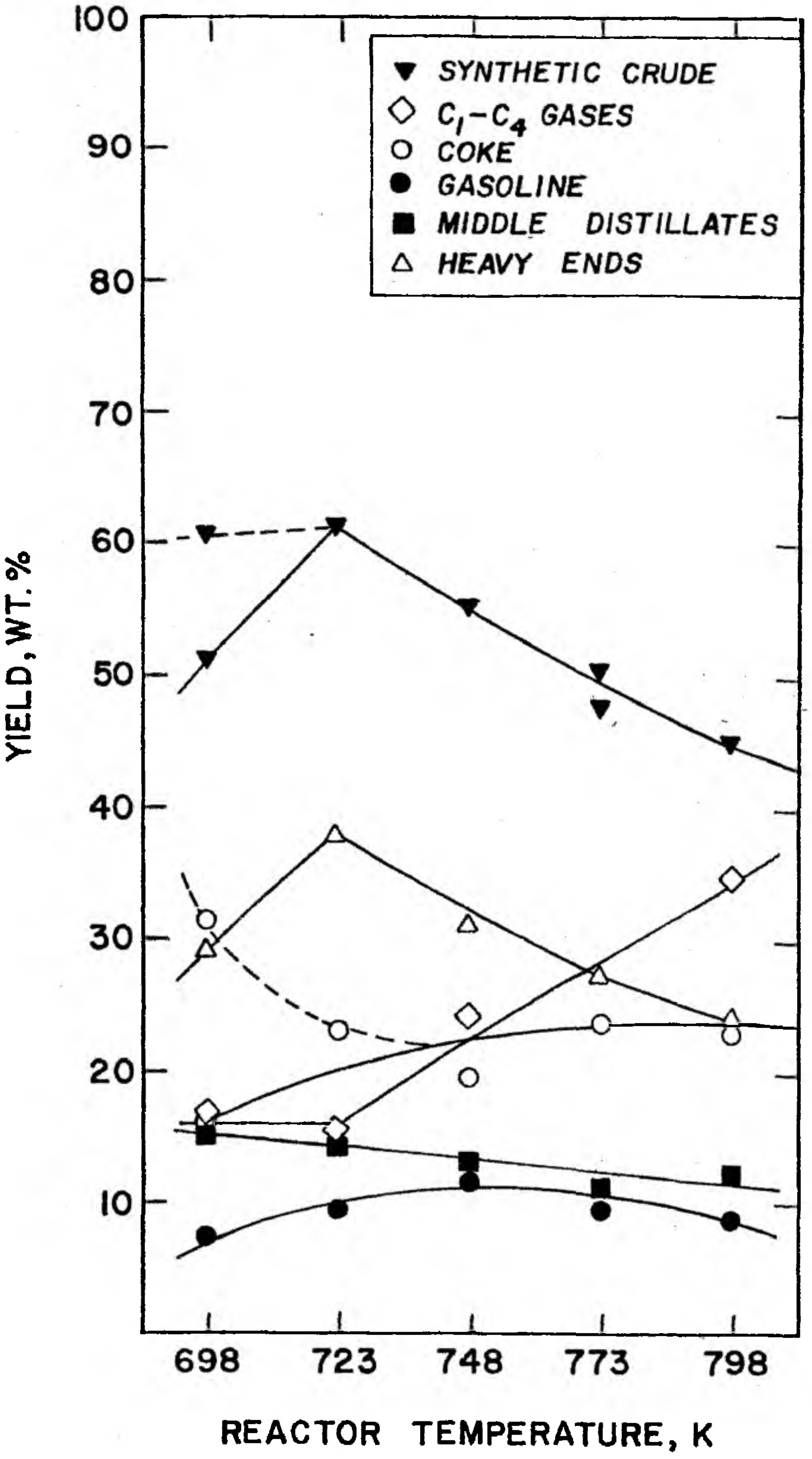
▼ SYNTHETIC CRUDE
◇ C_1-C_4 GASES
○ COKE
● GASOLINE
■ MIDDLE DISTILLATES
△ HEAVY ENDS
100
90
80
70
60
50
40
30
20
10
YIELD, WT. %
698
723
748
773
798
REACTOR TEMPERATURE, K

478 K), a middle distillate fraction (478 - 617 K), and the heavy ends (617 K plus). The weight percent yields of these individual fractions based on the bitumen fed are also presented in Figure 4.1. The yield of the high boiling, high molecular weight fraction (617 K plus) decreased with increasing reactor temperature exhibiting a trend similar to that of the synthetic crude. The yields of the gasoline fraction and the middle distillate fraction were insensitive to increasing reactor temperature. However, Filby, et. al.(122) have reported an increasing trend in the yield of naphtha (C_5^+ - 468 K) with increasing reactor temperature for the Canadian bituminous sands. The authors have corrected their yields to a 797 K end point and their correction factor (CF) was based on the weight percent residue (797 K plus), the weight percent bitumen converted to coke and the weight percent Conradson carbon residue (CCR) of the liquid residue (797 K plus). The correction factor (CF) was computed using the relationship

$$\text{Correction Factor (CF)} = \frac{\text{weight percent liquid residue } \left(1 - \frac{1.3\ \text{CCR}}{100}\right)}{100 - (\text{weight percent liquid residue}) - (\text{weight percent coke})} \qquad (4\text{-}1)$$

The weight percent liquid residue (697 K plus), the weight percent coke, and the Conradson carbon of the liquid residue (697 K plus) increased with increasing temperature in the uncorrected data. Consequently, the value of the correction factor increased. The corrected yield of naphtha was 10 percent higher than the weight percent yield of naphtha obtained before the correction. In the present investigation the yields were uncorrected.

The weight percent yield of synthetic crude at 698 K was low due to a solvent extractable liquid ("soft" coke) remaining on the sand particles with the coked bitumen (non-extractable "hard" coke). If this extractable liquid had also undergone pyro-distillation, then the synthetic crude yield would have been higher and would have stayed relatively constant between 698 - 723 K (dashed line in Figure 4.1). In spite of the incomplete pyro-distillation of the bitumen from the bituminous sand, the actual synthetic crude yield obtained at 698 K was about the same as the weight percent yield at 773 K. The energy requirements would be different for these two different reactor temperatures even though the synthetic crude yields were the same. In an integrated, high temperature fluidized bed pyro-distillation - combustion process for the production of synthetic crude from bituminous sands, the energy required for the pyro-distillation of the bitumen is produced by burning coke on the sand in a combustor and recycling the hot, spent sand to the coking reactor. The recycle ratio of the hot sand increases with the increase in the total heat demand in the coking reactor due to the change in the operating conditions, in particular the reactor temperature. At constant synthetic crude yield, the heat demand at a reactor temperature of 773 K would be higher than the heat demand at 698 K. Consequently, the recycle ratio of the hot sand would be lower at lower reactor temperature. This would minimize the erosion of process vessels due to sand abrasion. Furthermore, the quality of the synthetic liquid product obtained at a reactor temperature of 773 K would be different from the liquid product obtained at 698 K. Although the total heteroatoms content was nearly the same, the liquid product at 698 K had 11.1 weight percent hydrogen, 16 ^{o}API gravity and 97% of the liquid product boiled below 811 K, while the liquid product at 773 K had a lower hydrogen content (10.6 weight percent), lower ^{o}API gravity (12.7), and lower percentage of liquid boiling below 811 K (76%). The differences in the product qualities of the synthetic liquids obtained at 698 K and 773 K might influence the selection of the subsequent processing step.

When the experiment was repeated at a reactor temperature of 773 K the weight percent yields were 50% synthetic crude, 24% coke, and 26% light gases (C_1 - C_4) which agreed reasonably well with the yields obtained in experiment #53 (Table 4.1).

Up to 723 K, the total gas make (nitrogen free basis) remained constant at 7.3 liters per hour (LPH) measured at standard conditions. Beyond this temperature, the gas make increased rapidly with increasing reactor temperature (Figure 4.2). The increase in the gas make was accompanied by significant variations in the gas composition. Above 723 K, thermal cracking became progressively more severe compared to the direct distillation of the bitumen from the sand. This resulted in the sharp increase in the gas make reflecting the severity of the operation. The increase in the gas make was primarily due to the increase in C_1 - C_3 light hydrocarbon gases. The sharp increase in C_1 - C_3 weight percent yield beyond 723 K is due to the increase in ethylene, propylene, and methane weight percent yields with increasing reactor temperature. Similar observations were reported by Greensfelder, et. al.(128) in the thermal cracking of

Figure 4.2

Effect of Reactor Temperature on Gas Make
and Product Distribution

Sunnyside Feed

Retention Time of Solids, θ_{avg} = 27.2 min.

Feed Sand Particle Size, d_p = 358.5 microns

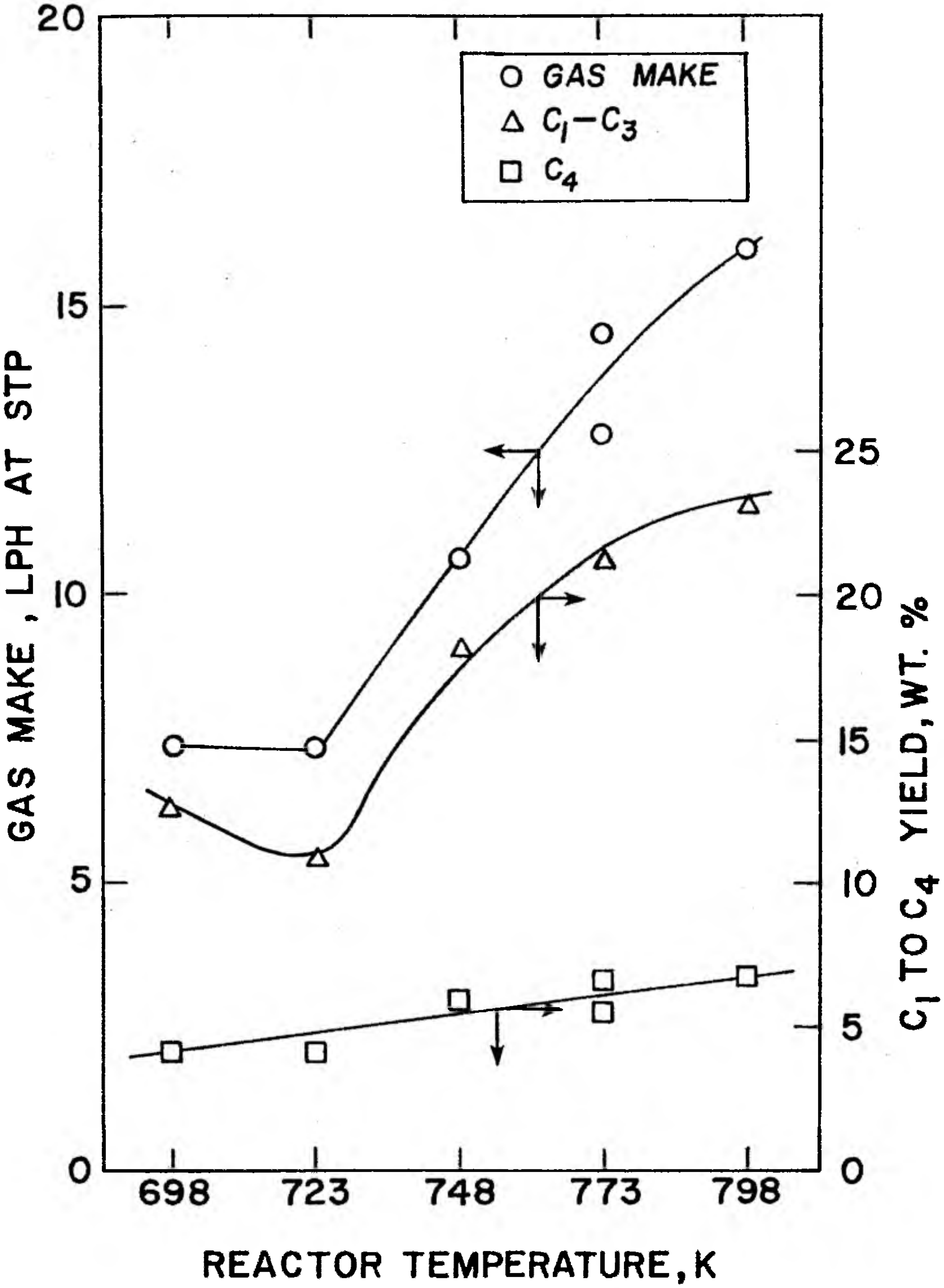

○ GAS MAKE
△ C_1-C_3
□ C_4
GAS MAKE , LPH AT STP
C_1 TO C_4 YIELD, WT. %
REACTOR TEMPERATURE, K
0
5
10
15
20
25
698
723
748
773
798

normal paraffins. This suggests that the rate of thermal cracking is much higher than the rate of distillation as the reactor temperature is increased. Furthermore, beyond 723 K the increase in the gas make is due to the thermal cracking of the synthetic crude as indicated by the decrease in synthetic crude yield.

The molal gas composition of the gas revealed that the total amounts of saturated and unsaturated hydrocarbons in C_1 - C_4 light gases were almost equal (Table 4.2). The yield of hydrogen was negligible, that is, less than 0.5 weight percent based on the bitumen fed which corresponds to less than five percent in the product gases. The data on the amount of molecular hydrogen in the product gases appears to be inconsistent in the thermal coking studies conducted with the Canadian bituminous sands, that is, Gishler(111) reported 15 percent hydrogen in the gas, while Filby, et. al.(122) reported no molecular hydrogen in the product gases. The yield of carbon dioxide based on the bitumen fed increased from 1.2 weight percent at 698 K to 2.7 weight percent at 798 K. The high percentage of oxygen (4.4 wt %) in the sand matrix may explain the presence of carbon dioxide in the product gas.

The amount of bitumen converted to "hard" coke, which is deposited on the sand particles, steadily increased (the solid line in Figure 4.1) with increasing reactor temperature and reached a stationary value at 21 - 24% by weight. Wenger, et. al.(57) have conducted coking studies on the Sunnyside bitumen obtained by the hot-water extraction process(49). The product yields of their study

Table 4.2

Typical Composition of the Gaseous Product[a]

Sunnyside Feed

Reactor Temperature = 773 K

Retention Time of Solids, θ_{avg} = 27.2 min.

Feed Sand Particle Size, d_p = 358.5 microns

Gas Composition	(Mole %)
H_2	4.7[b]
CO_2	3.2
CH_4	30.3
C_2H_4	19.9
C_2H_6	7.0
C_3H_6	14.2
C_3H_8	1.7
C_4H_8	6.8
C_4H_{10}	3.6
C_5	5.5
C_6	3.1

Notes: a. The gas composition reported excludes nitrogen and hydrogen sulfide.

b. Since the weight percent hydrogen based on bitumen is less than 0.5%, its value is excluded in the mass balance calculations.

were as follows: coker distillate (oil) 68.2 wt %, coke 22.9 wt %, and gas 8.9 wt %. The coke yield was almost identical to the present study, although the mode of processing was different. This suggests that the mineral matter in the bituminous sand is not participating in the thermal cracking reactions at these operating temperatures. The reported yield of coke in the direct distillation of Canadian bituminous sand appears to be around 20% by weight based on the bitumen fed and the yield of coke remained constant at 18 - 21% by weight beyond the reactor temperature of 803 K(111,122). Despite the differences in the chemical natures of the Canadian and Sunnyside bituminous sands and the reactor temperatures, the weight percent bitumen converted to coke was about the same for both of the sands. The effect of reactor temperature on the synthetic liquid product quality will be discussed in section 4.2.

4.1.2 Effect of Solids Retention Time on Yield and Product Distribution

In this investigation, the solids retention time (θ_{avg}, minutes) was defined as

$$\theta_{avg} = 60 \cdot W/F \tag{4-2}$$

where W is the weight of solids in the bed (kg) and F is the sand feed rate (kg hr^{-1}). According to the above definition, the average solids retention time can be changed either by changing the weight of solids in the bed at constant feed rate or by changing the sand feed rate at a constant bed weight. In this study, the bituminous sand feed rate was changed from 1.3 kg h^{-1} to 2.0 kg h^{-1} and the bed weight was maintained constant at 0.68 kg. This changed the solids retention time from 31.4 minutes to 20.4 minutes.

The effects of the retention time of solids on the product yield pattern are presented in Tables 4.3, 4.4, and 4.5 and in Figures 4.3, 4.4, and 4.5 for three different reactor temperatures.

The weight percent yield of synthetic crude increased with decreasing retention time of solids at a constant reactor temperature and with a uniform particle size of the feed sand. For example, at 773 K, the yield of synthetic crude was 47.5% by weight at 27.2 minutes and the yield increased to 67.5 weight percent at 20.4 minutes.

The increase in the synthetic crude yield was accompanied by a corresponding decrease in the yield of light gases. The weight percent coke (20 - 22 wt %) based on the bitumen fed remained relatively unchanged with respect to the retention time of solids for all the three different reactor temperatures. This suggests that the synthetic liquid liberated from the feed sand undergoes extensive secondary cracking at longer retention time of solids and this secondary cracking took place in the vapor phase.

The vapor phase cracking can possibly be explained based on the characteristic behavior of solids in a small diameter fluidized bed reactor. It has been widely observed that the phenomenon of slugging takes place in tubes whose diameters are 5 cm or less when the height to diameter ratio (aspect ratio) is in excess of one(129). A Vycor glass column which had an aspect ratio of nearly 30 (3.8 cm diameter, 100 cm in height) was used to simulate the

Table 4.3

Effect of Retention Time of Solids on Product Yield and Distribution

Sunnyside Feed

Experiment Number	68	52	61
Reactor Temperature, K	723	723	723
Retention Time of Solids, min.	31.4	27.2	20.4
Feed Sand Particle Size, μ	358.5	358.5	358.5
Fluidizing Gas Flow Rate, $SCM \cdot h^{-1}$	0.142	0.142	0.142
Gas Make, LPH at STP	9.3	7.3	7.7
Synthetic Liquid Yield, gm h^{-1}	25.1	23.9	32.6
Mass Balance (weight percent)			
CO_2	2.3	1.3	0.9
C_1 - C_3	15.2	10.8	8.3
C_4	4.3	4.0	2.6
C_5^+ liquid (synthetic crude)	55.8	61.2	50.4
Coke	22.5	22.6	37.9 (20.9)[a]

[a] Weight percent soft coke determined by solvent extraction.

Figure 4.3

Effect of Retention Time of Solids, θ_{avg},

on Product Yield and Distribution

Sunnyside Feed

Reactor Temperature, T = 723 K

Feed Sand Particle Size, d_p = 358.5 microns

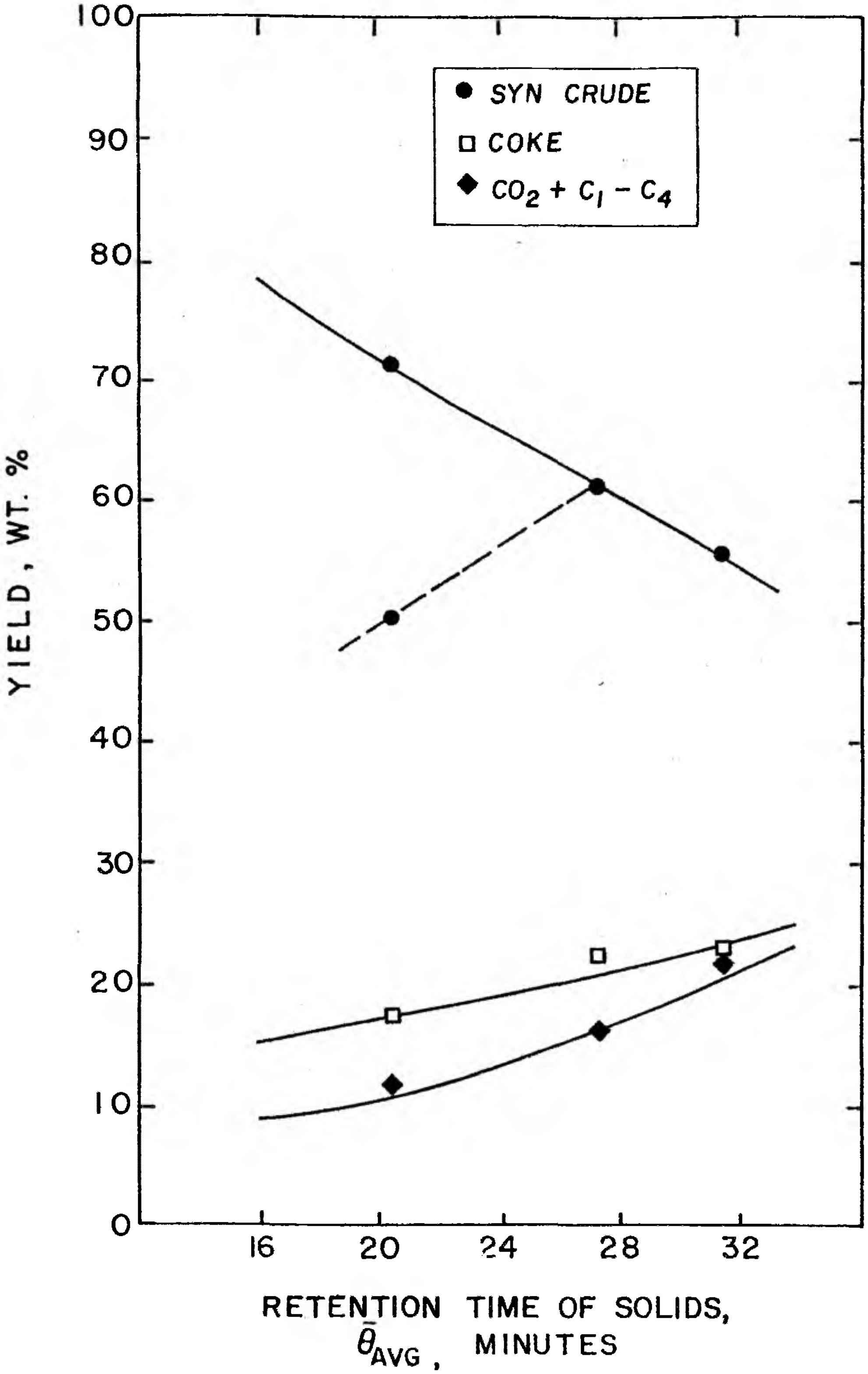
● SYN CRUDE
□ COKE
◆ $CO_2 + C_1 - C_4$
YIELD, WT. %
100
90
80
70
60
50
40
30
20
10
0
16
20
24
28
32
RETENTION TIME OF SOLIDS, $\bar{\theta}_{AVG}$, MINUTES

Table 4.4

Effect of Retention Time of Solids on Product Yield and Distribution

Sunnyside Feed

Experiment Number	67	53	64
Reactor Temperature, K	773	773	773
Retention Time of Solids, min.	31.4	27.2	20.4
Feed Sand Particle Size, μ	358.5	358.5	358.5
Fluidizing Gas Flow Rate, SCM·h^{-1}	0.142	0.142	0.142
Gas Make, LPH at STP	15.9	14.5	9.0
Synthetic Liquid Yield, gm h^{-1}	23.1	22.2	44.0
Mass Balance (weight percent)			
CO_2	2.8	1.5	1.3
C_1 - C_3	26.8	21.0	8.7
C_4	8.0	6.5	2.6
C_5^+ liquid (synthetic crude)	42.8	47.5	67.4
Coke	19.7	23.5	20.0

Figure 4.4

Effect of Retention Time of Solids, θ_{avg},

on Product Yield and Distribution

Sunnyside Feed

Reactor Temperature, T = 773 K

Feed Sand Particle Size, d_p = 358.5 microns

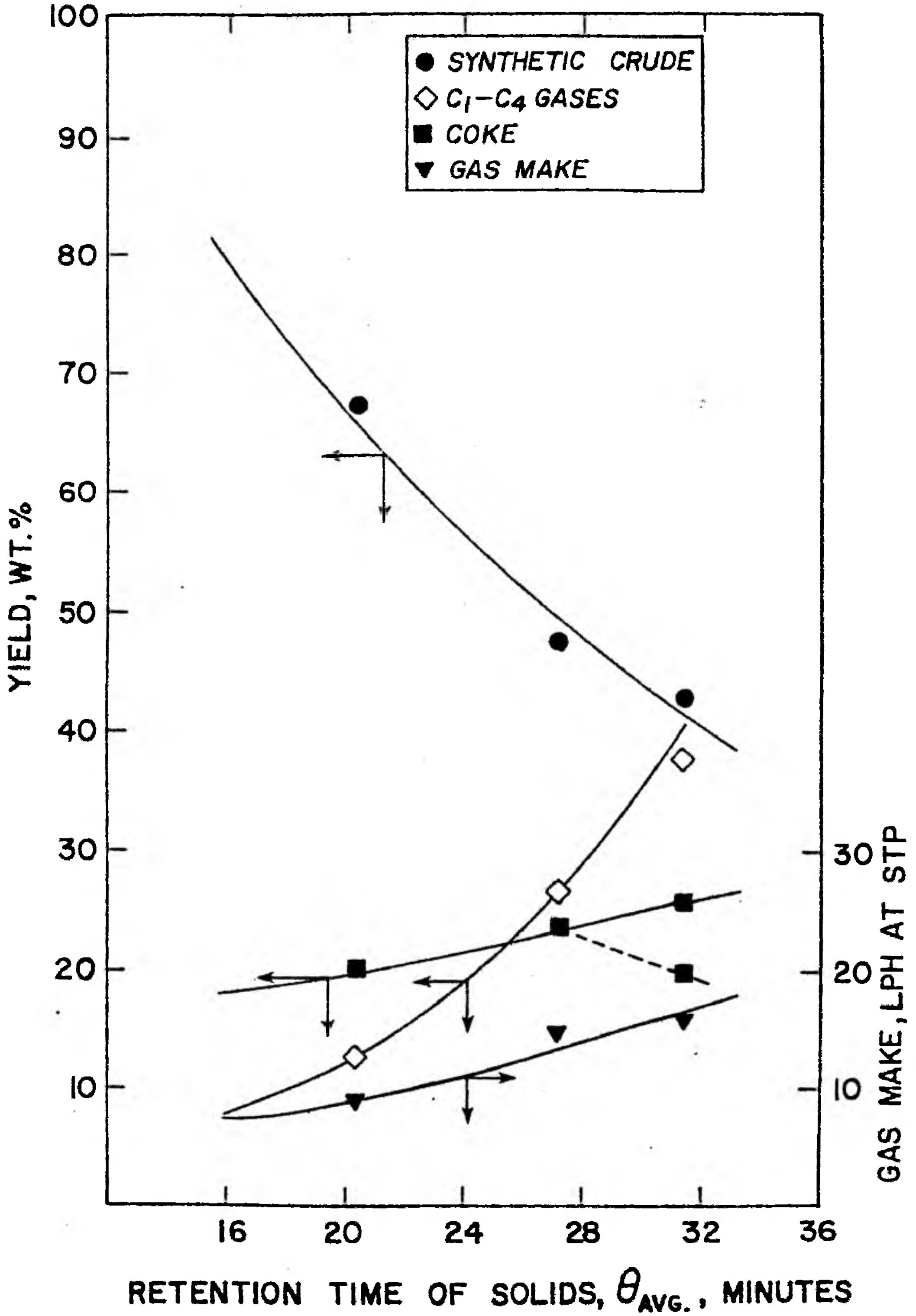
● SYNTHETIC CRUDE
◇ C1–C4 GASES
■ COKE
▼ GAS MAKE
YIELD, WT.%
100
90
80
70
60
50
40
30
20
10
GAS MAKE, LPH AT STP
30
20
10
16
20
24
28
32
36
RETENTION TIME OF SOLIDS, θAVG., MINUTES

Table 4.5

Effect of Retention Time of Solids on Product Yield and Distribution

Sunnyside Feed

Experiment Number	~~87~~	55	~~85~~ 67
Reactor Temperature, K	798	798	798
Retention Time of Solids, min.	31.4	27.2	20.4
Feed Sand Particle Size, μ	358.5	358.5	358.5
Fluidizing Gas Flow Rate, SCM·h^{-1}	0.142	0.142	0.142
Gas Make, LPH at STP	14.3	16.0	12.2
Synthetic Liquid Yield, gm h^{-1}	22.8	22.9	41.1
Mass Balance (weight percent)			
CO_2	5.2	2.7	1.6
C_1 - C_3	23.3	22.9	11.8
C_4	6.8	6.7	4.1
C_5^+ liquid (synthetic crude)	42.2	45.0	61.8
Coke	22.5	22.8	20.6

Figure 4.5

Effect of Retention Time of Solids, θ_{avg},

on Product Yield and Distribution

Sunnyside Feed

Reactor Temperature, T = 798 K

Feed Sand Particle Size, d_p = 358.5 microns

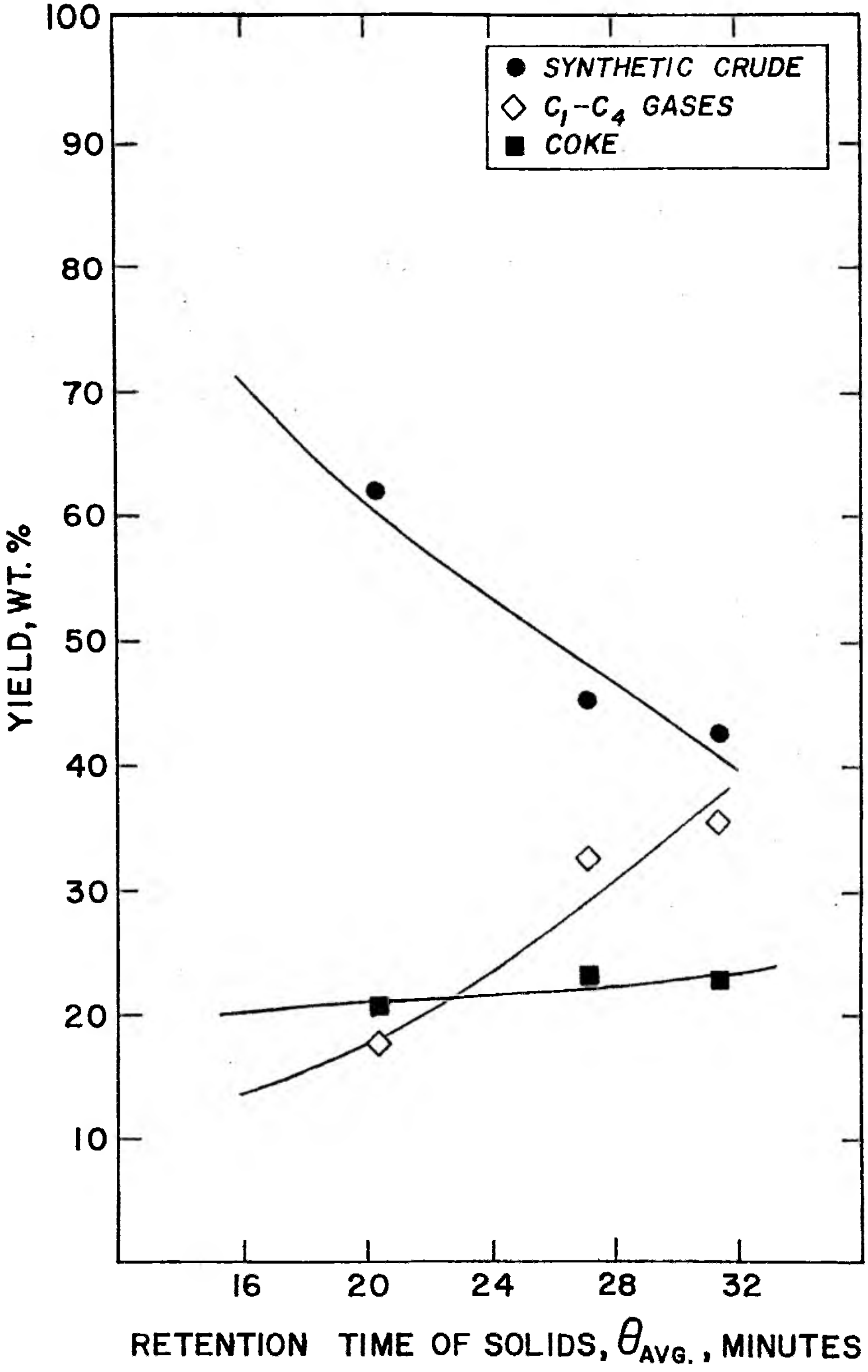

● SYNTHETIC CRUDE
◇ C_1-C_4 GASES
■ COKE
YIELD, WT. %
100
90
80
70
60
50
40
30
20
10
16
20
24
28
32
RETENTION TIME OF SOLIDS, $\theta_{AVG.}$, MINUTES

process and the aspect ratios of the glass column and the reactor were nearly equal. Furthermore, the behavior of a bed of coked sand was studied in the glass column when fluidized with air at ambient temperature. The bubble formation was initiated at or close to the distributor. In addition, square nosed slugs of gas (Figure 4.6) were observed rising through the bed at high flow rates. The minimum gas velocity at which slugging in the reactor commences can be determined using the Stewart and Davidson(130) equation,

$$U_s - U_o = 0.07 \, (gD)^{\frac{1}{2}} \tag{4.3}$$

where U_s is the gas velocity at the onset of slugging, U_o is the minimum fluidization velocity, g is the acceleration due to gravity, and D is the bed diameter. The minimum fluidization velocity was found to have a linear relationship with operating temperature of the reactor (Appendix C). The amount of gas in the bubble phase and the bubble velocity increased at higher reactor temperatures at constant mass flow rate. Furthermore, it is believed that the bubbles formed in the inlet region above the distributor coalesced due to the decrease in the effective hydrostatic pressure as the bubbles rose through the bed.

At a low sand feed rate and a high reactor temperature, the gas bubbles moved through the reactor rapidly causing adequate mixing of solids in the bed. The improved solids mixing facilitates the transfer of a portion of the hydrocarbon vapors liberated from the sand from the dense or particulate phase of the fluidized bed to the lean or bubble phase. The bubble phase passed through the reactor and

Figure 4.6

Solids Slugging

Fluidized Bed Reactor

Aspect Ratio = 30

Reactor Diameter = 3.6 cm

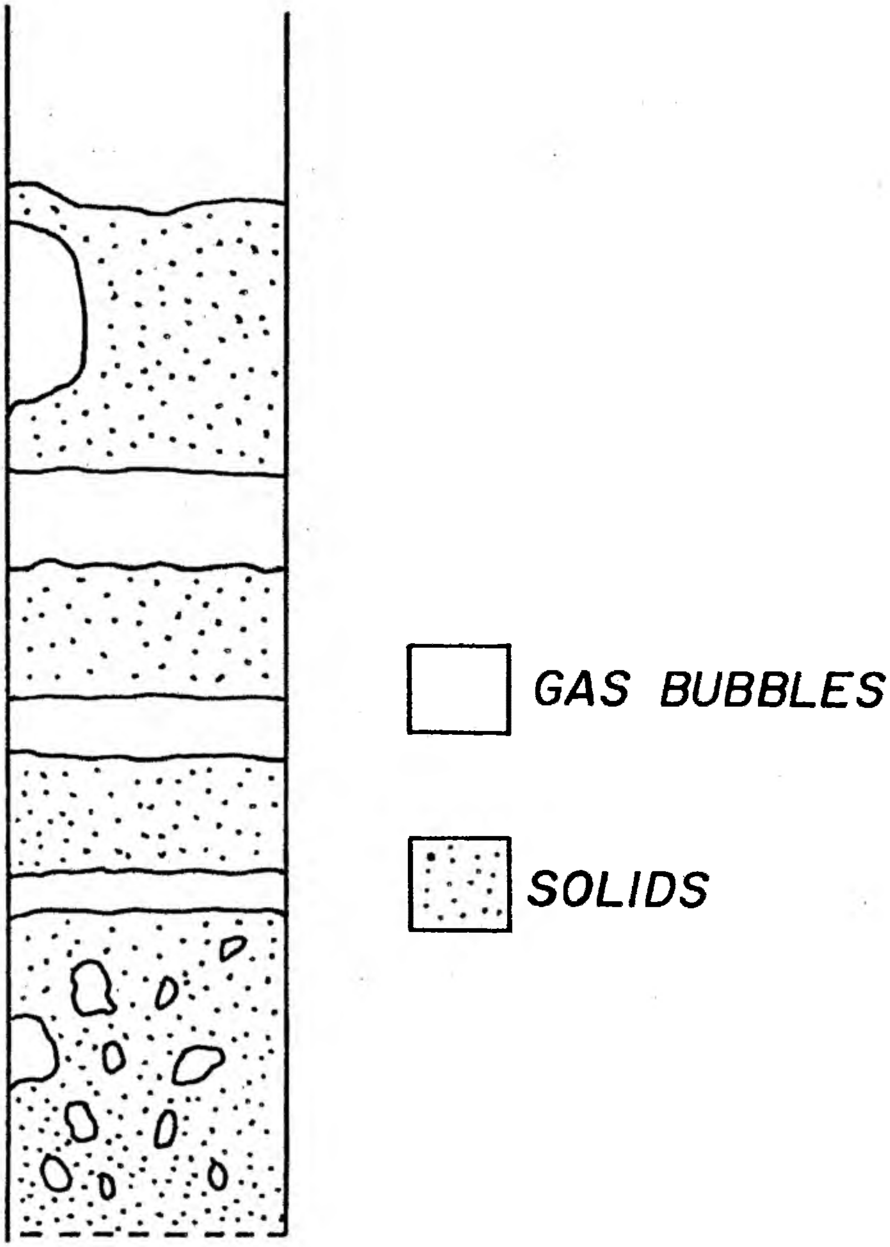
GAS BUBBLES
SOLIDS

may have behaved as a batch, thermal cracking reactor. Thus the vapors underwent cracking prior to leaving the fluidized bed region of the reactor. This additional vapor phase cracking was responsible for the higher light hydrocarbon gas make (C_1 - C_3 gases). At an average solids retention time of 31.4 minutes, the gas make increased from 9.3 liters per hour to 15.9 liters per hour for reactor temperatures 723 K and 773 K, respectively.

At high sand feed rate (2 kg/hr), the velocity of the rising bubble might have been decelerated due to an effective increase in the hydrostatic pressure acting on the bubble. Under similar conditions in the glass column, the addition of solids to the column caused poor mixing of the solids. This resulted in slugs of solids that moved up through the reactor in a piston-like manner by the slowly rising bubble (Figure 4.6). Under these conditions, it is speculated that the pyro-distillation of the bitumen mainly took place in the particulate phase and there was less transfer of vapor from the particulate phase to the bubble phase due to poor mixing of solids in the bed. This minimized the secondary cracking of the bitumen in the vapor phase. Consequently, the yield of light gases should be decreased with an increase in the synthetic crude yield. It is evident from Tables 4.4 and 4.5, at 773 K and 798 K, the synthetic crude yield obtained at a solids retention time of 20.4 minutes were considerably higher than the yields obtained at a solids retention time of 27.2 minutes. At 773 K, the yield of synthetic crude increased from 47.5 weight percent to 67.4 weight percent with a corresponding decrease in the yield of light gases (C_1 - C_3) from 21.0 percent to 8.7 percent, while at 798 K, the yield of synthetic crude increased from 45.0 weight percent to 62.0 weight percent with a decrease in the yield of light gases from 22.9 weight percent to 11.8 weight percent. The slight increase in the yield of light gases between 773 K and 798 K at a constant solids retention time of 20.4 minutes indicated the severity of operation and clearly confirmed the absence of vapor phase secondary cracking.

Decreasing the retention time of solids shifted the optimum temperature at which the maximum C_5^+ liquid (synthetic crude) yield was obtained to a higher temperature, that is, from 723 to 773 K. Furthermore, the yield of synthetic crude at the optimum temperature increased with decreasing solids retention time (Figure 4.7). At a retention time of 20.4 minutes, the maximum liquid yield was 67.4 weight percent at 773 K whereas at a retention time of 27.2 minutes, the maximum yield was 61.2 weight percent at 723 K. Increasing the feed sand rate also caused the following changes: (1) increased the "soft" coke yield at lower reactor temperatures, and (2) increased the lower limit of the temperature at which "soft" coke was produced. The "soft" coke yield was 15.8 weight percent for operating conditions of 698 K, 27.2 minutes, while at a solids retention time of 20.4 minutes and a reactor temperature of 723 K, the yield of "soft" coke was 20.9 weight percent. This suggests that any increase in sand feed rate should be accompanied by an increase in the operating temperature to minimize the yield of "soft" coke.

Retention times below 20 minutes could not be investigated due to the limitation in reactor throughput capacity. Although the screw feeder could be operated for a sand feed rate of 2.5 kg hr^{-1}, the

Figure 4.7

Effect of Retention Time of Solids on
the Optimum Temperature for Maximum
Yield of Synthetic Crude
Sunnyside Feed
Feed Sand Particle Size, d_p = 358.5 microns

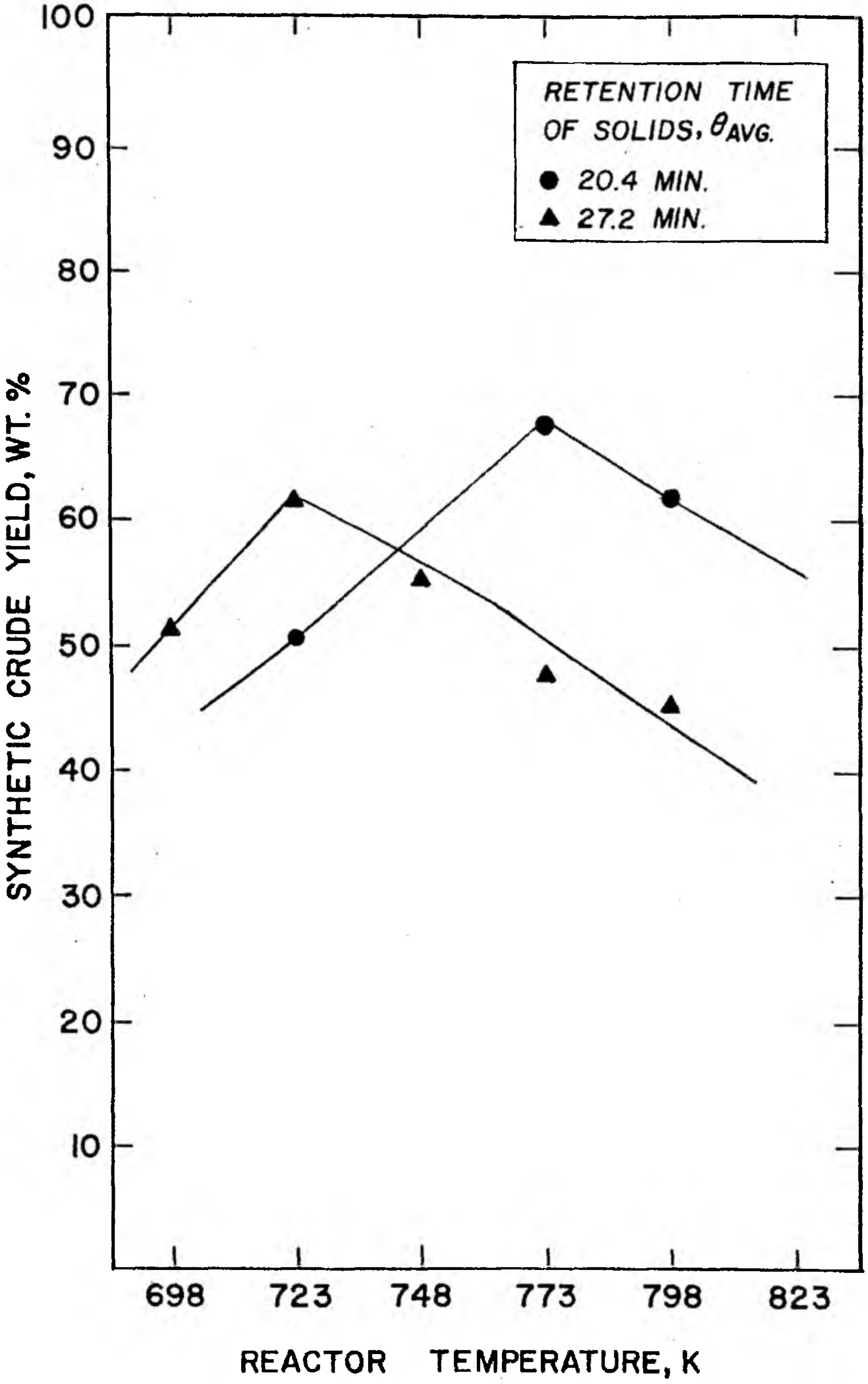

RETENTION TIME OF SOLIDS, $\theta_{AVG.}$
● 20.4 MIN.
▲ 27.2 MIN.
SYNTHETIC CRUDE YIELD, WT. %
100
90
80
70
60
50
40
30
20
10
698
723
748
773
798
823
REACTOR TEMPERATURE, K

reactor got plugged even at a reactor temperature of 773 K. A decrease in the solids retention time below 20 minutes could be achieved by decreasing the weight of solids in the bed at a constant feed rate. This would decrease the bed depth considerably and might increase the possibility of the vapor phase thermal cracking in the empty tube portion of the reactor above the sand bed.

If the data obtained at a reactor temperature of 773 K can be reasonably extrapolated (Figure 4.4), a liquid yield of 80% by weight based on the bitumen fed could be obtained at a solids retention time of 16 minutes (corresponds to a sand feed rate of 2.5 kg hr^{-1}). The solids retention time-liquid yield data in the literature lead to conflicting interpretations, that is, Peterson and Gishler(114,115), Safonov, et. al.(118), and Filby, et. al.(122) reported no effect of solids retention time on liquid yield. However, Rammler(120,121) observed that the plant capacity (directly related to the sand feed rate) has a definite influence on the liquid yield in the Lurgi-RühRgas direct coking process when processing a bituminous sand with a bitumen content of 9 - 10% by weight.

4.1.3 Effect of Feed Sand Particle Size and Particle Size Distribution on Yield and Product Distribution

The knowledge of the effect of feed sand particle size or particle size distribution is important because of the feed preparation step that might be involved in the mined above ground processing of consolidated bituminous sands of Utah. Moreover, the feed particle size influences the fluidization characteristics of the fluidized bed(131). No work has been reported in the literature regarding the effect of particle size on product yield and its distribution in the processing of bituminous sands. Canadian bituminous sands can be fed as lumps and do not require size reduction before being processed due to its unconsolidated nature. The consolidated bituminous sands of Utah dictate the necessity for size reduction before processing. Shea and Higgins(49) have reported the use of crushing and grinding apparatus such as the Jaw Crusher, Roll Crusher, and the Hammer Mill in the preparation of feed from Sunnyside bituminous sandstones for the hot water extraction process.

The effects of feed sand particle size and particle size distribution on the yield and product distribution are presented in Table 4.6. The particle size data were acquired at a coking bed temperature of 773 K and a solids retention time of 20.4 minutes. The reported value of the particle size (expressed in microns) is the mean value of the sieve openings of the two adjacent Tyler Standard Screens, the top screen through which the particles passed and the bottom screen where they were retained.

A reduction in the sand particle size from 358.5 microns to 253.5 microns had little or no effect on the product yield and its distribution. However, a significant shift in the product yield and its distribution was observed when the feed sand particle size was changed from 358.5 microns to 507.5 microns. The weight percent yield of the C_5^+ liquid (synthetic crude) decreased from 67.4 weight percent to 51.8 weight percent while the $C_1 - C_4$ light hydrocarbons yield

Table 4.6

Effect of Feed Sand Particle Size and Particle Size Distribution on Product Yield and Distribution

Sunnyside Feed

Experiment Number	71	64	69	59
Coking Reactor Temperature, K	773	773	773	773
Retention Time of Solids, min.	20.4	20.4	20.4	25.5
Feed Sand Particle Size, μ	253.5	358.5	507.5	162.0
Fluidizing Gas Flow Rate, $SCM \cdot h^{-1}$	0.142	0.142	0.142	0.142
Gas Make, LPH at STP	9.2	9.0	21.9	11.9
Synthetic Liquid Yield, gm h^{-1}	40.8	44.0	40.6	32.0
Mass Balance (weight percent)				
CO_2	2.3	1.3	2.3	1.3
C_1 - C_3	9.7	8.7	20.6	13.6
C_4	2.9	2.6	6.1	4.3
C_5^+ liquid (synthetic crude)	65.1	67.4	51.8	63.5
Coke	20.0	20.0	19.2	17.4

increased from 11.3% to 26.7% by weight. With no change in the yield of coke (19 - 20% by weight), it appears that the C_5^+ liquid hydrocarbons underwent thermal cracking to yield the light gaseous products, in particular, the C_1 - C_3 gases. It could be speculated that a fraction of the liberated hydrocarbon vapor was "trapped" in the pore structure of the large particles. The diffusion time for these species to transfer from the internal region of the sand particles to the bulk fluid phase was, therefore, increased. This increased residence time within a microscopic thermal cracker (i.e. the pore structure of the sand) led to conversion of the high molecular weight species to C_1 - C_4 gases.

A single experiment (Run #59) was made with a wide cut feed sand (Tyler sieve, 20 - 150 mesh fraction) to determine the effect of the particle size distribution on the synthetic crude yield. The retention time of solids was 25.5 minutes and the reactor temperature was 773 K. The product yield was similar to that obtained for smaller feed sand particles. A size distribution of the product coked sand is presented in Figure 4.8. It appears that 65% of the feed sand was finer than 358.5 microns and it would be expected to exhibit yields more nearly like the smaller feed sand particles ($\leq$ 385.5 microns) than like the large particles ($\geq$ 507.5 microns). Furthermore, during this experiment a large amount of sand fines was collected in the high temperature cyclones. If the yield pattern for the particle size of 358.5 microns was used to predict the yield for this particle size distribution at θ_{avg} = 20.4 minutes, the yield of synthetic crude

Figure 4.8

Particle Size Distribution of Coked Sand

Sunnyside Feed

Reactor Temperature, T = 773 K

Retention Time of Solids, θ_{avg} = 25.5 min.

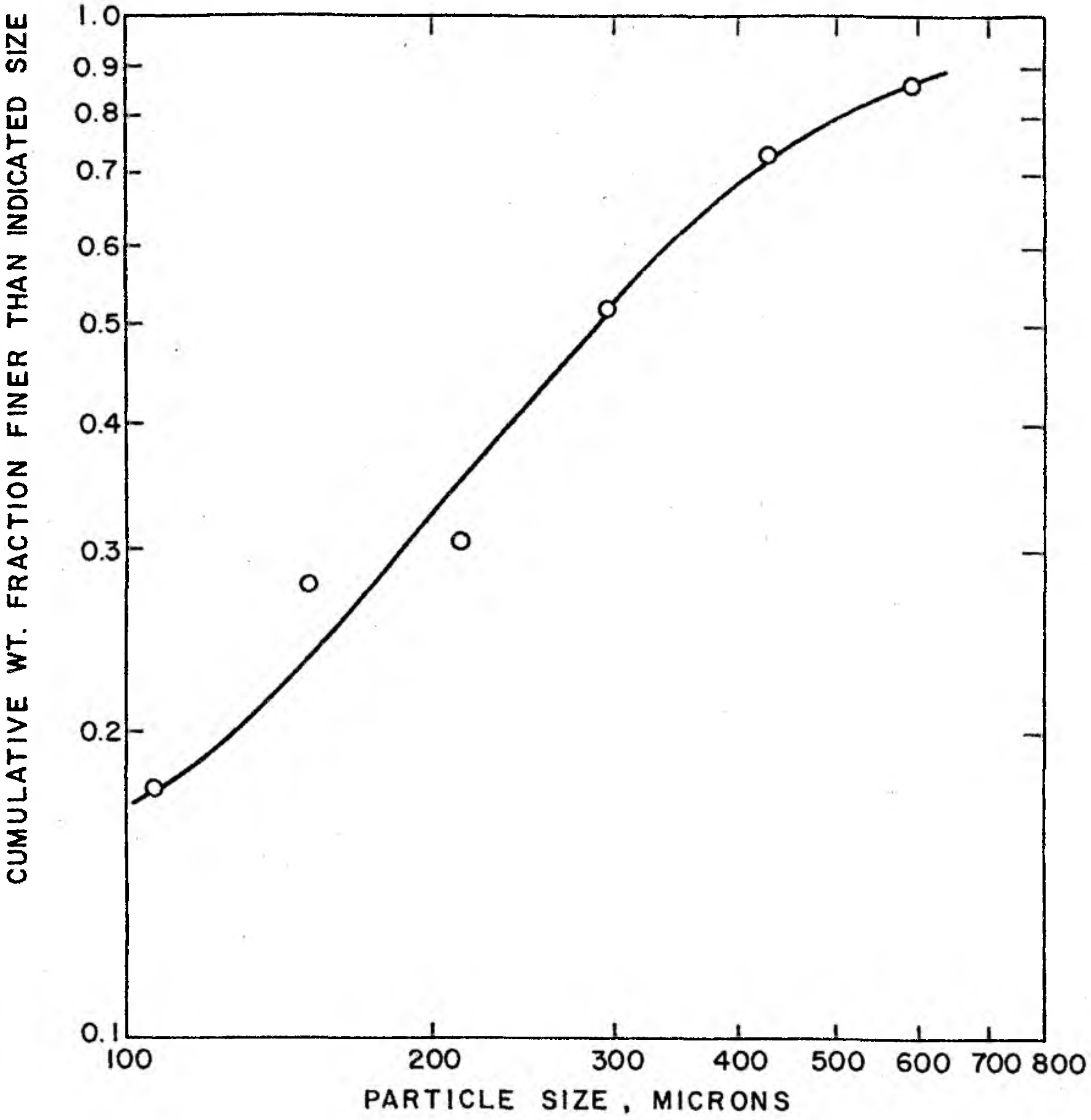
CUMULATIVE WT. FRACTION FINER THAN INDICATED SIZE
1.0
0.9
0.8
0.7
0.6
0.5
0.4
0.3
0.2
0.1
100
200
300
400
500
600
700
800
PARTICLE SIZE, MICRONS

could be about 84 weight percent. However, the data on the coke make would seem to indicate a limit of 80% synthetic crude yield.

The surface mined above ground recovery of bitumen or bitumen derived synthetic crude from the bituminous sands of Utah depends upon the energy requirements needed for size reduction. By proper selection of feed particle size distribution for smooth fluidized bed operation, the energy requirements can be minimized. Controlling and minimizing these energy requirements could make the mined above ground recovery processes attractive.

4.1.4 Effect of Feed Bituminous Sand Source and its Bitumen Content on Product Yield and Distribution

As mentioned in Chapter 1, the Tarsand Triangle deposit is the single biggest bituminous sand reserve and accounts for nearly 50% of the total bituminous reserves in Utah. The physical and chemical properties and origin of the bitumen are different from the Sunnyside bitumen, but are similar to the Canadian bitumen. The paucity of available process water and the low grade of the Tarsand Triangle deposit (4 - 5% bitumen by weight) make the thermal process attractive relative to the hot water process(47). Thus, the applicability of the fluidized bed thermal recovery method for processing this lean bituminous sand was investigated. Among the process variables, only the effect of temperature on yield and product distribution was studied. Results obtained with Tarsand Triangle feed sand are discussed first and a comparative study of the results obtained on the effect of temperature with regard to feed bituminous sand source (i.e. for Sunnyside and Tarsand Triangle bituminous sands) is then presented.

The effects of temperature on the yield and product distribution for Tarsand Triangle bituminous sand feed are presented in Table 4.7 and Figures 4.9 and 4.10. The "uncorrected" C_5^+ liquid (synthetic crude) changed from 45.8 weight percent at 723 K to 41.8 weight percent at 898 K, with a maximum liquid yield of 49.9 weight percent by weight occuring at the optimum reactor temperature of 798 K. The yields of synthetic crude were corrected, that is (i) to account for the loss of liquid condensing on the screw feeder outlet, and (ii) to account for the liquid lost with the solvent during the stripping of the solvent from the solvent-synthetic liquid mixture. The "uncorrected" synthetic crude yield was calculated from the relation,

$$\text{Yield of "Corrected" Synthetic Crude} = 100 - [\text{Yield of Coke} + \text{Yield of Light Gases } (C_1 - C_4)] \quad (4.4)$$

The "corrected" synthetic crude yield decreased linearly from 62.3 weight percent to 51.0 weight percent between the temperature range of 723 to 898 K.

The yield of synthetic crude for Tarsand Triangle feed sand appears to be insensitive to the change in the reactor temperature. This is evident from the shape of the "uncorrected" C_5^+ liquid yield curve with temperature. The Tarsand Triangle sample used in this study was leaner in bitumen content compared to the Sunnyside sample. Moreover, the feed was an outcrop sample and had undergone severe weathering over a long period of time. Ali(132) has studied the effect of aging phenomenon on the recovery of bitumen from the Canadian

Table 4.7

Effect of Reactor Temperature on Product Yield and Distribution

Tarsand Triangle Feed

Experiment Number	33	41	43	46	44	45
Reactor Temperature, K	723	773	798	823	853	898
Retention Time of Solids, min.	27.2	27.2	27.2	27.2	27.2	27.2
Feed Sand Particle Size, μ	358.5	358.5	358.5	358.5	358.5	358.5
Fluidizing Gas Flow Rate, SCM·h^{-1}	0.142	0.142	0.142	0.142	0.142	0.142
Gas Make, LPH at STP	7.5	12.0	14.3	17.3	14.0	19.8
Synthetic Liquid Yield, gm h^{-1}	27.6	26.5	27.9	25.2	26.6	22.1
Mass Balance (weight percent)						
CO_2[a]	2.3	2.4	4.2	4.4	3.0	4.4
C_1 - C_3	9.4	15.8	17.3	22.2	18.6	20.0
C_4	2.8	4.7	5.2	6.1	4.7	5.3
C_5^+ liquid (synthetic crude)	45.8 (62.3)[b]	47.9 (58.5)[b]	49.9 (55.6)[b]	47.4 (51.3)[b]	47.7 (54.9)[b]	41.8 (51.0)[b]
Coke	23.1	18.5	17.7	16.0	18.8	18.8

Notes: [a] Includes small percentage of carbon monoxide.

[b] The value in the parenthesis is the "corrected" C_5^+ liquid yield.

Figure 4.9

Effect of Reactor Temperature on Product Yield and Distribution

Tarsand Triangle Feed

Retention Time of Solids, θ_{avg} = 27.2 mins.

Feed Sand Particle Size, d_p = 358.5 microns

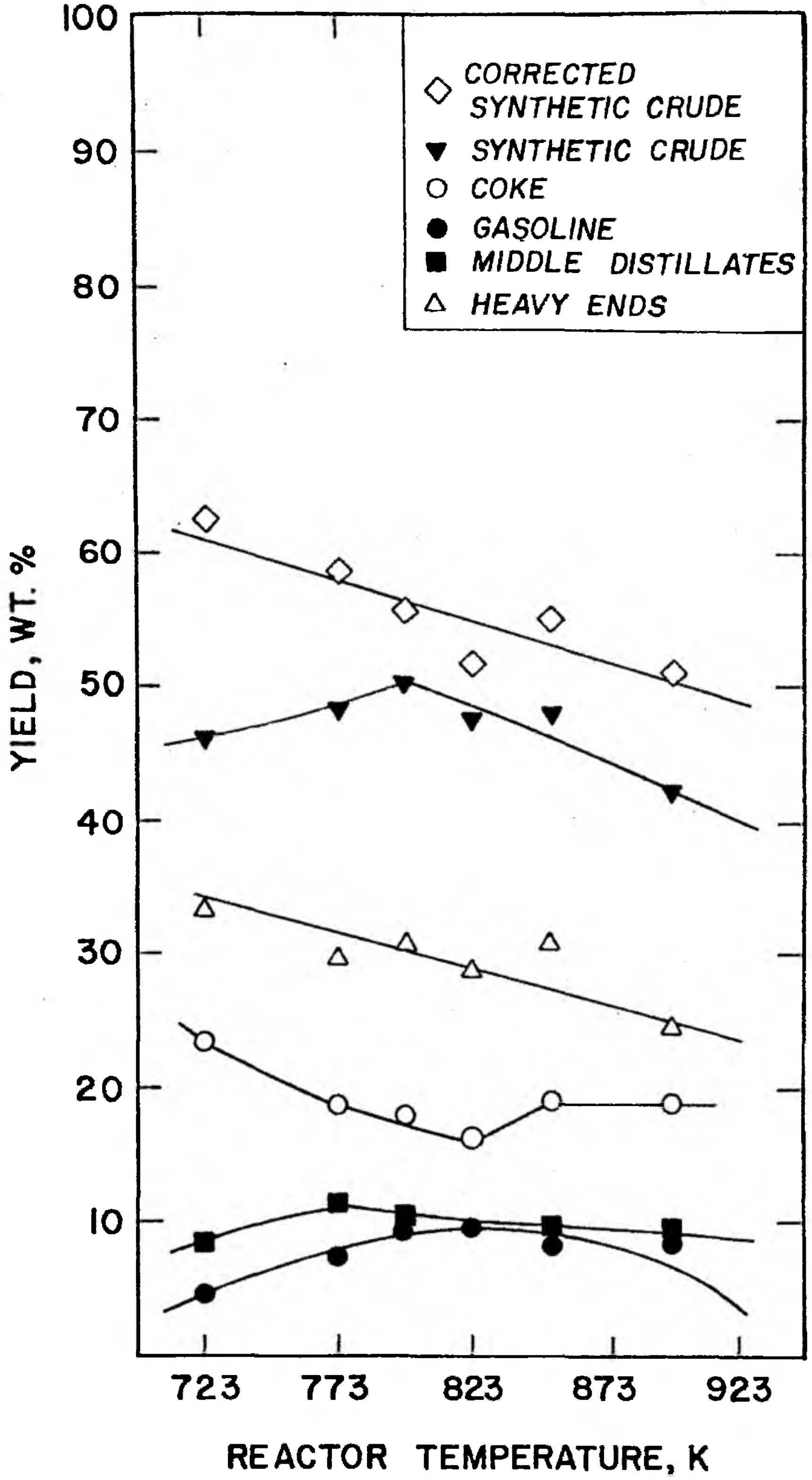
100
90
80
70
60
50
40
30
20
10
YIELD, WT. %
723
773
823
873
923
REACTOR TEMPERATURE, K
◇ CORRECTED SYNTHETIC CRUDE
▼ SYNTHETIC CRUDE
○ COKE
● GASOLINE
■ MIDDLE DISTILLATES
△ HEAVY ENDS

Figure 4.10

Effect of Reactor Temperature on Gas Make
and Product Distribution

Tarsand Triangle Feed

Retention Time of Solids, θ_{avg} = 27.2 min.

Feed Sand Particle Size, d_p = 358.5 microns

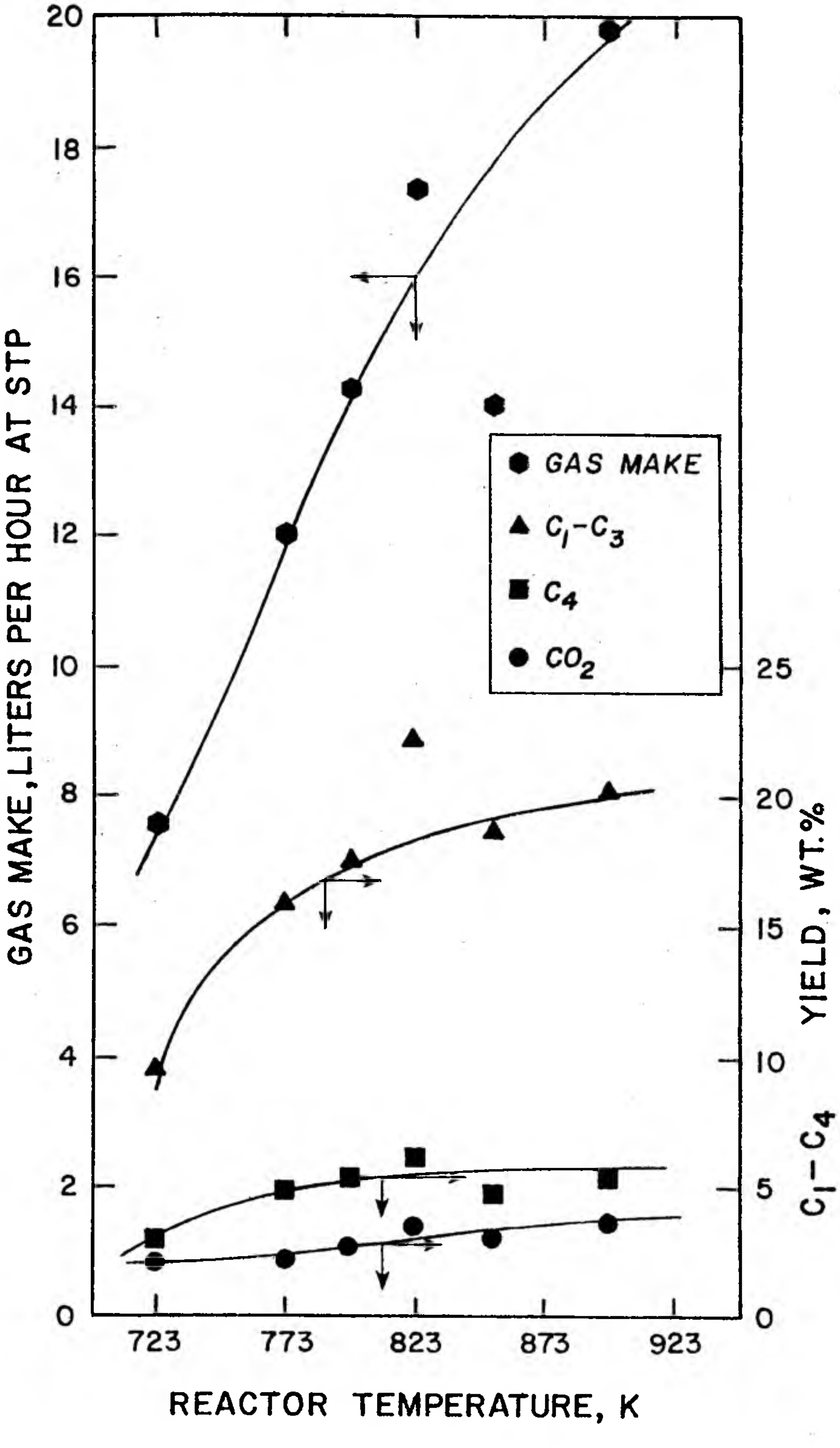
GAS MAKE, LITERS PER HOUR AT STP
0
2
4
6
8
10
12
14
16
18
20
C1–C4 YIELD, WT.%
0
5
10
15
20
25
REACTOR TEMPERATURE, K
723
773
823
873
923
⬢ GAS MAKE
▲ C1-C3
■ C4
● CO2

bituminous sands and has found that the percent bitumen recovered decreased with aged samples. Furthermore, the percent of the sand pore volume occupied by bitumen was very small for surface samples compared to the core samples for the Tarsand Triangle deposit, even though the sand porosity for both samples was about the same (Table 1.5)(51). Thus, the low yield of synthetic crude could be related to these factors.

The gas make, in particular the C_1 - C_3 gas yield, increased sharply between 723 K and 773 K. Beyond 773 K, the coke yield reached a stationary value of 18 - 19 percent by weight as the reactor temperature was increased. Again, it appears that coke yield is only slightly sensitive to a change in operating temperature.

The yields of the gasoline fraction and the middle distillate fraction did not change much with reactor temperature, while the yield of heavy ends decreased linearly as did the "corrected" synthetic crude yield.

A comparison was made for the effect of temperature on the C_5^+ liquid (synthetic crude) yield for the Sunnyside and Tarsand Triangle feeds. The yield and product distributions for three different reactor temperatures for Sunnyside and Tarsand Triangle feeds are presented in Table 4.8. The synthetic crude yield as a function of reactor temperature is presented in Figure 4.11. These data were obtained at a solids retention time of 27.2 minutes and a particle size of 358.5 microns. Interestingly, the over-all material balances for the Sunnyside feed were better than for the Tarsand Triangle feed. The "uncorrected" material balance based on the weight percent bitumen

Table 4.8

Comparison of Product Yield and Distribution with Feed Sand Source and its Bitumen Content

Feed Sand Source	Sunnyside			Tarsand Triangle		
Average Bitumen Content of Feed Sand (weight percent)	8.5			4.5		
Experiment Number	52	53	55	33	41	43
Reactor Temperature, K	723	773	798	723	773	798
Retention Time of Solids, min.	27.2	27.2	27.2	27.2	27.2	27.2
Feed Sand Particle Size, μ	358.5	358.5	358.5	358.5	358.5	358.5
Fluidizing Gas Flow Rate, SCM·h^{-1}	0.142	0.142	0.142	0.142	0.142	0.142
Gas Make, LPH at STP	7.3	14.5	16.0	7.5	12.0	14.3
Synthetic Liquid Yield, gm h^{-1}	23.9	22.2	22.9	27.6	26.5	27.9
Mass Balance (weight percent)						
CO_2	1.3	1.5	2.7	2.3	2.4	4.2
C_1 - C_3	10.8	21.0	22.9	9.4	15.8	17.3
C_4	4.0	6.5	6.7	2.8	4.7	5.2
C_5^+ liquid (synthetic crude)	61.2	47.5	45.0	45.8	47.9	49.9
Coke	22.6	23.5	22.8	23.1	18.5	17.7

Figure 4.11

Effect of Feed Sand Source and Bitumen Content
on the Optimum Temperature for Maximum
Yield of Synthetic Crude

Feed Sand Particle Size, d_p = 358.5 microns

Retention Time of Solids, θ_{avg} = 27.2 mins.

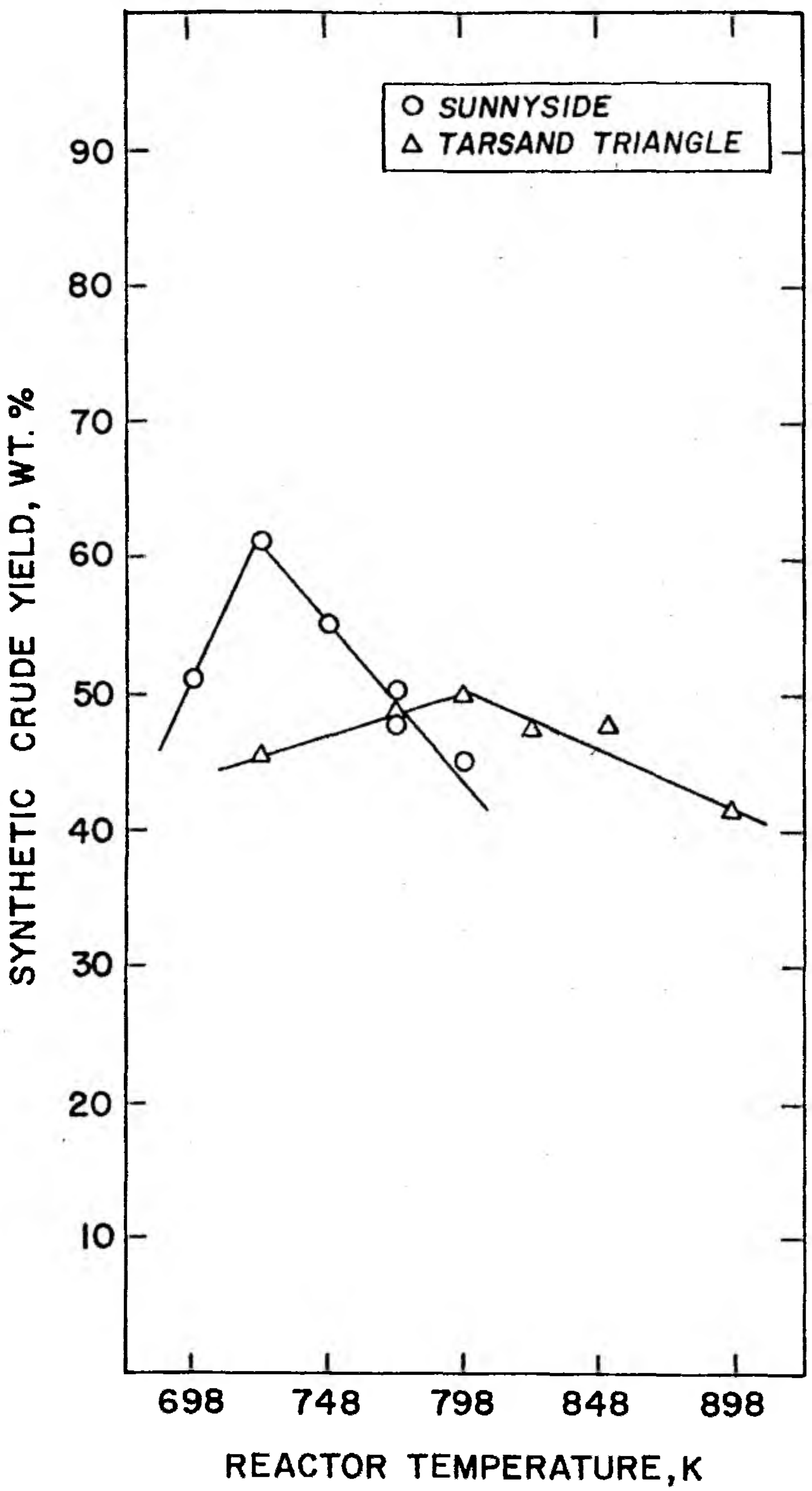

○ SUNNYSIDE
△ TARSAND TRIANGLE
SYNTHETIC CRUDE YIELD, WT. %
90
80
70
60
50
40
30
20
10
698
748
798
848
898
REACTOR TEMPERATURE, K

fed always exceeded 90% for the Sunnyside feed. The optimum temperature at which maximum liquid yield was obtained was about 723 K for the Sunnyside feed and was about 798 K for the Tarsand Triangle feed. Moreover, the maximum yield of synthetic crude was higher at the optimum temperature for Sunnyside feed. The Sunnyside feed was richer in bitumen content (8.5 wt %) compared to 4.5 weight percent for Tarsand Triangle feed. It was also more sensitive to higher cracking temperatures, giving higher yields of C_1 - C_4 light hydrocarbon gases than did the Tarsand Triangle feed. A high synthetic crude yield of 61.2 weight percent was obtained at a lower reactor temperature for the Sunnyside feed, thus the energy demand for liberating one kilogram of synthetic liquid is much lower than for the Tarsand Triangle feed. Using Peterson and Gishler's data(116), the energy required for distilling one kilogram of synthetic liquid for these two feed sands was 1670 kcal for the Sunnyside bituminous sand and 2900 kcal for the Tarsand Triangle bituminous sand.

A discussion comparing the qualities of liquid product from these two feed bituminous sands is presented in Section 4.2.

4.2 Characterization Studies on the Extracted Bitumens and the Synthetic Liquids

The quality of the synthetic liquid produced in the high temperature thermal recovery process was dependent upon the operating variables. A knowledge of the product quality could have a direct impact in the selection of the subsequent processing steps in the refining or the upgrading of this synthetic liquid. The synthetic liquid obtained from the thermal recovery scheme could be used for the production of motor fuels, cracking stock for making olefins, or as a fuel oil depending upon the nature of the liquid. Moreover, a knowledge of the properties of the synthetic liquid product and the bitumen could provide an insight to the thermal cracking reaction mechanisms for the bitumen.

The synthetic liquid and the solvent extracted bitumen were characterized using physical properties, elemental analysis, infra-red (IR) spectroscopy, and proton magnetic resonance (PMR) spectroscopy. The physical properties included the density expressed in terms of API gravity, viscosity, simulated distillation, Conradson carbon residue, ash content, and heating value. The density of the liquid product at 293 K was obtained using a Mettler/Paar DMA 40 digital density meter (manufactured by Metler Corporation, New Jersey). The viscosity of the liquid product was obtained using a Brookfield Viscometer Model LVT, 0.8^{o} Cone (manufactured by Brookfield Engineering Laboratories, Massachusetts). The Conradson carbon residue and ash content of the synthetic liquids and the bitumen were obtained using ASTM D189-65 and ASTM D482-63 methods, respectively. The net heat of combustion values were determined by the Bomb Calorimeter technique (ASTM D2382-65). The simulated distillation data for the extracted bitumens and for the synthetic liquid products were done on a 5730 A Series Hewlett-Packard Gas Chromatograph with dual flame ionization detectors (FID) using a 3% Dexil 300 on Anachrome Q column (6.35 mm O.D. x 0.46 m long). This procedure was similar to the ASTM D2887-70T method. Elemental analyses and the molecular weight determination of the bitumens and the synthetic liquids were performed by a commercial laboratory. Infra-red spectra were obtained on a Perkin Elmer Model 283 Spectrophotometer and a Beckman Acculab 3 Spectrophotometer. The proton magnetic resonance spectra of the synthetic liquids and the bitumens were obtained on a Varian EM360 60MHZ NMR Spectrometer. The properties of Sunnyside and Tarsand Triangle bitumens and the synthetic liquids are presented together for comparison.

4.2.1 Properties of the Extracted Bitumens

The physical properties of Sunnyside and Tarsand Triangle solvent-extracted bitumens are presented in Table 4.9. Data from the literature on the properties of hot water extracted bitumen from the Sunnyside bituminous sand and the solvent extracted bitumen from Athabasca sand are also included in Table 4.9 for comparison.

The density of Tarsand Triangle bitumen could not be estimated with reasonable accuracy, but a value in the range of 2.5 to 3.5 was obtained. The sulfur content of the Tarsand Triangle bitumen sample was high (3.8 - 3.9 wt %) compared to the Sunnyside bitumen (0.62 wt %) and was comparable to that for the Athabasca bitumens. This result was not unexpected since both the Tarsand Triangle and the Athabasca bitumens are of marine origin whereas the Sunnyside bitumen is of fresh water origin. The high oxygen content of the Tarsand Triangle and the Sunnyside bitumens was attributed to the fact that both were obtained from outcrop sand samples and might have undergone oxidation due to weathering. The nitrogen content of Sunnyside bitumen was much greater than the 0.2 to 0.3 weight percent nitrogen

Table 4.9

Properties of Extracted Bitumens

PROPERTIES	Sunnyside Bitumen (This Study)	Tarsand Triangle Bitumen (This Study)	Sunnyside Bitumen (Hot Water Extraction)[a]	Athabasca Bitumen[b]
Gravity, ^{o}API at 298 K	4.9 - 5.5	2.5 - 3.5[c]	6.7	5.8 -- 8.3
Viscosity at 298 K (poise)	>10,000[e]	NE	NA	5000 - 10,000
Elemental Analysis (weight percent)				
Carbon	83.3	77.8	NA	81.9 - 83.6
Hydrogen	10.8	8.7	NA	9.5 - 10.6
Nitrogen	0.7	0.5	1.0	0.3 - 0.4
Sulfur	0.6	3.8 - 3.9	0.5	3.8 - 5.5
Oxygen	4.4	5.0 - 6.0	NA	1.2 - 2.9
Molecular Weight (VPO benzene) $g.mol^{-1}$	1042	450	NA	540 - 800
Hydrogen/Carbon Atomic Ratio	1.56	1.35	NA	1.38- 1.53
Conradson Carbon (weight percent)	14.8	NE	19.1	10.0 - 14.0
Ash (weight percent)	2.4	NE	NA	4.0 - 5.0
Heat of Combustion at 298 K (calories per gram)	9900	NE	NA	9800 - 10,000

- Continued -

Table 4.9 - Continued

Distillation Data (weight percent)		Sunnyside Bitumen (This Study)		Tarsand Triangle Bitumen (This Study)		Sunnyside Bitumen (Hot Water Extraction)[a]		Athabasca Bitumen[b]	
Fraction	Cut Point Temperature, K	% Total	% Cumulative	% Total	% Cumulative	% Total[d]	% Cumulative	% Total	% Cumulative
1 - 7	<473	0.9	0.9	0.2	0.2	0.3	0.3	3.0	3.0
8	498	0.2	1.1	0.1	0.3	0.4	0.7	1.6	4.6
9	523	0.5	1.6	0.2	0.5	1.4	2.1	1.9	6.5
10	548	0.8	2.4	0.3	0.8	5.1	7.2	2.4	8.9
11	578	1.3	3.7	0.7	1.5	6.4	13.6	3.5	12.4
12	608	1.9	5.6	1.7	3.2			3.9	16.3
13	638	2.8	8.4	3.2	6.4			4.0	20.3
14	668	3.2	11.6	5.0	11.4			4.2	24.5
15	698	3.5	15.1	5.1	16.5			4.6	29.1
16	728	4.6	19.7	7.1	23.6			4.4	33.5
17	758	5.7	25.4	7.2	30.8			4.1	37.6
18	788	4.3	29.7	7.0	37.8			4.0	41.6
19	811	2.7	32.4	5.0	42.8			3.0	44.6
Residue	>811	67.6	100.0	57.2	100.0	86.4	100.0	55.4	100.0

Notes:

[a] Data from Reference 57.
[b] Data from References 5, 45, 50, and 55.
[c] Estimated with insufficient sample.
[d] Distillation data using Bureau of Mines routine method.
[e] Could not be measured in the operating range of the viscometer.
NE - Not estimated.
NA - Not available.

to be expected in typical black crude oils. The atomic hydrogen/carbon ratio and molecular weight for Sunnyside bitumen were 1.56 and 1042 $g.mol^{-1}$, respectively; while the values for the Tarsand Triangle sample were 1.35 and 450 $g.mol^{-1}$, respectively. These values for Tarsand Triangle bitumen were similar to the Athabasca bitumen. The hydrogen to carbon atomic ratio indicated that the Sunnyside bitumen was less aromatic, while the Tarsand Triangle bitumen was more aromatic. The high hydrogen content and the high molecular weight of the Sunnyside bitumen suggests that the bitumen maturation conditions have been less severe than for Tarsand Triangle bitumens. The higher percentage of volatility of the Tarsand Triangle bitumen seems to correspond with the lower molecular weight of the bitumen. The converse relationship of high molecular weight and low volatility held true for Sunnyside bitumen.

The viscosities of the Tarsand Triangle and Sunnyside bitumens could not be determined with the Brookfield Viscometer since the values appear to be beyond the operating range of the viscometer. But the data in the literature indicated that the viscosity of the Sunnyside bitumen was one order of magnitude higher than the Tarsand Triangle bitumen(54,55,57).

The experimental heat of combustion of Sunnyside bitumen was determined to be 9889 cals/gm. The heat of combustion can also be calculated from the elemental analysis of the bitumen using the Boie equation(132)

$$\begin{aligned} Q\ (\text{cals/gm}) &= \frac{1}{100}\,[8400\ (C) + 27{,}765\ (H) + 1500\ (N) \\ &\quad + 2500\ (S) = 2650\ (O)] \end{aligned} \tag{4.5}$$

where (C) is the percent carbon, (H) is the percent hydrogen, (N) is the percent nitrogen, (S) is the percent sulfur, (O) is the percent oxygen, and Q is the heat of combustion in calories per gram. The calculated value for heat of combustion was 9907 cals/gm. The high ash content (2.4 wt %) of the Sunnyside bitumen was due to the high percentage of sand fines in the crushed feed used for the extraction. This explains the reason for the large amount of sand fines collected in the high temperature cyclones in the experimental run with a wide cut (Tyler Sieve 20 - 150 mesh fraction) Sunnyside feed sand.

The Conradson carbon residue of the bitumen should provide an indication of relative coke-forming tendency of the bitumen during pyro-distillation. The Conradson carbon residue for the Sunnyside bitumen was about 15.0 weight percent, after correction for the ash content, which was comparable to the value determined for the bitumen obtained by the hot water extraction process(57) (Table 4.9). Thus, the method of extraction of the bitumen did not affect the Conradson carbon residue. The high Conradson carbon residue could explain the high coke yields (19 - 23 wt %) observed during the pyro-distillation of the bitumen. If a linear relationship between the carbon residue and coke make is accepted, about 15 - 16 weight percent of the bitumen would immediately be converted to coke during the pyro-distillation of the bituminous sand.

The Conradson carbon residue for the Tarsand Triangle bitumen could not be obtained due to inadequate availability of sample, however, a value of 20 weight percent was reported in the literature(55). Despite the difference in the Conradson carbon residues, the two feed sands gave nearly the same coke yield (18 - 22 wt %) at a solids retention time of 27.2 minutes and at reactor temperatures above 773 K.

The simulated distillation data for Sunnyside and Tarsand Triangle bitumens are presented in Table 4.9 and Figure 4.12. The data of the present study and that of Wenger, et. al.(57) indicated that the Sunnyside bitumen had a higher percentage of high boiling fraction, while low molecular weight Tarsand Triangle bitumen contained a higher percentage of low boiling material (< 811 K). This indicates that a relationship exists between the molecular weight, the weight percent volatility below 811 K, and the viscosity of the bitumen.

Infra-red spectra were obtained on the extracted bitumen from Sunnyside and Tarsand Triangle bituminous sands. Carbon tetrachloride was used both as reference and as solvent for the bitumen. The infra-red analyses were preliminary and the information reported here are general inferences relating to the functional groups present in the bitumen. Since the analyses are not sufficiently sophisticated, no attempt was made to relate the data to the molecular structure of the bitumen. The C - H stretch region (2750 - 3100 cm^{-1}) showed two strong intensity peaks at 2920 cm^{-1} and 2870 cm^{-1} corresponding to methylene and methyl stretching vibrations. Furthermore, two sharp peaks between 1350 - 1500 cm^{-1} indicating methyl and methylene C - H bending were observed. No distinct peak for the aromatic C - H bond between 300 - 3100 was observed, however, a medium intensity peak centering around 1600 cm^{-1} characteristic of

Figure 4.12

Distillation Curves for Extracted Bitumens

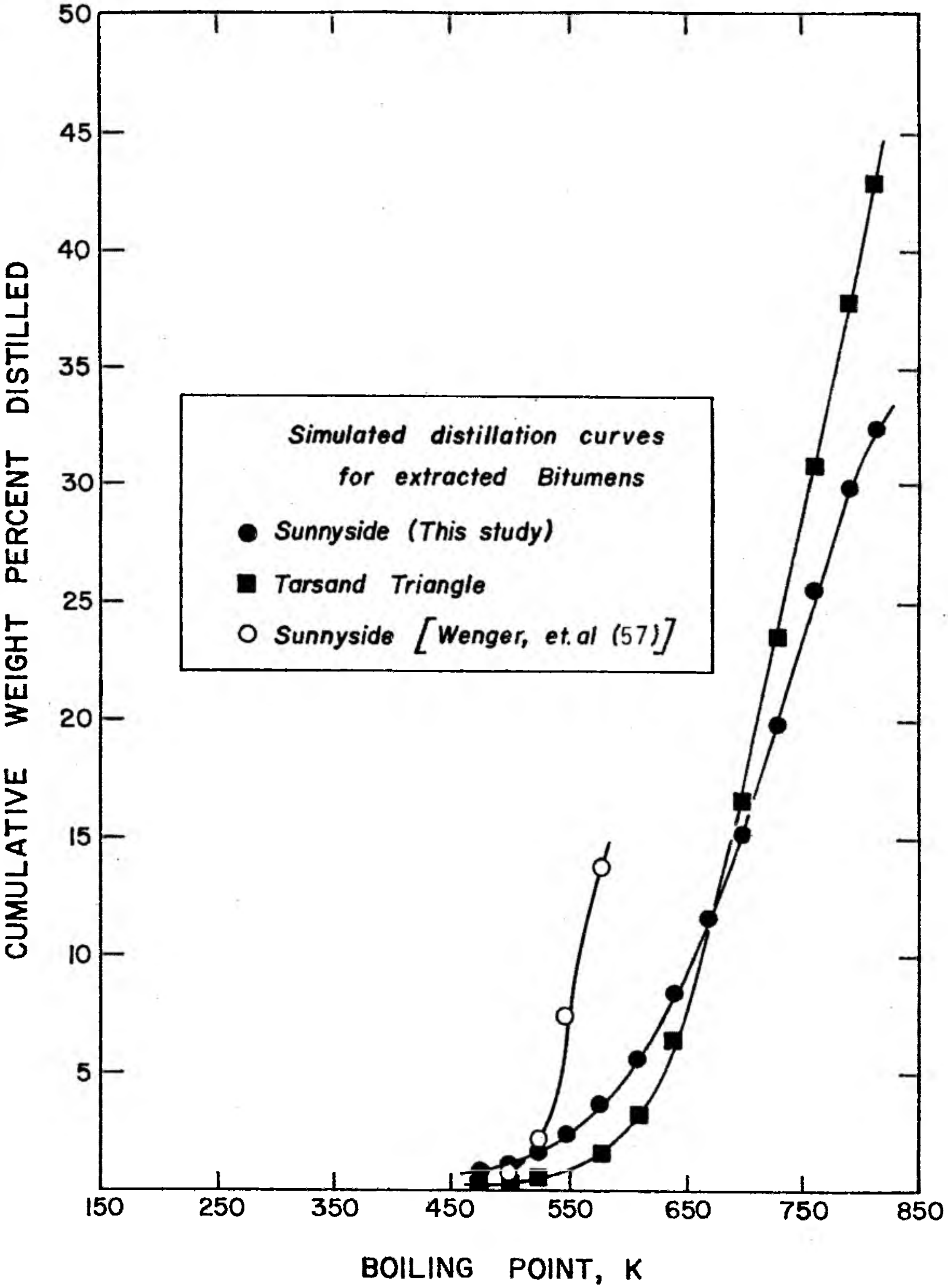
Simulated distillation curves for extracted Bitumens
● Sunnyside (This study)
■ Tarsand Triangle
○ Sunnyside [Wenger, et. al (57)]
CUMULATIVE WEIGHT PERCENT DISTILLED
BOILING POINT, K
50
45
40
35
30
25
20
15
10
5
150
250
350
450
550
650
750
850

the aromatic ring C = C vibration was observed. A moderate intensity peak centering at 1700 cm^{-1} wave number was indicative of the presence of carbonyl compounds, perhaps a result of the long term oxidation of the bituminous sand samples. A broad absorption band of very low intensity between 3000 - 3200 cm^{-1} characteristic of the O - H and N - H stretching vibrations was observed. A number of peaks of very low intensity between 700 - 900 cm^{-1}, characteristic of substituted aromatic ring systems, were also observed.

4.2.2 Effect of Temperature on Synthetic Liquid Product Quality

The effects of the coking reactor temperature on the selected physical properties of the synthetic liquid products from Sunnyside feed and Tarsand Triangle feed are presented in Tables 4.10 and 4.11. The change in the API gravities of the synthetic liquids with increasing reactor temperature for Sunnyside and Tarsand Triangle feed is presented in Figure 4.13. The API gravities of the heavy oil liquids obtained in the fluidized bed coking of Canadian bituminous sands(111) are also presented in Figure 4.13. The API gravities of the liquids decreased linearly with increasing reactor temperature perhaps due to an increase in the aromaticity of the liquid product. The API gravities of the Sunnyside synthetic liquids were higher than the API gravities of the Tarsand Triangle synthetic liquids produced at the same reactor temperature. The hydrogen content of the Sunnyside liquid obtained at a reactor temperature of 723 K was 11.1, whereas the hydrogen content of Tarsand Triangle liquid was 9.5, thus the Sunnyside synthetic liquid was more saturated and exhibited a

Table 4.10

Effect of Reactor Temperature on Synthetic Liquid Product Quality

Sunnyside Feed

Reactor Temperature, K	698	723	748	773	798
Retention Time of Solids, θ_{avg}, min.	27.2	27.2	27.2	27.2	27.2
Feed Sand Particle Size, μ	358.5	358.5	358.5	358.5	358.5
Fluidizing Gas Velocity, $SCM \cdot h^{-1}$	0.142	0.142	0.142	0.142	0.142
Properties					
Gravity, ^{o}API at 293 K	15.9	17.4	14.9	12.7	14.0
Viscosity, Centipoise at 298 K	159 ± 4	198 ± 4	133 ± 2	81 ± 1	86.5 ± 2
Elemental Analysis (weight percent)					
Carbon	87.1	87.1	87.3	87.6	87.5
Hydrogen	11.0	11.1	11.1	10.6	10.5
Nitrogen	0.5	0.6	0.6	0.8	0.7
Sulphur	0.4	0.4	0.4	0.4	0.4
Oxygen	0.6	0.6	0.5	0.5	0.9
Molecular Weight (VPO benzene) $g.mol^{-1}$	298	350	306	292	235
Hydrogen/Carbon Atomic Ratio	1.52	1.53	1.53	1.45	1.44
Heat of Combustion, Q, in cal/g at 298 K	--	10500	10300	10200	--
Conradson Carbon (weight percent)	--	3.2	5.3	7.3	7.1
Volatility below 811 K	97.6	88.6	82.0	75.6	85.0

Table 4.11

Effect of Reactor Temperature on Synthetic Liquid Product Quality

Tarsand Triangle Feed

Reactor Temperature, K	723	798	898
Retention Time of Solids, min.	27.2	27.2	27.2
Feed Sand Particle Size, μ	358.5	358.5	358.5
Fluidizing Gas Velocity, SCM·h^{-1}	0.142	0.142	0.142
Properties			
Gravity, ^{o}API at 293 K	12.2	10.8	7.5
Viscosity, Centipose at 298 K	102 ± 2	90 ± 1	108 ± 2
Elemental Analysis (weight percent)			
Carbon	83.7	84.0	83.9
Hydrogen	9.5	9.9	9.2
Nitrogen	0.3	0.7	0.3
Sulphur	3.1	3.3	3.5
Oxygen	3.2	2.4	3.0
Molecular Weight (VPO benzene) g.mol^{-1}	320	312	327
Hydrogen/Carbon Atomic Ratio	1.36	1.41	1.32
Heat of Combustion, Q, in cal/gm at 298 K	10,000	9700	9800
Conradson Carbon (weight percent)	4.9	6.8	7.8
Ash (weight percent)	0.03	0.03	0.07
Volatility below 811 K (weight percent)	64.3	75.7	76.1

Figure 4.13

Effect of Coking Reactor Temperature on the
API Gravity of Synthetic Liquid

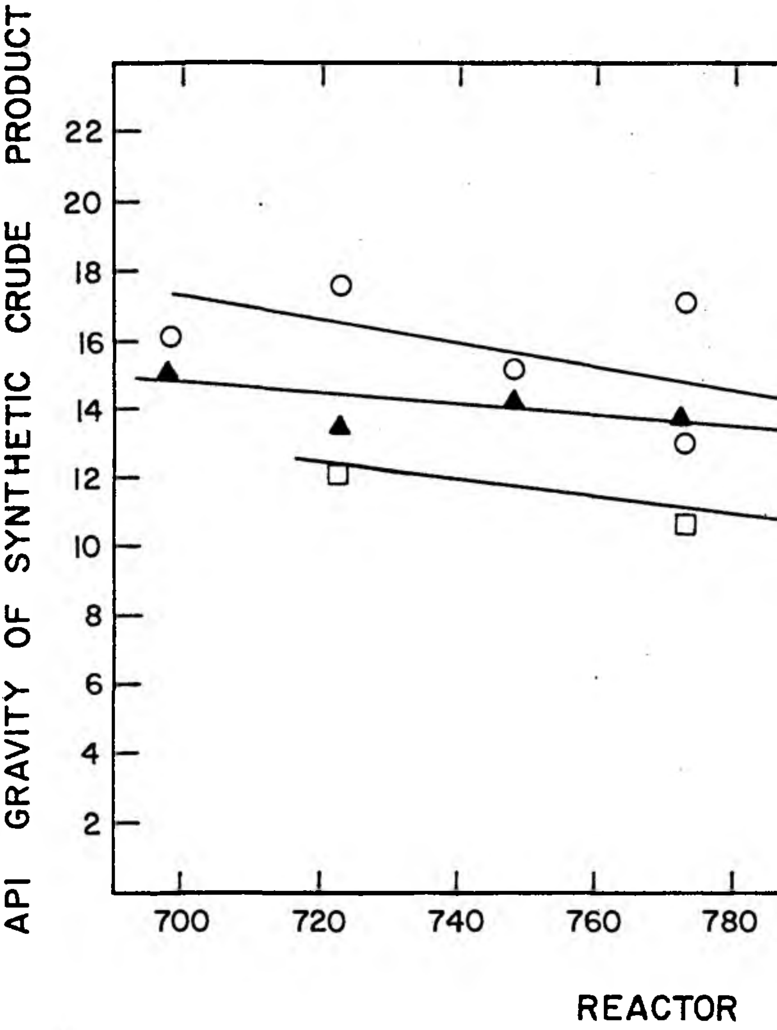
API GRAVITY OF SYNTHETIC CRUDE PRODUCT
22
20
18
16
14
12
10
8
6
4
2
700
720
740
760
780
REACTOR

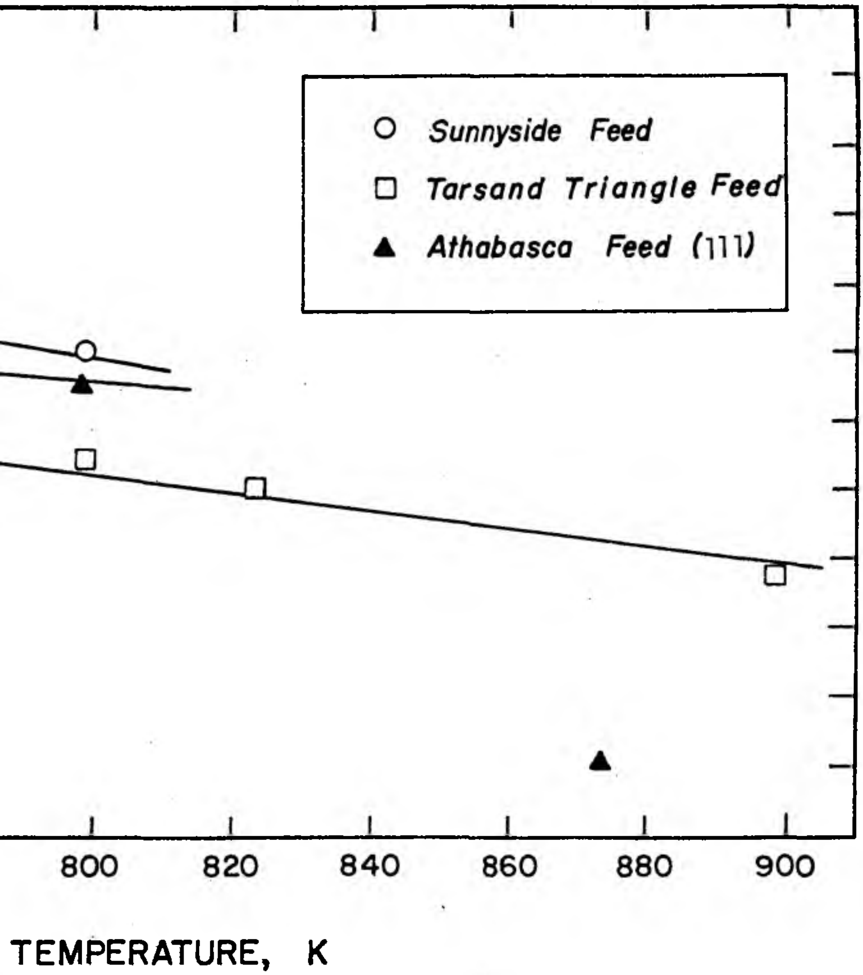
○ Sunnyside Feed
□ Tarsand Triangle Feed
▲ Athabasca Feed (111)
800
820
840
860
880
900
TEMPERATURE, K

higher API gravity. Schmidt(133) has obtained the following emperical relationship between the hydrogen content and specific gravities for petroleum fuels

$$\rho = \frac{25 - \langle H \rangle}{15} \tag{4.6}$$

where ρ is the specific gravity and $\langle H \rangle$ is the hydrogen content in weight percent. Thus, according to this relationship as the hydrogen content increases the specific gravity decreases or the API gravity increases. The hydrogen content of the Sunnyside synthetic liquids decreased with increasing reactor temperature and a more aromatic synthetic liquid was produced, thus a lower API gravity was obtained. The Conradson carbon residue of the synthetic liquid increased with increasing reactor temperature as shown in Figure 4.14. This indicated that the coke forming precursors are increased in the synthetic crude at higher reactor temperatures which is consistent with the increased aromaticity of the liquids. The change in the Conradson carbon residue of the synthetic liquid seems to be more sensitive for Sunnyside feed than for the Tarsand Triangle feed, that is, the Conradson residue of Sunnyside synthetic liquid increased from 3 to 7 weight percent for a 50 K increase in reactor temperature from 723 to 773 K. This is also reflected by the sharp decrease in the (H/C) atomic ratio of Sunnyside synthetic liquid between these temperatures. The ash content of Sunnyside synthetic liquid was negligible (0.03 - 0.05 wt %) compared to that for the extracted bitumen (2.4 wt %). This was an indication of the high operating efficiency of the sand fines collecting apparatus.

Figure 4.14

Effect of Coking Reactor Temperature on the Conradson Carbon Residue of the Synthetic Liquid

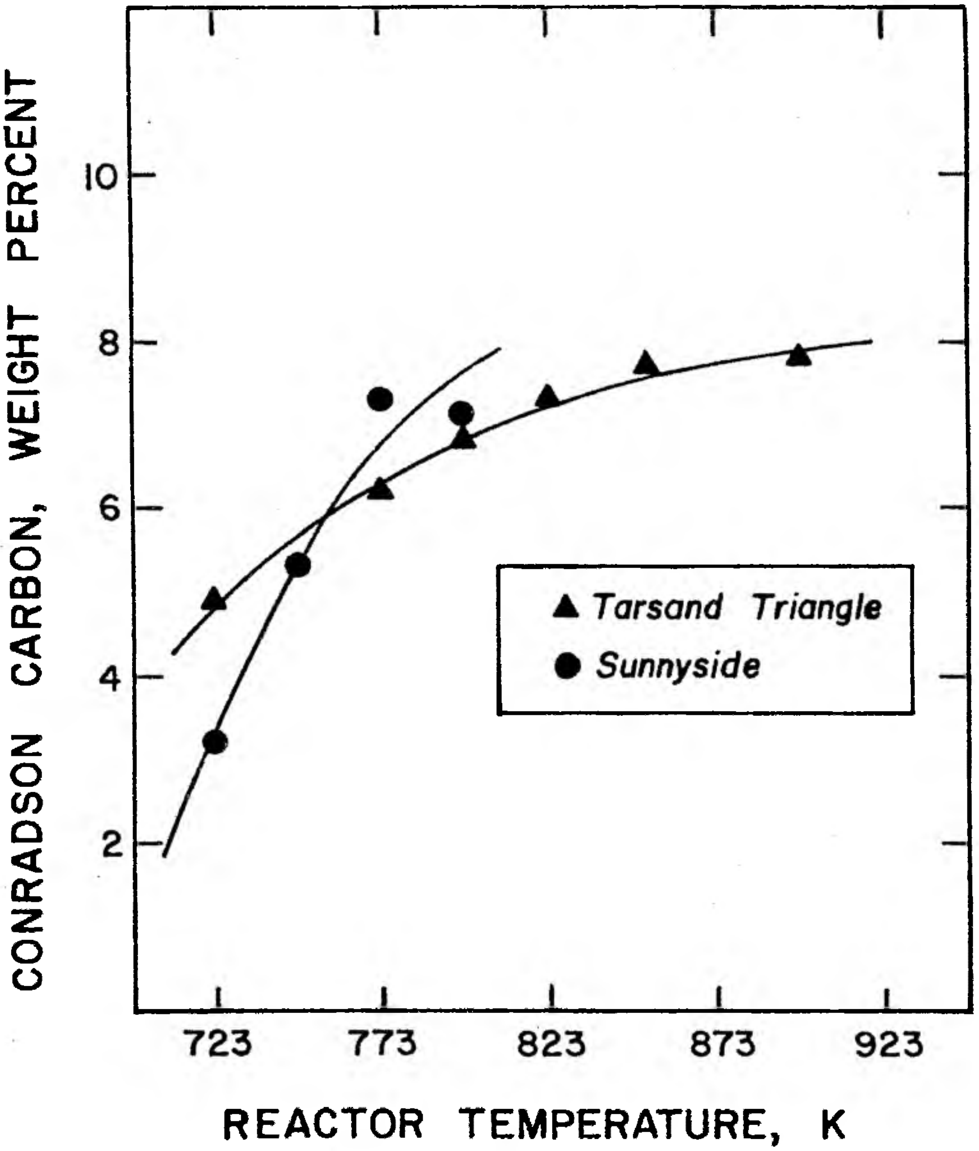
CONRADSON CARBON, WEIGHT PERCENT
10
8
6
4
2
723
773
823
873
923
REACTOR TEMPERATURE, K
▲ Tarsand Triangle
● Sunnyside

The viscosities of the Sunnyside and the Tarsand Triangle synthetic liquids as a function of reactor temperature are presented in Figure 4.15. The viscosity data on the synthetic liquid obtained from Canadian bituminous sand(111) are also included in Figure 4.15. Viscosities of synthetic liquids obtained from the Sunnyside and the Canadian bituminous sands exhibited a similar trend with increasing reactor temperature, while the viscosity of Tarsand Triangle synthetic crude was insensitive to the reactor temperature. The increase in the viscosity of Sunnyside synthetic liquid between 698 and 723 K was due to the increase in the molecular weight from 298 $g.mol^{-1}$ to 350 $g.mol^{-1}$ between these temperatures. The change in the molecular weight of the synthetic liquids from Tarsand Triangle was insensitive to reactor temperature which is consistent with the dependence of the viscosity on reactor temperature for Tarsand Triangle synthetic liquid.

The extracted bitumens from the Sunnyside and Tarsand Triangle bituminous sands were solids at room temperature and the standard ASTM procedure (ASTM-D97-66) could not be used for these solid-like materials, however, the pour points of the synthetic liquids from Sunnyside and Tarsand Triangle were determined. The pour points were in the range of 258 - 268 K. The dependence of the pour point on reactor temperature could not be evaluated due to the large sample sizes required for conducting the pour point measurements. The low viscosities and the low pour point temperatures indicated that the synthetic liquids could be transported in conventional pipelines to the refining site.

Figure 4.15

Effect of Coking Reactor Temperature on the
Viscosity of Synthetic Liquid

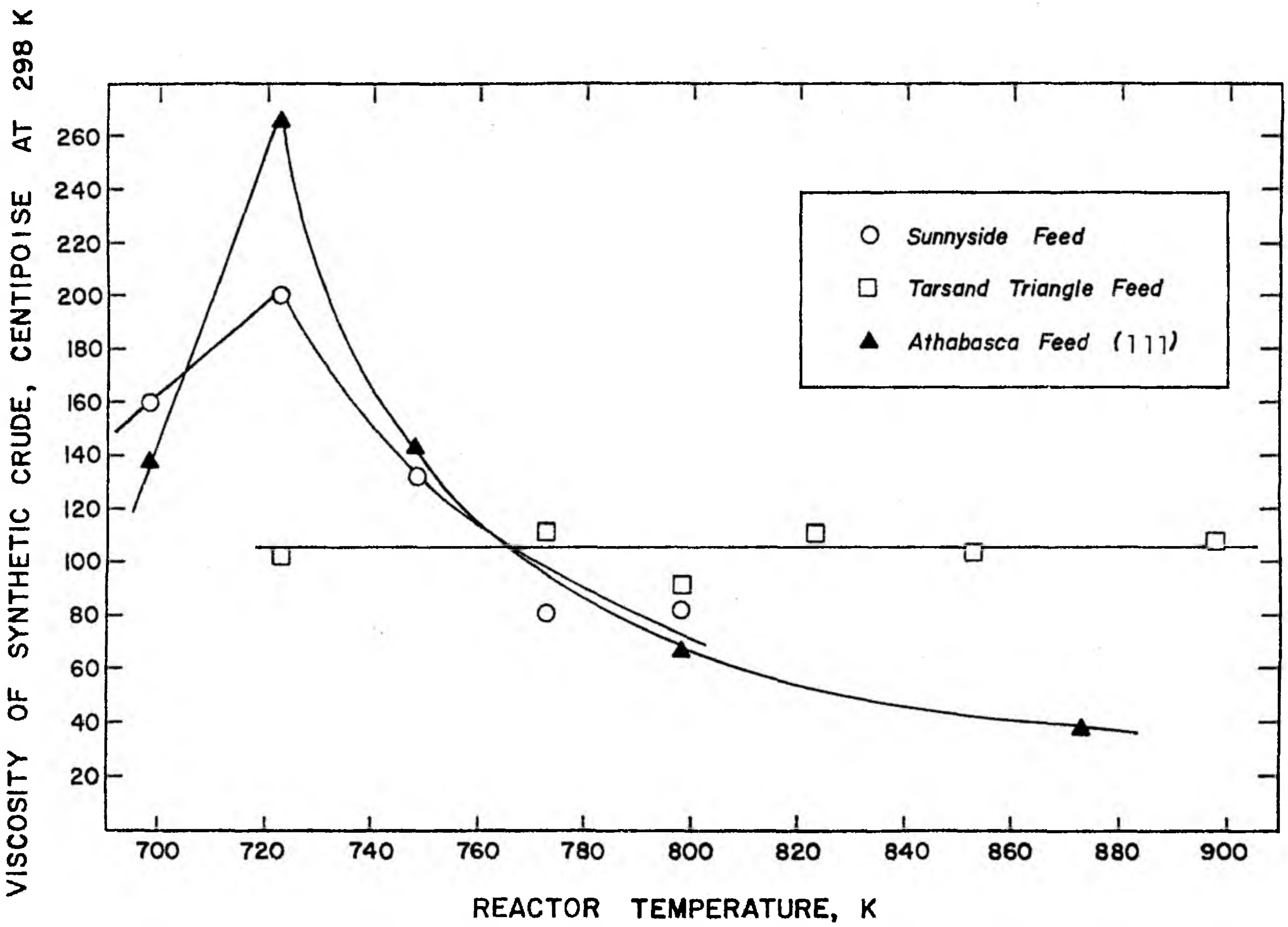
VISCOSITY OF SYNTHETIC CRUDE, CENTIPOISE AT 298 K
260
240
220
200
180
160
140
120
100
80
60
40
20
700
720
740
760
780
800
820
840
860
880
900
REACTOR TEMPERATURE, K
Sunnyside Feed
Tarsand Triangle Feed
Athabasca Feed (111)

The simulated distillation data for the Sunnyside synthetic liquids obtained at various reactor temperatures are presented in Table 4.12 and Figure 4.16, while the data for the Tarsand Triangle synthetic liquids are presented in Table 4.13 and Figure 4.17. The simulated distillation method allowed the determination of boiling range distribution of the synthetic liquid with a final boiling point of 811 K. The volatility below 811 K for both the Sunnyside and the Tarsand Triangle liquids did not correlate with molecular weight, however, the volatility of the extracted bitumen from both the Sunnyside and Tarsand Triangle did correlate with the molecular weight of the bitumens. With Sunnyside feed, the volatility below 811 K of the synthetic liquid was higher at lower reactor temperature (698 K) and decreased with increasing reactor temperature. However, the volatility below 811 K of the synthetic liquids was much greater than for the extracted bitumen. This was not unexpected because the bitumen was pyro-distilled to produce the synthetic liquid. The cumulative weight percent of liquid boiling below 675 K increases with increasing reactor temperature (Figure 4.16), perhaps an indication that the hydrocarbon species boiling above 675 K have undergone thermal cracking at the higher reactor temperatures. It is speculated that the molecular weight distribution perhaps becomes bimodal with increasing reactor temperature and this bimodal functionality could explain the decrease in the cumulative weight percent of liquid boiling below 811 K with simultaneous decrease in the average molecular weight of the synthetic liquid.

The Tarsand Triangle synthetic liquids exhibited an increase in the cumulative weight percent of liquid boiling below 811 K with

Table 4.12

Effect of Reactor Temperature on the Distillation Fractions for Synthetic Liquid

Sunnyside Feed

Temperature, K		698		723		748		773		798	
Fraction	Cut Point Temperature, K	Wt % Total	Wt % Cumulative	Wt % Total	Wt % Cumulative	Wt % Total	Wt % Cumulative	Wt % Total	Wt % Cumulative	Wt % Total	Wt % Cumulative
1 - 7	<473	4.0	4.0	3.3	3.3	3.5	3.5	4.7	4.7	4.5	4.5
8	498	3.3	7.3	2.8	6.1	3.4	6.9	3.6	8.3	3.4	7.9
9	523	4.8	12.1	3.5	9.6	4.1	11.0	4.7	13.0	5.2	13.1
10	548	5.8	17.9	4.9	14.5	5.4	16.4	5.4	18.4	6.0	19.1
11	578	7.1	25.0	6.4	20.9	6.5	22.9	5.9	24.3	7.0	26.1
12	608	8.0	33.0	7.0	27.9	6.8	29.7	6.1	30.4	7.6	33.7
13	638	9.2	42.2	7.8	35.7	7.7	37.4	6.4	36.8	8.4	42.1
14	668	9.6	51.8	8.3	44.0	7.5	44.9	6.6	43.4	8.3	50.4
15	698	8.9	60.7	9.0	53.0	8.1	53.0	6.9	50.3	7.2	57.6
16	728	10.1	70.8	9.4	62.4	8.0	61.0	6.8	57.1	8.1	65.7
17	758	11.8	82.6	10.8	73.2	8.6	69.6	7.3	64.4	8.8	74.5
18	788	9.3	91.9	9.1	82.3	7.2	76.8	6.6	71.1	6.7	81.2
19	811	5.7	97.6	6.3	88.6	5.2	82.0	4.5	75.6	3.8	85.0
Residue	>811	2.4	100.0	11.4	100.0	18.0	100.0	24.4	100.0	15.0	100.0

Figure 4.16

Effect of Coking Reactor Temperature on the Distillation Curve

Sunnyside Feed

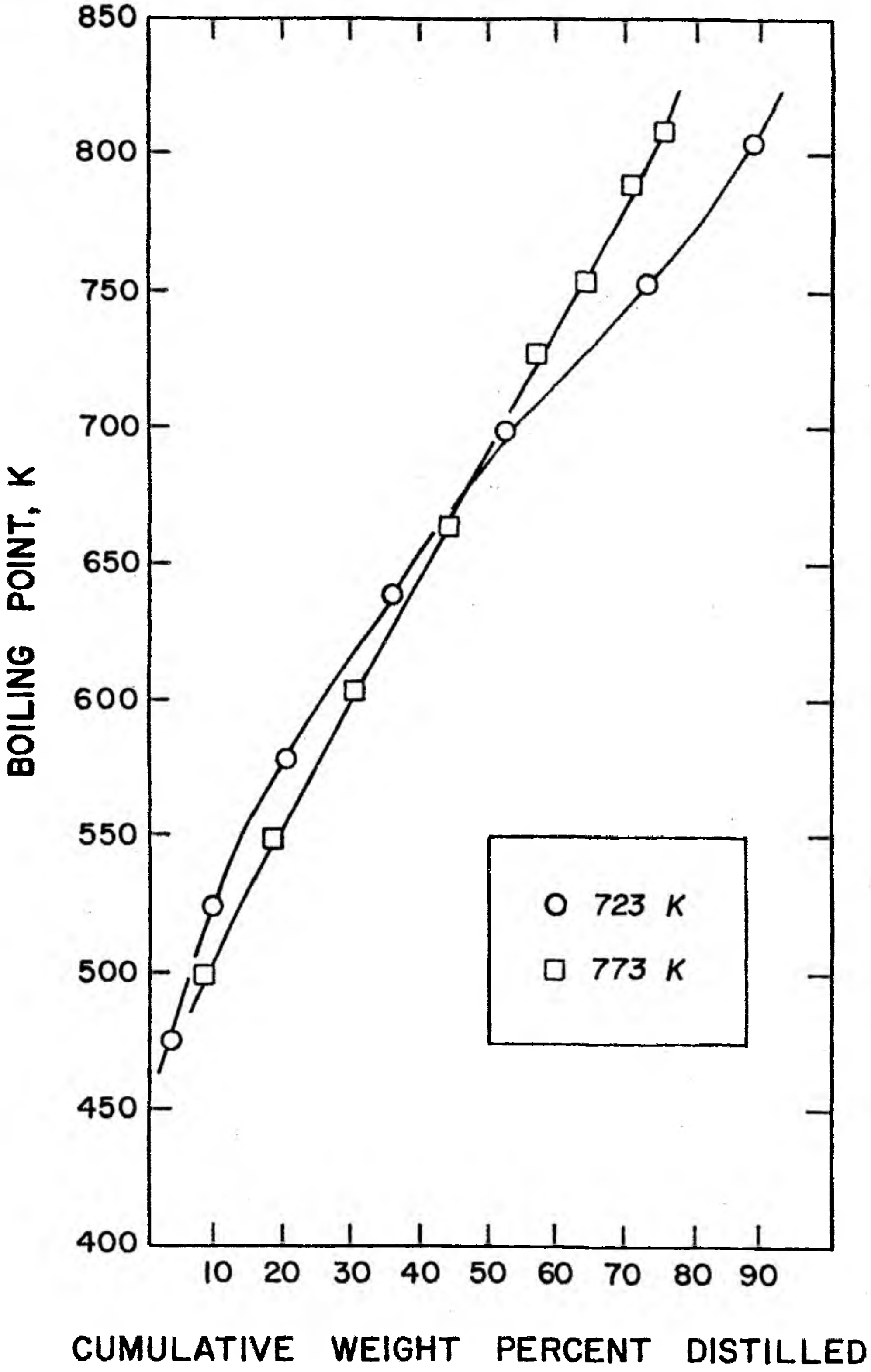
850
800
750
700
650
600
550
500
450
400
BOILING POINT, K
10
20
30
40
50
60
70
80
90
CUMULATIVE WEIGHT PERCENT DISTILLED
○ 723 K
□ 773 K

Table 4.13

Effect of Reactor Temperature on the Distillation Fractions for Synthetic Liquid Tarsand Triangle Feed

Temperature, K		723		798		898	
Fraction	Cut Point Temperature, K	Wt % Total	Wt % Cumulative	Wt % Total	Wt % Cumulative	Wt % Total	Wt % Cumulative
1 - 7	< 473	1.8	1.8	4.5	4.5	4.1	4.1
8	498	2.0	3.8	2.9	7.4	2.7	6.8
9	523	2.3	6.1	2.9	10.3	3.0	9.8
10	548	3.1	9.2	3.9	14.2	4.3	14.1
11	578	4.3	13.5	5.2	19.4	5.6	19.7
12	608	5.1	18.6	5.8	25.2	6.0	25.7
13	638	6.1	24.7	6.8	32.0	6.9	32.6
14	668	6.9	31.6	7.6	39.6	7.8	40.4
15	698	7.5	39.1	8.6	48.2	8.9	49.3
16	728	7.4	46.5	8.0	56.2	8.1	57.4
17	758	7.4	53.9	8.2	64.4	7.9	65.3
18	788	6.2	60.1	6.8	71.2	7.3	72.6
19	811	4.2	64.3	4.5	75.7	3.5	76.1
Residue	> 811	35.7	100.0	24.3	100.0	23.9	100.0

Figure 4.17

Effect of Coking Reactor Temperature on the Distillation Curves

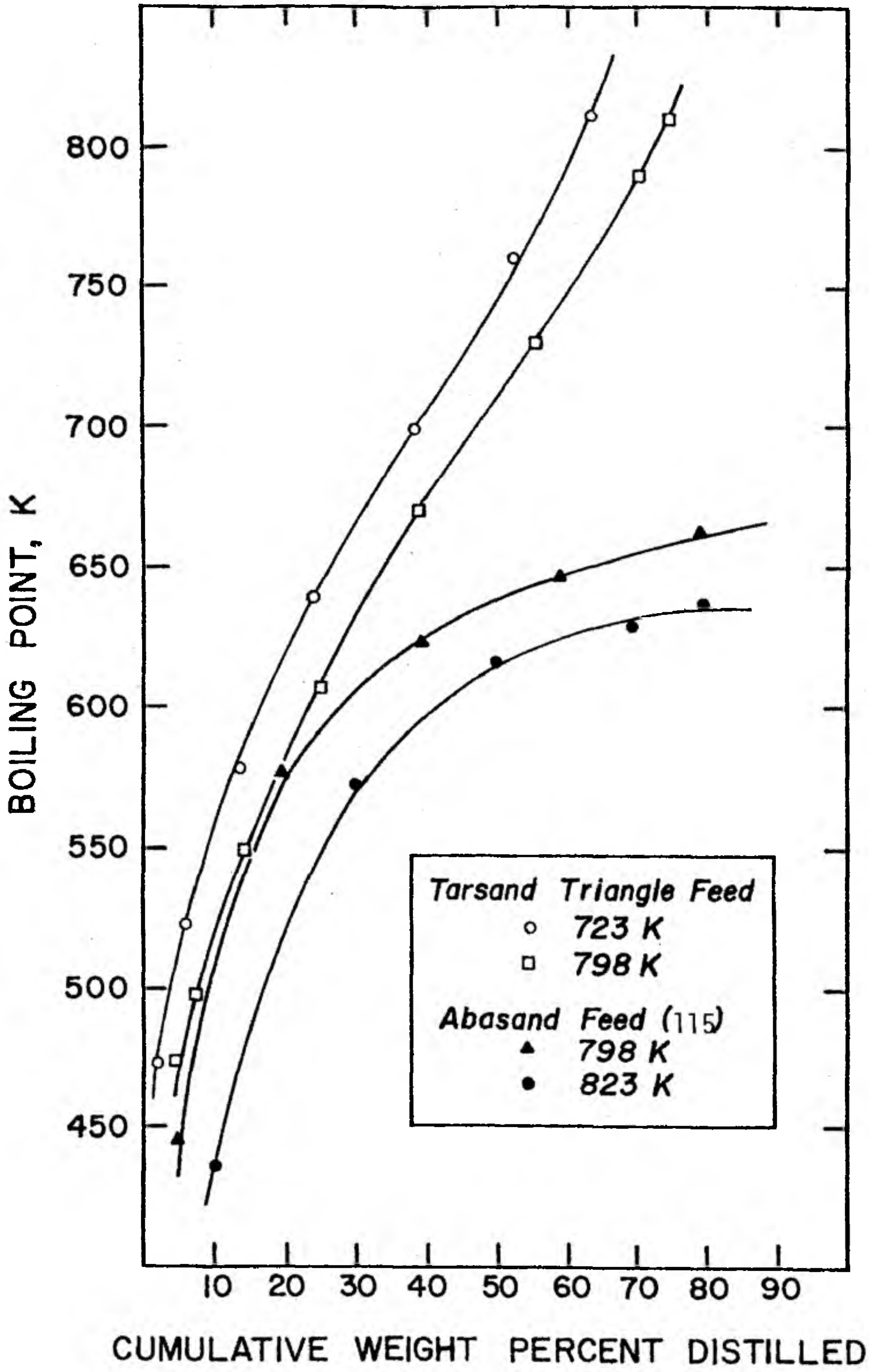
800
750
700
650
600
550
500
450
BOILING POINT, K
10
20
30
40
50
60
70
80
90
CUMULATIVE WEIGHT PERCENT DISTILLED
Tarsand Triangle Feed
○ 723 K
□ 798 K
Abasand Feed (115)
▲ 798 K
● 823 K

increasing reactor temperature. The synthetic liquids obtained in the fluidized bed direct coking of Abasand bituminous sand, Canada, whose properties were similar to Tarsand Triangle bituminous sand, displayed a similar trend in the distillation curves(115) (Figure 4.17). The shape of the distillation curves for Tarsand Triangle and Abasand synthetic liquids was similar up to 600 K, with the cumulative weight percent of liquid distillable being higher for Tarsand Triangle synthetic liquid as compared to Abasand synthetic crude at a given temperature. However, the differences in the shape of the curves beyond 600 K was due to the difference in the method for obtaining the data. Peterson and Gishler(115) used the ASTM D86-67 method for obtaining the distillation data, where evidence of thermal cracking at higher distillation temperatures have been observed. This could explain for the high percentage of liquid, that is 80 weight percent, boiling below 670 K.

The heats of combustion values for synthetic liquids fall in the range of 9500 - 10,500 calories per gram. This is comparable to the heats of combustion of coal derived liquids which are in the range of 9000 - 10,000 calories per gram(134). The heat of combustion values for Sunnyside synthetic liquids were higher than the heating values of Tarsand Triangle synthetic liquids, perhaps due to the higher hydrogen content of the Sunnyside synthetic liquids. From the results on the heats of combustion of coal derived liquids(134), the heat of combustion coal liquid from the H-coal process was 9700 calories per gram (hydrogen content 8.0 wt %), while the heat of combustion of SRC liquid was 8900 calories per gram (hydrogen content 5.7 wt %). The theoretical heat of combustion values computed from equation 4.5 agreed within one percent of the experimental values.

The elemental analyses and molecular weights determined for the synthetic liquids obtained at various reactor temperatures for the Sunnyside and Tarsand Triangle sands are presented in Tables 4.10 and 4.11. Up to 748 K, the atomic hydrogen/carbon ratio of Sunnyside synthetic liquids remained constant at 1.53 and did not differ very much from the value of extracted bitumen (atomic hydrogen/carbon ratio of extracted bitumen was 1.56). The atomic hydrogen/carbon ratio of the Sunnyside synthetic liquids decreased to a value of 1.44 for reactor temperatures above 748 K. The decrease in the atomic hydrogen/carbon ratio suggests an increase in the aromaticity of the synthetic crude which is a reflection of the severity in the thermal cracking of the bitumen and the synthetic liquid above 748 K. The atomic hydrogen/carbon ratio of Tarsand Triangle synthetic liquid was lower than that of the Sunnyside synthetic liquids, an indication that the liquids obtained from the Tarsand Triangle deposit were more aromatic. In addition, the total heteroatoms content of Tarsand Triangle synthetic liquid was three times higher than Sunnyside synthetic liquid. This would have a significant influence on the subsequent processing of the synthetic liquid. The weight percent sulfur (3.0 - 4.0) in the Tarsand Triangle liquid was comparable to the sulfur content of synthetic liquid obtained from the Canadian bituminous sand. The molecular weight of Sunnyside synthetic liquid decreased with increasing reactor temperature, while the molecular weight of Tarsand Triangle synthetic crude remained constant. The molecular weight of Sunnyside synthetic liquid was nearly one-third that of the extracted bitumen.

Infra-red spectra determined on the Sunnyside and Tarsand Triangle synthetic liquids showed functional group features similar to the bitumen. In addition, a small, sharp peak at 1640 cm^{-1} characteristic of unconjugated olefins was observed. This indicated that olefins are produced during the cracking of the bitumen. Also, a distinct peak of medium intensity around 3020 - 3060 cm^{-1} characteristic of aromatic C - H stretch was observed. This peak was not distinctly visible in the bitumen spectra. Again, as in the case with the bitumen, the analyses were not sufficiently sophisticated and, therefore, no attempt was made to relate the data either to the structure of the synthetic liquid or to elucidate the reaction pathways during cracking.

Since the yield of synthetic crude from the Sunnyside feed was more sensitive to the reactor temperature than the Tarsand Triangle feed, chemical structural analyses of the bitumen and the synthetic liquid product were carried out using the data of elemental analysis, proton magnetic resonance ('H-NMR) spectra, and molecular weight. The Speight Method(63) and the Brown-Ladner Method(135) were used to obtain the structural parameters of the bitumen and the synthetic liquid. The results obtained by each method are presented separately and are compared. The chemical nature of the Athabasca bitumen and the bituminous fractions have been studied using the Speight Method(63,64).

The Speight structural parameters (expressed in terms of the carbon-type distribution) were obtained from elemental analysis, 'H-NMR, and the average molecular weight of the sample.

A typical proton magnetic resonance spectra of the Sunnyside bitumen and the synthetic liquid product are presented in Figure 4.18. The spectra clearly indicated an increase in the aromatic protons in the synthetic liquid compared to the bitumen. A small amount of vinylic protons (chemical shift 4.6 - 5.9) was observed in the synthetic liquids obtained at reactor temperatures above 773 K. The proton distribution [aromatic (H_a), benzylic (H_α), naphthenic (H_n), paraffinic methylene (H_r), and paraffinic methyl (H_m)] was calculated according to the Speight Method(63). Using this information together with the elemental analysis and molecular weight, the carbon-type distribution was computed from the following relationships:

$$C_S = H_t \left(\frac{H_\alpha}{2} + \frac{H_n}{2} + \frac{H_r}{2} + \frac{H_m}{3}\right) \tag{4.7}$$

$$C_{Sa} = H_t \times \frac{H_\alpha}{2} \tag{4.8}$$

$$C_a = C_t - C_S \tag{4.9}$$

$$C_p = H_t \left(H_a + \frac{H_\alpha}{2}\right) \tag{4.10}$$

$$C_i = C_a - C_p \tag{4.11}$$

$$C_r = H_t \left(\frac{H_r}{2} + \frac{H_m}{3}\right) \tag{4.12}$$

Figure 4.18

Proton Magnetic Resonance Spectra of Extracted
Bitumen and Synthetic Liquid

Sunnyside Feed

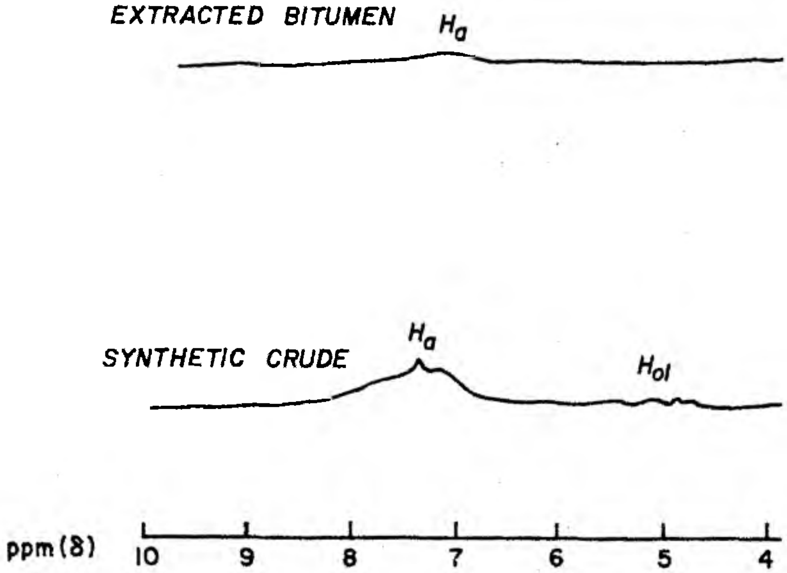
EXTRACTED BITUMEN
H_a
SYNTHETIC CRUDE
H_a
H_{ol}
ppm (δ)
10
9
8
7
6
5
4

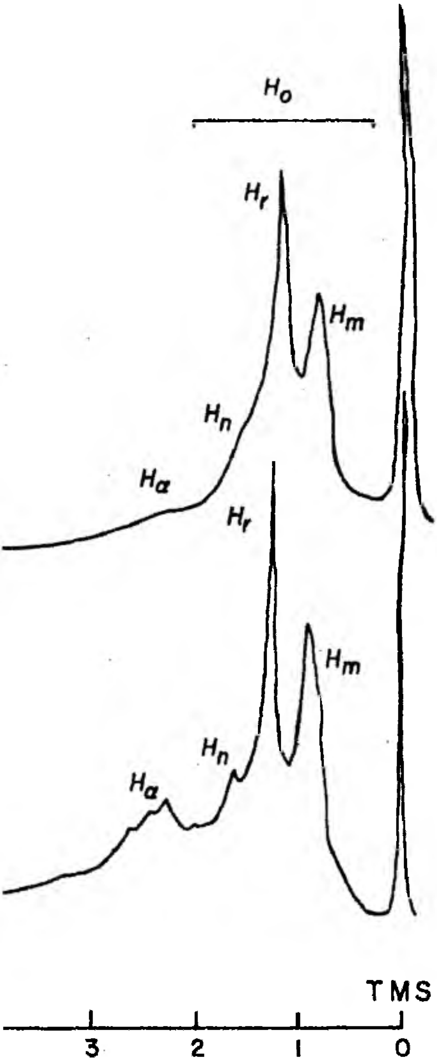
H_o
H_r
H_m
H_n
H_α
H_r
H_m
H_n
H_α
TMS
3
2
1
0

$$C_n = C_S - (C_{Sa} + C_r) \tag{4.13}$$

$$R_a = \left(\frac{C_i + 2}{2}\right) \tag{4.14}$$

where

C_S is the total number of saturated carbon atoms per molecule,

C_{Sa} is the total number of saturated carbon atoms α to an aromatic ring,

C_a is the total number of aromatic carbon atoms per molecule,

C_t is the total number of carbon atoms per molecule from elemental analysis and molecular weight,

C_p is the number of peripheral carbon atoms in a condensed aromatic cluster,

C_i is the number of internal carbon atoms in a condensed aromatic cluster,

C_n is the total number of naphthenic carbon atoms per molecule,

C_r is the total number of paraffinic carbon atoms per molecule in locations other than α- to an aromatic ring,

H_t is the total number of hydrogen atoms per molecule from elemental analysis and molecular weight, and

R_a is the number of aromatic rings per molecule.

The analysis of the bitumen and the synthetic liquids obtained at three reactor temperatures are presented in Table 4.14. The distribution of saturated carbon atoms is expressed as a percentage of total saturated carbon atoms. Similarly, the distribution of aromatic carbon atoms is expressed as percentage of total aromatic carbon

Table 4.14

Effect of Reactor Temperature on the Percentage Distribution of Carbon Type in the Bitumen and in the Synthetic Liquid

Sunnyside Feed

Temperature, K	353	698	723	773
H_t	112.5	32.9	39.0	30.9
C_t	72.3	21.6	25.4	21.3
C_s	67.0	65.9	66.5	60.3
C_{sa}	18.1	24.2	20.9	31.1
C_r	61.2	59.4	64.2	50.7
C_n	20.7	16.4	14.9	18.2
C_a	33.0	34.1	33.5	39.7
C_p	53.8	72.9	60.8	81.4
C_i	46.2	27.1	39.2	18.6
R_a	6.5	2.0	2.7	1.8
C_s/C_{sa}	5.5	4.1	4.8	3.2
C_{sa}/C_p	0.68	0.64	0.68	0.58
C_p/C_a	0.54	0.73	0.61	0.81

Notes: H_t - total number of hydrogen atoms per molecule from elemental analysis and molecular weight

C_t - total number of carbon atoms per molecule from elemental analysis and molecular weight

C_s - total number of saturated carbon atoms per molecule expressed as a percentage of total carbon atoms

- Continued -

Table 4.14 - Continued

C_{sa} - total number of saturated carbon atoms α to an aromatic ring expressed as a percentage of total saturated carbon atoms

C_r - total number of paraffinic carbon atoms per molecule in locations other than α to an aromatic ring expressed as a percentage of total saturated carbon atoms

C_n - total number of naphthenic carbon atoms per molecule expressed as a percentage of total saturated carbon atoms

C_a - total number of aromatic carbon atoms per molecule expressed as a percentage of total carbon atoms

C_p - total number of peripheral carbon atoms in a condensed aromatic cluster expressed as a percentage of total aromatic carbon atoms

C_i - total number of internal carbon atoms in a condensed aromatic cluster expressed as a percentage of total aromatic carbon atoms

R_a - total number of aromatic rings per molecule

C_s/C_{sa} - the average number of carbon atoms in an alkyl substituent attached to the peripheral aromatic carbon atom of a condensed aromatic cluster

C_{sa}/C_p - the average degree of substitution of an aromatic cluster

C_p/C_a - the average shape of an aromatic cluster atoms. The percentage of aromatic carbon increased with increasing reactor temperature with a concomitant decrease in the number of aromatic rings per molecule (Table 4.14). The ratio C_{Sa}/C_p represents the average degree of substitution of the aromatic cluster. As seen from Table 4.14, the C_{Sa}/C_p ratio remained constant, indicating at least 60 - 70% of the peripheral carbon atoms of the aromatic cluster carry saturated substituents. With a low percentage of naphthenic carbon atoms, it is highly probable that the majority of the substituents are alkyl groups rather than hydroaromatic groups. The ratio C_S/C_{Sa}, which represents the average number of carbon atoms attached to the edge of an aromatic cluster, decreased with increasing reactor temperature. The length of the alkyl group attached to the aromatic cluster is a five to six carbon unit in the bitumen, while the length of the alkyl group attached to the aromatic cluster in the synthetic liquid decreased with increasing reactor temperature, that is, the length of the alkyl group attached to the aromatic cluster is a four to five carbon unit in the synthetic liquid obtained at 723 K and this alkyl length was reduced to a three carbon unit at 773 K. On the basis of the C_p/C_a ratio, which represents the average shape of the aromatic cluster, the bitumen contained a condensed aromatic cluster approximating to eight rings if the cluster is cata-condensed or six rings if the cluster is peri-condensed. In addition, the value of R_a for the extracted bitumen suggested that there were six to seven aromatic rings per molecule. The number of aromatic clusters per molecule can be obtained by dividing the total number of aromatic rings per molecule (as indicated by R_a) with the number of aromatic rings per cluster (as obtained from the C_p/C_a ratio). This indicated that the bitumen had only one aromatic cluster per molecule. However, the synthetic liquid contained on an average of two to three rings per molecule corresponding to the R_a value and the average shape of the aromatic cluster (C_p/C_a) contained two to three aromatic rings. Thus, the synthetic liquid contained one aromatic cluster per molecule.

The proton magnetic resonance (PMR) analysis (Speight method) indicated that the bitumen molecule contained six to eight aromatic rings as a single cluster having 65 - 70% of the peripheral hydrogen atoms replaced with a saturated alkyl group of five to six carbon units. The alkyl side chains attached to the aromatic cluster were cleaved when the bitumen was thermally cracked to produce light gases resulting in the decrease in the length of the alkyl side chain. The structural information for the synthetic liquid indicated that the liquid molecule contained one aromatic cluster with two to three aromatic rings having the same percentage of peripheral hydron substitution but the length of the alkyl group is a three carbon unit. Since it is not possible to decrease the size of the aromatic cluster of the bitumen molecule having six to eight rings to an aromatic cluster having two to three rings in the synthetic liquid by thermal cracking, the bitumen cracking could not be adequately explained using Speight's parameters.

In the Brown-Ladner method, the structural parameters are computed from the elemental analysis and the proton magnetic resonance spectra. Yoshida, et. al.(136) have estimated the structural parameters for the Athabasca bitumen using the Brown-Ladner method and compared their results with the Speight method(63). In this method the fractional distribution of protons among the aromatic (H_a), benzylic (H_α), and other non-aromatic saturated (H_o) attachments were calculated. The parameter H_o includes H_n, H_r, H_m (Figure 4.18). The hydrogen distribution results are presented in Table 4.15. The following relationships were used in determining the structural parameters

$$f_a = \frac{\frac{C}{H} - \frac{H_\alpha^*}{x} - \frac{H_o^*}{y}}{\frac{C}{H}} \qquad (4.15)$$

$$\sigma = \frac{\frac{H_\alpha^*}{x} + \frac{O}{H}}{\frac{H_\alpha^*}{x} + \frac{O}{H} + H_a^*} \qquad (4.16)$$

$$\frac{H_{au}}{C_a} = \frac{\frac{H_\alpha^*}{x} + H_a^* + \frac{O}{H}}{\frac{C}{H} - \frac{H_\alpha^*}{x} - \frac{H_o^*}{y}} \qquad (4.17)$$

where

f_a is the aromaticity, defined as the ratio of aromatic carbon atoms to total carbon atoms,

σ is the degree of substitution of the aromatic cluster,

H_{au}/C_a is the atomic hydrogen to carbon ratio of the hypothetical unsubstituted aromatic cluster unit,

x is the atomic ratio of hydrogen to carbon for the α- carbons,

y is the atomic ratio of hydrogen to carbon for the carbon atoms in locations other than α- to an aromatic ring,

Table 4.15

Chemical Structure of Bitumen and Synthetic Liquid

Sunnyside Feed

	1[c]	2	3	4	5	6
Reactor Temperature, K	353[a]	698	723	748	773	798
Retention Time of Solids, min.	--	27.2	27.2	27.2	27.2	27.2
Feed Sand Particle Size, μ	--	358.5	358.5	358.5	358.5	358.5
Fluidizing Gas Velocity, $SCM \cdot h^{-1}$	--	0.142	0.142	0.142	0.142	0.142
Hydrogen Distribution						
H_a^*	0.027	0.069	0.053	0.114	0.115	0.109
H_α^*	0.125	0.190	0.169	0.173	0.221	0.187
H_o^*	0.848	0.744	0.766	0.694	0.640	0.688
H_{olefin}^*	--	--	0.012	0.020	0.022	0.016

- Continued -

Table 4.15 - Continued

	1^c	2	3	4	5	6
Structural Parameters						
f_a	0.24 $(0.21)^b$	0.29	0.28	0.33	0.38	0.36
σ	0.76	0.59	0.63	0.44	0.55	0.54
H_{au}/C_a	0.75	0.87	0.78	0.94	0.88	0.90
H_o^*/H_α^*	6.8	3.9	4.5	4.0	2.9	2.9
M_n	718	378	598	279	281	261
M_v	1042	298	350	306	292	235
M_v/M_n	1.5	0.8	0.6	1.1	1.04	0.9

Notes: [a] Temperature during the solvent extraction of Sunnyside bituminous sand using benzene.

[b] Value of f_a obtained from ^{13}C-NMR.

[c] Values in column 1 are for the extracted bitumen.

- Continued -

Table 4.15 - Continued

H_a^* - fraction of the total hydrogen attached to aromatic carbon atoms

H_α^* - fraction of the total hydrogen attached to the carbon atoms α to an aromatic ring

H_o^* - fraction of the total hydrogen attached to non-aromatic carbon atoms

H_{olefin}^* - fraction of the total hydrogen attached to vinyl carbon atoms

f_a - aromaticity, defined as the ratio of aromatic carbon atoms to total carbon atoms

σ - the degree of substitution of the aromatic cluster

H_{au}/C_a - the atomic hydrogen to carbon ratio of the hypothetical unsubstituted aromatic structural unit

H_o^*/H_α^* - measure of the aliphatic chain attached to the peripheral aromatic carbon atom of a condensed aromatic cluster

M_n - weight of the average structural unit calculated numerically from the values of the structural parameters

M_v - molecular weight determined by vapor-pressure osmometry

M_v/M_n - measure of the number of aromatic cluster per molecule

H_a^* is the fraction of the total hydrogen attached to aromatic carbon atoms,

H_α^* is the fraction of the total hydrogen attached to α-carbon atoms, and

H_o^* is the fraction of the total hydrogen attached to other non-aromatic carbon atoms.

Brown and Ladner have commented, "the major consideration in the calculations is the choice of x and y. Both these quantities are unknown although their limits can be fixed. There are insufficient data to decide whether x and y differ statistically, and in these circumstances it will be assumed that they are equal, that is, that the average atomic H/C ratios of the α- carbon structures are equal to those of the other non-aromatic carbon systems". In this study, 2 was adopted for the values of x and y as an approximation. The close agreement between the aromaticity (f_a) calculated by the Brown-Ladner method and that determined from ^{13}C-NMR spectra should indicate the validity of this approximation. The calculated structural parameters are presented in Table 4.15 and in Figure 4.19. Furthermore, the weight of the average aromatic cluster unit (M_n) can be calculated numerically from the values of the structural parameters with the following relationship

$$M_n = 12\ C_a + 12\ C_p\ \sigma_{al}\ (\frac{H_o^*}{H_\alpha^*} + 1) + C_p\ (1 - \sigma) + C_p\ \sigma_{al} \cdot x + C_p\ \sigma_{al}\ (\frac{H_o^*}{H_\alpha^*}) \cdot x + 16\ C_p\ \sigma_o \qquad (4.18)$$

where

Figure 4.19

Effect of Coking Reactor Temperature on the
Chemical Nature of Synthetic Liquid

Sunnyside Feed

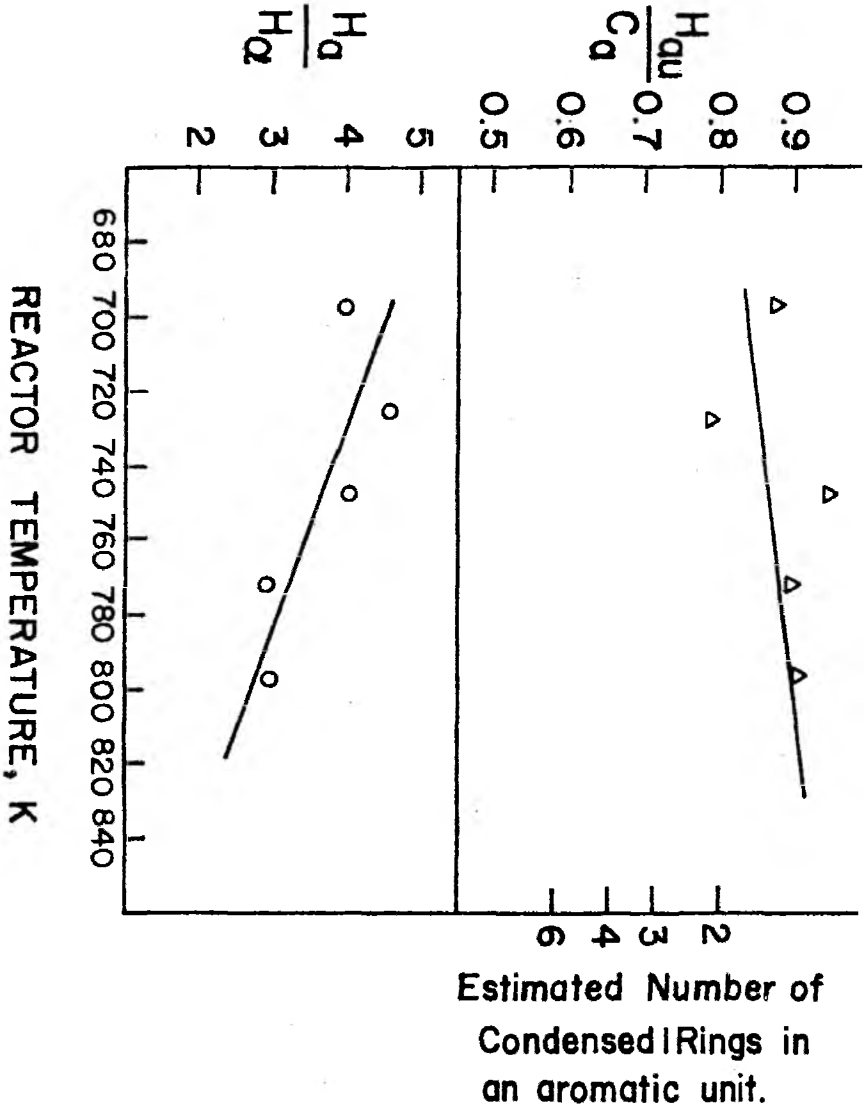
Hau/Ca
0.5
0.6
0.7
0.8
0.9
Ha/Hα
2
3
4
5
680
700
720
740
760
780
800
820
840
REACTOR TEMPERATURE, K
2
3
4
6
Estimated Number of Condensed Rings in an aromatic unit.

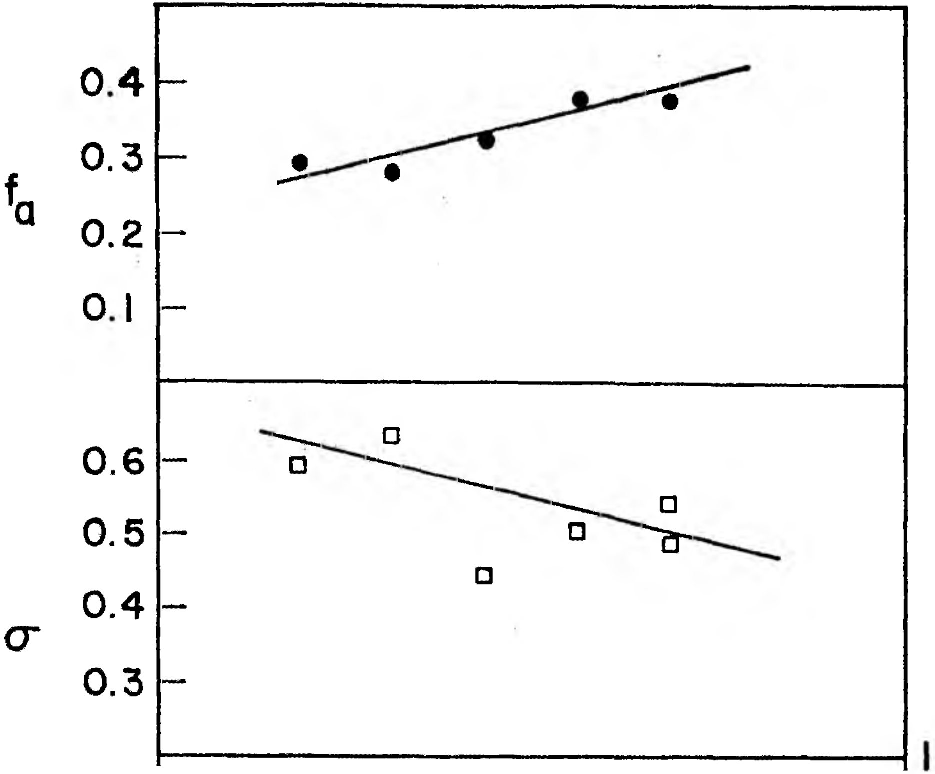
0.4
0.3
f_a
0.2
0.1
0.6
0.5
0.4
σ
0.3

C_p is the number of peripheral carbon atoms per unit cluster,

C_a is the number of aromatic carbon atoms in the cluster unit,

$$\sigma_{al} = \frac{\frac{H_\alpha^*}{x}}{\frac{H_\alpha^*}{x} + \frac{0}{H} + H_a^*} \tag{4.19}$$

$$\sigma_0 = \frac{\frac{0}{H}}{\frac{H_\alpha^*}{x} + \frac{0}{H} + H_a^*} \tag{4.20}$$

The number of aromatic cluster units was computed by M_v/M_n where M_v is the molecular weight determined by vapor pressure osmometry. The calculated values of M_n and M_v/M_n are also presented in Table 4.15.

Based on the results obtained by the Brown-Ladner method, the bitumen molecules are low in aromaticity ($f_a = 0.24$). The aromatic rings per unit cluster being 2 corresponding to $H_{au}/C_a = 0.75$ and the number of aromatic cluster units per molecule (M_v/M_n) was approximately 2. Thus, the bitumen molecules contained four aromatic rings. It is highly substituted ($\sigma = 0.76$) with a seven or eight carbon unit aliphatic chain ($H_0^*/H_\alpha^* = 6.8$). The chemical nature of the synthetic liquid product changed with increasing reactor temperature. The length of the aliphatic chain decreased from eight to four, the aromaticity of the product increased from 0.24 to 0.38, and the extent of substitution of the aromatic cluster decreased from 0.76 to 0.5 with increasing reactor temperature (Figure 4.19).

A comparison of the results obtained by the Brown-Ladner method and the Speight method indicated that the structural parameters for the synthetic liquid product were nearly the same irrespective of the method of computation. However, differences exist in the structural parameters for the extracted bitumen. The results obtained by the Brown-Ladner method indicated that the number of aromatic rings per unit cluster was in the range of two to three rings, corresponding to a value of $H_{au}/C_a = 0.75$. However, this value was six to eight rings corresponding to a value of $C_p/C_a = 0.54$ using the Speight method. It is appropriate to mention that terms C_p/C_a in the Speight method and H_{au}/C_a in the Brown-Ladner method have the same meaning, that is, both the terms represent the average size of the aromatic cluster. This low value of $C_p/C_a = 0.54$ may have been due to lack of consideration for the heteroatoms in the Speight method. The percentage of oxygen in the Sunnyside bitumen sample was high (4.4 wt %) compared to the percentages of sulfur (0.6 wt %) and nitrogen (0.7 wt %). The Brown-Ladner method assumed that all the oxygen present in the sample was phenolic oxygen and this assumption is incorporated into the estimation of structural parameters. The infra-red spectra on the extracted bitumen showed a broad absorption band of low intensity between 3600 - 3200 cm^{-1}, indicating the presence of phenolic oxygen. The presence of phenols in the bitumens from the Asphalt Ridge and P. R. Spring sands have been reported(55). However, if the value of O/H is omitted in the calculations, the value of H_{au}/C_a using equation 4.17 becomes 0.57, which is now in good agreement with the value of $C_p/C_a = 0.54$ obtained using the Speight method. In addition, the close agreement between the f_a values obtained by the Brown-Ladner method (f_a = 0.24) and by ^{13}C-NMR (f_a = 0.21) for the Sunnyside bitumen indicated the assumption in the Brown-Ladner method of 2 for the atomic H/C ratio of aliphatic structures was reasonable. Although the difference in the value between C_p/C_a and H_{au}/C_a for the two methods was explained by correcting the equation for H_{au}/C_a in the Brown-Ladner method instead of including a correction term in the Speight method for the oxygen present in the bitumen, the present approach was easier compared to incorporating the correction term for calculating C_p/C_a in the Speight method.

4.2.3. Potential Reaction Pathways for Bitumen Cracking

The thermal cracking of the Sunnyside bitumen can be explained based on the above structural information. Examination of the structural parameters of the feed bitumen and the synthetic liquid indicated that the cleavage of alkyl side chains attached to the aromatic clusters account for the reduction in molecular weight. The molecular size reduction of the bitumen during the thermal cracking was accomplished in two ways: (i) the removal of aliphatic carbons as low molecular weight hydrocarbons, and (ii) the cleavage of linkages connecting the aromatic clusters. The production of light hydrocarbon products via cleavage of alkyl side chains resulted in an increase in aromaticity (f_a) of the synthetic liquid relative to the native bitumen. The cleavage of the alkyl linkages connecting the aromatic clusters caused a significant reduction of molecular size, but does not affect the aromaticity as long as the species produced remain with the liquid product. Since the aromaticity (f_a) of the synthetic liquid increased with increasing reactor temperature and the molecular weight of the synthetic liquid decreased with increasing reactor temperature, it is concluded that both the cleavage of aliphatic carbons from the aromatic cluster and the breaking of alkyl linkages between the aromatic clusters are operative. Furthermore, the aliphatic carbons cleaved from the aromatic cluster do not form liquid paraffinic products but produce the light hydrocarbon gases.

A comparison of the aromaticity (f_a) of the bitumen and the synthetic liquid obtained, for example at 773 K, indicates that 37% of the molecular weight of the bitumen was removed as light hydrocarbon gases. The total reduction in the molecular size is 71% from the molecular weight of 1042 to 292. Since 37% is accounted in the production light hydrocarbon gases, the remaining 34% is attributable to the cleavage of linkages between aromatic clusters. The estimated number of aromatic clusters (corresponding to the M_v/M_n value in Table 4.15) in the bitumen was approximately two, and in the synthetic liquid it was 1.0. The reduction in the number of aromatic clusters confirmed that the cleavage of the linkages produced smaller molecules in the synthetic liquid product. The formation of smaller molecules from a portion of bitumen molecules via cleavage of the linkage could explain the bimodal distribution in the molecular weight of the liquid product.

The formation of coke can occur via condensation reactions between aromatic clusters. It is speculated that the aliphatic free radicals were stabilized by hydrogen abstraction from a portion of the bitumen. This portion of the bitumen could then undergo cyclization and polymerization reactions forming coke on the sand. The coke thus formed was in addition to the direct coke formed from asphaltenes present in the bitumen.

A better understanding of the complex reaction mechanism involved in the thermal cracking of the bitumen could be obtained by knowing the compound type distribution (saturates, MNA-DNA, DNA, etc.) of bitumen and of synthetic liquid products obtained at various reactor temperatures. A gradient elution chromatographic (GEC) separation technique has been selected to provide the information on the compound type distribution in the synthetic liquid and in the bitumen. This method, developed by the Mobil Research and Development Corporation, has been extensively used for the compound type separation of heavy petroleum residues(137) and coal liquids(134). The GEC separation technique was adopted for analysis of the extracted Sunnyside bitumen and the synthetic liquids produced from the fluidized bed thermal recovery process. The results of these analyses have been reported by Utley(138).

4.2.4 Effect of Solids Retention Time on Synthetic Liquid Product Quality

The effects of solids retention time on the physical properties of the synthetic liquids from Sunnyside feed sand are presented in Tables 4.16 and 4.17. The API gravity of the synthetic liquids increased slightly with decreasing solids retention time due to an increase in hydrogen content of the liquid at reactor temperatures of 773 K and 798 K. The weight percent hydrogen content increased from 10.6 to 11.2

Table 4.16

Effect of Retention Time of Solids on Synthetic Liquid Product Quality

Sunnyside Feed

Retention Time of Solids, min.	20.4	27.2	31.4	20.4	27.2	31.4	20.4	27.2	31.4
Reactor Temperature, K	723	723	723	773	773	773	798	798	798
Feed Sand Particle Size, μ	358.5	358.5	358.5	358.5	358.5	358.5	358.5	358.5	358.5
Fluidizing Gas Velocity, SCM·h^{-1}	0.142	0.142	0.142	0.142	0.142	0.142	0.142	0.142	0.142
Properties									
Gravity, ^{o}API at 293 K	16.2	17.4	16.1	17.8	12.7	15.0	16.8	14.0	15.8
Viscosity, CP at 298 K	158.3±2	198±4	198±4	109±2	81±1	138.8±2	115.1±2	86.5±2	169.6±2
Volatility below 811 K	88.1	88.6	NE	80.5	75.6	NE	81.1	85.0	NE
Distillation Fractions									
Gasoline	12.9	15.0	NE	10.3	19.6	NE	11.4	19.1	NE
Middle Distillate	27.2	23.4	NE	24.6	23.2	NE	25.7	27.1	NE
Heavy Ends	59.9	61.6	NE	65.1	57.2	NE	62.9	53.8	NE

Notes: NE - Not Estimated

Table 4.17

Properties of Synthetic Liquid at Optimum Reactor Temperatures

Sunnyside Feed

Reactor Temperature, K	723	773	773
Retention Time of Solids, min.	27.2	20.4	27.2
Feed Sand Particle Size, μ	358.5	358.5	358.5
Fluidizing Gas Velocity, $SCM{\cdot}h^{-1}$	0.142	0.142	0.142
Synthetic Crude Yield (weight percent)	61.2	67.4	47.5
Properties			
Gravity, ^{o}API at 293 K	17.5	17.8	12.7
Viscosity, Ceitipose at 298 K	198 ± 4	110 ± 2	81 ± 1
Elemental Analysis (weight percent)			
Carbon	87.1	87.0	87.6
Hydrogen	11.1	11.2	10.6
Nitrogen	0.6	1.3	0.8
Sulfur	0.4	< 0.1	0.4
Oxygen	0.6	0.5	0.5
Molecular Weight (VPO benzene) $g.mol^{-1}$	350	302	292
Hydrogen/Carbon Atomic Ratio	1.53	1.54	1.45
Volatility below 811 K (weight percent)	88.6	81.7	75.6

for a corresponding decrease in solids retention time from 27.2 to 20.4 minutes (Table 4.17). The API gravity of the synthetic liquid changed from 12.7 to 17.8(133) for this decrease in solids retention time.

The relationship between the viscosity of the synthetic liquid and the solids retention time for two reactor temperatures is shown in Figure 4.20. Because the data was limited, the increase in viscosity of synthetic liquids at higher solids retention time (31.4 minutes) could not be explained, however, the increase in the viscosity with decreasing retention time was due to the highly paraffinic nature of the synthetic liquid which was confirmed by the increase in the atomic hydrogen/carbon ratio (Table 4.17). This was substantiated by the reduction in the light gas make.

At higher reactor temperatures and lower retention time of solids, the amount of heavy ends in the synthetic liquid increased with a concomitant decrease in the gasoline fraction, indicating less secondary cracking at lower solids retention time. The properties of the synthetic liquids obtained at optimum reactor temperatures and at different solids retention times are given in Table 4.17. No significant differences were observed in the physical properties of the liquids. But, at a constant reactor temperature (773 K), the decrease in the solids retention time caused the following changes in the properties of the synthetic liquid: (i) increased API gravity, (ii) increased viscosity, (iii) increased atomic H/C ratio, and (iv) decreased gasoline yield and a simultaneous increase in heavy ends.

Figure 4.20

Effect of Solids Retention Time on the
Viscosity of Synthetic Liquid

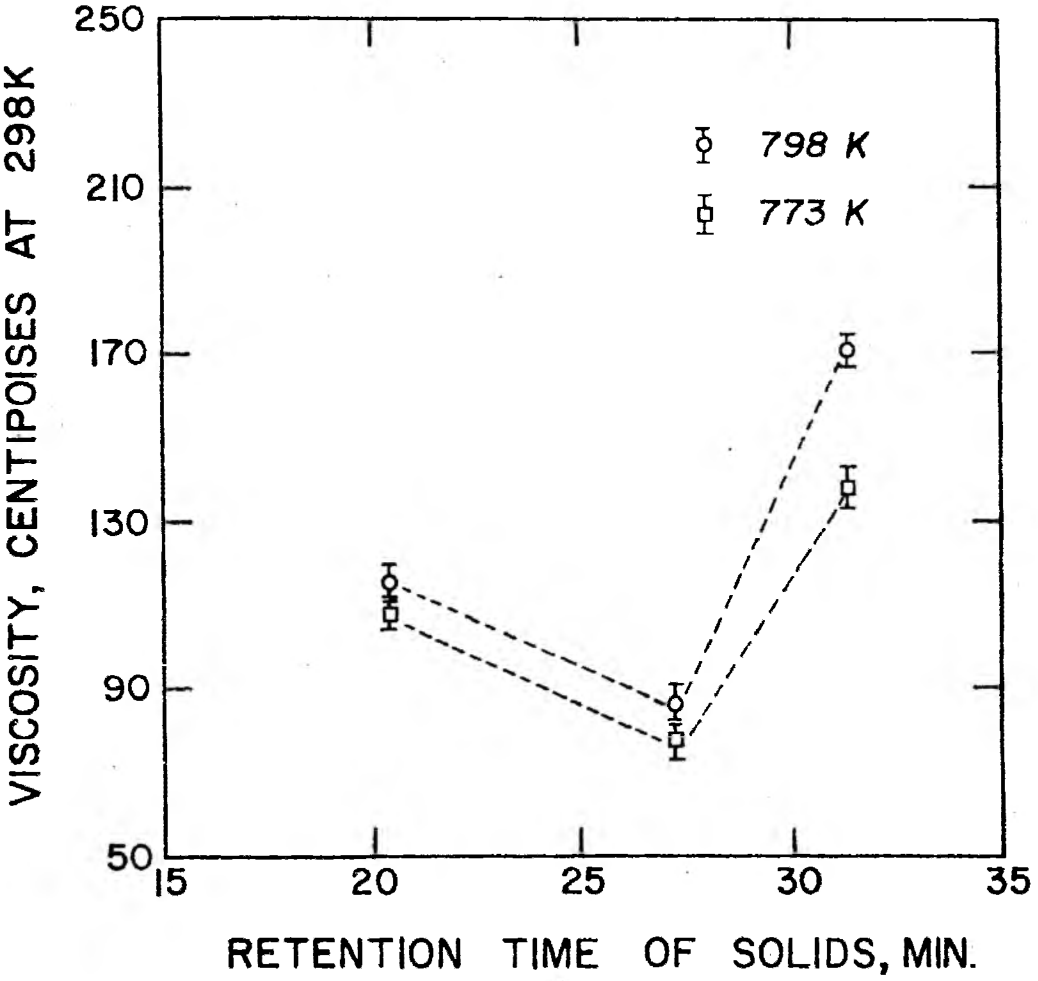
250
210
170
130
90
50
15
20
25
30
35
VISCOSITY, CENTIPOISES AT 298K
RETENTION TIME OF SOLIDS, MIN.
798 K
773 K

CHAPTER 5

CONCLUSIONS AND RECOMMENDATIONS

5.1 Conclusions

The development of the technology for the production of synthetic crudes from alternate fossil energy resources appears to be gaining importance in the wake of the increasing demand for energy and the higher prices for imported petroleum crude. The bituminous sand deposits of Utah appear to be a readily accessible alternate fossil energy resource. A fluidized bed thermal process has certain advantages over direct coking processes such as the Lurgi-Ruhrgas process(120-121) and could offer a feasible alternative to a modified hot water process for the recovery of a synthetic crude from bituminous sands, particularly for lean grade deposits. The application of the fluidization technology developed by the petroleum industry for the fluid catalytic cracking process to the recovery of synthetic liquids from bituminous sands would reduce the technological risk involved in commercializing a synthetic crude process. In this investigation, an effort has been made to ascertain the feasibility of a fluidized bed thermal process for the recovery of a synthetic crude from the bituminous sands of Utah. The Sunnyside and Tarsand Triangle bituminous sands were evaluated as potential feeds for the process and the following conclusions were drawn:

(1) The process variable data obtained in this exploratory investigation indicate the above ground, fluidized bed thermal process could be a feasible alternative to a modified hot water process for the production of synthetic crude from the bitminous sands of Utah.

(2) In the range of reactor temperatures studied (650 - 900 K), an optimum temperature exists at which the synthetic crude (C_5^+ liquid) yield was maximized. Moreover, the yield of coke did not change with temperature, but remained reasonably constant (19 - 22%). At low reactor temperatures (673 - 700 K), the liberation of the bitumen is incomplete with a portion remaining on the sand in the form of solvent extractable "coke" on the sand withdrawn from the unit.

(3) The bitumen content of feed sand appears to influence the optimum reactor temperature and the corresponding maximum synthetic crude yield. Bituminous sands with bitumen content in the range of 4 - 10 wt % were processed indicating the flexibility of the process to handle a variety of bituminous sand feed sources.

(4) The weight percent yield of synthetic crude increased as the retention time of solids decreased. Synthetic crude yields in excess of 80% by weight of bitumen fed might be attainable at solids retention times in the range 12 - 16 minutes.

(5) The consistency of the coke yields (18 - 22 wt %) indicates a commercial or large scale pilot plant could be maintained in thermal balance regardless of the coking bed temperature or the feed sand retention time.

(6) The temperature required to liberate the synthetic crude resulted in considerable cracking of the bitumen, producing a

synthetic liquid with properties that differ markedly from the extracted bitumen. The paraffinic nature, the high hydrogen content, and the low heteroatoms content of the synthetic crude from Sunnyside bituminous sand indicate it would be excellent catalytic cracking feedstock.

5.2 Recommendations

The yields and product distribution obtained in this bench scale fluidized bed reactor for the recovery of synthetic crude from bituminous sands of Utah appear to be comparable to the ultimate yields obtained in the hot water extraction of the bitumen followed by coking of the bitumen (two step process). Since the fluidized bed reactor has been shown to be a reasonable alternate scheme for processing a wide variety of Utah's bituminous sands, further research is needed in the following areas:

(1) The bituminous sand deposits of the United States, in particular the Utah deposits, are small and widely dispersed unlike the Athabasca (Canada) deposit, and have different bitumen contents. The fluidized bed thermal process was successfully applied to the processing of bituminous sands from the Sunnyside and Tarsand Triangle deposits. The effect of process variables on the yield of synthetic crude from the Asphalt Ridge (unconsolidated deposit), P. R. Spring, and Hill Creek bituminous sand deposits of Utah and the Edna deposit of California needs to be assessed in order that the effect of feed sand source and bitumen content can be fully understood. The bench scale unit developed in this study can be used for these studies.

(2) The effect of the Aspect ratio (length to diameter ratio of the fluidized bed) on synthetic liquid yield should be studied in the context of scale-up. A reactor with a 15 - 30 cm diameter will be required to study this problem.

(3) The effect of steam partial pressure upon the yield and product quality of synthetic liquid should be investigated by injecting steam along with the fluidizing gas. Additionally, the effect of steam on the yield of coke should be assessed to evaluate the extent of the steam-carbon reaction.

(4) The effect of a reducing atmosphere such as H_2, H_2-CO mixture during the coking of the bituminous sand on the yield and chemical composition of synthetic liquid should be assessed in comparison to the liquids obtained under inert conditions.

(5) Steam reforming studies with the Canadian bituminous sands indicated an increase in the gas production occurred(111). This suggests that bituminous sand can be used for the production of C_2-C_4 gases. The steam reforming of bituminous sands should be evaluated as an alternative for the utilization of the various minor bituminous sand deposits.

(6) The effect of high pressure (up to 6900 kPa) on the yield and product quality of synthetic liquid and upon the quality of fluidization should be evaluated.

(7) The effects of fluidizing gas composition and its residence time upon the yield and product distribution should be determined.

(8) The thermodynamics and kinetics of the combustion of the

coke on the sand should be studied to obtain data for the combustor design.

(9) Gradient elution chromatography (GEC) should be used in conjunction with spectroscopic analysis of the fractions for the determination of the compound types present in the extracted bitumens and synthetic liquids.

APPENDIX A

THERMOGRAVIMETRIC ANALYSIS OF THE BITUMINOUS SANDS OF UTAH

Thermogravimetric analysis (TGA) has been used as one of the primary techniques for the study of the decomposition reactions for coal, oil shale, and bituminous sands. The TGA studies and small scale pyrolysis studies conducted in the past have been concentrated on the decomposition of coal and oil shale in order to elucidate the pyrolysis mechanism and to determine the rate of the pyrolysis of these fossil fuels. Coking studies have been conducted on the extracted bitumen instead of bituminous sand to obtain information on the rate of bitumen coking. The information obtained from these studies can be used for designing a reactor to upgrade the bitumen via coking processes for the production of synthetic crude. However, the data obtained in these studies could not be utilized to design a bench scale thermal recovery unit to carry out the pyro-distillation of the bitumen from the bituminous sands because the feed to the thermal coking unit is a bitumen-sand mixture instead of bitumen itself. Furthermore, there is a paucity of data in the literature on the effects of the inorganics associated with sand particles on the pyrolysis of the bitumen.

Barbour, et. al.(139) investigated the pyrolysis of the bituminous sands of Utah in a small scale reactor to which 140 - 170 g of the sand were charged. Nitrogen was used as a sweep gas to carry out the hydrocarbon vapors from the reactor to the product collection system. Samples from the Asphalt Ridge, P. R. Spring, Sunnyside, and Tarsand Triangle deposits were studied. The liquid yield increased with increasing pyrolytic temperature for each deposit studied. They also investigated the kinetics of the bitumen pyrolysis reaction which was expressed as

$$\text{Bitumen} \rightarrow \text{Oil} + \text{Gas} + \text{Coke} \tag{A-1}$$

and the reaction was found to follow the first order kinetics with respect to the unreacted bitumen in the sand with an activation energy of 33 kcal/mole.

The main objective of the thermal analysis was to obtain a weight loss - time - temperature relationship for the pyro-distillation of the bitumen from the bituminous sands of Utah. In thermogravimetric analysis, the weight of the sample is constantly measured as it is heated either at constant temperature or at constant heating rate. The rate of weight loss with time or temperature can then be computed from the weight loss curve.

The thermograms for Asphalt Ridge and Sunnyside bituminous sands were obtained using an experimental unit equipped with a Cahn RG Electrobalance, Fisher TGA Accessory Model 120, Cahn control unit for the electrobalance and a Rikadenki three-pen recorder. The description and operating procedures for the TGA unit have been described in detail by Lee(140). The analysis was conducted in a nitrogen atmosphere under isothermal conditions. The inert gas sweep was used in a down-flow mode. A 10 - 20 mg sample of the bituminous sand was used for each analysis. The thermogravimetric studies on Tarsand Triangle sand were conducted at the Flammability Research Center, University of Utah.

The results of the TGA experiments for Asphalt Ridge and Sunnyside bituminous sand samples are given in Figures A-1 and A-2, respectively. The bitumen content for these samples was 16 - 18 weight percent for the Asphalt Ridge sample and 8 - 9 weight percent for the Sunnyside sample. The Asphalt Ridge sample was obtained from the Asphalt Quarry near Vernal, Utah. The sample locations for the Sunnyside and Tarsand Triangle sands are given in Chapter 3. From the isotherms presented in Figures A-1 and A-2, it is clear that as the temperature is increased the time required to reach a constant weight decreases. Also, the initial rate of devolatilization increases with increasing reactor temperature. Similar observations were made by Barbour, et. al.(139). In the temperature range studied the optimum operating temperature appears to be between 773 - 873 K for the Asphalt Ridge bituminous sand and between 723 - 773 K for the Sunnyside sample at a nominal solids retention time of five minutes in the reactor. At this retention time of five minutes, nearly 80% of the bitumen was converted to product vapors in the optimum temperature range for both the Asphalt Ridge and Sunnyside samples studied. In view of the limited data obtained from TGA studies, the kinetics of the pyro-distillation of the bitumen from the bituminous sand was not attempted.

Figure A-1

Isothermal Thermal Analysis (TGA) Curves

Asphalt Ridge Bituminous Sand

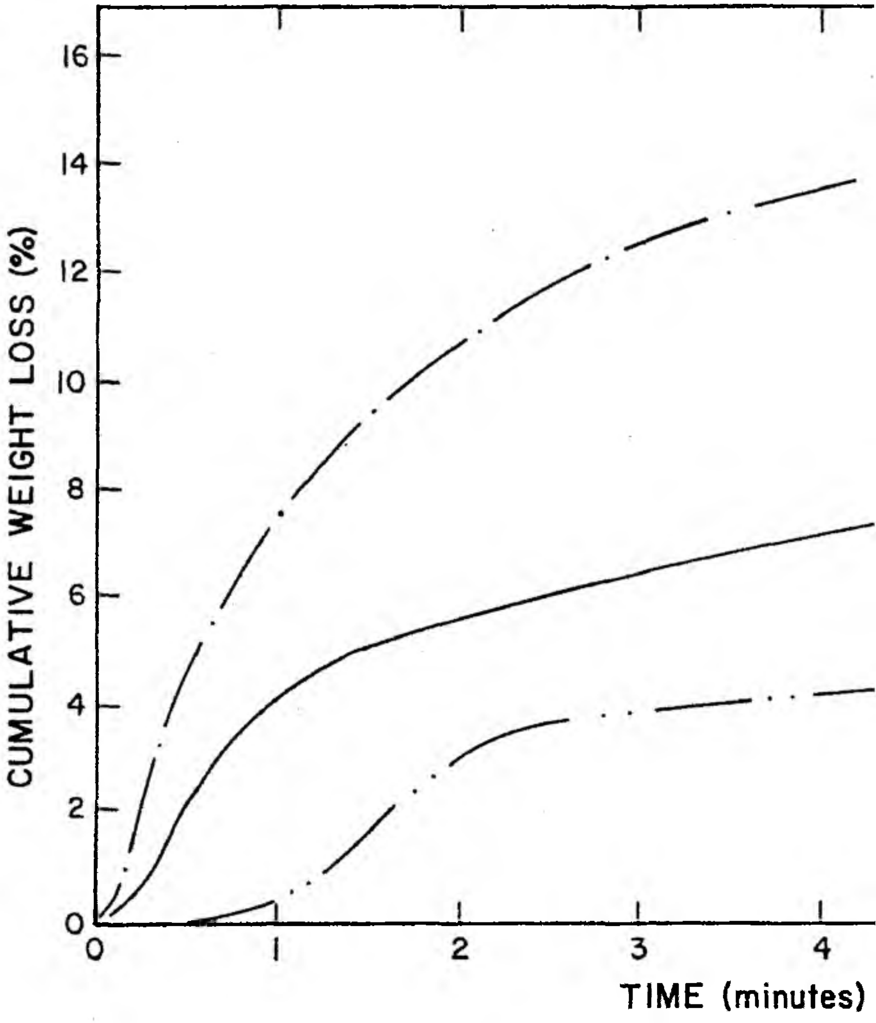

CUMULATIVE WEIGHT LOSS (%)
16
14
12
10
8
6
4
2
0
0
1
2
3
4
TIME (minutes)

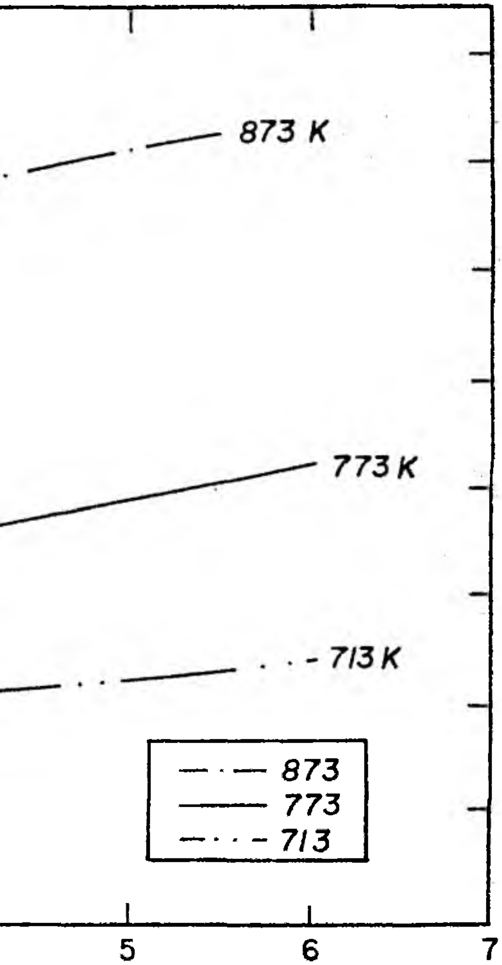
873 K
773 K
713 K
873
773
713
5
6
7

Figure A-2

Isothermal Thermal Analysis (TGA) Curves

Sunnyside Bituminous Sand

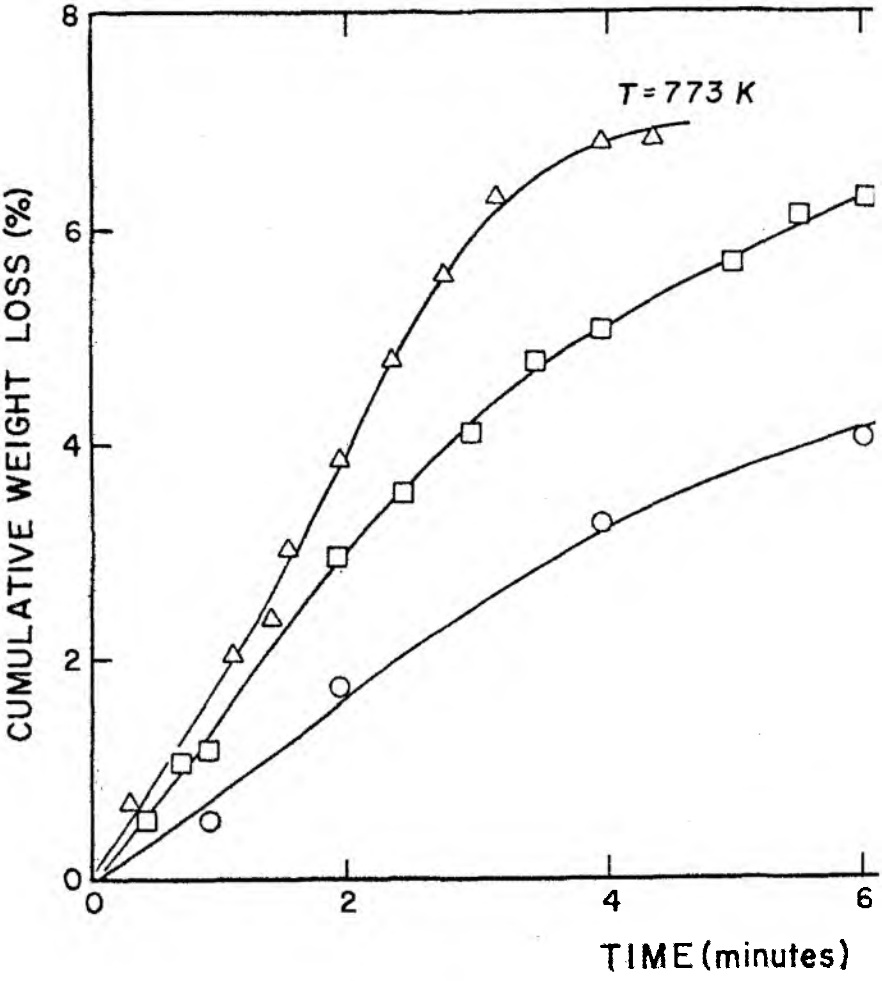
T = 773 K
CUMULATIVE WEIGHT LOSS (%)
8
6
4
2
0
0
2
4
6
TIME (minutes)

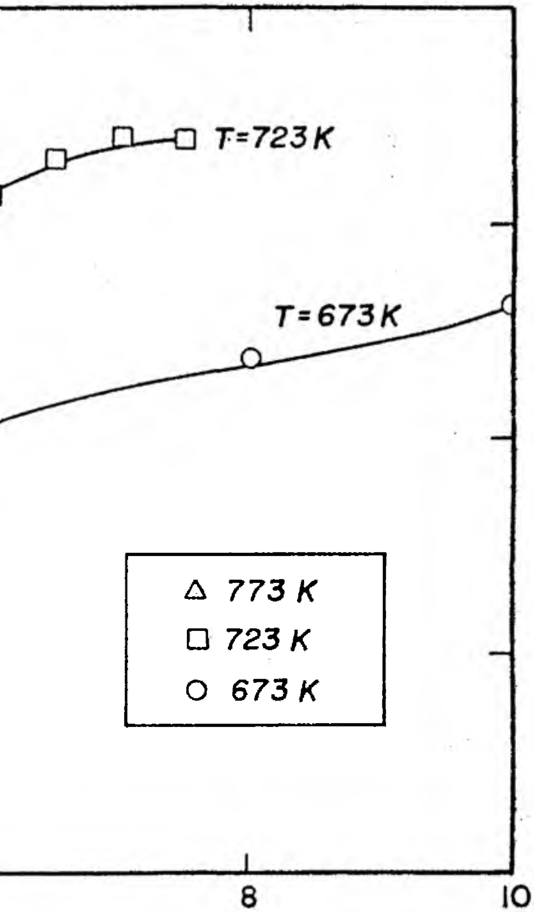
T=723K
T=673K
△ 773 K
□ 723 K
○ 673 K
8
10

In the case of the Tarsand Triangle bituminous sand samples, thermograms were obtained at constant heating rate of 10 K per minute in the temperature range of 298 - 1273 K with helium as the sweeping gas. The thermograms are presented in Figures A-3 and A-4. The thermogram as shown in Figure A-4 was obtained by heating the sample up to 773 K and holding the temperature constant till the weight loss became constant. Following this, the heating rate was continued until the final temperature of 1273 K was reached. The following conclusions were drawn from these two thermograms:

(i) The production of hydrocarbon vapors from the bituminous sand commences at temperatures as low as 373 K.

(ii) The pyro-distillation of the bitumen was completed at a temperature of 823 K and the rate of production of hydrocarbon vapor was maximum in the temperature range of 523 - 723 K.

Furthermore, in the temperature range of 873 - 1073 K, a sharp differential weight loss was observed. This may be, perhaps, due to the decomposition of carbonate materials present in the inorganic portion of the bituminous sand. Carbonate materials such as dolomite, calcite, and ankerite have a decomposition temperature in the range of 873 - 1023 K. Since the heat requirements for these decomposition reactions are large, these reactions have strong influence on the coking of bituminous sand, in particular the burning of coke on the sand.

A TGA study on the coked sand (obtained in the fluidized bed thermal recovery scheme at a reactor temperature of 773 K) was also conducted at a heating rate of 10 K per minute. The thermograms were

Figure A-3

Temperature Programmed Thermal Analysis (TGA) Curve

Tarsand Triangle Bituminous Sand

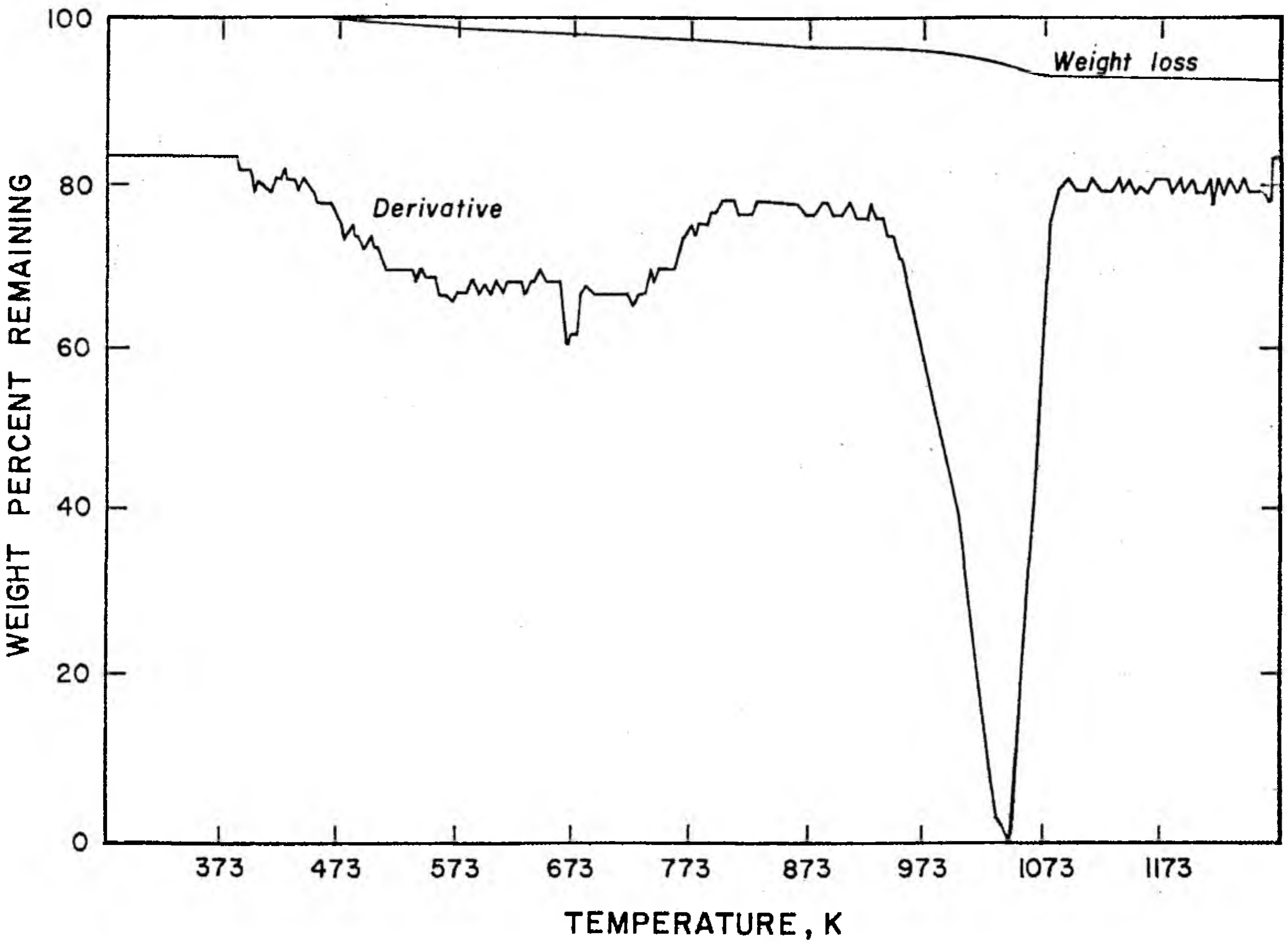

100
80
60
40
20
0
WEIGHT PERCENT REMAINING
373
473
573
673
773
873
973
1073
1173
TEMPERATURE, K
Weight loss
Derivative

Figure A-4

Temperature Programmed Thermal Analysis (TGA) Curve

Tarsand Triangle Bituminous Sand

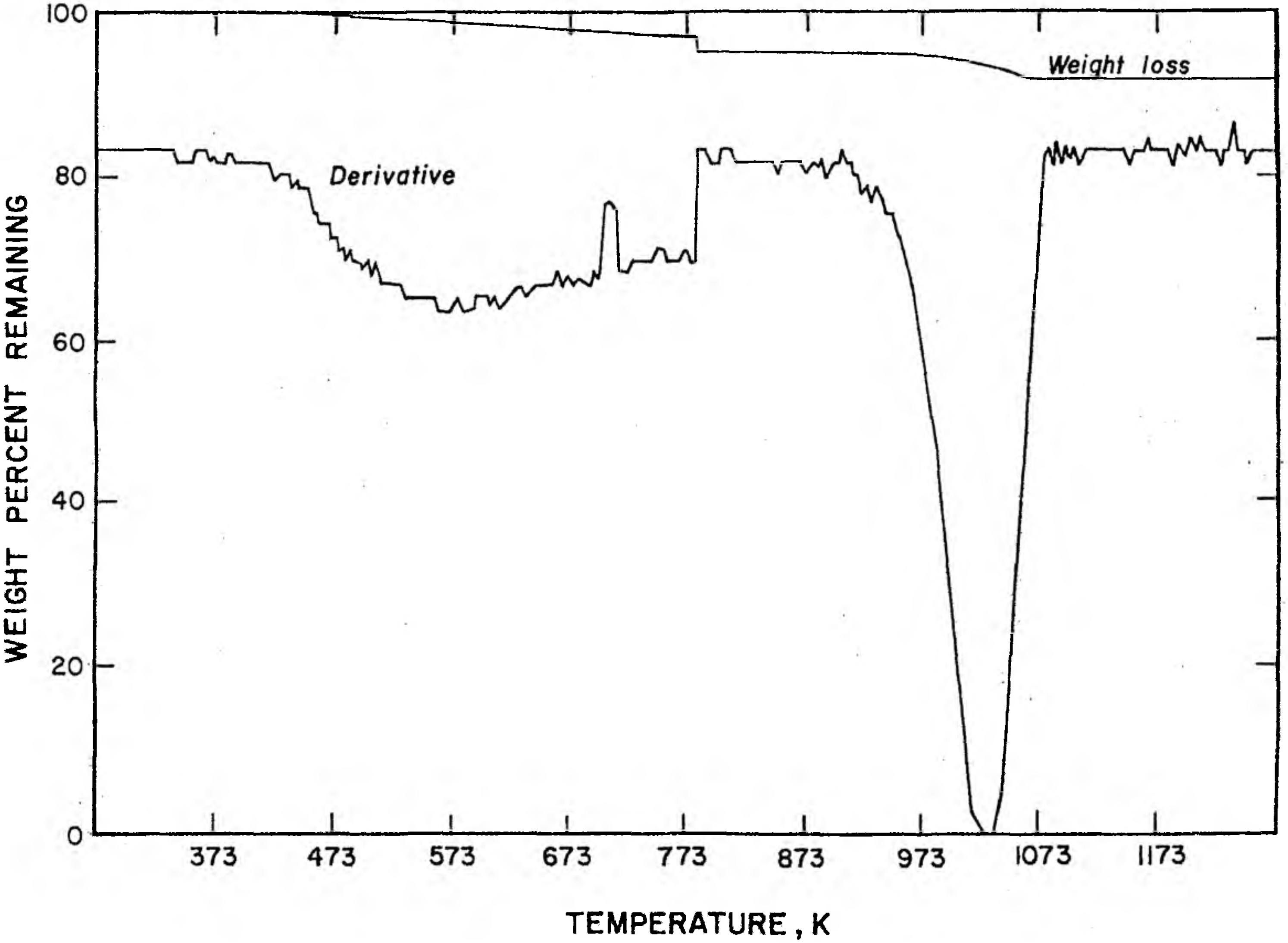
Weight loss
Derivative
100
80
60
40
20
0
WEIGHT PERCENT REMAINING
373
473
573
673
773
873
973
1073
1173
TEMPERATURE, K

obtained both in an inert atmosphere (helium) and in an oxidizing atmosphere (air) and are presented in Figures A-5 and A-6, respectively. In the inert atmosphere, a small weight loss was observed in the temperature range of 723 - 873 K. However, no solvent extractable material was present in the coked sand. It is speculated that a portion of the coke-like material left on the sand may be weakly associated with the sand and was released depending upon the temperature at which the thermal analysis was conducted. Additionally, the total burning of coke from the sand (Figure A-6) was completed at a lower temperature, that is, below 798 K. Therefore, the coke on the sand was determined in the temperature range of 773 - 798 K as indicated in Chapter 3.

Figure A-5

Temperature Programmed Thermal Analysis (TGA) Curve

Tarsand Triangle Coked Sand

Helium Atmosphere

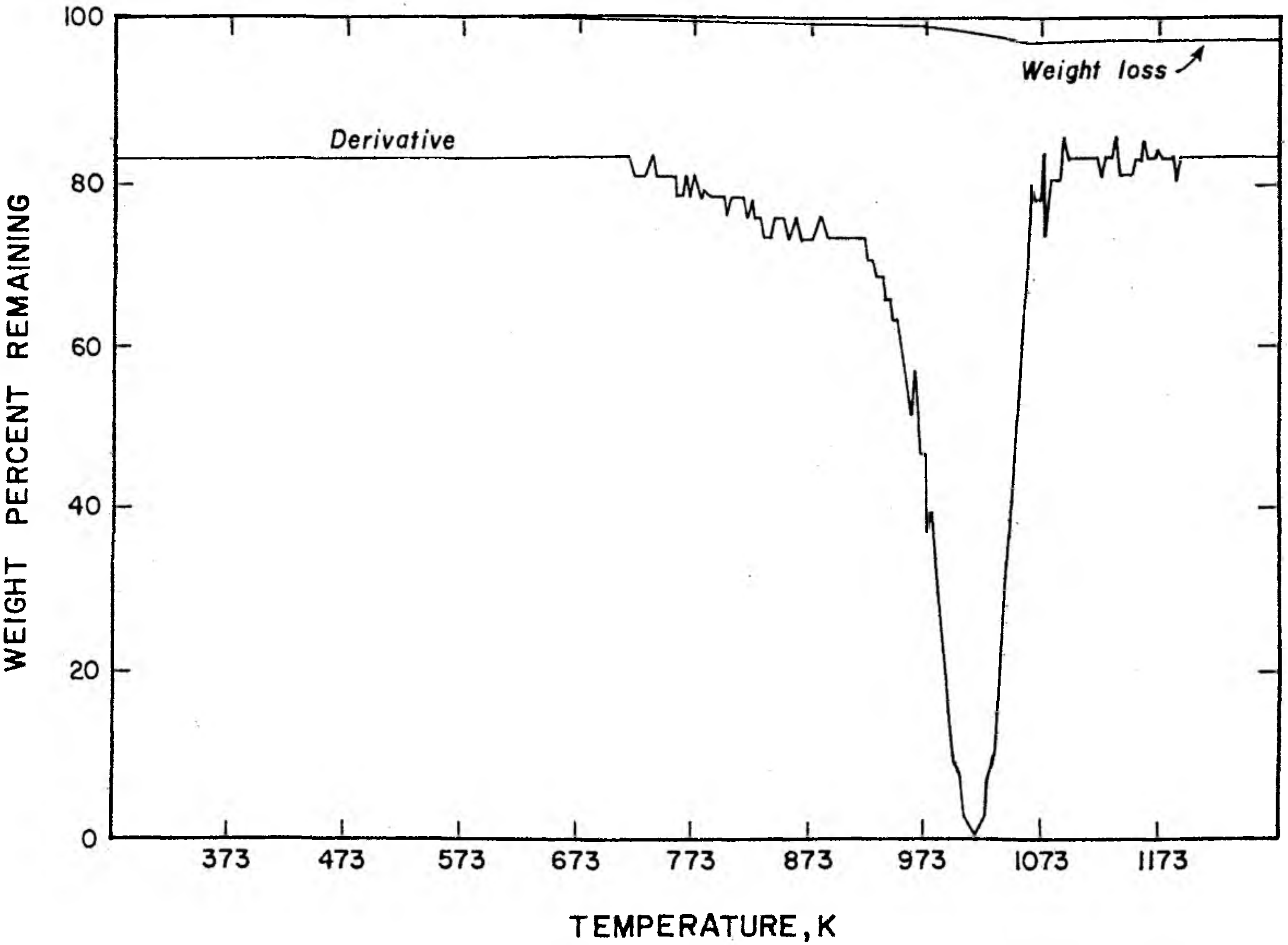
100
80
60
40
20
0
WEIGHT PERCENT REMAINING
373
473
573
673
773
873
973
1073
1173
TEMPERATURE, K
Derivative
Weight loss

Figure A-6

Temperature Programmed Thermal Analysis (TGA) Curve

Tarsand Triangle Coked Sand

Oxidizing Atmosphere

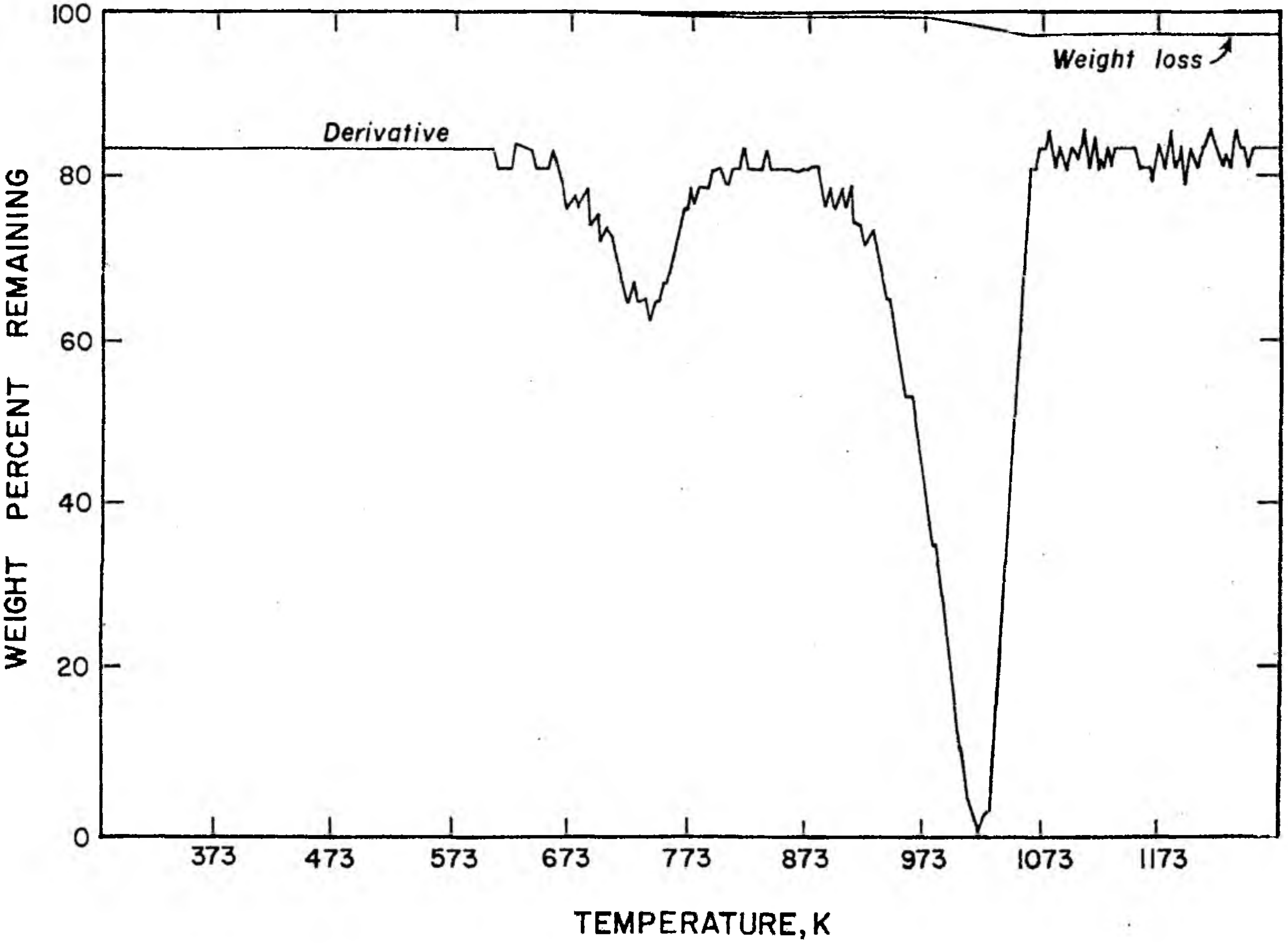
100
80
60
40
20
0
WEIGHT PERCENT REMAINING
373
473
573
673
773
873
973
1073
1173
TEMPERATURE, K
Derivative
Weight loss

APPENDIX B

DESIGN OF THE FLUIDIZED BED REACTOR

The design of a continuous, bench-scale fluidized-bed reactor for processing the bituminous sands of Utah required the development of an understanding of the following:

1. the rheological properties of the bituminous sand,
2. the behavior of bituminous sand under fluidizing conditions,
3. the heat demand for the pyro-distillation of the bituminous sand.

B.1 Rheological Properties of the Bituminous Sands

The appearance and rheological properties of bituminous sands depend upon the bitumen content. The free-flowing behavior of the bituminous sand sample decreased with increasing bitumen content of the sample. Furthermore, with decreasing bitumen content the bituminous sands are a consolidated rock. The medium grade (bitumen content 4 - 10 weight percent), consolidated bituminous sands of Utah could be ground and size classified by conventional grinding and sieving apparatus. The size classified bituminous sand sample exhibited acceptable free-flowing properties from the standpoint of material handling and feeding to the processing apparatus. On the contrary, the rich grade (bitumen content more than 10 weight percent) bituminous sand samples from the Asphalt Ridge and the Athabasca deposits did not exhibit free-flowoing characteristics, but rather tended to agglomerate.

The medium grade bituminous sand sample lacked the free-flowing properties exhibited at ambient temperature when a sample was heated in a test-tube above 423 K. Above 423 K, the sample formed a hard, cylindrical solid mass.

B.2 Behavior of Bituminous Sand Under Fluidizing Conditions

The use of a fluidized bed thermal process for the production of the synthetic crude from the bituminous sands depended upon the fluidization characteristics of the bituminous sand at the high temperature at which the bitumen is pyro-distilled. A small Vycor glass fluidized-bed reactor, 3.8 cm I.D. by 45 cm long with a porous quartz disc as a distributor plate, was fabricated to observe the movement of particles inside the reactor under fluidizing conditions in the temperature range of 673 - 973 K. The reactor was electrically heated by a heating coil rated for 1200 watts at 115 volts. Two hundred grams of dry sand were poured into the reactor to form a bed of 20 cm in height. Nitrogen was metered and admitted at the bottom of the reactor to cause fluidization. About 200 g of Sunnyside bituminous sand (bitumen content 8.5 weight percent) were slowly added to the hot bed of solids at 773 K. The behavior of bituminous sand, when added to the reactor, was studied by visual observation through windows in the insulated tube. The following observations were made:

(a) oil vapor flashed off the sand, however, it formed an aerosol; (b) the bituminous sand particles did not stick to the wall nor did they agglomerate during the addition of fresh bituminous sand; (c) a portion of the bitumen was converted to coke which was deposited on the sand.

B.3 Heat Demand for the Pyro-Distillation of the Bituminous Sand

The heat requirement for the pyro-distillation of bitumen from bituminous sand was of paramount importance for design considerations. The heat of reaction for the pyro-distillation of the bitumen is endothermic and the bituminous sand must be heated from ambient temperature to the required temperature inside the reactor. No data on the thermal properties of the sand were available in the literature. Therefore, the data for the Canadian bituminous sands were used to compute the energy requirements.

B.4 Fluidized Bed Reactor Design

The bench scale unit was designed to process bituminous sands at a maximum feed rate of 2.25 $kg.h^{-1}$ in the temperature range of 673 - 923 K at atmospheric pressure. The bitumen content of the feed sand was assumed to be 10 weight percent for the design calculations. This value was chosen because the bituminous sand samples investigated in the thermal analysis studies had bitumen contents ranging from 4 to 16 weight percent. The minimum fluidization velocity of the sand with nitrogen as the fluidizing gas in the Vycor glass reactor was about 20 $g.h^{-1}$ cm^{-2} at 293 K for an average particle size of 500 microns.

According to Leva$^{(131)}$, the ratio of operating mass velocity of the gas (G_f) to the minimum fluidization velocity (G_{m_f}) corresponding to the particle size of 500 microns is in the range of 2 to 3. Taking an average value of 2.5 for G_f/G_{m_f}, the value for G_f is 50 g.h^{-1} cm^{-2}. The reactor diameter is chosen such that the linear gas velocity in the fluidized bed falls in the range of 15 - 305 cm.s$^{-1(131)}$ at the operating temperature. For a reactor diameter of 3.66 cm I.D., this corresponds to a linear gas velocity of 14 cm.s^{-1} at 293 K or about 38 cm.s^{-1} at 773 K. With the diameter of the reactor chosen based on the operating linear velocity of the fluidizing gas, the height of the reactor must be chosen to ensure a sufficient solids retention time in the reaction zone for the liberation of the bitumen. The thermogravimetric analysis indicated five minutes were required for the liberation of the bitumen at a bitumen content of 8 - 16 weight percent. Therefore, for a solids retention time of five minutes, the static bed height needed is about 17 cm assuming a bed voidage of 0.55.

Alternatively, the bed height can be determined from the required heat transfer area to permit the energy input necessary to liberate the synthetic crude, that is, the sensible heat for vaporization and the endothermic heat for cracking the bitumen. The calculation of the heat transfer area required a knowledge of the bed-wall heat transfer coefficient. Leva$^{(131)}$ expressed the bed-wall heat transfer coefficient (h_w) for an externally heated fluidized bed as

$$h_w = 0.16\left(\frac{k_g}{d_p}\right)\left[\frac{C_s \rho_s d_p^{1.5} g_c^{0.5}}{k_g}\right]^{0.4}\left[\frac{G d_p n}{\mu_g R}\right]^{0.36} \qquad \text{(B-1)}$$

where k_g is the thermal conductivity of the gas, d_p is the particle size, C_s is the heat capacity of the solids, ρ_s is the density of the solids, G is the operating mass velocity of the fluidizing gas, μ_g is the viscosity of the fluidizing gas, η is the fluidization efficiency, R is the bed expansion ratio, and g_c is the conversion factor. The total energy input required for the coking operation at the design throughput capacity of 2.25 $kg.h^{-1}$ was about 290 $kcal.h^{-1}$. The value for the bed-wall heat transfer coefficient determined from equation (B-1) was about 160 $kcal/(h)(m^2)(^oC)$. The required bed height of the reactor was calculated to be 60 cm for the operating temperature range of 673 - 923 K. The actual reactor length including the freeboard above the bed surface was 90 cm.

APPENDIX C

FLUIDIZATION STUDIES AT HIGH TEMPERATURES

The purpose of the fluidization studies conducted during the course of this investigation was to obtain the minimum fluidization velocity as a function of temperature for the coked sand which was obtained during the direct coking of a bituminous sand.

C.1 The Fluidized State

The utilization of fluidized beds has become common place in the petroleum refining industry (i.e. catalytic cracking) and in the chemical process industry (i.e. fluid bed drying). Several comprehensive text books on fluidization have been published(129,131,141,142).

A bed of solids undergoes a transformation from a fixed bed regime to a fluidized state with increasing gas flow rate. At low gas flow rate, the bed behaves like a fixed bed and the pressure drop across the bed increases linearly with increasing gas flow rate. The increase in pressure drop continues until a point is reached at which the packed bed suddenly unlocks and the particles of solids are freely agitated. At this flow rate, it appears that the particles are suspended in the gas and the pressure drop across the bed is equal to the bouyant weight of the solids per unit cross sectional area. For any further increase in gas flow rate, the pressure drop across the bed remains almost constant. The gas velocity at which the pressure drop is equal to the bouyant weight of the bed per unit area is called minimum fluidization velocity and the point at which this occurs is called the minimum fluidization point. The minimum fluidization velocity is determined using a pressure drop versus gas velocity diagram. The pressure drop-gas velocity diagram for an ideal bed of fluidized solids is presented in Figure C.1. However, many solids exhibit irregularities in the pressure drop-gas velocity relationships. These irregularities can be caused either by the characteristics of the solid phase (such as shape, density and moisture content of the solid) resulting in channeling in the bed or by the choice and design of the equipment resulting in slugging behavior.

Slugging is a condition in which gas bubbles coalesce and increase in size until their diameters are equal to the diameter of the containing apparatus. The particle layers or slugs of granular solids between such gas bubbles travel upward in a piston-like manner, reach a certain height at which bed expansion is maximized and then disintegrate. The granular solids rain through the ascending gas bubble as small aggregates and/or as individual particles. Slugging phenomenon is related to the height to diameter ratio of the bed (aspect ratio) and is commonly observed in small diameter (less than 5 cm) vertical tubes having an aspect ratio greater than unity(129). Stewart and Davidson(130) have discussed various types of solids slugging and have adequately reviewed the slug flow behaviour in small diameter fluidized beds. Recently, Geldart, et. al.(143) have reported square-nosed solid. slugs in tubes up to 20 cm diameter using coarser size particles. They also observed that the bed pressure drop increased with

Figure C-1

Ideal Pressure Drop-Gas Velocity Diagram

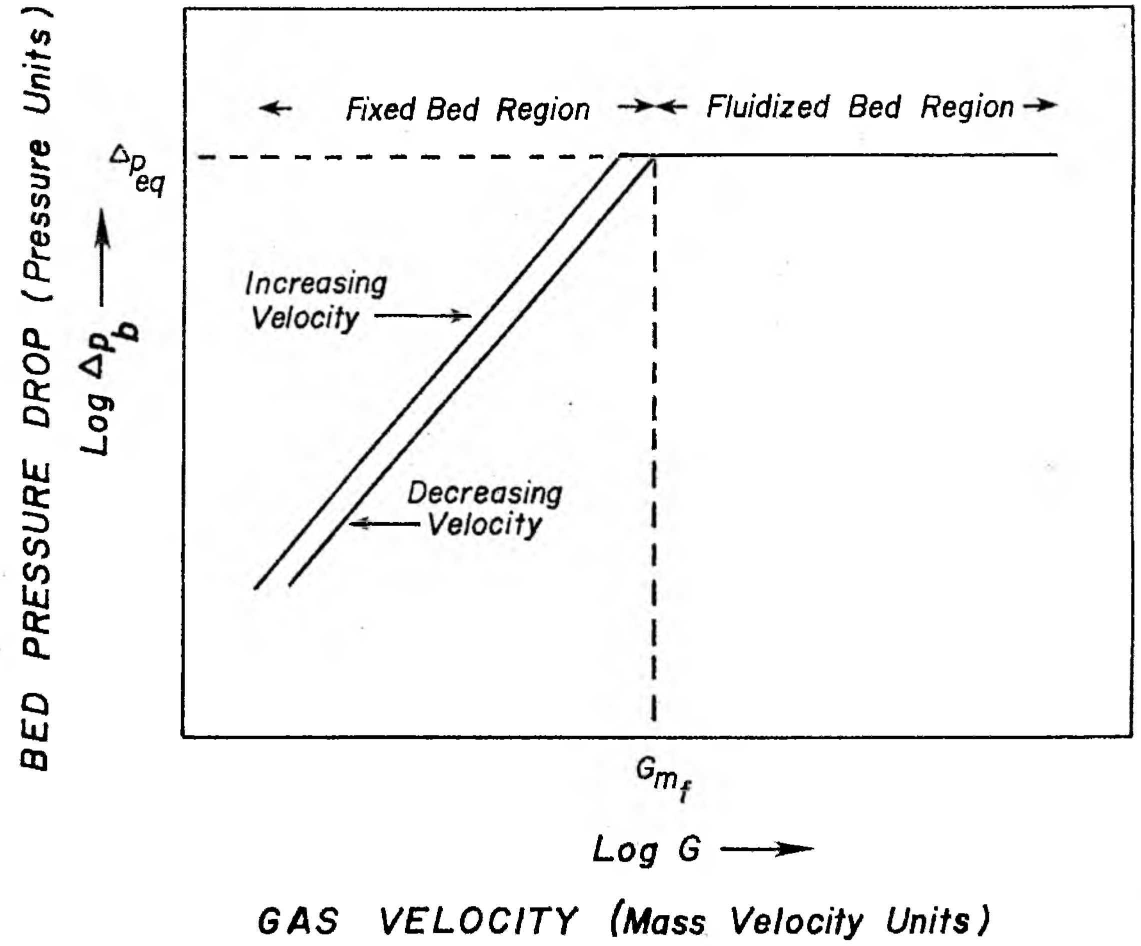
Fixed Bed Region
Fluidized Bed Region
Δp_{eq}
Increasing Velocity
Decreasing Velocity
G_{m_f}
BED PRESSURE DROP (Pressure Units)
Log Δp_b
Log G
GAS VELOCITY (Mass Velocity Units)

increasing gas velocity beyond the minimum fluidization point. They attributed this to the energy required to accelerate the solid slugs.

C.2 Estimation of Minimum Fluidization Velocity

The minimum fluidization velocity can be estimated theoretically and determined experimentally. Leva(131) has summarized the equations used to predict the minimum fluidization gas velocity as proposed by various authors. However, the most commonly used equation for estimating the minimum fluidization gas velocity, G_{m_f}, as given by Leva

$$G_{m_f} = \frac{688\ d_p^{1.82}\ [\rho_g(\rho_s-\rho_g)]^{0.94}}{\mu_g^{0.88}} \tag{C-1}$$

This is a dimensional equation giving G_{m_f} in pounds per hour per square foot if d_p is expressed in inches, ρ_s and ρ_g in pounds per cubic foot and μ_g in centipoises. Additionally, equation (C-1) is valid for Reynolds number less than 5.0, where the Reynolds number, N_{Re}, is given by

$$N_{Re} = \frac{d_p\ G_{m_f}}{\mu_g} \tag{C-2}$$

The effect of temperature on the minimum fluidization velocity has been investigated by several authors(144, 145). Desai, et. al.(144) obtained the expression

$$\log G_{m_f} = - A \log T + B \tag{C-3}$$

where A and B are constants. The above relationship was derived from the Frantz(146) equation for minimum fluidization velocity, which is

$$G_{m_f} = \frac{k\, d_p^2\, \rho_g(\rho_s - \rho_g)}{\mu_g} \tag{C-4}$$

where G_{m_f} is the minimum fluidization gas velocity, d_p is the particle size of the solids, ρ_s is the density of the solids, ρ_g and μ_g are the density and viscosity of the fluidizing gas respectively, and k is a constant.

Desai, et. al.(144) have suggested a value of 1.5 for the constant 'A' in equation (C-3) based on equation (C-4), but their experimental value of 'A' based on eight different bed materials was in the range of 0.8 to 1.35. On the other hand, Singh, et. al.(145) have developed the following equation for predicting the minimum fluidization velocity

$$G_{m_f} = \frac{\rho_g}{\mu_g} \cdot f\,(d_p,\, \rho_s - \rho_g, \Phi_s, \varepsilon) \tag{C-5}$$

They studied the effect of temperature on G_{m_f} using silica sand as the bed material and different fluidizing gases in the temperature range of 288-973 K.

The experimental value of G_{m_f} is always determined from the pressure drop-gas velocity diagram, but discrepancies exist among various authors in determining the minimum fluidization point. Richardson(147) has suggested that the minimum fluidization velocity corresponds to a pressure drop, Δp_{eq}, which is the ratio of bouyant weight of the bed (W) per unit cross-sectional area (A_c) as given by

$$\Delta p_{eq} = \frac{W}{A_c} \tag{C-6}$$

Several investigators have defined the minimum fluidization velocity as the point of intersection of the fixed and fluidized bed pressure drop lines(145,148), however, the estimation of G_{m_f} by this technique may be erroneous due to the possibility of extending the straight line of the fluidized region through the transitional region between fixed and fluidized state, especially if the transitional region was large. The ratio of $\Delta p_b/\Delta p_{eq}$ (where Δp_b is the bed pressure drop in the fluidized region) can be either more than or less than unity. In such cases different values for G_{m_f} would be expected. In this present investigation, G_{m_f} values will be estimated corresponding to Δp_{eq} from the pressure drop versus velocity diagram.

C.3 Fluidization Studies on Coked Sand

Fluidization studies were made with coked sand obtained in the preliminary thermal coking runs made with the bituminous sand from Tarsand Triangle. The screw feeder and product recovery train were disconnected during fluidization experiments (Figure 3.17). A manometer was connected to tap 3 of the reactor (Figure 3.4) located 22.5 cm from the distributor. The pressure reading (P_5) indicated by this manometer was used to estimate the bed height (H) from the relation

$$H = \frac{(P_2 - P_3)\cdot 22.5}{(P_2 - P_5)} \qquad \text{(C-7)}$$

where P_2 is the pressure measured below the distributor (tap 1) and P_3 is the pressure measured above the bed of solids (tap 7). The fluidization studies were conducted at four different reactor temperatures in the range, 293 - 773 K. The size distribution of the coked sand used is given as

Particle Size, d_p, in Microns	Weight Fraction in Coked Sand
358.5	0.17
253.5	0.40
179.5	0.43

The average particle size based on this size distribution was 225.1 microns. The bed solids hold-up in all fluidization runs was 680 grams.

The results obtained in the fluidization studies are given in Table C-1 and Figures C-2 and C-3. The value for minimum fluidization velocity was obtained corresponding to a pressure drop equivalent to bouyant bed weight, Δp_{eq} = 65 cm water column, as calculated using equation (C-6). These values are compared with the G_{m_f} values obtained using equation (C-1) and are given in Table C-2. A log-log plot of minimum fluidization velocity versus temperature, according to equation (C-3), gave a straight line relationship (Figure C-4) with a value for constant 'A' of 1.17. From Figure C-4 and Table C-2, there appears to be a substantial difference between theoretical and experimental values of minimum fluidization velocity indicating that equation (C-1) cannot be used for predicting minimum fluidization velocities for coked sand.

Fluctuations in the pressure drop were observed beyond the minimum fluidization point and the fluctuations increased severely at higher temperatures. Also, it is clear from Figure C-3 that the pressure drop across the bed increased with increasing gas velocities beyond the minimum fluidization point. This increase in pressure

Table C-1

Bed Pressure Drop Versus Gas Velocity at Different Reactor Temperatures

Solids Hold-up: 680 g Average Particle Size: 225.1 μ

Temperature, K 293		Temperature, K 473	
G,(gm/cm^2-hr)	ΔP_b(cm H_2O)	G,(gm/cm^2-hr)	ΔP_b(cm H_2O)
8.07	17.78	4.71	12.5
10.09	22.50	6.05	15.0
14.12	31.25	6.72	21.25
16.81	40.00	7.40	25.00
19.50	45.00	8.07	30.0
21.85	51.25	9.08	35.63
23.20	54.38	10.09	41.25
24.21	57.50	11.43	46.88
26.90	61.88	12.44	52.50
28.24	62.50	14.12	57.50
28.91	64.38	14.79	62.50
31.60	68.75	15.46	67.50
32.27	70.00	16.81	72.50
33.96	70.00	18.15	72.25
36.64	67.50	21.85	69.5-75.6
37.65	68.13	31.27	66.2-77.8
40.34	64.2-72.0		
44.38	63.0-74.0		
57.82	61.5-77.0		

Temperature, K 723		Temperature, K 773	
G,(gm/cm^2-hr)	ΔP_b(cm H_2O)	G,(gm/cm^2-hr)	ΔP_b(cm H_2O)
4.03	20.0	4.03	20.0
5.72	28.13	4.68	23.75
6.73	36.88	5.70	32.50
7.41	46.25	6.73	45.0
8.09	55.63	7.41	52.5
9.41	65.0	8.09	65.0
10.09	72.5	9.41	61.25
11.46	72.5	10.09	62.5
13.8	65.0-78.0	11.46	63.75
15.8	60.0-82.5	12.43	59.5-70.0
18.14	60.0-85.0	13.80	60.3-73.8
19.16	58.0-85.0		

Figure C-2

Bed Pressure Drop Versus Gas Velocity

Coked Sand

Tarsand Triangle Deposit

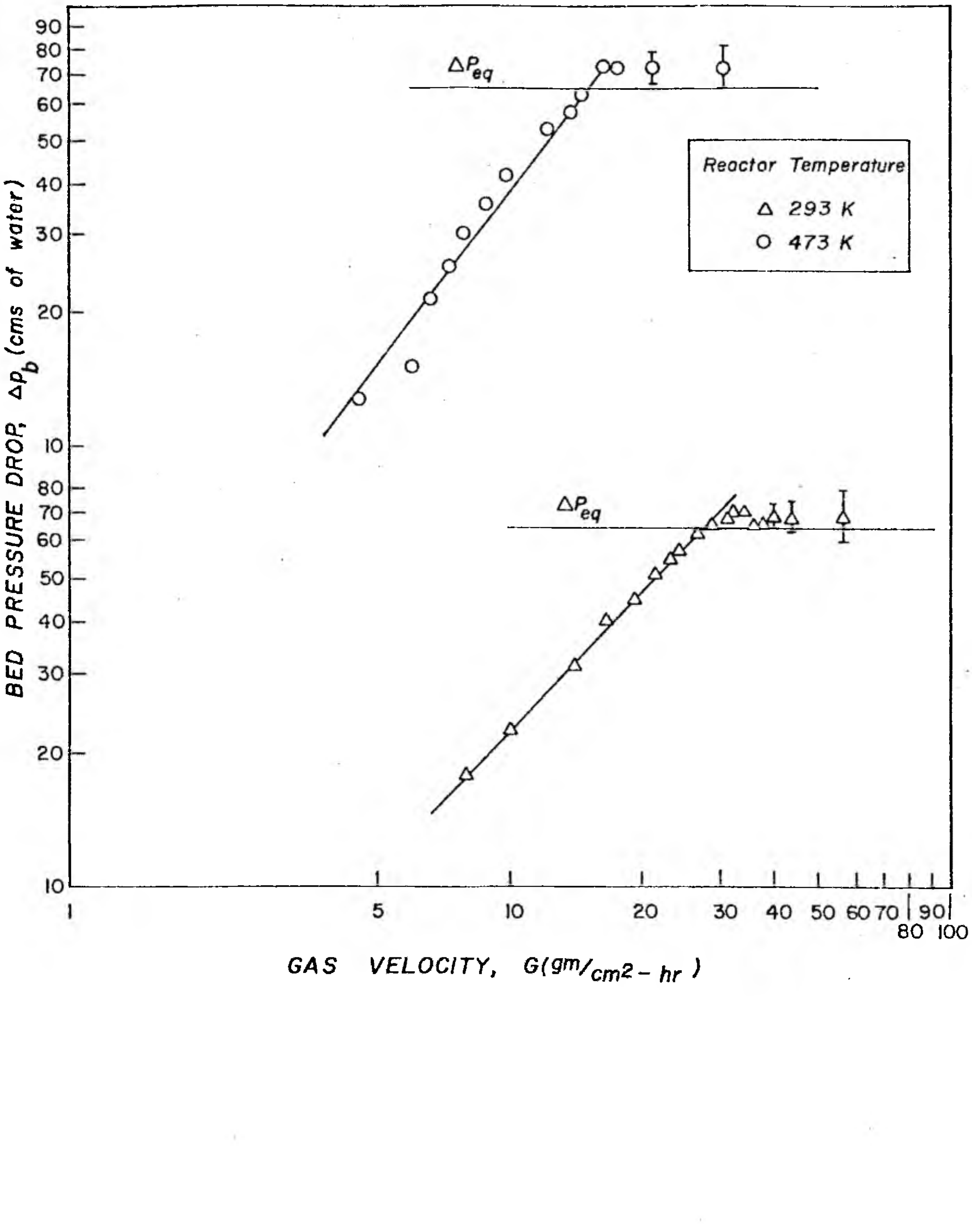

BED PRESSURE DROP, Δp_b (cms of water)
90
80
70
60
50
40
30
20
10
80
70
60
50
40
30
20
10
ΔP_{eq}
ΔP_{eq}
Reactor Temperature
△ 293 K
○ 473 K
1
5
10
20
30
40
50
60
70
80
90
100
GAS VELOCITY, G(gm/cm2 - hr)

Figure C-3

Bed Pressure Drop Versus Gas Velocity

Coked Sand

Tarsand Triangle Deposit

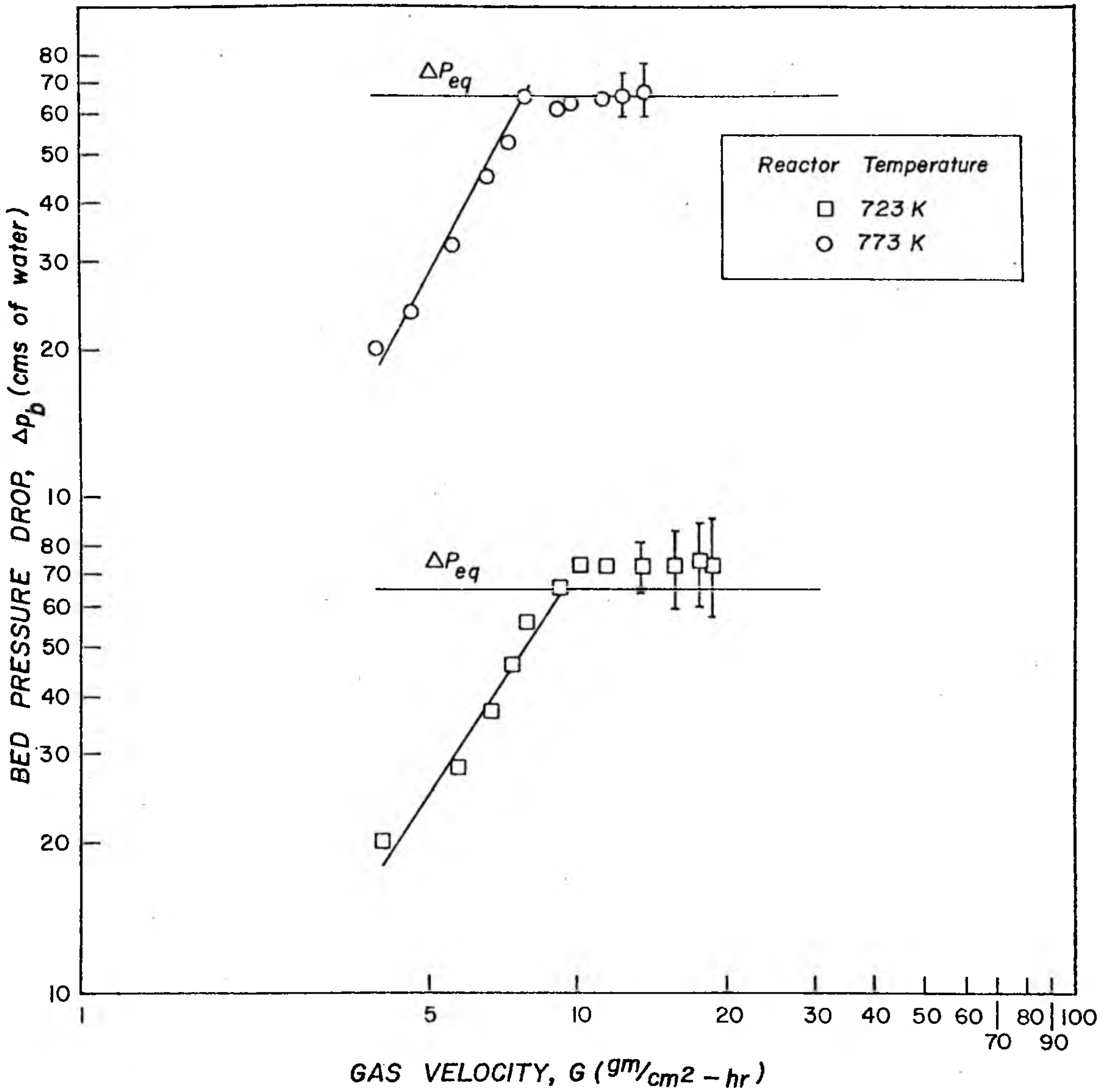
ΔP_eq
ΔP_eq
Reactor Temperature
□ 723 K
○ 773 K
BED PRESSURE DROP, Δp_b (cms of water)
80
70
60
50
40
30
20
10
80
70
60
50
40
30
20
10
1
5
10
20
30
40
50
60
70
80
90
100
GAS VELOCITY, G (gm/cm2 – hr)

Table C-2

Comparison of Experimental and Theoretical Values of Minimum Fluidization Velocity

Reactor Temperature, K	Minimum Fluidization Velocity, G_{m_f} (gm/cm^2-hr)	
	Theoretical[a]	Experimental
293	18.3	28.0
473	8.8	15.2
723	4.5	9.4
773	4.0	8.0

[a] Theoretical values of G_{m_f} from Leva's equation.

Figure C-4

Effect of Reactor Temperature on Minimum Fluidization Velocity

Coked Sand

Tarsand Triangle Deposit

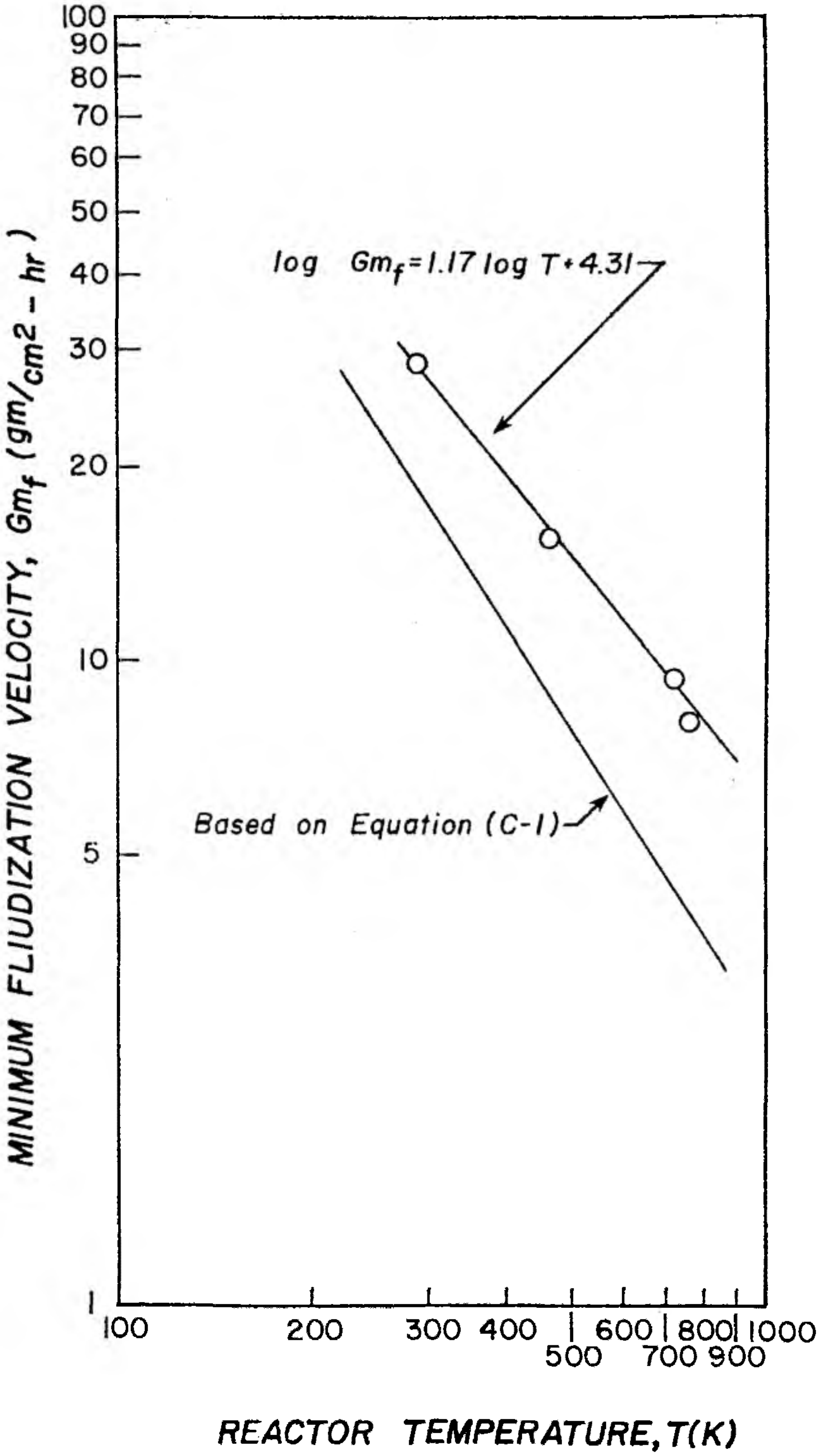
100
90
80
70
60
50
40
30
20
10
5
1
100
200
300
400
500
600
700
800
900
1000
MINIMUM FLUIDIZATION VELOCITY, Gm_f (gm/cm2 - hr)
REACTOR TEMPERATURE, T(K)
log Gm_f = 1.17 log T + 4.31
Based on Equation (C-1)

drop is perhaps due to the extra energy associated with acceleration of solids during slugging. According to Stewart and Davidson(130) slugging will occur if $u_s - u_{m_f} = 0.07\ (gD)^{\frac{1}{2}}$, where D is the bed diameter, u_{m_f} is the minimum fluidization velocity and u_s is the superficial gas velocity at which slugging commences. For example, at 773 K for the bed diameter of 3.66 cm and $u_{m_f} = 5.96$ cm s^{-1}, the excess gas velocity needed for slugging is $u_s - u_{m_f} = 4.2$ cm s^{-1}, that is, a superficial gas velocity of 10.16 cm s^{-1}. During the direct thermal coking experiments, a superficial gas velocity of 12.6 cm s^{-1} was maintained which suggested that solids slugging would occur.

The fluidization studies have indicated that theoretical predictions of minimum fluidization velocities are far below the experimental values, although there exists a linear relationship between minimum fluidization velocity and reactor temperature. These observations raise important questions regarding the validity of scale-up of gas fluidized beds from bench scale data. It is clear from the limited data, further fluidization studies should be conducted, perhaps using a reactor size of 15 - 30 cm diameter, to formulate scale-up procedure for the thermal recovery of synthetic crude from bituminous sands using fluidized beds.

APPENDIX D

HYDROCARBON MIST REMOVAL

A hydrocarbon vapor was produced whenever fresh bituminous sand was added to a fluidized bed of sand particles at temperatures above 673 K. When the hydrocarbon vapor-carrier gas mixture was cooled in the condenser, a hydrocarbon mist or aerosol was observed. Several recovery schemes were tried in the course of developing an efficient recovery system. The recovery of the hydrocarbon mist was essential to obtaining a good material balance. The coalescence of mist becomes more difficult as the droplet size becomes finer. Brink, Jr., et. al.(149) have classified the effectiveness of the various demisting devices according to the droplet size of the aerosol. The demisting devices such as packed-bed scrubbers, electrostatic precipitators, and fiber mist eliminators are more effective for the coalescence of aerosols over a wide range of droplet sizes (10 to 0.01 microns and below), while cyclone separators and impingement separators such as demisting wire mesh pads are effective over a narrow size range of mist droplets (5 - 10 microns). Several of the above mentioned demisting devices were used either alone or in combination for the coalescence of the mist in this investigation.

The effectiveness of each of the devices was evaluated by visual observation of the exit gas stream from the device.

In the present study, the first piece of equipment tested (experiment #5) as a potential demister was a cyclone separator. A portion of the liquid was collected in the cyclone separator, much of the aerosol or mist passed through unaffected. Cyclone separators have higher efficiency of operation when the droplet size being removed is above five microns(127). The performance of the cyclone separator indicated that the hydrocarbon mist has a wide range of mist droplets and required additional demisting devices which were used in combination with the cyclone separator.

A packed-bed scrubber was tried in series with the cyclone separator (experiment #9 and #10). The mild steel scrubbing column, which was 7.5 cm I.D., 90 cm in height, was packed to a height of 75 cm with 1.25 cm porcelain berl saddles. The scrubber was operated in the countercurrent mode with the aerosol from the outlet of the cyclone separator entering at the bottom of the scrubbing column. Various solvents including benzene, toluene, xylenes, n-decane, and n-heptane were used and the solvent was sprayed at the top of the column packing material. The solvent collected at the bottom of the scrubber was recirculated using a pump. The color of the circulating solvent changed from clear to yellow; much of the aerosol was leaving at the scrubber outlet indicating the performance was poor. Moreover, solvent entrainment at higher gas velocities restricted the range of operation.

Next, a plate-type electrostatic precipitator was used in series with the cyclone separator (experiment #7). Tubular-type electrostatic precipitators have been successfully used in recovering heavy oil fractions in the fluidized bed thermal recovery of synthetic crude from Canadian bituminous sands(111). An Electro-Air model (manufactured by Emerson Electric Co., Connecticut) two-stage electrostatic precipitator with a plant area of approximately 1.67 square meters gave a better performance than the scrubber; but a small portion of the aerosol still passed through uncondensed.

A two-stage stainless steel knitted mesh demister unit (manufactured by Diversified Metal Products Inc., New Jersey), similar to that reported by Ellington(150) in the thermal recovery of oil from shale, was used in combination with the cyclone separator (experiment #15). The gas stream leaving the demister contained an aerosol and no liquid product was obtained.

Fiber mist eliminators have been widely used for the removal of acid mist(149). The collection efficiencies reported were high (> 95%) because of the combined effects of the three mechanisms operative during demisting, that is, inertial impaction, direct interception, and absorption. When a gas stream containing aerosol moved across the fibers, the large size droplets were coalesced and condensed on the fibers by inertial impaction and by direct interception and became a part of the liquid film which wet the fibers. Small mist droplets in the gas stream exhibited considerable Brownian movement and did not move uniformly along the gas stream.

As the small droplets diffused from the gas to the surface of the wet fibers, they were absorbed by the liquid film.

Two glass columns, each 3.0 cm I.D. and 75 cm in length, were packed with white cellulose fibers and were used in series as fiber mist eliminators (experiments #11 and #12). The fiber mist eliminators were used in series with the cyclone separator. The outlet of the cyclone separator was connected to the bottom of the first fiber mist eliminator. The aerosol travelled from bottom to top in the first mist eliminator column, while a downward flow direction was used in the second column. During demisting, the color of the cellulose fibers in the first column changed from white to dark brown due to the absorption of hydrocarbon liquid. The gas exiting from the second column contained no aerosol. In addition, a sample of the exit gas was analyzed using a chromosorb 102 column (3.18 mm O.D. x 6.1 m long) in a 5830 A Hewlett-Packard Gas Chromatograph. The entire product recovery unit during experimental runs #11 and #12 consisted of a double pipe, single pass, water-cooled condenser, a cyclone separator, and the fiber mist eliminators. The collection efficiency of the product recovery unit was greater than 92% (collection efficiency is defined for this recovery unit as 100- vol % of C_5^+ in the product gas). The synthetic crude product absorbed in the cellulose fibers was extracted with solvent and the solvent was stripped off in a roto-evaporator under vacuum.

A comparison of the various demisting devices used in this investigation is presented in Table D-1. The electrostatic precipitator and the cellulose fiber mist eliminators were clearly superior to the other alternatives tested, however, the precipitator collected

Table D-1

Comparison of the Performance of Various Liquid Recovery Systems

Pyro-Distillation of Bituminous Sand

Experiment Number	Reactor Temperature, K	Liquid Recovery Scheme	Remarks
5	773	Cyclone Separator	Condensed part of the oil from the mist
7	773	Cyclone Separator - Electrostatic Precipitator	Light oil fraction could not be collected (API gravity of the product is 11.0 - 11.5)
9,10	773	Cyclone Separator - Packed Bed Absorption Column (packing material - porcelain berl saddle)	Poor performance. Solvent entrainment severe at higher gas velocities
11	703	Cyclone Separator - Cellulose Fiber Mist Eliminators	No visible aerosol stream in the exit gas (API gravity of the product is 17.0)
12	703	Cyclone Separator - Cellulose Fiber Mist Eliminators	API gravity of the product is 15.5
15	773	Cyclone Separator - Stainless Steel Demisting Pad	No liquid product collected

only the "heavy ends" of the hydrocarbon mist, while the "light ends" passed through. The API gravity of the liquid product was in the range of 11.0 - 11.5. On the contrary, the fiber mist eliminators also collected the "light ends" giving a higher API gravity for the liquid product, that is, 15.0 - 17.0. Since the fiber mist eliminator gave better performance compared to the Electrostatic precipitator for the removal of condensable vapor from the gas stream, it was used for the removal of mist in this investigation.

APPENDIX E

MATERIAL BALANCE CALCULATIONS

The material balance calculations for a typical experimental run are presented in this Appendix. The analytical procedures for the determination of the composition of the product gas and the quantity of synthetic liquid and of the weight percent coke on the sand were discussed in Chapter 3.

The compositional analysis of gas obtained by gas chromatography included the percent volume of the fluidizing gas, nitrogen, in the exit gas. The volumetric hourly rate at standard temperature and pressure (STP) of the light hydrocarbon gas was computed using the volume percent of nitrogen and the volumetric flow rate of nitrogen at STP conditions. The composition of the product gas was reported on a nitrogen, hydrogen, and hydrogen sulfide free basis. The percentage of hydrogen in the product gas could not be determined accurately due to the low sensitivity of the thermal conductivity detector to hydrogen. Thus, it was not included in the calculation of the material balance.

Material Balance for A Typical Run

Run I.D. #52

Reactor Temperature: 723 K

Average Retention Time of Solids: 27.2 min.

Particle Size of Feed Sand: 358.5 microns

Source of Feed Sand: Sunnyside

Average Bitumen Saturation of Feed Sand: 8.5 weight percent

Bitumen Feed Rate to the Reactor: 54.4 g h^{-1}

Fluidizing Gas (N_2) Flow (at STP): 142 LPH

Product Analysis:

Synthetic Liquid Rate: 24.5 g h^{-1}

Gas Make (at STP): 7.3 LPH

Gas Composition	(Mole %)
CO	1.11
CO_2	4.71
CH_4	26.59
C_2H_4	18.84
C_2H_6	6.37
C_3H_6	13.30
C_3H_8	1.94
i-C_4H_8	0.83
n-C_4H_8	6.93
C_4H_{10}	3.88
C_5	9.70
C_6	5.82
Total	100.00

Coke on Sand before the Run: 0.88 weight percent

Coke on Sand after the Run: 1.40 weight percent

Material Balance Calculations:

$$\text{Component Wt \%} = (\text{Mol.\%})(\text{MW})\left(\frac{\dot{Q}}{V_{STP}}\right)\left(\frac{1}{\dot{W}}\right)$$

where

MW is the molecular weight of the component, g mol^{-1}

$\dot{W}$ is the bitumen feed rate to the reactor, g h^{-1}

$\dot{Q}$ is the volumetric flor rate of the product gases measured at standard conditions, lit. h^{-1}

		Wt % Bitumen	
		Actual	Normalized
CO	$1.11 \times 28 \times \frac{7.34}{22.414} \times \frac{1}{54.4}$ =	0.19	0.19
CO_2	$4.71 \times 44 \times$ " " =	1.25	1.25
CH_4	$26.59 \times 16 \times$ " " =	2.56	2.56
C_2H_4	$18.84 \times 28 \times$ " " =	3.18	3.18
C_2H_6	$6.37 \times 30 \times$ " " =	1.15	1.15
C_3H_6	$13.30 \times 42 \times$ " " =	3.36	3.36
C_3H_8	$1.94 \times 44 \times$ " " =	0.51	0.51
i-C_4H_8	$0.83 \times 56 \times$ " " =	0.28	0.28
n-C_4H_8	$6.93 \times 56 \times$ " " =	2.34	2.34
C_4H_{10}	$3.88 \times 58 \times$ " " =	1.35	1.35
Synthetic Crude (C_5^+ liquid)	$9.70 \times 72 \times$ " + $5.82 \times 86 \times$ " " $\frac{24.44}{54.4} \times 100$ =	52.17	61.23
Coke	$(1280.5 \times 1.4 - 640.25 \times 0.88)\frac{1}{54.4}$ =	22.60	22.60
	Total	90.94	100.00

REFERENCES

1. Wilson, C. L., Energy: Global Prospects 1985-2000, McGraw-Hill Book Co., Inc., New York, (1977).
2. "End Seen for Slump in Global Oil Output", Oil and Gas Journal, 73 (12), 38, (1975).
3. Parent, J. D., Glenn, Seay J. and Linden, H. R., "A Survey of United States and Total World Production, Proved Reserves, and Remaining Recoverable Resources of Fossil Fuels and Uranium as of December 31, 1976", Preprints, Div. Fuel Chemistry (ACS), 24 (1), 1, (1979).
4. Howard, J. B. and Hottel, H. C., New Energy Technology-Some Fact and Assessments, MIT Press, Cambridge, Massachusetts, (1973).
5. Hendrickson, T. A., Compiler, Synthetic Fuels Data Handbook, Cameron Engineers, Inc., Denver, Colorado, (1975).
6. Abraham, H., Asphalts and Allied Substances: Their Occurances, Modes of Production, Uses in the Arts, and Methods of Testing, Vol. I, Ch. 2, D. Van Nostrand Co., Inc., Princeton, New Jersey, (1960).
7. Demaison, D. J., "Tarsands and Supergiant Oil Fields", Amer. Assn. of Petrol. Geologists Bull. 61 (11), 1950, (1977).
8. McRae, A. and Dudas, J. L., Editors , Energy Source Book, Aspen Systems Corporation, Germantown, Maryland, (1977).
9. Holmgren, D. A., Moody, J. D. and Emmerich, H. H., "The Structural Setting for Giant Oil and Gas Fields", Proceedings, Ninth World Petroleum Congress, 2, 45, (1975).
10. Jardine, D., "Cretaceous Oil Sands of Western Canada", in "Oil Sands, Fuel of the Future", Hill, L. V., Editor, Can. Soc. of Petrol. Geologists, p. 56-67, (1974).
11. Outtrim, C. P. and Evans, R. G., "Alberta Oil Sands Reserves and Their Evaluation", in "The Oil Sands of Canada-Venezuela 1977", Redford, D. A. and Winestock, A. G., Editors, Can. Inst. Mining and Metallurgy, Special Volume 17, p. 36-66, (1977).
12. Swabb, L. E., Jr., "Synthetic Fuel Activities in the Western Hemisphere", Erdol und Kohl, 26 (4), 183, (1975).

13. Walters, E. J., "Review of the World's Major Oil Sand Deposits", in "Oil Sands, Fuel of the Future", Hill, L. V., Editor, Can. Soc. Petrol. Geologists, p. 240-263, (1974).

14. Phizackerley, P. H. and Scott, L. O., "Major Tarsand Deposits of the World", Proceedings, Seventh World Petroleum Congress, 3, 551, (1967).

15. Ball Associates Ltd., "Surface and Shallow Oil-Impregnated Rocks and Shallow Oil Fields in the United States", U.S. Bureau of Mines, Monograph 12, (1965).

16. Herkenkoff, E. C., "When are We Going to Mine Oil?", Eng. and Mining Journal, 173 (6), 132, (1972).

17. Ritzma, H. R., "Oil-Impregnated Rock Deposits of Utah", Utah Geological and Mineralogical Survey, Map 33, (1973).

18. Covington, R. E., "Bituminous Sandstone and Limestone Deposits of Utah", in "Oil and Gas Possibilities of Utah, Re-evaluated", Crawford, A. L., Editor, Utah Geological and Mineralogical Survey Bull. 54, Salt Lake City, Utah, (1963).

19. Campbell, J. A., "Oil-Impregnated Sandstone Deposits of Utah", Mining Eng., 27 (5), 47, (1975).

20. Tirastoo, E. N., Oil Fields of the World, Gulf Publishing Co., Houston, Texas, (1976).

21. Oblad, A. G. and Dorrence, S. M., "Future of Utah Tarsands", Symposium on Implications of Energy Conservation and Supply Alternatives, Science Applications Inc., New Brunswick, New Jersey, Jan. 30-Feb. 2, 1978.

22. Lowe, R. M., "The Asphalt Ridge Tarsand Deposits", AIChE Symp. Series, 72 (155), 55, (1976).

23. Bailey, N. L. J., Jobson, A. M. and Roger, M. A., "Bacterial Degradation of Crude Oil: Comparison of Field and Experimental Data", Chemical Geology, 11, 202, (1973).

24. James, D. P. and Oliver, T. A., "The Sedimentology of the McMurray Formation, East Athabasca", in "The Oil Sands of Canada-Venezuela 1977", Redford, D. A. and Winestock, A. G., Editors, Can. Inst. Mining and Metallurgy, Special Volume 17, p. 17-26, (1977).

25. Deroo, G. and Powell, T. G., "The Oil Sand Deposits of Alberta: Their Origin and Geochemical History", Preprints, Div. Fuel Chemistry (ACS), 22 (3), 183, (1977).

26. Galavis, J. A. S. and Velarde Ch., H. M., "Geological Study and Preliminary Evaluation of Potential Reserves of Heavy Oil of the Orinoco Tar Belt Eastern Venezuelan Basin", Proceedings, Seventh World Petroleum Congress, 3, 229, (1967).

27. Gutierrez, F. J., Vasquez, E. and Santos, A. C., "Formation of Crude Oil Characteristics of Oil Reservoirs in the Orinoco Petroleum Belt as related to the Geology", in "The Oil Sands of Canada-Venezuela 1977", Redford, D. A. and Winestock, A. G., Editors, Can. Inst. Mining and Metallurgy, Special Volume 17, p. 69-77, (1977).

28. "Bacteria Have Destroyed 10% of World's Crude", World Oil, 174 (2), 28, (1972).

29. Ritzma, H. R., "Commercial Aspects of Utah's Oil-Impregnated Sandstone Deposits", Interstate Oil Compact Commission Committee Bull., XV, 2, (1973).

30. Ritzma, H. R., "Exploration and Development of Oilshale and Oil-Impregnated Rocks, 1970-75", Quarterly, Colorado School of Mines, 70, 81, (1975).

31. Campbell, J. A., "Oil-Impregnated Sandstone Deposits of Utah", Utah Geological and Mineralogical Survey, Reprint 99, (1975).

32. Speiker, E. M., "Bituminous Sandstone near Vernal, Utah", U.S. Geological Survey Bull., 822, (1931).

33. Kayser, R. B., "Bituminous Sandstone Deposits, Asphalt Ridge, Uintah County, Utah", Utah Geological and Mineralogical Survey, Special Studies 19, (1966).

34. Byrd, W. D. III, "P. R. Spring Oil-Impregnated Sandstone Deposit, Uintah and Grand Counties, Utah", Utah Geological and Mineralogical Survey, Special Studies 31, (1970).

35. Peterson, P. R. and Ritzma, H. R., "Informational Core-Drilling in Utah's Oil-Impregnated Sandstone Deposits, South East Uinta Basin, Utah", Utah Geological and Mineralogical Survey, Rept. Investigation 88, (1974).

36. Merchant, L. C., Johnson, L. A. and Cupps, C. Q., "Properties of Utah Tarsands-Three Mile Canyon Area, P. R. Spring Deposit", U.S. Bureau of Mines, Rept. Investigation 7923, (1974).

37. Holmes, C. N., Page, B. M. and Averitt, P., "Geology of the Bituminous Sandstone Deposits near Sunnyside, Carbon County, Utah", U.S. Geol. Survey, Oil and Gas Prelim. Investigation Map 86, (1948).

38. Davidson, E. S., "Geology of the Circle Cliff Area, Garfield and Kane Counties, Utah", U.S. Geological Survey Bull. 1299, (1967).

39. Baar, D. L. and Seager, W. R., "Stratigraphic Control of Petroleum in White Rim Sandstone (Permian) in and Near Canyonlands National Park, Utah", Amer. Assn. Petrol. Geologists, Bull. 54 (5), 709, (1970).

40. Ismail, M., "Engineering Evaluation of Alabama Tarsands", Alabama Geol. Surv. Circ. 89, 1, (1973).

41. Brimhall, R. M. and Dickman, J., "Reserves of Heavy Oil from the Santa Rosa Sandstone, Guadalupe County, New Mexico", Paper presented at the Fourth Rocky Mountain Fuel Symposium, Salt Lake City, Utah, February, 1979.

42. Harris, M. C. and Sobkowicz, J. C., "Engineering Behaviour of Oil Sands", in "The Oil Sands of Canada-Venezuela 1977", Redford, D. A. and Winestock, A. G., Editors, Can. Inst. Mining and Metallurgy, Special Volume 17, p. 270-281, (1977).

43. Sepulveda, J. E., Miller, J. D. and Oblad, A. G., "Hot-Water Extraction of Bitumen from Utah Tarsands", Preprints, Div. Fuel Chemistry (ACS), 21 (6), 110, (1976).

44. Carrigy, M. A., "The Physical and Chemical Nature of a Typical Tarsand: Bulk Properties and Behaviour", Proceedings, Seventh World Petroleum Congress, 3, 573, (1967).

45. Camp, F. W., The Tarsands of Alberta, Canada, Second Ed., Cameron Engineering Inc., Denver, Colorado, (1974).

46. Wood, R. E. and Ritzma, H. R., "Analysis of Oil Extracted from Oil-Impregnated Sandstone Deposits in Utah", Utah Geological and Mineralogical Survey, Special Studies 39, Salt Lake City, Utah, (1972).

47. Sepulveda, J. E., "Hot-Water Separation of Bitumen from Utah Tarsands", M.S. Thesis, University of Utah, Salt Lake City, Utah, (1977).

48. Oblad, A. G., Seader, J. D., Miller, J. D. and Bunger, J. W., "Recovery of Bitumen from Oil-Impregnated Sandstone Deposits of Utah" in "Oil Shale and Tar Sands", Smith, J. W. and Atwood, M. T., Editors, AIChE Symp. Series, 72 (155), 69, (1976).

49. Shea, G. D. and Higgins, R. V., "Separation and Utilization Studies of Bitumens from Bituminous Sandstones of the Vernal and Sunnyside, Utah, Deposits, Part I-Laboratory Hot-Water Separation Tests", U.S. Bureau of Mines. Rept. Investigation 4871, (1952).

50. Bowman, C. W., "Molecular and Interfacial Properties of Athabasca Tarsands", Proceedings, Seventh World Petroleum Congress, 3, 583, (1977).

51. Cupps, C. Q., Land, C. S. and Marchant, L. C., "Field Experiment of In-situ Oil Recovery from a Utah Tarsand by a Reverse Combustion" in "Oil Shale and Tar Sands", Smith, J. W. and Atwood, M. T., Ed., AIChE Sym. Series, 72 (155), 61, (1976).

52. Oblad, A. G., Personal Communication, 1978.

53. Boyd, M. L. and Montgomery, D. S., "Structural Group Analysis of the Asphaltene and Resin Components of the Athabasca Bitumen", Fuel, 41, 335, (1962).

54. Misra, M. and Miller, J. D., "The Effect of Feed Source in the Hot Water Processing of Utah Tar Sand", Preprints, 1979 AIME Ann. Meeting, New Orleans, LA, Feb. 18-22, (1979).

55. Bunger, J. W., Thomas, K. P. and Dorrence, S. M., "Compound Types and Properties of Utah and Athabasca Tarsand Bitumens", Fuel, 58, 183, (1979).

56. Rojas, G. G., Barrios, T., Scudiero, B. and Ruiz, J., "Rheological Behaviour of Extra-Heavy Crude Oil from the Orinoco Tar Belt" in "The Oil Sands of Canada-Venezuela 1977", Redford, D. A. and Winestock, A. G., Ed., Can. Inst. Mining and Metallurgy, Special Volume 17, p. 284-302, (1977).

57. Wenger, W. J., Hubbard, R. L. and Whisman, M. L., "Separation and Utilization Studies of Bitumens from Bituminous Sandstones of the Vernal and Sunnyside, Utah, Deposits, part II - Analytical Data on Asphalt Properties and Cracked Products of the Separated Bitumens", U.S. Bureau of Mines, Rept. Investigation 4871, (1952).

58. "Boiling Range Distribution of Petroleum Fractions by Gas Chromatography", Annual Book of ASTM Standards, part 17, p. 1069, (1973).

59. Bunger, J. W., "Techniques of Analysis of Tar Sand Bitumens", Preprints, Div. Petroleum Chemistry (ACS), 22 (2), 716, (1977).

60. Strauz, O. P., "The Chemistry of Alberta Oil Sand Bitumen", in "The Oil Sands of Canada-Venezuela 1977", Redford, D. A. and Winestock, A. G., Ed., Can. Inst. Mining and Metallurgy, Special Volume 17, p. 146-153, (1977).

61. Jones, J. H. and Moote, T. P., "Studies on the Composition of Athabasca Tar Fractions", Preprints, Div. Petroleum Chemistry, 8 (2), A-29, (1963).

62. Boyd, M. L. and Montgomery, D. S., "A Study of the Oil Component of the Athabasca Bitumen", Jour. Inst. Petroleum, 49, 345, (1963).

63. Speight, J. G., "A Structural Investigation of the Constituents of Athabasca Bitumen by Proton Magnetic Resonance Spectroscopy", Fuel, 49, 76, (1970).

64. Speight, J. G., "Structural Analysis of Athabasca Asphaltenes by Proton Magnetic Resonance Spectroscopy", Fuel, 50, 102, (1971).

65. Ruberto, R. G., Jewell, D. M., Jensen, R. K. and Cronauer, D. C., "Characterization of Synthetic Liquid Fuels", in "Shale Oil, Tar Sands and Related Fuel Sources", Yen, T. F., Ed., Adv. Chem. Series, (ACS), 151, Ch. 3, (1976).

66. Jewell, D. M., Weber, J. H., Bunger, J. W., Plancher, H. and Latham, D. R., "Ion-Exchange, Coordination, and Adsorption Chromatographic Separation of Heavy End Petroleum Distillates", Anal. Chem., 44, 1391, (1972).

67. Bachman, W. A. and Stormont, D. H., "Plant Starts, Athabasca now Yielding its Hydrocarbons", Oil and Gas J., 65 (10), 69, (1967).

68. Humphreys, R. D., "Oil from Alberta Oil Sands", Chem. Eng. Prog., 70 (9), 66, (1974).

69. Nulty, P., "Canada Goes after the Energy in the Tarsands", Fortune, 97 (5), 72, (1978).

70. McMillan, J. C., "The Challenge in Financing Canadian Oil Sands Development", Preprints, First International Conference on the Future of Heavy Crude and Tar Sands, Edmonton, Alberta, Canada, June 4-12, (1979).

71. Glassett, J. M. and Glassett, J. A., "The Production of Oil from Intermountain West Tarsands Deposits", Final Report, U.S. Dept. of the Interior, Bureau of Mines, Contract No. SO 241129, (1976).

72. Decora, A. W. and Schrider, L. A., "In-situ Recovery Processing", Hydrocarbon Processing, 55 (5), 117, (1976).

73. Bader, B. E., Fox, R. L. and Stosur, J. J., "The Potential of Downhole Steam Generation to the Recovery of Heavy Oils", Preprints, First International Conference on the Future of Heavy Crude and Tarsands, Edmonton, Alberta, Canada, June 4-12, (1979).

74. Doscher, T. M., Labelle, R. W., Sawatsky, L. H. and Zwicky, R. W., "Steam Drive Successful in Canada's Oil Sands", Petrol. Engr., 36, 71, (1964).

75. Dillabough, H. A. and Prats, M., "Recovering Bitumen from Peace River Deposits", Oil and Gas J., 72 (11), 186, (1974).

76. Faroug Ali, S. M., "Application of In-situ Methods of Oil Recovery to Tarsands", in "Oil Sands - Fuel of the Future", Hills, L. V., Ed., Can. Soc. Petrol. Geologist, Memoir 3, p. 199-211, (1974).

77. Redford, D. A. and Winestock, A. G., The Oil Sands of Canada-Venezuela 1977, Can. Inst. Mining and Metallurgy, Special Volume 17, (1977).

78. McConville, L. B., "The Athabasca Tarsands", Mining Engineering, 27 (1), 19, (1975).

79. Camp, F. W., "Tarsands" in Kirk-Othmer Encyclopedia of Chemical Technology", 2nd Ed., 19, 682, (1969).

80. McIntyre, H., "Imperial Plans Giant Syncrude Works", Can. Chem. Proc., 61 (12), 25, (1977).

81. Thurber, J. L. and Welbourn, M. E., "How Shell Attempted to Unlock Utah Tarsands", Petrol. Engr., 49 (11), 31, (1977).

82. Doscher, T. M., "Technical Problems in In-situ Methods for Recovery of Bitumen from Tarsands", Proceedings, Seventh World Petroleum Congress, 3, 625, (1967).

83. Redford, D. A. and Cotsworth, P. F., "Development of Communication Paths within a Tarsand Bed", in "Shale Oil, Tarsands, and Related Fuel Sources", Yen, T. F., Ed., Advances in Chemistry Series (ACS), 151, Ch. 9, (1976).

84. Perry, R. H., Green, D. W. and Campbell, J. M., "Reverse Combustion - A New Oil Recovery Technique", Jour. of Petrol. Tech., 12 (5), 11, (1960).

85. Warren, J. E., Reed, R. L. and Price, H. S., "Theoretical Considerations of Reverse Combustion in Tarsands", Jour. of Petrol. Tech., 12 (5), 14, (1960).

86. Berry, Jr., V. J. and Parrish, D. R., "A Theoretical Analysis of Heat Flow in Reverse Combustion", Jour. of Petrol. Tech., 12 (5), 15, (1960).

87. Nelson, T. W. and McNeil, J. S., "In-situ Combustion Project", Oil and Gas J., 59 (6), 58, (1961).

88. Alexander, A. D., Martin, W. L. and Dew, J. W., "Factors Affecting Fuel Availability and Composition during In-situ Combustion", Jour. of Petrol. Tech., 14 (10), 1154, (1962).

89. Marchant, L. C., Land, C. S. and Cupps, C. Q., "Experimental Approach to In-situ Oil Recovery from Tarsands", Energy Sources, 2 (3), 293, (1975).

90. Reed, R. L. and Reed, D. W., "Experimental Aspects of Reverse Combustion in Tarsands", Jour. of Petrol. Tech., 12 (5), 13, (1960).

91. Marchant, L. C. and Johnson, L. A., "U.S. Energy Research and Development Administration Tarsand Research - Updata", in "The Oil Sands of Canada-Venezuela 1977", Redford, D. A. and Winestock, A. G., Ed., Can. Inst. Mining and Metallurgy, Special Volume 17, p. 520-524, (1977).

92. Johnson, L. A., Fahy, L. J., Thornton, M. W., Romanowski, Jr., L. J. and Marchant, L. C., "Oil Recovery from Utah Tarsand Deposit by In-situ Combustion", Proceedings, Fourth DOE Symposium on Enhanced Oil and Gas Recovery and Improved Drilling Methods, Tulsa, Oklahoma, pp. D-6/1-16, Aug., (1978).

93. Marchant, L. C., Cupps, C. Q. and Stosur, J. J., "Current Activity in Oil Production from U.S. Tarsands", Preprints, First International Conference on the Future of Heavy Crude and Tarsands, Edmonton, Alberta, Canada, June 4-12, (1979).

94. Mungen, R. and Nicholls, J. H., "Recovery of Oil from Athabasca Oil Sands and from Heavy Oil Deposits of Northern Alberta by In-situ Methods", Proceedings, Ninth World Petroleum Congress, 5, 29, (1975).

95. Funk, E. W., "Behaviour of Tarsand Bitumen with Paraffinic Solvents and Its Application to Separation for Athabasca Bitumen", Preprints, Div. Fuel Chemistry (ACS), 23 (4), 81, (1978).

96. Clark, K. A., "Hot-Water Separation of Alberta Bituminous Sand", Transactions, Can. Inst. Mining and Metallurgy, 47, 257, (1944).

97. Perrini, E. M., Oil from Shale and Tarsands, Chem. Tech. Review 51, Noyes Data Corporation, Park Ridge, New Jersey, (1975).

98. Djingheuzian, L. E., "Cold Water Method of Separation of Bitumen from Alberta Bituminous Sands", Can. Min. Met. Bull. 45, 2, (1952).

99. Clark, K. A. and Pasternack, D. S., "Hot Water Separation of Bitumen from Alberta Bituminous Sand", Ind. Eng. Chem., 24, 1410, (1932).

100. Innes, E. D. and Fear, J. V. D., "Canada's First Commercial Tarsand Development", Proceedings, Seventh World Petroleum Congress, 3, 633, (1967).

101. Leja, J. and Bowman, C. W., "Application of Thermodynamics to the Athabasca Tarsands", Can. J. Chem. Eng., 46, 479, (1968).

102. Bartel, F. E. and Miller, F. L., "Displacement of Crude Oil and Benzene from Silica by Aqueous Solutions", Ind. Eng. Chem., 24, (3), 335, (1932).

103. Nutting, P. G., "Chemical Problems in the Water Driving of Petroleum from Oil Sands", Ind. Eng. Chem., 17 (10), 1035, (1925).

104. Nutting, P. G., "Principles Underlying the Soda Process", Oil and Gas J., 25 (5), 32, (1927).

105. The Syncrude Story, Public Affairs Department, Syncrude, Edmonton, Alberta, Canada, (1979).

106. Camp, F. W., "Processing Athabasca Tarsands - Tailing Disposal", Can. J. Chem. Eng., 55 (10), 581, (1977).

107. Flynn, P. C., Porteous, K. C. and Sulzle, R. K., "Heat and Mass Balance Implications for Direct Coking of Athabasca Tarsands", Energy Processing (Canada), pp. 42-48, October, 1976.

108. Vermeulen, F. E. and Stephenchute, F., "Electrical Extraction of Oil from Tarsand", IEEE Transactions on Industry Applications, 1A-13 (6), 604, (1977).

109. Sepulveda, J. E. and Miller, J. D., "Extraction of Bitumen from Utah Tarsands by a Hot Water Digestion - Flotation Technique", Mining Engineering, 30 (9), 1311 (1978).

110. Moore, R. G., Bennion, D. W. and Donnelly, J. K., "Anhydrous Extraction of Hydrocarbons from Oil Sands", Energy Processing (Canada), p 48, October, (1975).

111. Gishler, P. E., "The Fluidization Technique Applied to Direct Distillation of Oil from Bituminous Sand", Can. J. Research, 27, Sec. F, 104, (1949).

112. Steinhofer, A., Frey, O. and Nonnenmacher, H., "Make Ethylene from Crude Oil", Hydrocarbon Processing and Petroleum Refiner., 42 (7), 119, (1963).

113. Adonik, S. B., Green, E. J. and Hallee, L. P., Manufacture Ethylene, Petroleum Publishing Co., Oklahoma, (1970).

114. Peterson, W. S. and Gishler, P. E., "A Small Fluidized Solids Pilot Plant for the Direct Distillation of Oil from Alberta Bituminous Sands", Can. J. Research, Sec. F, 62, (1950).

115. Peterson, W. S. and Gishler, P. E., "Oil from Alberta Bituminous Sand", Petrol. Engr., 23, C-66, (1951).

116. Peterson, W. S. and Gishler, P. E., "The Fluidized Solids Technique Applied to Alberta Oil Sands Problem", Proceedings, First Athabasca Oil Sands Conference, Edmonton, Alberta, Canada, p 207-236, September, (1951).

117. Safonov, V. A., Indyukov, N. M., Shevtsov, I. S., Markaryan, S. M. and Rustamov, M. I., "Utilization of Fluidized Bed Thermal Conversion Process for Oil Bearing Kirmak Sands", Sb. Tr. Azer-Nauch-Issledovatel, Inst. Neft, Prom. im. V. V. Kurbysheva, 2, 288, (1958).

118. Safonov, V. A., Indyukov, N. M., Loginova, S. M. and Shevtsov, I. S., "Improvement in the Technology of Treating Oil-Bearing Sands and Utilization of Oil Thus Produced", Sb. Tr. Inst. Nebtekhim Protssov, Akad. Nauk Azerb. SSR, 4, 272, (1959).

119. Haensel, V., "Separating and Cracking of Oil from Oil-Bearing Sands", U.S. Patent 2,733,193 (1956).

120. Rammler, R. W., "One Process Retorts Three Feeds for Synthetic Crude", Mining Engineering, 22 (9), 63 (1970).

121. Rammler, R. W., "The Production of Synthetic Crude Oil from Oil Sand by Application of the Lurgi Ruhrgas Process", Can. J. Chem. Eng., 48 (10), 552, (1970).

122. Filby, J. E., Flynn, P. C. and Porteous, K. C., "Bench Scale Studies of Direct Coking of Athabasca Tarsand", Paper presented at the 27th Canadian Chemical Engineering Conference, Oil Sands Symposium, Calgary, Alberta, Canada, Oct. 23-27, (1977).

123. Berg, C. H. O., "Retorting and Coking Process with Hot Sand Recycle", U.S. Patent 2,905,595 (1959).

124. Steinmetz, I., "Coking a Mixture of Tarsand and Froth Product", U.S. Patent 3,466,240 (1969).

125. Gallagher, J. P., Humes, W. H., and Siemssen, J. O., "Cat-Cracking to Upgrade Synthetic Crudes", Chem. Eng. Prog., 75 (6), 56, (1979).

126. Thomson, F. M., "Smoothing the Flow of Materials Through the Plant:Feeders", Chemical Engineering, 85 (24), 77, (1978).

127. Chemical Engineers' Handbook, Fifth Edition, Perry, R. H. and Chilton, C. H., Editors, McGraw-Hill Book Co., Inc., New York, 1973.

128. Greensfelder, B. S., Voge, H. H. and Good, G. M., "Catalytic and Thermal Cracking of Pure Hydrocarbons", Ind. Eng. Chem., 41, 2573 (1949).

129. Hovmand, S. and Davidson, J. F., "Pilot Plant and Laboratory Scale Fluidized Reactors at High Gas Velocities; the Relevance of Slug Flow", in Fluidization, Davidson, J. F. and Harrison, D., Editors, Academic Press, London, Ch. 5, 1971.

130. Steward, P. S. B. and Davidson, J. F., "Slug Flow in Fluidized Beds", Powder Tech., 1, 61, (1967).

131. Leva, M., Fluidization, McGraw-Hill Book Co., Inc., New York, 1959.

132. Boie, W., "Contributions to Pyrotechnic Computations", Wissenschaftliche Zeitschrift der Technischen Hochschule, Dresden, 2, 687, (1952/53).

133. Schmidt, P. F., Fuel Oil Manual, 3rd Ed., Industrial Press, New York, (1969).

134. Callen, R. B., Bendoraitis, J. G., Simpson, C. A. and Voltz, S. E., "Upgrading Coal Liquids to Gas Turbine Fuels. I. Analytical Characterization of Coal Liquids", Ind. Eng. Chem., Prod. Res. Dev., 15 (4), 222, (1976).

135. Brown, J. K. and Ladner, W. R., "A Study of the Hydrogen Distribution in Coal-like Materials by High Resolution Nuclear Magnetic Resonance Spectroscopy II - A Comparison with Infrared Measurement and the Conversion to Carbon Structure", Fuel, 39, 87, (1960).

136. Yoshida, R., Yoshida, T., Ikawa, Y., Okutani, T., Hirama, Y., Nakata, Y., Yokoyama, S., Makabe, M and Hasegawa, Y., "The Nature of Athabasca Tar Sand (Canada) and Derivatives. A Comparison with Coal-Hydrogenolysis Products", Bulletin of the Chemical Society of Japan, 52 (5), 1464, (1979).

137. Middleton, W. R., "Gradient Elution Chromatography Using Ultraviolet Monitors in the Analytical Fractionation of Heavy Petroleums", Anal. Chem., 39, 1839, (1967).

138. Utley, J. K., "The Adoptation of Gradient Elution Chromatography to the Analysis of the Bitumen and Synthetic Liquids Derived from Bituminous Sand", Senior Project Report, Department of Mining and Fuels Engineering, University of Utah, Salt Lake City, Utah, 1979.

139. Barbour, R. V., Dorrence, S. M., Vollmer, T. L. and Harris, J. D., "Pyrolysis of Utah Tarsands - Products and Kinetics", Preprints, Div. Fuel Chemistry (ACS), 21 (6), 278, (1976).

140. Lee, H., "A Thermal Study of Coal Impregnated with Hydrogenation Catalysts", Ph.D. Dissertation, University of Utah, Salt Lake City, Utah, 1974.

141. Kunii, D. and Levenspiel, O., Fluidization Engineering, John Wiley and Sons, Inc., New York, 1969.

142. Zenz, F. A. and Othmer, D. F., Fluidization and Fluid Particle Systems, Reinhold Publishing Corp., New York, 1960.

143. Geldart, D., Hurt, J. M. and Wadia, P. H., "Slugging in Beds of Large Particles", AIChE Sym. Series, 74 (176), 60, (1978).

144. Desai, A., Kikukawa, H. and Pulsifer, A. H., "The Effect of Temperature upon Minimum Fluidization Velocity", Powder Tech., 16, 143, (1977).

145. Singh, B., Rigby, G. R. and Callcott, T. G., "Measurement of Minimum Fluidization Velocities at Elevated Temperature", Trans. Inst. Chem. Engrs., 51, 93, (1973).

146. Frantz, J. F., "Design of Fluidization, Part I", Chem. Eng., 69 (9), 161, (1962).

147. Richardson, J. F., "Incipient Fluidization and Particulate Systems", in "Fluidization", Davidson, J. F. and Harrison, D., Editors, Academic Press, New York, 1971.

148. Mori, S., "High Pressure Fluidization and Momentum Equations", Ph.D. Dissertation, Department of Mining and Fuels Engineering, University of Utah, Salt Lake City, Utah, 1973.

149. Brink, Jr., J. A., Burggrabe, W. F. and Greenwell, L. E., "Mist Removal from Compressed Gases", Chem. Eng. Prog., 62 (4), 60, (1966).

150. Ellington, R. T., "Fluidized Bed Retorting of Oil Shale", Annual SME of AIME Meeting, Preprints No. 72, AIME 41, (1972).

VITA

Name	Valadi Natarajan Venkatesan
Birthdate	January 21, 1944
Birthplace	Madras, Tamilnadu, India
High School	Sri Ramakrishna Mission High School (North Branch) T. Nagar, Madras, India
College 1961-1963	Loyola College, Madras University, Tamil Nadu, India
University 1963-1968	Annamalai University, Annamalainagar, Tamil Nadu, India
1968-1970	Indian Institute of Technology Madras, Tamil Nadu, India
1973-1979	University of Utah Salt Lake City, Utah, U.S.A.
Degrees May, 1968	B.E., Chemical Engineering Annamalai University Annamalainagar, India
May, 1970	M. Tech., Chemical Engineering Science Indian Institute of Technology Madras, India
Professional Positions	Research Assistant, Fuels Engineering University of Utah, 1973-1979
	Assistant Foreman, Dept. of Energy and Economy, Hindustan Steel Limited, Bhilai, India, 1971-1973